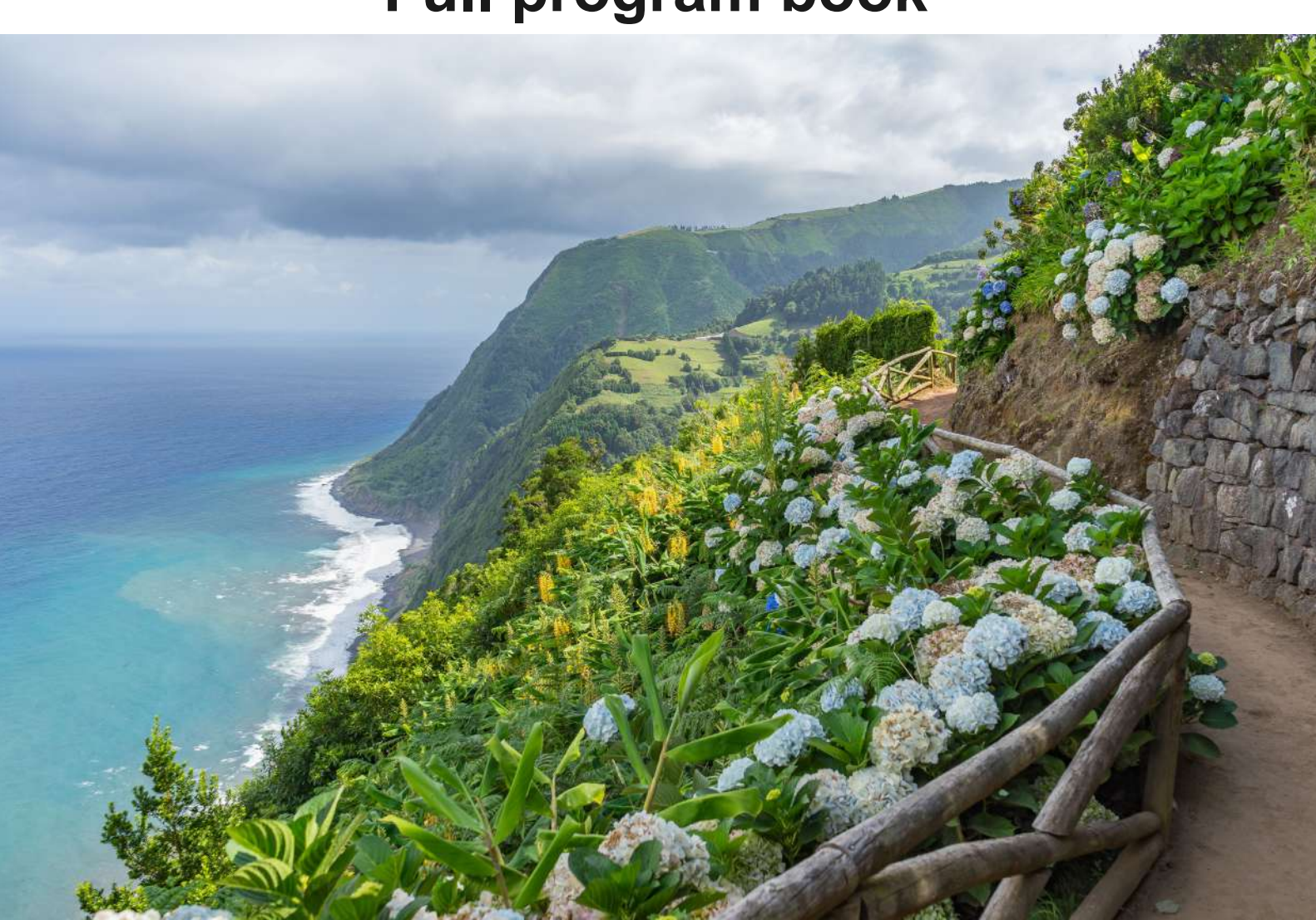
https://ufo2025.fc.up.pt/info@ultrafastoptics2025.org

UltrafastOptics UJFOXIV

Azores (Portugal), 5-10 October 2025

Full program book





General Chairs

Rosa Romero, Sphere Ultrafast Photonics, Portugal Helder Crespo, Central Laser Facility, STFC, UK

Program Chairs

Cord Arnold, Lund University, Sweden Xinkui He, Institute of Physics, Chinese Academy of Sciences, China Jeffrey Moses, Cornell University, USA

Local Organizing Committee

Helena Cristina Vasconcelos, University of the Azores, Portugal Maria Gabriela Meirelles, University of the Azores, Portugal

General Organizing Committee

Michelle Young, Stanford University, USA Ritu Khurana, Stanford University, USA Sheetal Singh, Stanford University, USA Martin Saraceno, Ruhr University Bochum, Germany

























Program Committee

Topical Leads

Federico Furch, Max-Born Institute, Germany

Yuxin Leng, Shanghai Institute of Optics and Fine Mechanics, China

Thomas Metzger, Trumpf Scientific, Germany

Michael Chini, Ohio State University, USA

Íñigo Sola, University of Salamanca, Spain

Derryck T. Reid, Heriot-Watt University, Scotland

Liang Jie Wong, Nanyang Technological University, Singapore

Clara Saraceno, Ruhr-Universitet Bochum, Germany

Anne-Lise Viotti, Lund University, Sweden

Michelle Sander, Boston University, USA

Marc Jankowski, Stanford University, USA

Geory Genty, Tampere University, Finland

Committee Members

Alan Fry, SLAC, Stanford University, USA

Anne-Laure Calendron, DESY, Germany

Bojan Resan, University of Applied Sciences and Arts, Northwestern Switzerland

Bruno Schmidt, Few-cycle Inc., Canada

Camille Sophie-Bres, EPFL, Switzerland

Caterina Vozzi, CNR-IFN, Italy

Emma Springate, Central Laser Facility, STFC, UK

Giulio Cerullo, Politecnico di Milano, Italy

Günter Steinmeyer, Max Born Institute, Germany

Igor Jovanovic, University of Michigan, USA

Jan Rothhardt, University of Jena, Germany

Juliet Gopinath, University of Colorado at Boulder, USA

Jungwon Kim, KAIST, South Korea

Marta Fajardo, IST Lisbon, Portugal

Michael Hemmer, KM Labs, USA

Minglie Hu, Tianjin University, China

Oliver Heckl, University of Vienna, Austria

F. Ömer Ilday, Ruhr-Universität Bochum, Turkey

Óscar Martinez, FIUBA, Universidad de Buenos Aires, Argentina

Rocio Borrego Varillas, CNR-IFN, Italy

Rodrigo Lopez-Martens, Laboratoire d'Optique Appliquée, France

Selçuk Akturk, Bruker Nano Surfaces Division, USA

Shu-Wei Huang, University of Colorado Boulder, USA

Sterling Backus, Thorlabs Inc., USA

Yi Liu, University of Shanghai for Science and Technology, China



About the Ultrafast Optics conference

Since the first edition in Monterey, California, in 1997, Ultrafast Optics (UFO) has been a dedicated forum for scientists and researchers to discuss the science and technology of ultrashort laser pulses. UFO thrives thanks to the dedicated efforts of its general chairs, program chairs, and local organizers, with guidance from an executive committee of past chairs. Its intentionally small size (typically 150–200 attendees), single-session format, strong involvement from exhibitors, inspiring locations, and engaging social activities all work together to create a welcoming, interactive, and tightly connected international ultrafast optics community.

Over the years, UFO has journeyed across the globe, bringing together the international ultrafast optics community in a series of inspiring locations:

I: 1997 - Monterey, California, USA

II: 1999 - Ascona, Switzerland

III: 2001 - Château Montebello, Quebec, Canada

IV: 2003 - Vienna, Austria

V: 2005 - Nara, Japan

VI: 2007 - Santa Fe, New Mexico, USA

VII: 2009 - Arcachon, France

VIII: 2011 - Monterey, California, USA

IX: 2013 - Davos, Switzerland

X: 2015 - Beijing, China

XI: 2017 - Jackson Hole, Wyoming, USA

XII: 2019 - Bol, Croatia

XIII: 2023 - Bariloche, Argentina

The 14th edition in the Azores provides a special opportunity to reconnect and share the latest advances, as well as enjoy the breathtaking island landscapes while forging lasting collaborations. We hope you take full advantage of the program, discussions, and unique environment to learn about the latest advances in the field.



São Miguel, the largest island in the Azores archipelago, is often called "the Green Island" thanks to its lush landscapes, volcanic lakes, and rolling pastures. Located in the middle of the Atlantic Ocean, this island is a remarkable blend of natural beauty, rich history, and vibrant culture. Measuring about 62 kilometers in length and 16 kilometers at its widest point, São Miguel is home to nearly half of the Azorean population, with



its capital, Ponta Delgada, serving as the main gateway to the archipelago.

What makes São Miguel so special is its unique volcanic origin, which has shaped both the geography and the lifestyle of its inhabitants. The island boasts stunning calderas such as Sete Cidades and Furnas, each home to emerald and sapphire-colored lakes nestled within steep crater walls. Visitors are often captivated by the view from Vista do Rei, overlooking the twin lakes of Sete Cidades, a scene that has become one of the most iconic images of the Azores. In Furnas, volcanic activity is still very much alive, with bubbling hot springs, fumaroles, and geysers scattered across the valley. Locals have turned this geothermal energy into tradition by cooking the famous Cozido das Furnas, a hearty stew slow-cooked underground by volcanic steam.

Nature lovers find São Miguel a paradise. The island is covered with endemic vegetation, colorful hydrangeas lining country roads, and tea plantations that are unique in Europe. The Gorreana and Porto Formoso tea estates have been producing black and green tea for over a century, offering a glimpse into the island's agricultural heritage. The climate, mild and humid year-round, allows for an extraordinary variety of plant life, giving São Miguel its characteristic green appearance in every season.



The coastline of São Miguel is equally impressive. Dramatic cliffs rise above the Atlantic, interspersed with natural pools, sandy beaches, and fishing villages that still preserve their charm. Surfers are drawn to Santa Bárbara beach, while others enjoy swimming in the warm, iron-rich waters of Caldeira Velha or relaxing in the oceanfront hot pools of Ferraria, naturally heated by underwater volcanic vents. Whale watching is another highlight, as the waters around the island are one of the best places

in the world to spot both resident and migratory species, from playful dolphins to majestic sperm and blue whales.

Beyond its natural wonders, São Miguel offers a rich cultural experience. The capital, Ponta Delgada, combines modernity with tradition: cobblestone streets, whitewashed churches with black basalt trim, and lively squares filled with cafés and restaurants. Throughout the year, festivals bring the community together, with the Festas do Senhor Santo Cristo dos Milagres being the largest religious celebration in the Azores. The local cuisine is another attraction, featuring fresh seafood, locally grown pineapples, and the signature volcanic-cooked stew.

São Miguel is more than just a beautiful island—it is a place where nature and people live in harmony, shaped by centuries of resilience and connection to the sea. Whether hiking along crater rims, soaking in hot springs, tasting unique teas and wines, or simply enjoying the hospitality of its people, visitors leave with the sense that São Miguel is both timeless and alive.



A word to our sponsors:

We would like to express our deepest gratitude to our sponsors for their invaluable support of this year's UFO conference. Their contributions have not only made this gathering possible, but have also helped create an environment where scientists, students, and industry partners can share their latest discoveries, spark new collaborations, and inspire future directions in the field. The advancement of ultrafast science depends on strong partnerships between academia, industry, and the wider community, and we are truly grateful to our sponsors for recognizing the importance of investing in this endeavor. Their commitment ensures that we can continue to celebrate innovation, nurture the next generation of researchers, and strengthen the global ultrafast optics community.

Gold sponsors





Silver sponsors































Bronze sponsors











Anne L'Huillier, Lund University, Sweden The world of atoms at the attosecond time scale

Abstract: Extreme Ultraviolet light sources based on high-order harmonic generation in gases consist of extremely short light bursts, in the 100-attosecond range, allowing for outstanding temporal resolution. Attosecond pulses enable the study of atoms in an entirely new way. It is now possible to measure tiny time delays in photoionization, the phase change across a resonance, or the quantum state of a photoelectron. This presentation will outline some of the main steps of attosecond science, from the sources to the applications.



About the speaker: Anne L'Huillier is a Swedish/French researcher in attosecond science. She started her career at the

Commissariat à l'Énergie Atomique, in Saclay, France, as a PhD student until 1986, then as a permanent researcher until 1995. She moved to Lund University, Sweden, and became full professor there in 1997. Her research is focused on high-order harmonic generation in gases and its applications, particularly in attosecond science. She was awarded the Nobel Prize in Physics 2023 with Pierre Agostini and Ferenc Krausz "for experimental methods that generate attosecond pulses of light for the study of electron dynamics in matter".

Sponsored by Light Conversion.



Matthias Kling, SLAC, Stanford University, USA Breaking Boundaries: Next-Generation Ultrafast Lasers for Transformative Research



Abstract: Ultrafast laser technology is fundamental to breakthroughs in scientific research, enabling applications that range from probing fundamental atomic processes at the attosecond scale to generating and manipulating bright particle beams. However, many established laser systems are approaching their performance limits, highlighting the need for innovative approaches to enhance capabilities in intensity, wavelength diversity, and high average power. This presentation will outline recent advancements in both table-top and free-electron laser systems and emphasize the required architectures, components, and techniques critical for driving transformative discoveries across

various scientific disciplines.

About the speaker: Matthias Kling is a leading expert in ultrafast science, serving as Professor of Photon Science and Applied Physics (by courtesy) at Stanford University and Director of the Science and R&D Division at the Linac Coherent Light Source (LCLS) at SLAC National Accelerator Laboratory. With a background spanning physics, laser physics, and physical chemistry, he earned degrees from the Universities of Göttingen and Jena before completing postdoctoral research at UC Berkeley and AMOLF in Amsterdam. From 2007 to 2021, he led a research group within the Laboratory of Attosecond Physics at the Max Planck Institute of Quantum Optics and held faculty positions at Kansas State University and the University of Munich. Since joining SLAC and Stanford in 2021, he has been shaping the scientific program at LCLS, advancing cutting-edge research in ultrafast dynamics. Matthias also chaired the 2023 Basic Research Needs Workshop on Laser Technology, contributing to the strategic direction of the field.

Sponsored by Thorlabs.



Invited Speakers

Benjamin Wetzel, XLIM Research Institute - Photonics Department, Limoges, France

Birgitta Bernhardt, Technische Universität Graz, Austria

Carmen Menoni, Colorado State University, USA

Caterina Vozzi, Politecnico di Milano, Italy

Charles Durfee, Colorado School of Mines, USA

Clara Saraceno, Ruhr Universität Bochum, Germany

Christopher Barty, Lumitron/University of California Irvine, USA

Cristina Hernandez-Gomez, Central Laser Facility, STFC, UK

Darko Zibar, Danish Technical University, Copenhagen, Denmark

Derryck T. Reid, Heriot-Watt University, Edinburgh, UK

Jens Biegert, ICFO, Spain

Jinping Yao, Shanghai Institute of Optics and Fine Mechanics, Shanghai, China

John Travers, Heriot-Watt University, Edinburgh, UK

Laura Sinclair, NIST, University of Colorado, USA

Lucia Caspani, Università degli Studi dell'Insubria, Italy

Marc Hanna, Institut d'Optique, Palaiseau, France

Maria Chernysheva, Leibniz Institute of Photonics Technology, Jena, Germany

Ming-Chang Chen, National Tsing Hua University, Taiwan

Pieter Nethling, University of Stellenbosch, South Africa

Regina Gumenyuk, Tampere University, Finland

Tamas Nagy, Max-Born Institute, Berlin, Germany

Zsuzsanna Heiner, Humboldt University, Berlin, Germany



SUNDAY	OCTOBER 5TH
18:00 - 20:30	RECEPTION
MONDAY	OCTOBER 6TH
Session	M1: Novel methods for generating and manipulating ultrashort pulses Chair: Bruno Schmidt
09:15 - 09:45	INVITED M1.1: John C Travers Advances in soliton-driven light sources and their characterisation
09:45 - 10:15	INVITED M1.2: Zsuzsanna Heiner High-repetition-rate 1-µm pumped mid-IR OPAs for interface-specific spectroscopy
10:15 - 10:30	ORAL M1.3: Daniel Walke A 52 W few-cycle OPCPA for soft X-ray generation
10:30 - 10:45	ORAL M1.4: Nikoleta Kotsina Terawatt-scale optical attosecond pulses and 30 GW-scale far-ultraviolet pulses through extreme soliton dynamics
10:45 - 11:15	COFFEE BREAK
Session	M2: Spectral broadening and pulse compression I Chair: Anne-Lise Viotti
11:15 - 11:45	INVITED M2.5: Marc Hanna Multipass cells: multimode behavior and soliton self-frequency shift
11:45 - 12:00	ORAL M2.6: Jonas Manz 10 mJ Compression in Gas-Filled and Bulk-Based Multipass Cells of a kHz Thin-Disk Laser



12:00 - 12:15	ORAL M2.7: Victor Koltalo Yb-based multi-pass cell post-compression scheme reaching 0.6 TW limited by quasi-phase-matched four-wave mixing
12:15 - 12:30	ORAL M2.8: Peer Biesterfeld Towards a New HHG Driver Laser Platform: Post-Compression of Q-Switched Lasers in Multi-Pass Cells
12:30 - 12:45	ORAL M2.9: Ana Silva High-energy, blue shifted 100x spectral broadening from strong space-time focusing in a dispersion-managed hybrid multi-pass cell
12:45 - 14:15	LUNCH + POSTER SESSION 1
Session	M3: Frequency-combs and carrier envelope phase control Chair: Ursula Keller
14:15 - 14:45	INVITED M3.10: Derry T. Reid New technologies for visible to infrared astrocombs
14:45 - 15:00	ORAL M3.11: Muhammad Thariq How to Generate XUV Frequency Combs Without Enhancement Resonators?
15:00 - 15:15	ORAL M3.12: Eric Cormier Generation of sub 100 fs femtosecond pulses with tunable repetition rates up to 1 THz at 1030 nm
15:15 - 15:30	ORAL M3.13: Günter Steinmeyer Gauging Vacuum Fluctuations: Rogue Wave Emergence in Optical Parametric Generation
15:30 - 15:45	ORAL M3.14: Li Zheng Efficient SHG from a Low-noise GHz Yb:CYA femtosecond oscillator
15:45 - 16:15	COFFEE BREAK



Session	M4: Ultrafast Mid-infrared and Terahertz sources Chair: Clara Saraceno
16:15 - 16:45	INVITED M4.15: Maria Chernysheva Advances and challenges of mid-infrared ultrafast all-fibre lasers
16:45 - 17:00	ORAL M4.17: Nadia Berndt Integrated terahertz generation with high spectral brightness
17:00 - 17:15	ORAL M4.18: Caroline Juliano High-power, few-cycle, short-wave infrared source for high-flux, soft X-ray generation at 200 kHz repetition rate
17:15 - 17:30	ORAL M4.19: Ugaitz Elu High-energy self-CEP-stable seeder for a 2.2 μm OPCPA
TUESDAY	OCTOBER 7TH
08:45 - 09:45	PLENARY TALK 1: Matthias Kling Breaking Boundaries: Next-Generation Ultrafast Lasers for Transformative Research
Session	Tu1: Ultrafast spectroscopy and quantum photonics Chair: Günter Steinmeyer
09:45 - 10:15	INVITED Tu1.1: Lucia Caspani Enhanced Entangled Second Harmonic Generation Beyond the Photon Pairs Regime
10:15 - 10:45	INVITED Tu1.2: Jinping Yao Air Lasing: from strong-field molecular physics to ultrafast spectroscopy
10:45 - 11:15	COFFEE BREAK



Session	Tu2: Spectral broadening and pulse compression II Chair: Benjamin Alonso
11:15 - 11:45	INVITED Tu2.3: Tamas Nagy Full characterization of tunable few-fs vacuum ultraviolet pulses
11:45 - 12:00	ORAL Tu2.4: Uwe Griebner Bulk self-compression of millijoule 5 µm pulses to 37 fs in the spatio-temporal soliton regime
12:00 - 12:15	ORAL Tu2.5: Boldizsar Kassai 525-MW peak power, 100-kHz, sub-100 femtosecond Holmium laser at 2.1 µm
12:15 - 12:30	ORAL Tu2.6: Rajaram Shrestha Generation of 1.5-cycle optical pulses with 60 μJ energy at 3.2 μm.
12:30 - 12:45	ORAL Tu2.7: Christian Brahms Ytterbium-laser-driven resonant dispersive emission generating wavelength-tuneable few-femtosecond far-ultraviolet pulses
12:45 - 14:00	LUNCH + POSTER DISPLAY 1
Session	Tu3: High repetition rate sources and dual comb techniques Chair: Derryck T. Reid
Session 14:00 - 14:30	Tu3: High repetition rate sources and dual comb techniques
	Tu3: High repetition rate sources and dual comb techniques Chair: Derryck T. Reid INVITED Tu3.8: Birgitta Bernhardt UV/VIS Frequency Combs for Novel Applications in Dual Comb
14:00 - 14:30	Tu3: High repetition rate sources and dual comb techniques Chair: Derryck T. Reid INVITED Tu3.8: Birgitta Bernhardt UV/VIS Frequency Combs for Novel Applications in Dual Comb Spectroscopy ORAL Tu3.9: Carolin P. Bauer Ultrafast 1-GHz dual-comb optical parametric oscillator from a single
14:00 - 14:30 14:30 - 14:45	Tu3: High repetition rate sources and dual comb techniques Chair: Derryck T. Reid INVITED Tu3.8: Birgitta Bernhardt UV/VIS Frequency Combs for Novel Applications in Dual Comb Spectroscopy ORAL Tu3.9: Carolin P. Bauer Ultrafast 1-GHz dual-comb optical parametric oscillator from a single cavity ORAL Tu3.10: Jiayang Chen Dual-comb Fiber Laser with Dual-phase-biased Nonlinear Amplifying



15:30 - 15:45	ORAL Tu3.13: Andrea Monzani Generation of burst of pulses at 3 µm with widely tunable multi GHz repetition rate
15:45 - 16:15	COFFEE BREAK
Session	Tu4: Ultrafast applications: novel methods and technology I Chair: Sterling Backus
16:15 - 16:45	INVITED Tu4.14: J. Biegert Attosecond technology deciphering a chemical reaction
16:45 - 17:00	ORAL Tu4.15: Samuel Sahel-Schackis Multi-Modal X-ray Probing of Catalytic Activity in Photo-driven Nanosystems
17:00 - 17:15	ORAL Tu4.16: Daniel Santiago Penagos Molina Ångström-scale surface metrology enabled by a compact milliwatt-class HHG source
17:15 - 17:30	ORAL Tu4.17: Peter Dombi Ultrafast Field Sampling Reveals Sub-Cycle Absorption
17:30 - 17:45	ORAL Tu4.18: Martin Kozák Ultrafast valleytronics in bulk crystals
17:45 - 18:00	ORAL Tu4.19: Matteo Clerici Quantum-enhanced THz time-domain sensing
18:00 - 18:30	DRINKS AND APERITIF
18:30 - 20:30	INDUSTRY SESSION



WEDNESDAY	OCTOBER 8TH
Session	W1: Spatio-temporal manipulation and ultrashort pulse characterization Chair: Íñigo Sola
09:00 - 09:30	INVITED W1.1: Charles G. Durfee Spatio-temporal control and characterization for ultrafast nonlinear interactions
09:30 - 09:45	ORAL W1.2: Daniel Díaz Rivas Spatially-dependent group delay dispersion from a grating and its application for single-shot d-scan
09:45 - 10:00	ORAL W1.3: Joleik Nordmann Generation and characterisation of TW-scale sub-fs optical pulses
10:00 - 10:15	ORAL W1.4: Stefan Bock Advanced Laser Pulse Metrology through 2D Self-Referenced Spectral Interferometry
10:15 - 10:30	ORAL W1.5: Benjamín Alonso Visible and NIR optical vortices measured in space-time with BLASHI
10:30 - 10:45	ORAL W1.6: Klaus Steiniger Analytically describing and analyzing spatio-temporal couplings in focusing laser pulses
10:45 - 11:15	COFFEE BREAK + PICTURE
Session	W2: Machine learning and artificial intelligence for ultrafast optics Chair: Geory Genty
11:15 - 11:45	INVITED W2.7: Darko Zibar Advancing the next generation of photonic measurement systems using machine learning
11:45 - 12:15	INVITED W2.8: Benjamin Wetzel Machine learning for the control of ultrafast nonlinear spectral broadening processes



12:15 - 12:30	ORAL W2.9: Utsa Chattopadhyay AI-Driven Design of Ultra-Broadband Dispersive Mirrors
12:30 - 12:45	ORAL W2.10: Francesco Corazza High Harmonic Generation driven Extreme Ultraviolet 0-th order Scatterometry for Nanostructure Characterization
12:45 - 14:00	LUNCH + POSTER SESSION 2
Session	W3: Methods for shaping and measuring ultrashort pulses Chair: Tamas Nagy
14:00 - 14:30	INVITED W3.11: Pieter H Neethling i2PIE for broadband pulse measurement and compression
14:30 - 14:45	ORAL W3.12: Eric Cormier PI-FROSt to reveal driving mechanisms in harmonic generation from solid-state media
14:45 - 15:00	ORAL W3.13: Arno Klenke Detection of pulse-duration fluctuations and drifts with attosecond precision
15:00 - 15:15	ORAL W3.14: Haim Suchowski Shaping Exciton Polarization Dynamics in 2D Semiconductors by Tailored Ultrafast Pulses
15:15 - 15:30	ORAL W3.15: Chen Guo Single-Shot Carrier-Envelope Phase Measurement at 586 kHz Using Optical Fourier-Transform Interferometry
15:30 - 15:45	ORAL W3.16: Miguel Miranda d-scan ultrashort pulse characterization implemented with a 4-f pulse stretcher/compressor
15:45 - 16:15	COFFEE BREAK



Session	W4: Ultrahigh peak-power laser systems and related technologies Chair: Charles Durfee
16:15 - 16:45	INVITED W4.17: Cristina Hernandez-Gomez Progress on the commissioning of 10 Hz Petawatt beamline at the Extreme Photonics Applications Centre
16:45 - 17:00	ORAL W4.18: Samy Ferhat Picosecond contrast improvement for PW class lasers based on modified stretcher design
17:00 - 17:15	ORAL W4.19: Jan Heye Buss Advancing Short-Pulse Laser Drivers for Fusion Applications
17:15 - 17:45	INVITED W4.20: Carmen S. Menoni Multilayer dielectric coatings for ultrahigh intensity lasers and their challenges to achieve long term operation without damage
17:45 - 18:00	ORAL W4.21: Adeline Kabacinski Toward 100Hz Joule class ultra-short pulses TiSa laser
18:00 - 18:15	ORAL W4.22: Roland S. Nagymihály Towards a sub-10 fs hybrid frontend with $>10^{14}$ temporal contrast for high intensity lasers
THURSDAY	OCTOBER 9TH
08:45 - 09:45	PLENARY TALK 2: Anne L'Huillier The world of atoms at the attosecond time scale
Session	Th1: Attosecond science and pulse generation I Chair: Emma Springate
09:45 - 10:15	INVITED Th1.1: Caterina Vozzi Innovative Microfluidic Sources for XUV and Soft-X Ray Generation
10:15 - 10:30	ORAL Th1.2: Robert Klas Intrinsic Limits to Achieving Application-Relevant Soft X-ray Flux in High Harmonic Generation



10:30 - 10:45	ORAL Th1.3: Antoine Cavagna Continuous Relativistic High-Harmonic Generation from a Liquid-Leaf Plasma Mirror at kHz Repetition Rate
10:45 - 11:15	COFFEE BREAK
Session	Th2: Attosecond science and pulse generation II Chair: Rodrigo Lopez-Martens
11:15 - 11:45	INVITED Th2.4: Ming-Chang Chen Bright Isolated Attosecond Pulses from Post-Compressed Yb Laser Filaments
11:45 - 12:00	ORAL Th2.5: Melvin Redon Low-Divergence Harmonic Generation with Hollow Gaussian Beams for Compact, High-Intensity Attosecond Sources
12:00 - 12:15	ORAL Th2.6: Rodrigo Martin-Hernandez Synthesis of isolated attosecond extreme-ultraviolet spatiotemporal optical vortices via high-order harmonic generation
12:15 - 12:30	ORAL Th2.7: Rafael De Queiroz Garcia On-demand isolated attosecond pulses: the optimal in-situ and in silico tailored waveforms
12:30 - 12:45	ORAL Th2.8: Lauren Drescher All-attosecond transient reflection spectroscopy
12:45 - 13:00	ORAL Th2.9: Marta Arias Velasco Sub-20-fs UV Pump – XUV Probe Beamline for Ultrafast Molecular Spectroscopy
13:00 - 14:00	LUNCH + POSTER DISPLAY 2
14:00 - 18:30	EXCURSION Whale and Dolphin Watching Tour – Vila Franca do Campo, Azores



19:30 - 22:30	CONFERENCE BANQUET
FRIDAY	OCTOBER 10TH
Session	F1: High average power ultrafast lasers, Coherent beam combining Chair: Thomas Metzger
09:00 - 09:30	INVITED F1.1: Regina Gumenyuk Compact yet mighty: tapered double-clad amplifiers for picosecond pulses
09:30 - 09:45	ORAL F1.2: Tobias Witting 44 W, 100 kHz, 2.5-cycle pulses from a flat-top pumped OPCPA
09:45 - 10:00	ORAL F1.3: Maksym Ivanov Pulse compression of 300W, 12mJ with 83% transmission in hollow-core fiber
10:00 - 10:15	ORAL F1.4: Lauren Cooper Tailored Ultrashort Pulse Bursts in a Gain-Managed Nonlinear Fiber Amplifier for Coherent 50fs Pulse Stacking at mJ Energies
10:15 - 10:30	ORAL F1.5: Sergei Tomilov Energy Scaling of Kerr-Lens Modelocked Ho:YAG Thin-Disk Oscillators to the Microjoule Level
10:30 - 10:45	ORAL F1.6: Zhiyi Wei High Power Kilohertz Thin Disk Amplifier with 600mJ Pulse Energy Developed for OPCPA
10:45 - 11:15	COFFEE BREAK



Session	F2: Ultrafast applications: novel methods and technology II Chair: Jan Rothhardt
11:15 - 11:45	INVITED F2.7: Clara Saraceno High average power Terahertz time-domain systems
11:45 - 12:00	ORAL F2.8: Malte Schroeder Extended Length Femtosecond Laser Filamentation via High Repetition Rate Effects
12:00 - 12:15	ORAL F2.9: Hollie Wright Two-Photon Dual-Comb LiDAR Imaging
12:15 - 12:30	ORAL F2.10: Yuk Shan Cheng Offset tunable 650–1050 nm astrocomb
12:30 - 14:00	LUNCH + STEERING COMMITTEE MEETING
Session	F3: Ultrafast applications: novel methods and technology III Chair: Caterina Vozzi
14:00 - 14:15	ORAL F3.11: Jeffrey Moses A Simple, Multi-Channel Architecture for 10-fs Spectroscopy Covering Visible to Mid-IR
14:15 - 14:30	ORAL F3.12: Margarita Khokhlova Chiral optical tweezers – efficient enantioseparation of molecules
14:30 - 14:45	ORAL F3.13: Leona Licht HHG-Based Lensless Imaging: Unique Insights into Material and Life Sciences
14:45 - 15:00	ORAL F3.14: Kevin Murzyn Ultrafast Imaging Below the Diffraction Limit with High Harmonic Deactivation Microscopy
15:00 - 15:15	ORAL F3.15: Arash Aghigh Tunable Femtosecond Source Based on Spatiotemporal Nonlinear Enhancement



15:15 - 15:45	COFFEE BREAK
Session	F4: Ultrafast optics with x-rays and electrons Chair: John Travers
15:45 - 16:15	INVITED F4.16: C. P. J. Barty Distributed Charge Compton Sources & Applications
16:15 - 16:30	ORAL F4.17: Maximilian Benner High flux femtosecond fiber laser driven hard X-ray source
16:30 - 16:45	ORAL F4.18: Daniel Lesko Optical control of electrons in a Floquet topological insulator
16:45 - 17:00	ORAL F4.19: Robert Carley A soft X-ray timing tool based on spintronic THz emission
17:00 - 17:15	ORAL F4.20: Jack Hirschman Linking Adaptable and Optimized Ultrafast Photoemission to Brighter X-rays
17:15 - 17:45	CONFERENCE CLOSURE

Monday October 6th

Advances in soliton-driven light sources and their characterisation

John C Travers, Nikoleta Kotsina, Michael Heynck, Joleik Nordmann, Teodora Grigorova, Deepjyoti Satpathy, Mohammed Sabbah, Martin Gebhardt, and Christian Brahms
School of Engineering and Physical Sciences, Heriot-Watt University, Edinburgh, EH14 4AS, United Kingdom
*j.travers@hw.ac.uk

Abstract

We will provide a perspective on the latest advances in soliton-driven light sources, their characterisation, their applications, and their future direction. Highlights include high-energy few-cycle pulses across the far ultraviolet, field-resolved measurements of optical attosecond pulses at the terawatt scale, miniaturised sources with compact pump lasers, and a plethora of application demonstrations.

Harnessing optical soliton dynamics in gas-filled hollow-core fibres has enabled a new class of ultrafast light source [1]. The two foundational techniques are the generation of optical attosecond pulses through soliton-effect self-compression, and the generation of few-cycle pulses tuneable across the vacuum, deep ultraviolet, and visible, through resonant dispersive-wave emission from solitons. Over the last decade, both of these techniques have been significantly advanced, with major milestones including the demonstration of soliton dynamics at high energy in hollow capillaries [2, 3], the characterisation of sub-3 fs pulses across the ultraviolet and visible [4, 5, 6, 7, 8, 9], field-resolved measurements of self-compressed optical attosecond pulses [7, 8, 10], and a range of applications in ultrafast spectroscopy and photoelectron imaging [11, 12, 13, 14, 15]. It is noticeable that many of these advances occurred in just the last few years.

While soliton-driven light-sources can already address several of the most pressing technology gaps in ultrafast science—chief among them extreme (few-cycle or better) temporal resolution across the vacuum ultraviolet, visible and near-infrared spectral region—there remain multiple important challenges. First, characterising and modelling such extreme pulse durations is difficult, and we will present a new approach to frequency-resolved optical gating pulse retrieval that helps with this, along with tests of the accuracy of our modelling tools. Second, the majority of work so far has been with simple polarisation states (linear, circular), while more exotic states are interesting for wide-ranging applications [16]. Third, the use of soliton-driven light sources to drive secondary sources of radiation is a developing area, enabled by a new regime of high peak power RDW emission in the ultraviolet [8] and visible [17]. Fourth, raising the repetition-rate, and moving to more industrialised ytterbium-laser architectures, are key to maximising usability and applications [18, 19]. Fifth, routes to even shorter ultraviolet pulses are being explored [20]. Finally, shrinking soliton-driven light sources to a much more compact form-factor, will enable applications outside of ultrafast laser laboratories [21]. We will provide a perspective on all of these directions.

- [1] J. C. Travers, Opt. Commun. **555**, 130191 (2024).
- [2] J. C. Travers et al., Nat. Photonics 13, 547–554 (2019).
- [3] C. Brahms et al., Phys. Rev. Res. 2, 043037 (2020).
- [4] C. Brahms et al., Opt. Lett. 44, 731-734 (2019).
- [5] M. Reduzzi et al., Opt. Express 31, 26854–26864 (2023).
- [6] J. R. C. Andrade et al., ArXiv:2411.11769 (2024).
- [7] A. M. Heinzerling et al., Nat. Photonics 19, 772-777 (2025).
- [8] N. Kotsina et al., "Terawatt-scale optical attosecond pulses and 30 GW-scale far-ultraviolet pulses through extreme soliton dynamics," Ultrafast Opt. XIV (2025).
- $[9]\ \ \, {\rm K.\ A.\ Larsen}\ \, et\ \, al.,\, {\rm Opt.\ Lett.}\ \, {\bf 50}\ \, 4962\text{--}4965\ \, (2025).$
- [10] J. Nordmann, et al., "Generation and characterisation of TW-scale sub-fs optical pulses," Ultrafast Opt. XIV (2025).
- [11] H. Bromberger et al., Appl. Phys. Lett. 107, 091101 (2015).
- [12] N. Kotsina et al., The J. Phys. Chem. Lett. 10, 715-720 (2019).
- [13] N. Kotsina et al., Chem. Sci. 13, 9586-9594 (2022).
- [14] J. P. Lee et al., Optica 11, 1320-1323 (2024).
- [15] C. Brahms et al., Nat. Commun. 16, 3714 (2025).
- [16] M. Heynck et al. "Generation of multi-octave millijoule-level radial vector beams," Ultrafast Opt. XIV (2025).
- [17] M. Gebhardt et al. "Generation of multi-GW, sub-10 fs tuneable visible pulses," Ultrafast Opt. XIV (2025).
- [18] C. Brahms *et al.* "Ytterbium-laser-driven resonant dispersive emission generating wavelength-tuneable few-femtosecond far-ultraviolet pulses," Ultrafast Opt. XIV (2025).
- [19] L. Silletti et al., APL Photonics 10, 070801 (2025).
- [20] M. F. Galán et al. "Tunable sub-2 fs ultraviolet pulse generation," Ultrafast Opt. XIV (2025).
- [21] M. Sabbah et al., Optica ${f 12}$, 728–731 (2025).

High-repetition-rate 1-µm pumped mid-IR OPAs for interface-specific spectroscopy

Zsuzsanna Heiner, 1,2,* Valentin Petrov³ and Mark Mero³

³Max-Born-Institut, Max-Born-Straße 2 A, 12489 Berlin, Germany **<u>zsuzsanna.heiner@hu-berlin.de</u>

Abstract

We demonstrate efficient broadband mid-infrared generation using wide-bandgap sulfur-based crystals in supercontinuum-seeded few-cycle OPAs, achieving μ J-level output up to 13 μ m. Building on this, we present the first MHz-repetition-rate broadband VSFG spectrometer, enabling ultrafast, interface-sensitive microscopy of 2D and hybrid materials with unprecedented sensitivity, resolution, and spectral coverage.

Results and Discussion

Many fundamental processes in chemistry and biology are governed by interactions at surfaces and interfaces. Vibrational sum-frequency generation (VSFG) spectroscopy is a powerful, non-invasive, and intrinsically surfacespecific technique that provides direct insight into interfacial molecular structure and dynamics. Conventional broadband VSFG systems, however, are limited by spectral resolution, acquisition speed, and inefficient midinfrared pulse generation, restricting their use in real-time or in situ studies of complex interfaces and macromolecular assemblies. Recent advances in nonlinear optical materials now allow highly efficient generation of broadband, few-cycle mid-infrared pulses in the molecular fingerprint region. Wide-bandgap sulfur-based crystals such as LiGaS₂, BaGa₄S₇, and Cd_xHg_{1-x}Ga₂S₄ combine superior transparency and damage thresholds with scalability, enabling stable, high-energy sources beyond 6 µm. Using supercontinuum-seeded few-cycle OPAs pumped by a 100-kHz Yb laser, we directly compared these crystals, demonstrating µJ-level MIR output, fewcycle pulse durations, and overall efficiencies far surpassing cascaded OPA/DFG schemes (Fig. 1a). The generated MIR output covers the important molecular fingerprint region up to 13 µm (Fig. 1b), with high quantum efficiency in a compact configuration [1,2]. Building on these advances, we now report the construction of the first MHzrepetition-rate broadband VSFG spectrometer, delivering ultrabroadband mid-infrared spectra across the fingerprint region (Fig. 1c). Designed for interface-sensitive microscopy, this system addresses the demands of ultrafast studies in 2D and hybrid materials, including electron transfer at surfaces and interfaces. Its compact design, broad spectral coverage, and high repetition rate provide powerful new opportunities for probing interfacial chemistry and structure with unprecedented temporal and molecular resolution.

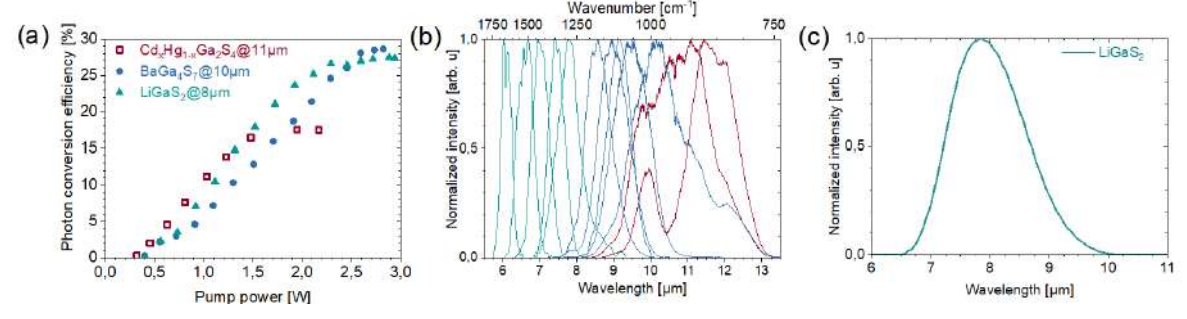


Figure 1: Comparison of photon conversion efficiencies (a) and spectral tunability (b) of sulfur crystal-based 100-kHz OPAs. (c) Mid-infrared spectrum from the 1.33 MHz OPA driving the VSFG spectrometer.

References

[1] Z. Heiner, V. Petrov, V.L. Panyutin, et al. "Efficient generation of few-cycle pulses beyond 10 µm from an optical parametric amplifier pumped by a 1-µm laser system," Scientific Reports 12, 5082 (2022).

[2] Z. Heiner, A. Der, V. Petrov, M. Mero, "Nonlinear vibrational spectrometer for bioapplications featuring narrowband 1-µm pulses and a recycled OPA pump beam", Optics Express **32**, 45029-45040 (2024).

¹Department of Chemistry, Humboldt-Universität zu Berlin, Brook-Taylor-Str. 2, 12489 Berlin, Germany ²School of Analytical Sciences Adlershof (SALSA), Humboldt-Universität zu Berlin, Albert-Einstein-Str. 5-9, 12489 Berlin, Germany

A 52 W few-cycle OPCPA for soft X-ray generation

Daniel Walke,^{1,*}Azize Koç,¹ Florian Gores,¹ Minjie Zhan,² Nicolas Forget,³ Raman Maksimenka³ and Iain Wilkinson¹

Abstract

We present a high-average-power (52 W), few-cycle, CEP stable, short-wave infrared (2.1 µm central wavelength) optical parametric chirped pulse amplifier. This system is applied to generate soft x-rays in helium, resulting in a low-divergence broadband soft x-ray emission extending beyond 600 eV.

The latest generation of kW-class, picosecond pulse duration lasers are ideal pump sources for optical parametric chirped pulse amplifiers (OPCPA). In combination, these technologies offer a route to ultrashort (i.e. few-optical-cycle), carrier-envelope-phase (CEP) stable pulses at high average power levels in the short-wave infrared (SWIR, $\sim 1.4 - 3.0 \,\mu m$) spectral region. Although highly desirable as drivers for soft x-ray (SXR, $\sim 0.1 - 1 \,keV$) generation, there are only a handful of reports of such high-average power SWIR-OPCPAs. [1,2]

We have developed a high-average-power (52 W in the amplified signal), CEP stable, SWIR-OPCPA generating pulses of 20 fs duration [3]. In the first tests, the pulses were focused to an intensity of \sim 7 x 10^{14} W/cm² in a high-pressure helium gas cell, yielding a low-divergence (< 2 mrad half-angle) broadband SXR emission extending beyond 600 eV. The on-target SWIR power of 45 W represents the highest average-power SXR driver to date.

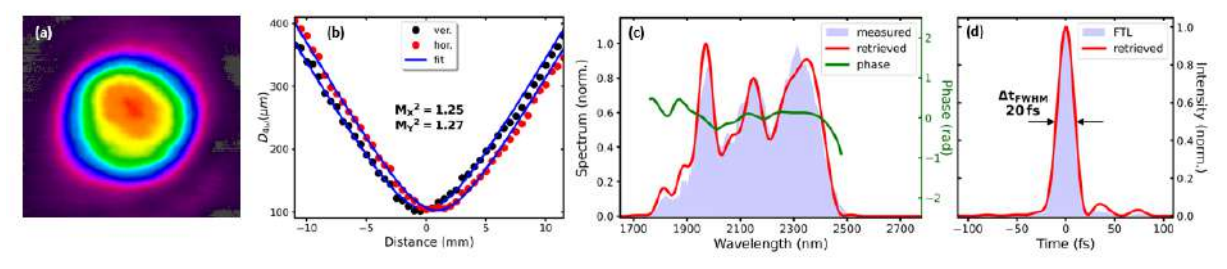


Figure 1: Spatial, spectral and temporal characterization of the OPCPA output: (a) beam profile before focusing. b) M² measurement (c) spectrum and spectral phase (d) temporal profile.

The OPCPA pump source is 465 W from a Yb:YAG thin-disk amplifier that outputs 1.03 μ m, 850 fs pulses at 52.6 kHz repetition rate. The OPCPA is split into two parts; a commercial 'front-end' OPCPA, that incorporates an acousto-optic programmable dispersive filter, and a high-power 'booster' OPCPA. In the high-power booster, 100 μ J, passively CEP stable (160 mrad rms, single-shot) SWIR pulses are amplified to ~ 1 mJ in two OPCPA stages based on lithium niobate (LN), which was chosen for its high parametric figure of merit, broadband phase-matching and transparency at 2.1 μ m. This architecture supports high quantum efficiencies of 30% and 25% in the first and second stage respectively. Mitigating potentially deleterious processes induced by the high peak intensities and average powers of the pump and signal beams was crucial in achieving optimal on-target beam characteristics (see Fig. 1). An M^2 < 1.3 in both axes was determined with a scanning slit profiler (Fig. 1b). After compression in bulk IR-fused silica, the temporal profile and spectral phase was measured with self-referenced spectral interferometry (Fig. 1c & d)). The pulse-to-pulse energy fluctuations were measured to be ~ 1%.

Current work focuses on the amplified-pulse CEP stability (presently ~ 600 mrad rms, single-shot) and optimization of the SXR yield. Given its state-of-the-art performance, this system will empower further growth of laser-based sources as key tools for element-specific interrogations of ultrafast electronic-structure dynamics.

References

[1] M. F. Seeger, D. Kammerer, J. Blöchl, et al., "49 W carrier-envelope-phase-stable few-cycle 2.1 μm OPCPA at 10 kHz," Opt. Express 31(15), 24821 (2023).

[2] J. H. Buss, S. Starosielec, M. Schulz, et al., "Mid-infrared optical parametric chirped-pulse amplifier at 50 W and 38 fs pumped by a high-power Yb-InnoSlab platform," Opt. Express 32(21), 36185–36192 (2024).

[3] D. Walke, A. Koç, F. Gores, M. Zhan, N. Forget, R. Maksimenka, and I. Wilkinson, "High-average-power, few-cycle, 2.1 µm OPCPA laser driver for soft-X-ray high-harmonic generation," Opt. Express 33, 10006-10019 (2025).

¹ Helmholtz-Zentrum Berlin für Materialien und Energie GmbH, Hahn-Meitner-Platz 1, 14109 Berlin, Germany

² Ultrafast Innovations GmbH, Dieselstr. 5, 85748 Garching (Munich), Germany

³ FASTLITE, 165 rue des Cistes, 06600 Antibes, France

^{*}daniel.walke@helmholtz-berlin.de

△ UFO XIV Azores 2025

Terawatt-scale optical attosecond pulses and 30 GW-scale far-ultraviolet pulses through extreme soliton dynamics

Nikoleta Kotsina¹, Michael Heynck¹, Joleik Nordmann¹, Martin Gebhardt¹, Teodora Grigorova¹, Christian Brahms¹, and John C Travers^{1,*}

¹School of Engineering and Physical Sciences, Heriot-Watt University, Edinburgh, EH14 4AS, United Kingdom *i.travers@hw.ac.uk

Abstract

We describe the XSOL (Extreme Soliton) beamline designed to up-scale soliton dynamics, delivering new drivers for strong-field physics. We have generated and characterised terawatt-scale sub-femtosecond self-compressed pulses and sub-3 fs deep ultraviolet pulses with greater than $170\,\mu\mathrm{J}$ energy through resonant dispersive-wave emission. Tunability to $140\,\mathrm{nm}$ has been achieved.

Optical soliton dynamics in gas-filled hollow capillaries enable extreme pulse self-compression in the visible-infrared

region and efficient, tuneable, few-femtosecond pulse generation in the deep and vacuum ultraviolet (DUV/VUV) through resonant dispersive-wave emission (RDW) [1]. This technique is scalable in peak power and energy by adjusting the fibre core size and length. The first demonstration achieved 40 GW peak power, 1.2 fs self-compressed pulses, and tuneable DUV/VUV generation with tens of µJ energy. Similar experiments have shown that few-µJ DUV RDW pulses can have a sub-3 fs pulse duration [2]. Here we describe our new XSOL (Extreme Soliton) beamline that has been designed to up-scale soliton dynamics, delivering a more than ten-fold peak power and energy upgrade. We utilise three stretched capillary fibres (4.7 m long, 530 µm core diameter) as illustrated in Fig. 1(a). The first two stages pre-compress 40 fs input pulses through spectral broadening and phase compensation with chirped mirrors to obtain 5.5 fs, ~3 mJ pulses with the option for pre-pulse contrast enhancement. The third stage is for the soliton dynamics. The input and output of all three fibre stages are maintained in large vacuum chambers to avoid free-space nonlinearity and ionisation, and to manage the low-divergence high-fluence beams emerging from larger core fibres. The helium gas used in all three stages is injected by side ports along the fibre length.

We have achieved self-compression to 0.77 fs (envelope full-width at half-maximum), multi-mJ pulses, corresponding to terrawatt-class peak power (Fig. 1(b)), characterised using an in-vacuum TIPTOE setup. Driving RDW emission yields tuneable deep-ultraviolet pulses with energy exceeding 170 µJ. We measured a DUV pulse duration shorter than 3 fs with an in-vacuum TG-FROG—Fig. 1(c). These DUV pulses exceed the 30 GW peak power level. Extended tuneability down to 140 nm (Fig. 1(d)) has also been obtained, with full vacuum-ultraviolet energy and temporal characterisation in progress. Our next goal is to utilise these extreme pulses for strong-field physics experiments.

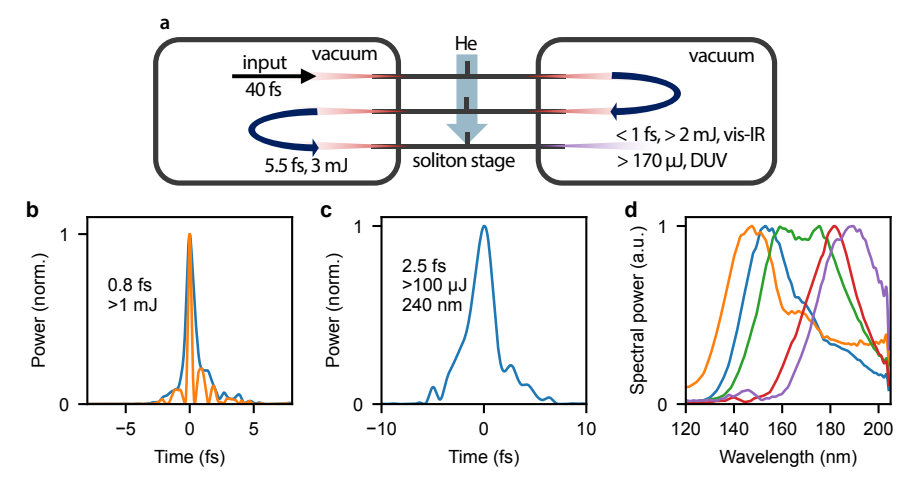


Figure 1: (a) Experimental setup used for extreme soliton dynamics. (b) Measured sub-femtosecond TW-scale pulse. (c) Measured sub-3 fs RDW at 240 nm. (d) Pressure-tuned VUV generation.

References

[1] J C Travers et al., Nat. Phot. 13, 547 (2019).

[2] M Reduzzi et al., Opt. Express 31, 26854 (2023).

Multipass cells: multimode behavior and soliton self-frequency shift

Marc Hanna¹, Giovanni Cichelli², Gautier Parize^{1,3}, Ania Ierano^{1,3}, Michele Natile³, Xavier Délen¹, Paolo Laporta², Nicola Coluccelli², and Patrick Georges¹

Abstract

In a first part, we describe how higher-order Laguerre-Gaussian modes and multimode beams propagate in nonlinear multipass cells, and how this could be used to scale the energy of post-compression setups. In a second part, an experimental effort aiming at observing soliton self-frequency shift inside a multipass cell is reported.

Multipass cells (MPCs) have become an important platform to implement subsystems based on nonlinear optics in recent years, particularly for temporal compression of femtosecond pulses. In this contribution, we will describe some recent development on the physics of nonlinear MPCs.

In a first part [1], we describe the propagation of higher-order Laguerre-Gaussian modes in MPCs, and how the presence of nonlinearity induces or not energy coupling between the modes. Our findings indicate that single higher-order modes are stable upon nonlinear propagation, which could provide an interesting avenue to scale the energy of compression setups while keeping the size of these setups reasonable.

In a second part [2], we report on an experiment that combines negative dispersion mirrors and propagation in a molecular gas to observe soliton self-frequency shift for the first time in a MPC. Using 130 μ J 24 fs pulses at a central wavelength of 1030 nm at the input of a nitrogen-filled MPC, we demonstrate the generation of Fourier transform-limited pulses with a central wavelength around 1100 nm and peak power up to 0.5 GW.

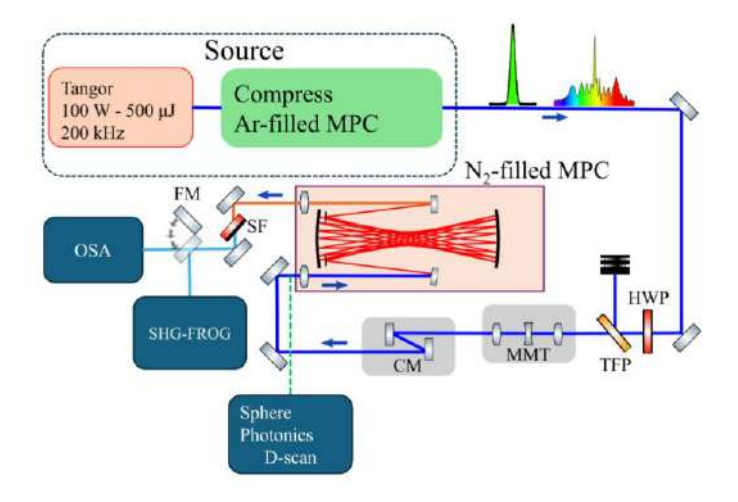


Figure 1: Experimental setup for the soliton self-frequency shift experiment.

References

[1] Marc Hanna, Michele Natile, Florent Guichard, Gautier Parize, Xavier Délen, and Patrick Georges, "Higher-order-and multimode properties of nonlinear multipass cells for temporal compression," J. Opt. Soc. Am. B 42, 631-638 (2025). [2] Giovanni Cichelli, Gautier Parize, Michele Natile, Xavier Délen, Florent Guichard, Paolo Laporta, Nicola Colucelli, Marc Hanna, and Patrick Georges, "High-energy soliton frequency shifting in a nitrogen-filled multipass cell", submitted (2025).

¹Université Paris-Saclay, Institut d'Optique Graduate School, CNRS, Laboratoire Charles Fabry, 91127 Palaiseau, France

²Department of Physics, Politecnico di Milano, Piazza Leonardo da Vinci, 32 - 20133 Milano, Italy

³Amplitude, 11 Avenue de Canteranne, Cité de la Photonique, 33600 Pessac, France

^{*}marc.hanna@institutoptique.fr

10 mJ Compression in Gas-Filled and Bulk-Based Multipass Cells of a kHz Thin-Disk Laser

Jonas Manz,^{1,2*} Gaia Barbiero,¹ Sandro Klingebiel,¹ Michael Rampp,¹ Catherine Y. Teisset,¹ Haochuan Wang,¹ Dominik Ertel,¹ Ronak N. Shah,¹ Martin Hoffmann,² Clara J. Saraceno,² and Thomas Metzger¹

¹TRUMPF Scientific Lasers GmbH + Co. KG, Feringastr. 10a, 85774 Unterföhring, Germany ²Ruhr University Bochum, Universitätstrasse 150, 44801 Bochum, Germany ^{*}jonas.manz@trumpf.com

Abstract

We present spectral broadening experiments for 10 mJ, 50 W pulses of a Yb-doped thin-disk amplifier using a gas- and bulk-based multipass cell setup. Compressability to sub-40 fs and sub-50 fs pulse duration is shown for the gaseous and solid approach, respectively.

Experimental description

To overcome the bandwidth limitation of Yb-doped amplifiers [1], gas-filled multipass cells (MPC) have prevailed in the last years for high energy and average power nonlinear pulse compression systems [2]. However, their energy scaling is constrained by the need for longer cell lengths to prevent gas ionization and mirror damage. Replacing the nonlinear medium to bulk material positioned away from the focus allows for a shorter cell length, since ionization can be neglected. Here we demonstrate the efficient generation of sub-50 fs pulses inside a gas-filled MPC and a bulk-based MPC. Reaching up to 10 mJ, this is the highest pulse energy achieved in a bulk-based MPC confirming the potential of the latter approach for increasing peak power in a compact setup.

We use a commercial DIRA 1000-5 from TRUMPF Scientific Lasers as a seed. This 200-mJ thin-disk amplifier system delivers 1 kW of average power with sub-500 fs pulse duration and M² value < 1.2 [1]. In these experiments we limit the output to 10 mJ and 50 W. First, we implement a state-of-the-art gas-filled MPC with a mirror separation distance of ~2 m. The pulses are spectrally broadened using argon along the 25 passes inside the MPC. The output pulses are attenuated to ~8% of the pulse energy and temporally compressed to ~34 fs after 11 bounces on chirped mirrors with -250 fs² group delay dispersion (GDD) each. The post compression reaches an overall optical efficiency of 97% while preserving the beam quality $M^2 < 1.3$. The setup (Fig. 1a) is then slightly modified by placing thin fused silica plates as nonlinear media in front of the MPC mirrors and operating the chamber in vacuum. Given that the nonlinear interaction per pass is limited in bulk media when compared to gas, a double pass configuration is implemented to achieve comparable broadening [3,4]. The beam is reflected from an end mirror back through the MPC under a small angle. On its return, the beam is picked off by a scraper mirror and coupled out. In this configuration, a total of 106 passes through 0.8 mm thick fused silica plates are achieved. The output pulses are attenuated and temporally compressed to 49.5 fs (Fig. 1b), using 24 reflections on chirped mirrors introducing a total GDD of -6000 fs2. The nonlinear pulse compression scheme exhibits an optical efficiency of 83.5% with a minimally deteriorated beam quality of $M^2 < 1.5$. In a next step we aim to reduce the footprint of our 200 mJ MPC (Herz 200) and demonstrate pulse energy scaling in a bulk-based MPC to 200 mJ.

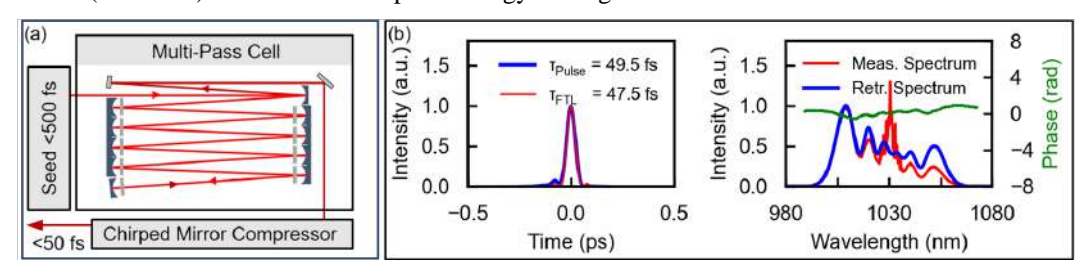


Fig. 1: (a) Schematic of the bulk-based nonlinear pulse compression setup. (b) Temporal and spectral analysis of the compressed output pulses using a second-harmonic frequency resolved optical gating (SH-FROG).

Acknowledgement: The project is funded by the German Federal Ministry of Education and Research (BMBF) under the funding code 13N16652. The responsibility for the content of this publication lies with the author.

- [1] C. Wandt, et al., OSA Technical Digest (Optica Publishing Group, 2020), paper HM2B.4.
- [2] Y. Pfaff, et al., Opt. Express **31**, 22740–22756 (2023).
- [3] A.-L. Viotti et al., Optica 9, 197-216 (2022).
- [4] M. Hanna et al., OSA Continuum 4, 732-738 (2021).

Yb-based multi-pass cell post-compression scheme reaching 0.6 TW limited by quasi-phase-matched four-wave mixing

Victor Koltalo,^{1,*} Louis Daniault,¹ Cédric Sire,² François Sylla,² and Rodrigo Lopez-Martens¹

Abstract

We show the implementation of a 4 m-long multi-pass cell (MPC) that increases the peak power of a kHz Ytterbium (Yb) laser up to 0.6 TW (21 fs, 15.9 mJ). We experimentally show that the main factor limiting post-compression down to shorter pulses is quasi-phase-matched four-wave mixing.

Main Text

There is currently a strong push towards Yb-based lasers, as they are more compact, deliver higher average power and exhibit much higher wall-plug efficiency than the conventional Ti:Sa systems, making experimental value chains more efficient and sustainable. To compensate for the long pulse duration from such lasers, we designed a MPC [1] post-compression setup tailored to a 18.1 mJ, 350 fs commercial Yb-based laser system (MAGMA 25, Amplitude), operating at 1 kHz repetition rate, in order to achieve compression around 20 fs with more than 15 mJ output energy. The 4 m-long MPC is implemented using a classical Herriott pattern with a total of 30 passes through 310 mbar of argon (Fig. 1 a)), leading to a transmission above 97 %. The pulses are compressed at full energy under vacuum using a dispersive mirror compressor, which allows a compression down to 21 fs (measured using TIPTOE) (Fig. 1 b)) and a spectral bandwidth of 150 nm (Fig. 1 c)). The total transmission of the setup is 88%, leading to a usable energy of 15.9 mJ and a peak power of 0.6 TW. The push towards larger spectral broadening factors is limited by quasiphase-matched four-wave mixing (FWM), as shown theoretically in [2]. We measured the spectra of FWM-induced idler and signal through leaks of the MPC end mirrors (Fig. 1 d)), showing that FWM appears alongside a decrease in MPC transmission (Fig. 1 e)).

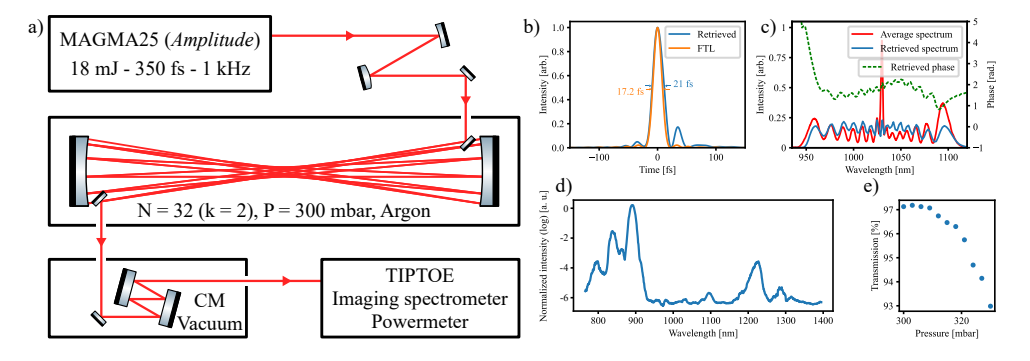


Figure 1: a) Experimental setup (CM = Chirped mirrors). b) Reconstructed pulse and FTL. c) Measured and retrieved spectra (solid lines), reconstructed spectral phase (dashed line). d) Spectral content leaked through the MPC mirror at P = 330 mbar. e) Transmission of the MPC as a function of the argon pressure.

- [1] A.-L. Viotti et al., "Multi-pass cells for post-compression of ultrashort laser pulses," Optica 9, 197–216 (2022).
- [2] M. Hanna et al., "Hybrid pulse propagation model and quasi-phase-matched four-wave mixing in multipass cells", JOSAB 37, 2982-2988 (2020).

¹Laboratoire d'Optique Appliquée (LOA), Institut Polytechnique de Paris, ENSTA Paris - CNRS - Ecole Polytechnique, 91120 Palaiseau, France

²SourceLAB, 7 rue de la Croix Martre, Palaiseau 91120, France

 $^{^*}$ victor.koltalo@ensta.fr

Towards a New HHG Driver Laser Platform: Post-Compression of Q-Switched Lasers in Multi-Pass Cells

Peer Biesterfeld^{1,*}, Marc Seitz², Arthur Schönberg², Nayla Jimenez², Prannay Balla², Sven Fröhlich¹, Philip Mosel¹, Lutz Winkelmann², Tino Lang², Marcus Seidel^{2,4,5}, Ingmar Hartl², Francesca Calegari^{2,3}, Uwe Morgner¹, Milutin Kovacev¹, Christoph M. Heyl^{2,4,5} and Andrea Trabattoni^{1,2}

Abstract

We demonstrate post-compression of 0.5ns pulses to 24ps in a bulk-rod multi-pass cell. This novel approach overcomes limitations of previous post-compression approaches in the nanosecond region, representing a very promising method for reaching the parameter regime of mode-locked lasers using compact Q-switched laser sources.

The generation of high peak power laser pulses is essential to drive non-linear processes in numerous applications e.g. high-harmonic generation (HHG) [1]. The application of Q-switched laser technology, which provides a compact, robust and cost-effective setup, is appealing. However achievable peak powers are limited by their typical pulse durations in the pico- to nanosecond-region. SPM-based compression in multi-pass cells (MPCs) has emerged as a standard method in the pico- to femtosecond regime in recent years [2]. In this work, we demonstrate the adaptation of MPC technology to Q-switched lasers, showing the potential to obtain the required peak powers.

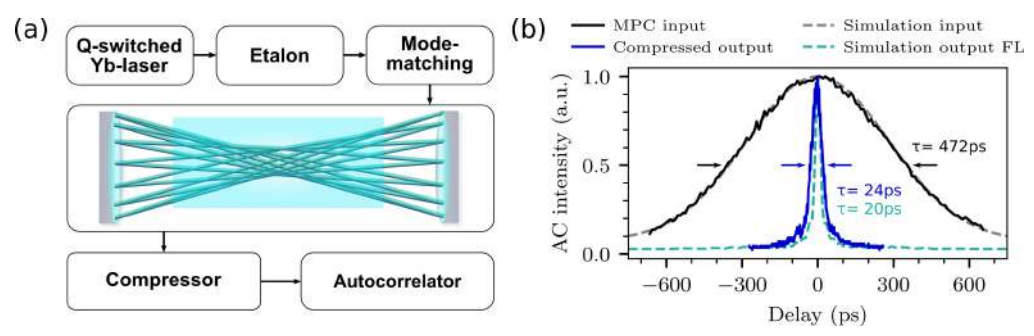


Figure 1: Schematic of the experimental setup (a). Autocorrelation measurements of the MPC input and the compressed output pulses, compared to simulation results (b).

For our experiments, we employ a Q-switched laser source and a Herriot-type MPC using a 10cm fused silica (FS) rod as non-linear medium. The pulses are spectrally broadened via 62 passes in the FS-rod, compressed in a transmission grating compressor and then characterized in an autocorrelator, resulting in a temporal compression factor of 20 (Fig. 1(b)). Based on the experimental results, we investigate the scalability of the concept using simulations and show the potential to achieve temporal compression factors up to two orders of magnitude. With this, we believe that the method shows great potential to achieve high peak power radiation using Q-switched lasers. In particular, we envision our technology to enable Q-switched lasers to be used as direct drivers for HHG sources.

- [1] E. Appi et al., "Synchronized beamline at flash2 based on high-order harmonic generation for two-color dynamics studies", Rev. Sci. Instruments 92, 123004 (2021)
- [2] A.-L. Viotti et al., "Multi-pass cells for post-compression of ultrashort laser pulses", Optica 9, 197-216 (2022)

¹Leibniz University Hannover, Institute of Quantum Optics, Welfengarten 1, 30167 Hannover, Germany

²Deutsches Elektronen-Synchrotron DESY, Notkestraße 85, 22607 Hamburg, Germany

³Universität Hamburg, Department of Physics, Notkestraße 9-11, 22607 Hamburg, Germany

⁴Helmholtz-Institute Jena, Fröbelstieg 3, 07743 Jena, Germany

⁵GSI Helmholtzzentrum für Schwerionenforschung GmbH, Planckstraße 1, 64291 Darmstadt, Germany *biesterfeld@iqo.uni-hannover.de

High-energy, blue shifted 100× spectral broadening from strong space-time focusing in a dispersion-managed hybrid multi-pass cell

Ross Powell, 1[†] Ana Silva, 2[†] Pedro Oliveira, 1 and Helder Crespo^{1,*}

¹Central Laser Facility, STFC, Rutherford Appleton Laboratory, Didcot OX11 0QX, United Kingdom ²IFIMUP, Dep. Física e Astronomia, Fac. de Ciências, Univ. do Porto, R. Campo Alegre s/n, 4169-007 Porto, Portugal [†]These authors contributed equally to this work

Abstract

We demonstrate the generation of high-energy, blue shifted broadband spectra with 800-1100 nm via strong space-time focusing in a dispersion-managed hybrid multi-pass cell (MPC) pumped by 450 fs pulses at 1030 nm. This source and spectra show promise as seed for petawatt laser systems.

Ultra-high-power petawatt lasers are unique tools for exploring extreme states of matter, advancing particle acceleration, and probing fundamental physics at unprecedented energy densities [1]. Systems targeting 20 PW peak power with sub-30 fs pulse durations are currently under development, relying on broadband amplification of low-energy seed pulses with spectra carefully matched to the amplifying medium. Such seed pulses are typically generated either by broadband laser oscillators at nanojoule energies, or via supercontinuum generation of relatively narrowband laser amplifier pulses with microjoule energies. Both approaches require further broadband amplification- typically via multiple laser-pumped optical parametric amplification (OPA) stages - to reach the millijoule-level. An interesting alternative is the direct spectral broadening of millijoule-level pulses from femtosecond laser amplifiers, where the multi-pass cell (MPC) technique stands out for its versatility and performance [2]. Very recently, high-energy 35 fs pulses from a Ti:Sapphire laser amplifier at 800 nm were compressed down to 3.8 fs in a 3-meter-long gas-filled MPC [3]. Recently, a hybrid MPC employing a fused silica plate has enabled compressing mJ-level Yb laser pulses from 220 fs down to 27 fs from a compact system operating in ambient air [4]. Here, we demonstrate the direct generation of mJ-level broadband spectra extending from 800 to 1100 nm - a region of particular interest for high-energy OPA in DKDP crystals - starting from 3nm-wide, 450-fs pulses from an Yb laser (s-pulse, Amplitude), by using a novel dispersion-managed hybrid MPC, based on the design in [4], and where custom broadband chirped mirrors (Ultrafast Innovations GmbH) enable overcompensating the material dispersion to experimentally achieve strong space-time focusing [5] within an MPC for the first time. This regime is characterized by a pronounced blue shift, which is due to self-steepening and not plasma formation, enabling efficient energy transfer from the pump laser to the bandwidth of interest.

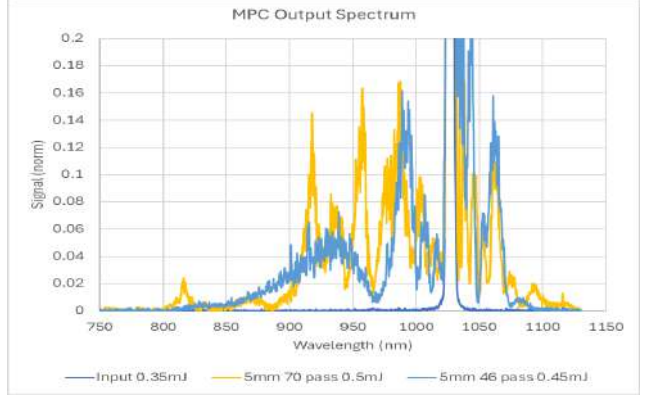


Figure 1: Spectra from the dispersion-managed hybrid MPC.

- [1] C. N. Danson et al., High Power Laser Science and Engineering, 7, e54 (2019).
- [2] A.-L. Viotti et al., Optica 9, 197-216 (2022).
- [3] L. Daniault et al., Opt. Lett. **49**, 6833-6836 (2024).
- [4] A. Omar et al., Opt. Express 32, 13235-13248 (2024).
- [5] C. Mei and G. Steinmeyer, Phys. Rev. Res. 3, 013259 (2021).

^{*}helder.crespo@stfc.ac.uk

Time Programmable Frequency Combs: Attosecond Control for Future Quantum Sensor Networks

Laura C. Sinclair¹

¹National Institute of Standards and Technology, 325 Broadway, Boulder, Colorado, 80305, USA *laura.sinclair@nist.gov

Abstract

A time programmable frequency comb provides enables user-defined control of the pulse output time and phase of an optical frequency comb. Here, I will present how this control enables precision time transfer to support future quantum sensor networks.

The optical frequency comb has enabled a wide range of frequency, time and distance metrology applications due to its precise, rigid, and referenced optical output. In addition, frequency combs' inherent connection of the optical and microwave domains removed the need for cumbersome frequency chains. However, the very rigidity which makes the frequency comb an excellent time-frequency ruler places limits on its applicability for comb-based sensing applications with many operating far from quantum-limited sensitivity. Both comb-based ranging or time transfer rely on the detection of an incoming optical comb pulse train from a distant location. These incoming comb pulse trains may be weak and amplification is costly – operation close to the quantum limit would dramatically increase the scope of what is possible in terms of range, SWaP (size, weight and power), and link loss.

Here, I will present our development of a quantum-limited approach to optical time transfer that relies upon a time programmable frequency comb to break the inherent trade-offs which result from the rigid operation of a traditional comb. These programmable combs have a pulse time and phase which can be digitally controlled with ± 2 -attosecond accuracy allowing for their use as an optical tracking oscillator [1,2]. Using frequency combs as optical tracking oscillators to reach the quantum limit for optical time transfer, we have been able to demonstrate subfemtosecond time transfer across a 300-km terrestrial free-space link with greater than 100 dB of loss, a factor of 10,000 times lower received power threshold than previous frequency-comb-based approaches [2]. I will show results from this 300-km demonstration as well as more recent work connecting optical atomic clocks across open air paths including an all-optical three-node iodine clock network spanning 14-km of air.

- 1. E. D. Caldwell, L. C. Sinclair, N. R. Newbury, and J.-D. Deschenes, "The time-programmable frequency comb and its use in quantum-limited ranging," Nature **610**, 667–673 (2022).
- 2. E. D. Caldwell, J.-D. Deschenes, J. Ellis, W. C. Swann, B. K. Stuhl, H. Bergeron, N. R. Newbury, and L. C. Sinclair, "Quantum-limited optical time transfer for future geosynchronous links," Nature **618**, 721–726 (2023).

How to Generate XUV Frequency Combs Without Enhancement Resonators?

Muhammad Thariq,^{1,2,*} Johannes Weitenberg,^{1,3} Theodor W. Hänsch,^{1,2} Thomas Udem,^{1,2} and Akira Ozawa^{1,4}

Abstract

We have performed high harmonic generation of a frequency comb without enhancement resonators. This is achieved by reducing the repetition rate to 40 kHz using an AOM-based pulse-picking scheme and a low noise solid-state amplifier. This method simplifies the laser system and enables easier accessibility for extreme ultraviolet frequency metrology.

The frequency comb is an indispensable tool for performing precision spectroscopy due to its ability to directly measure the frequency (not wavelength) of a specific laser tuned to a particular atomic transition. Though frequency combs are common in the visible and NIR regimes, extending this to the extreme ultraviolet regime is expected to be an exciting extension of this tool. An extreme ultraviolet (XUV) frequency comb allows precision spectroscopy for fundamental physics, optical clocks, and laser cooling to be extended into the XUV regime. This includes the spectroscopy of highly charged ions, the recently measured nuclear excitation of 229m Th, and our planned experiment on the spectroscopy of the He⁺ 1S-2S transition for testing quantum electrodynamics [1, 2].

Historically, the generation of XUV lasers has been a daunting task, requiring either particle accelerators or high harmonic generation (HHG) techniques with peak intensities on the order of $10^{13} - 10^{15}$ W/cm². In particular, generating XUV frequency combs at a repetition rate exceeding 10 MHz involves cavity-enhanced high harmonic generation (CE-HHG). Our current implementation consists of amplifying the average power to 400 W before feeding the laser to an enhancement resonator, where an average circulating power approaching 10 kW is used to generate gas-based HHG [2]. Considering this is a frequency comb, the comb structure must be maintained at high average powers, ensuring low phase noise to prevent carrier collapse during HHG [2]. The use of enhancement resonators (and high-power lasers in general) requires additional complexity and special measures to protect the optical components from the rigors of high-power lasers.

We have generated high harmonics with solid-state HHG using an average power of less than 10 W without an enhancement resonator, significantly simplifying the laser system. This is achieved by reducing the repetition rate by three orders of magnitude to 40 kHz while maintaining sufficient peak power for HHG [3]. The technique relies on pulse picking using an acousto-optic modulator (AOM) that selects pulses at specific intervals, effectively reducing the repetition rate. The dense comb structure resulting from the low repetition rate is not an issue when addressing ultra-narrow spectroscopic transitions; otherwise, it can be resolved via dual-comb spectroscopy.

The laser system uses a Kerr-lens mode-locked Yb:KYW oscillator (1030 nm, 40 MHz). After pulse picking with an AOM, which reduces the repetition rate to 40 kHz, the pulses are amplified by diode-pumped Yb:LuAG amplifiers to 10 μ J. The pulses are further compressed to 35 fs using two stages of Multi-Pass Cell Spectral Broadening [4]. The frequency comb structure is maintained by stabilizing one comb mode to an ultra-stable CW laser at 1033 nm. Solid-state HHG is achieved using MgO, generating odd harmonics from the amplified infrared frequency comb. Further XUV comb characterization, such as beam profiling and beat note measurements in the extreme ultraviolet, is currently underway.

This work offers a tantalizing prospect: XUV frequency combs with significantly reduced complexity and average power, making it more accessible and fostering exciting opportunities for exploration across disciplines.

- J. Moreno, et. al., "Toward XUV frequency comb spectroscopy of the 1S-2S transition in He⁺", Eur. Phys. J. D 77, 67 (2023).
- [2] F. Schmid, et. al., "An ultra-stable high-power optical frequency comb", APL Photonics 9, 026105 (2024).
- [3] F. Canella, et. al., "Low-repetition-rate optical frequency comb", Optica 11, 1 (2024).
- [4] J. Schulte, et. al., "Nonlinear pulse compression in a multi-pass cell", Opt. Lett. 41, 4511 (2016).

¹Max-Planck-Institut für Quantenoptik, 85748 Garching, Germany

²Fakultät für Physik, Ludwig-Maximilians-Universität München, 80799 Munich, Germany

³Fraunhofer-Institut für Lasertechnik ILT, 52074 Aachen, Germany

⁴Institute for Multidisciplinary Sciences, Yokohama National University, Yokohama City, 240-8501 Kanagawa, Japan

^{*}muhammad.thariq@mpq.mpg.de

Generation of sub 100 fs femtosecond pulses with tunable repetition rates up to 1 THz at 1030 nm

Abdelkrim Bendahmane^{1,*}, Fedele Pisani^{1,2,3}, Gianluca Galzerano³, Giorgio Santarelli¹, Eric Cormier¹

Abstract

We report on the generation of bursts of sub 100 fs pulses at tunable repetition rates ranging from 300 GHz up to 1 THz at a wavelength of 1030 nm. The repetition rates i.e. the comb free spectral range is stabilized with a feedback loop.

Ultrafast pulses are commonly generated with mode-locked oscillators. Depending on the cavity optical length, the repetition rates typically range from a few tens of MHz to 250 MHz and exceptionally up to 1 or even 10 GHz. However, recent applications such as astronomical spectrograph calibration or novel laser processing request repetition rates above 10 GHz. Such a set of parameters is routinely achieved by means of electro-optical modulation of a CW laser. Although theoretically extendable to very high frequencies, actual components set a practical limit of this approach to 30 GHz. Here, we propose an alternative road to reach the generation of ultrashort pulses at tunable repetition rates ranging from several hundreds of GHz up to 1 THz. It is based on nonlinear compression of an initial optical beat signal through multiple four-wave mixing processes in the anomalous chromatic dispersion region of an optical fiber. Recent studies have linked this compression process to Akhmediev Breathers, a periodic analytical solution to the nonlinear Schrödinger equation [1], which is of significant interest due to its connection with modulation instability, supercontinuum generation and rogue waves [2,3]. To date, the experimental studies have been limited to pulses with a duration of few hundred of femtosecond at wavelengths above 1300 nm where standard optical fibers exhibit anomalous chromatic dispersion.

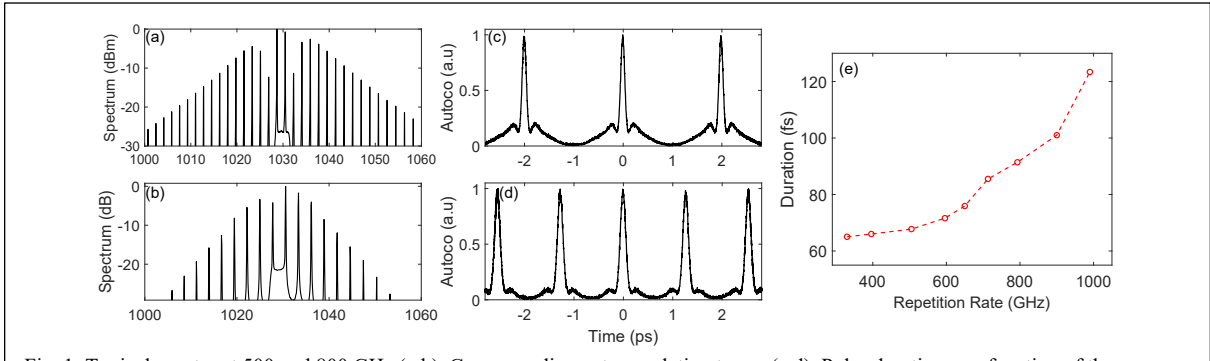


Fig. 1: Typical spectra at 500 and 800 GHz (a,b). Corresponding autocorrelation traces (c,d). Pulse duration as a function of the repetition rate (e).

In this work, we demonstrate the ability to achieve pulse durations shorter than 100 fs (> 60 fs) around 1030 nm using an all Polarization Maintaining (PM) fibered system and only a few meters of commercially available PM photonic crystal fiber (PM-PCF) with zero dispersion wavelength around 930 nm. The system emits pulse trains (bursts) of 1 ns (1000 pulses at 1 THz repetition rate) at a burst repetition rate of 1 MHz. The repetition rate can be continuously adjusted and actively stabilized between 300 GHz and 1 THz. Such a compact seed laser can directly be amplified in high-power Yb-doped fibers up to 10s to 10s W for scientific or industrial applications.

¹Laboratoire Photonique Numérique et Nanosciences (LP2N), UMR 5298, CNRS-IOGS-Université Bordeaux, 33400 Talence, France

²Dipartimento di Fisica, Politecnico di Milano, piazza Leonardo da Vinci 32, Milano, Italy

³Istituto di Fotonica e Nanotecnologie – CNR, piazza Leonardo da Vinci 32, Milano, Italy

^{*} abdelkrim.bendahmane@u-bordeaux.fr

^[1] N. Akhmediev and V. I. Korneev, "Modulation instability and periodic solutions of the nonlinear Schrödinger equation," Theor. Math. Phys. 69, 1089 (1986).

^[2] B. Kibler, J. Fatome, C. Finot, G. Millot, F. Dias et al., "The Peregrine soliton in nonlinear fibre optics," Nature Physics 6, 790-795 (2010).

^[3] J. Dudley, F. Dias, M., Erkintalo, et al., "Instabilities, breathers and rogue waves in optics," Nature Photonics 8, 755 (2014).

Gauging Vacuum Fluctuations: Rogue Wave Emergence in Optical Parametric Generation

Wenbin Chen¹, Haosen Shi², Günter Steinmeyer^{3,4,*}, Yuanbo Lu⁴, Jintao Fan¹, and Minglie Hu¹

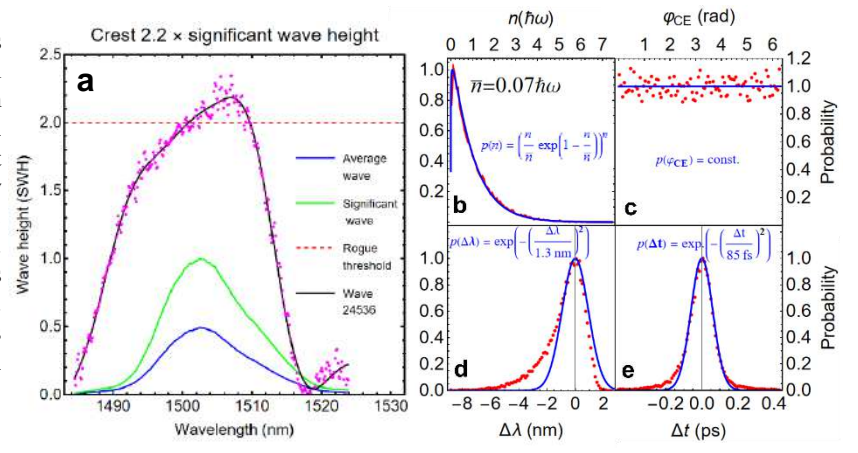
- 1. Ultrafast Laser Laboratory, Key Laboratory of Opto-electronic Information Science and Technology of Ministry of Education, School of Precision Instruments and Opto-electronics Engineering, Tianjin University, Tianjin 300072, China
- 2. State Key Laboratory of Precision Spectroscopy, East China Normal University, Shanghai 200062, China
- 3. Max-Born-Institut, Berlin 12489, Germany
- 4. Physics Department, Humboldt University, Berlin 12489, Germany

Abstract

Using real-time measurement techniques for recording spectra and spectral interferograms, we measure the statistical distributions of timing jitter, carrier-envelope phase, spectral shifts, and pulse energies of an optical parametric generator. The latter exhibit the emergence of rogue events as has been predicted for short-crested ocean waves.

Optical rogue waves have been first reported for Raman-shifted solitons in supercontinuum generation [1]. In this scenario, the extreme red tails clearly exhibit extreme-value statistics, i.e., with much larger events than anticipated from Gaussian statistics. However, at the same time, the energy of these rogue waves is much smaller than the total pulse energy in the supercontinuum. Here we present the emergence of rogue waves from an optical parametric generator (OPG), i.e., vacuum seeded parametric amplification in a PPLN crystal, pumped by a 1030 nm fiber laser at 53 MHz repetition rate. The output of the OPG is characterized by dispersive Fourier transform (DFT) and dispersive temporal interferometry (DTI), which provides the complete statistics of pulse energy fluctuations, timing jitter, Schawlow-Townes noise and carrier-envelope phase fluctuations at 53 MHz sampling rate. Analyzing the measured 26,500 individual DFT spectra, one can extract the significant wave height (SWH) from the average of the largest third of the waves. According to the established definition in oceanography, rogue waves exceeds the SWH by a factor >2. Our measured data set contains exactly one such rogue event, which is shown in Fig. 1a.

Figure 1: DFT and DTI results based on 26500 individual measurements. a: rogue spectrum (magenta symbols) in comparison to average (blue) and significant wave (green). b: pulse energy statistics with Poissonian fit (blue). c: measured univariate CEP noise. d: skewed Schawlow-Townes noise in comparison to Gauss fit. e: timing jitter noise. Excess kurtosis becomes apparent in comparison with Gaussian fit.



Pulse energy fluctuations follow Poisson statistics with effective photon number \bar{n} close to zero, see Fig. 1b. The measured distribution exhibits a heavy tail, with extreme energies exceeding the average pulse energies by a factor ~5. Quite remarkably, the histogram of OPG pulse energies in Fig. 1b appears identical to the predicted distributions of the surface slope in the short-crest limit of ocean waves [2]. CEP noise [Fig. 1c] is univariate in $[0,2\pi[$, which further confirms the quantum noise nature of the seed mechanism. Wavelength variations follow skewed statistics with a heavy wing on the anti-Stokes side [Fig. 1d]. Timing jitter distributions [Fig. 1e], in contrast, bear large resemblance with the heavily leptokurtic probability distributions of the direction of surface gradients in oceanography. Considering that the calculations in [2] for short-crested waves are classically throughout, this close agreement with vacuum-seeded parametric amplifiers appears truly remarkable. Coherent seeding at the few-photon level then allows studying the transition to long-crested waves, which exhibit perfect Gaussian statistics.

[1] D.R. Solli, C. Ropers, P. Koonath, and B. Jalali, "Optical Rogue Waves," Nature **450**, 1054-1057 (2007).

[2] M.S. Longuet-Higgins, "The statistical analysis of a Random, Moving Surface," Phil. Trans. Roy. Soc. London A **249**, 321-387 (1957).

^{*}steinmey@mbi-berlin.de

Efficient SHG from a Low-noise GHz Yb:CYA Femtosecond Oscillator

Li Zheng, Junxiao Bai, 2, Geyang Wang, Wenlong Tian, 2, Zhiyi Wei, and Jiangfeng Zhu

Abstract

We present a low-noise Kerr-lens modelocking Yb:CYA oscillator providing 8.2 W average power with a pulse duration of 108 fs at a repetition rate of 1.08 GHz. The second harmonic generation with average power of 4.5 W from the GHz oscillator is demonstrated, corresponding a frequency doubling efficiency of 56%.

GHz-repetition-rate femtosecond lasers play an important role in precision spectroscopy, biomedical microscopy and ablation-cooled materials processing. Throught the development of GHz femtosecond laser, the near-infrared (NIR) laser has played a dominate role. However, green lasers with GHz repetition rate are usually difficult to generate from oscillators directly. Second harmonic generation (SHG) via cascading a 1-µm GHz femtosecond oscillator is a simple method, the key is that the fundamental frequency femtosecond laser has a high peak power.

Here, we report on a high-power and low-noise Kerr-lens modelocking (KLM) Yb:CYA oscillator providing 8.2 W average power with a pulse duration of 108 fs at a repetition rate of 1.08 GHz (Fig. 1(a)(b)(c)). The oscillator exhibits low noise characteristics and excellent stability, the free-running integrated timing jitter is 155 fs in the span from 1 kHz and 1 MHz and the measured root mean square (RMS) of power fluctuation is 0.15% over eighteen hours in the laboratory environment, as shown in Fig. 1(d) and Fig. 1(e). By cascading a 5-mm-long LBO crystal, second harmonic is generated with over 4.5 W of average power at 519 nm when the incident fundamental frequency laser is 8.08 W, which corresponds a high conversion efficiency of 56% even if the pump intensity is only 4.3 GW/cm² [1]. The measured optical spectra and power conversion curves of the green laser are shown in Fig. 1(f)(g). It also shows good power stability, as shown in Fig. 1(h).

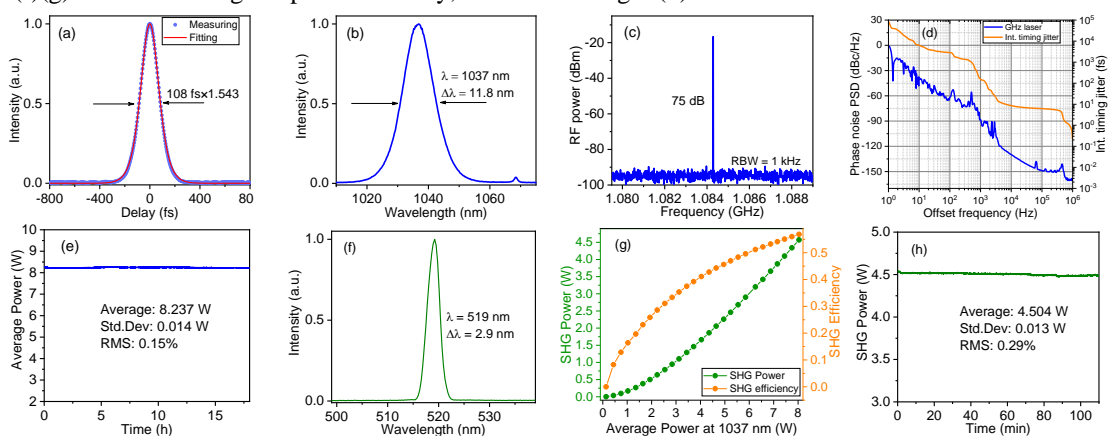


Figure 1: Modelocking diagnostics of the GHz oscillator and the second harmonic generation.

In conclusion, we have demonstrated an efficient SHG from a homemade GHz KLM Yb:CYA oscillator. The high-power GHz-class green laser could serve as an ideal pump for optical parametric oscillators (OPOs), capable of generating wavelength-tunable femtosecond pulses around 650-1350 nm for biomedical microscopy [2].

References

[1] W. L. Tian, X. Tian, Q Li, G. Y. Wang, C. Bai, Y. Yu, X. D. Xu, J. Xu, Z. Y. Wei, J. F. Zhu, "Kerr-lens mode-locked femtosecond Yb:CALYO oscillator with more than 20-W average power," Opt. Lett. **48**, 4789-4792 (2023). [2] N. Ji, J. C. Magee, E. Betzig, "High-speed, low-photodamage nonlinear imaging using passive pulse splitters," Nat. methods, **5**, 197-202 (2008).

¹School of Physics and Telecommunication Engineering, Shaanxi University of Technology, Hanzhong, 723001, China

²School of Optoelectronic Engineering, Xidian University, Xi'an 710071, China

³Beijing National Laboratory for Condensed Matter Physics, Institute of Physics, Chinese Academy of Sciences, Beijing 100190, China

^{*}wltian@xidian.edu.cn

Advances and challenges of mid-infrared ultrafast all-fibre lasers

Maria Chernysheva¹

¹Leibniz Institute of Photonic Technology, Albert-Einstein-Str 9, 07745 Jena, Germany *maria.chernysheva@leibniz-ipht.de

Abstract

While only a few mid-IR laser technologies have matured beyond $2.5 \,\mu m$, fibre lasers are rapidly emerging as a compelling platform for high-brightness sources, opening new possibilities for a wide application range. This talk focuses on the properties and design potential of ultrafast fluoride-based fibre lasers and outlines future development directions.

Main Text

Harnessing a mid-IR wavelength range has become an urgent challenge as it can enable the accurate detection of molecular vibrational modes in biological tissues, lying, for example, at around 3 μm (C-H, N-H, O-H stretches). Thus, since the 2000s, Mid-IR light sources and sensors have become an object for extensive research and industrial interest, also triggered by high demand for greenhouse gases and pollutants monitoring, optical frequency standards for global positioning systems and optical clocks, free space and fibre optic communications, LIDAR systems, medical diagnostics and surgery. A few mid-IR laser technologies have reached maturity, such as optical parametric oscillators, bulk Cr/Fe-doped solid-state lasers, sources employing nonlinear effects, such as supercontinuum generation or soliton-self-frequency shift, and quantum cascade lasers (QCLs). Fibre-based laser systems present a more promising platform compared to QCLs due to their high stability, cost-effectiveness, and flexibility in output parameters. Unfortunately, the silica fibre technology is not a remedy for all photonics applications and demonstrates strong attenuation beyond 2.5 μm.

Unique soft-glass materials have to replace silica fibres to expand beneficial fibre optics platforms towards the Mid-IR wavelength range[1,2]. Recent works of the research community have demonstrated great success in the first fluoride and chalcogenide fibre-based ultrafast laser systems operating beyond 2.8 µm[3]. Still, currently deployed systems rely on free-space coupling from bulk laser components into an active fibre[4,5]. This approach drastically limits the possibilities of manipulating the dynamics of ultrashort pulses. The translation to transparency in Mid-IR soft glass materials does not call for a straightforward engineering solution, yet brings forth immersing fundamental and methodological gaps due to drastically different material, thermal and chemical properties.

The talk will discuss the choice of gain media with an operational wavelength range across $2.8-5~\mu m$ of rare earth elements, chemical, optical and mechanical properties of soft glass fibres, followed by the development of efficient novel fibre arrangements and laser components. Overall, the talk will provide a promising outlook for the exploration of laser generation regimes and flexible fibre laser designs, significantly surpassing the performance of QCLs.

- [1] G. Tao, et al. "Infrared fibres," Advances in Optics and Photonics 7(2) 379-458 (2015)
- [2] A. B. Seddon, et al. "Short review and perspective: Chalcogenide glass mid-infrared fibre lasers," European Physical Journal Plus 139, 1–10 (2024)
- [3] F. Jobin, et al, "Recent developments in lanthanide-doped mid-infrared fluoride fiber lasers (invited)," Optics Express 30, 8615–8640 (2022)
- [4] S. D. Jackson "Mid-infrared fiber laser research: Tasks completed and the tasks ahead," APL Photonics 9, 070904 (2024)
- [5] K. Grebnev, et al. "Fluoride and chalcogenide glass fiber components for mid-infrared lasers and amplifiers: Breakthroughs, challenges, and future perspective," APL Photonics 9, 110901 (2024)

Integrated terahertz generation with high spectral brightness

Nadia Berndt, 1,* David Rohrbach, 1 Xi Zhang, 1 and Keith A. Nelson 1

¹Department of Chemistry, Massachusetts Institute of Technology, Cambridge, Massachusetts 02139, USA *nadiaber@mit.edu

Abstract

We present a novel approach for generating multicycle terahertz (THz) pulses using a nonlinear slab waveguide, optimized for on-chip THz spectroscopy and signal processing. Our method produces spectrally bright THz pulses with more than 20 cycles, each with a peak amplitude surpassing 10 kV/cm.

While most existing terahertz (THz) sources are configured to yield free-space propagating THz fields, the "THz polaritonics" platform enables THz generation, interaction, and detection entirely within a compact, solid-state waveguide.[1] Within this platform, THz pulses are typically broadband and single-cycle. However, achieving spectrally bright THz fields is crucial for selectively targeting specific excitations or signal processing frequencies, enhancing both the precision and sensitivity of the technique. It has been theoretically proposed [2] and experimentally demonstrated [3] that velocity-matching a femtosecond optical pulse at 800 nm to a THz waveguide mode via the lateral excitation method shown in Fig. 1a, leads to the buildup of multicycle THz fields within the waveguide. In the previous works the optical pump pulse was short in duration compared to a single lobe of the THz field. Therefore, during the co-propagation of the optical pulse and the multicycle THz pulse that it generates, each THz field lobe only gets pumped for a short propagation length, severely limiting the THz generation efficiency and the resulting THz spectral amplitude. We build on the previous methods through the use of an intensity modulated optical pulse (Fig. 1b), which is produced by a sequence of pairs of partial and high reflectors. Due to the modulated optical pulse, each THz lobe can be continuously pumped as it propagates resulting in higher THz generation efficiency. Using a modulated optical pulse with 0.8 mJ energy, THz fields with >20 cycles and up to 30 kV/cm peak fields are generated, as shown in Fig. 1c. Spectral full-width-halfmaxima of 36 GHz (12% of peak central frequency) are achieved (Fig. 1d). This method also allows for frequency tuning by adjusting the waveguide dispersion through changing the waveguide thickness or by introducing metallic or dielectric boundaries. Already at this modest pump power, THz fields generated in the waveguides have similar spectral brightness to our free-space propagating THz fields generated by tilted pulse front in LiNbO₃ using 6 mJ laser pulses. Therefore, this method offers significant potential for on-chip THz spectroscopy and signal processing.

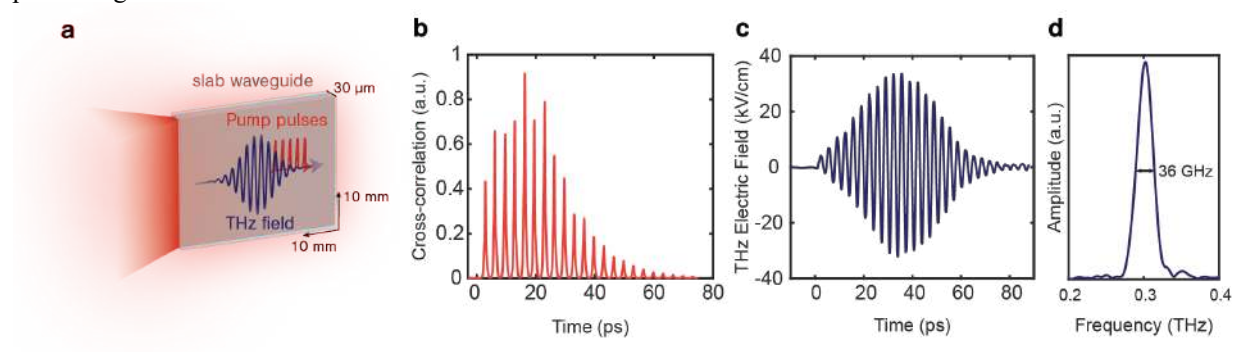


Figure 1: (a) Multicycle THz field generation by velocity-matching an 800 nm pump pulse with co-propagating THz field in a nonlinear slab waveguide. (b) Intensity modulated optical pulse used for THz generation. (c) Measured THz electric field inside the waveguide and (d) corresponding frequency spectrum.

[1] T. Feurer, N. S. Stoyanov, D. W. Ward, J. C. Vaughan, E. R. Statz, and K. A. Nelson, "Terahertz polaritonics," Annu. Rev. Mater. Res. 37, 317–350 (2007).

[2] H. Yang, J. Qi, C. Pan, Y. Lu, Q. Wu, J. Yao, and J. Xu, "Efficient generation and frequency modulation of quasi-monochromatic terahertz wave in Lithium Niobate subwavelength waveguide," Opt. Express **25**(13), 14766 (2017).
[3] Y. Lu, H. Xiong, Q. Wu, and J. Xu, "Propagation phase elimination of light pulses by an initial phase-locked synchronized moving source," Opt. InfoBase Conf. Pap. **Part F181**-(c), 2–3 (2020).

△ UFO XIV Azores 2025

High-power, few-cycle, short-wave infrared source for high-flux, soft X-ray generation at 200 kHz repetition rate

Caroline Juliano,^{1,*} Ivan Sytcevich,¹ Chen Guo,¹ Roya Garayeva,¹ Nikolas Rupp,¹ Anne-Lise Viotti,¹ Anne L'Huillier¹ and Cord L. Arnold¹

¹Department of Physics, Lund University, P. O. Box 118, SE-22100 Lund, Sweden *caroline.juliano@fysik.lth.se

Abstract

We present a 200 kHz, high average power, ytterbium-based optical parametric chirped pulse amplification system delivering CEP-stable, few-cycle pulses around 2 μ m with an anticipated average power of 50 W. The source is designed to drive a pump-probe beamline with high-flux, soft X-ray attosecond pulses.

Advances in laser technology have enabled the development of tabletop soft X-ray (SXR) radiation via high-order harmonic generation (HHG), driven by mid- and short-wave infrared (SWIR) sources [1, 2, 3]. However, the HHG conversion efficiency scales unfavorably with longer driving wavelengths, limiting the SXR flux [4]. To address this, we present the development of a high-power SWIR driver designed to generate high-flux SXR reaching the water window via HHG in gases. The system, presented in Fig.1(a), is based on optical parametric chirped pulse amplification (OPCPA), centered at 2 µm and operating at 200 kHz repetition rate. The front-end relies on an Ytterbium (Yb) CPA laser, including an Yb:YAG thin-disk multipass amplifier, delivering 1 ps-long pulses at 1030 nm and 500 W of average power, while preserving a high beam quality (M² <1.2). A part of the 1030 nm is used for both whitelight generation in a YAG crystal and second harmonic generation (SHG), the latter pumping the white-light in a noncollinear optical parametric amplification (NOPA) stage. Difference frequency generation (DFG) between the resulting amplified visible spectrum and another fraction of the 1030 nm yields passively CEP-stable idler pulses with a broadband SWIR spectrum (1.6-2.6 µm) supporting a Fourier transform limit of ∼15 fs. The CEP can be manipulated by a piezo-driven delay stage in the 1030 nm arm. The SWIR pulses are then amplified in three consecutive NOPA stages, targeting 250 µJ of pulse energy. In the current development phase, the first stage is realized and delivers 15 μJ of pulse energy using 40 W of pump. Compression to the few-cycle regime is achieved using a combination of bulk materials with positive and negative dispersion (zinc sulfide and Al₂O₃, respectively), along with chirped mirrors for third-order dispersion management. Pulse characterization via third-harmonic generation (THG) dispersion scan (d-scan) in a thin Al_2O_3 plate shows a retrieved pulse duration of 21 fs after the first stage, as shown in Fig. 1(b). The shot-to-shot CEP stability is evaluated using nonlinear interferometry techniques, similar as in [5]. A high-flux SXR beamline is currently being designed for attosecond pump-probe photoelectron spectroscopy in the gas phase.

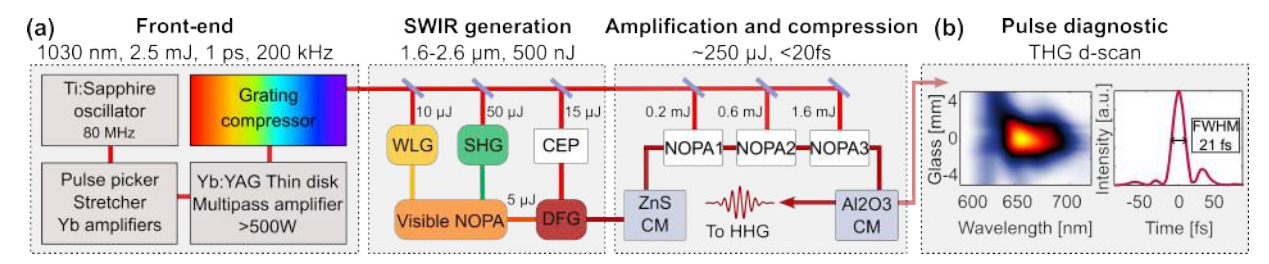


Figure 1: (a) SWIR OPCPA layout (b) THG d-scan trace and retrieved pulse intensity profile

- G J Stein et al., "Water-window soft x-ray high-harmonic generation up to the nitrogen K-edge driven by a kHz, 2.1 µm OPCPA source", J. Phys. B: At. Mol. Opt. Phys. 49, 155601 (2016)
- [2] J Pupeikis et al., "Water window soft x-ray source enabled by a 25 W few-cycle 2.2 μm OPCPA at 100 kHz", Optica 7, 168-171 (2020)
- [3] M F Seeger et al., "49 W carrier-envelope-phase-stable few-cycle 2.1 μm OPCPA at 10 kHz", Opt. Express 31, 24821-24834 (2023)
- [4] A DiChiara et al., "Scaling of High-Order Harmonic Generation in the Long Wavelength Limit of a Strong Laser Field", IEEE J. Sel. Top. Quantum Electr. 18, 419 (2012).
- [5] I Sytcevich et al., "Few-cycle short-wave-infrared light source for strong-field experiments at 200 kHz repetition rate," Opt. Express 30, 27858-27867 (2022)

High-energy self-CEP-stable seeder

for a 2.2 µm OPCPA

Ugaitz Elu,^{1,*} Marcel Krenz,¹ Maria Pawliszewska,¹ Michael H. Frosz,² Francesco Tani,^{2,3} Philip St.J. Russell,² Jens Biegert,^{4,5} and Martin Wolf¹

¹FHI-MPG – Fritz-Haber-Institut der Max-Planck-Gesellschaft, Faradayweg 4-6, 14195, Berlin, Germany

Abstract

We present a novel front-end for self-CEP-stable 2.2 µm OPCPA driven by Yb lasers. Gas-filled ARPCFs broaden the narrowband pulses, which are then compressed with chirped mirrors followed by intra-pulse-DFG. This design provides robustness and high energy seeding for contrast-improved OPCPA, crucial for plasma physics, wakefield acceleration, and attosecond physics.

Main Text

Over the past decade, significant advancements in attosecond science [1,2] have enabled in-house, time-resolved Soft-X-ray spectroscopy for condensed matter physics [3]. To advance bright tabletop Soft-X-ray beamlines, the ultrafast optics community has explored various pulse broadening and compression techniques to generate carrier-envelope phase (CEP)-stable infrared pulses directly from narrowband high-energy lasers [4,5].

Here, we present a groundbreaking compact scheme for generating self-CEP-stable 2.2 μ m pulses using a Dira 200 Thin Disc laser from TRUMPF Laser GmbH. The front-end system, with a footprint of 1.2 m \times 0.5 m, incorporates pulse compression from 650 fs to 9 fs at 1 μ m utilizing a gas-filled antiresonant reflection photonic crystal fiber (ARR-PCF), followed by self-CEP-stable, 100 nJ, 2.2 μ m pulse generation in BiBO via intra-pulse-DFG, and amplification to microjoule energy levels in an OPA stage. While BiBO produces self-CEP-stable 2.2 μ m pulses, BBO combines intra-pulse-DFG and DFG between the fundamental and its second harmonic (Fig. 1c). We anticipate that this methodology will be instrumental in developing robust self-CEP-stable front-end systems for high-energy tabletop infrared OPCPA setups, ultimately enabling next-generation attosecond experiments and advancing the field of ultrafast X-ray science.

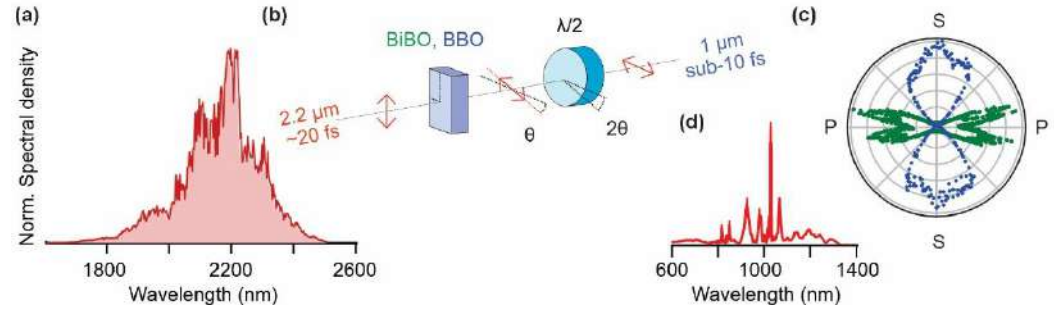


Figure 1: Intra-pulse-DFG diagram. (a) Measured spectrum of the passively CEP-stable 2.2 µm pulses. (b) Intra-pulse-DFG sketch. (c) Polar plot of the intra-pulse-DFG signal in BiBO (green dots) and mixture between DFG and intra-pulse-DFG signals in BBO (blue dots), as a function of input polarization, measured rotating the achromatic half-wave plate. (d) Measured broadband 1030 nm spectrum.

- [1] P. B. Corkum & F. Krausz, "Attosecond science." Nature Physics 3, (2007).
- [2] J. Biegert, et al. "Attosecond technology(ies) and science." Journal of Physics B: Atomic, Molecular and Optical Physics **54**, (2021).
- [3] A. M. Summers, et al. "Realizing Attosecond Core-Level X-ray Spectroscopy for the Investigation of Condensed Matter Systems." Ultrafast Science 3, (2023).
- [4] F. Köttig, et al. "Generation of μJ pulses in the deep ultraviolet at megahertz repetition rates." Optica 4, (2017).
- [5] L. Lavenu, et al. "Nonlinear pulse compression based on a gas-filled multipass cell," Opt. Lett. 43, (2018).

²Max Planck Institute for the Science of Light, Staudtstraße 2, 91058 Erlangen, Germany

³PhLAM – Physique des Lasers Atomes et Molécules, Université Lille, CNRS, UMR 8523, Lille, France

⁴ICFO – Institut de Ciencies Fotoniques, 08860 Castelldefels, Barcelona, Spain

⁵ICREA – Institució Catalana de Recerca i Estudis Avançats, 08010 Barcelona, Spain

<u>*elu@fhi-berlin.mpg.de</u>

Tuesday October 7th

Enhanced Entangled Second Harmonic Generation Beyond the Photon Pairs Regime

T. Dickinson,^{1,2} I. Afxenti,³ G. Astrauskaite,⁴ L. Hirsch,³ S. Nerenberg,⁴ O. Jedrkiewicz,^{1,5} D. Faccio,⁴ C. Müllenbroich,⁴ A. Gatti,⁵ M. Clerici,^{1,3} and L. Caspani^{1,2,*}

Abstract

We report quantum-enhanced second harmonic generation driven by parametric down-conversion, with efficiencies surpassing those of classical light beyond the photon-pair regime. Experiments confirm a persistent quantum advantage up to ~ 10 photons per mode, extending nonlinear quantum enhancement toward practical applications.

Entangled photons from parametric down-conversion (PDC) can enhance nonlinear processes such as second harmonic generation (SHG) and two-photon absorption (TPA) compared to classical light [1]. Previous demonstrations, for both SHG [2] and TPA [3], focused on the photon-pair regime, with less than one photon per mode, where signals remain weak, casting doubts on the usefulness of this enhancement [4]. In our work, we investigate SHG stimulated by broadband, strongly multimode PDC light, with more than ten thousand spatiotemporal modes. We benchmark the results against SHG driven by a classical source matched in energy and spatiotemporal properties. The comparison reveals a robust quantum advantage persisting up to excitation levels of about ten photons per mode (see Fig. 1)—nearly an order of magnitude beyond the quantum-classical boundary commonly assumed so far [5].

Our findings extend the regime where quantum enhancement can be observed, showing that efficient two-photon interactions can be realized even at intensities far above the photon-pair limit. This not only addresses ongoing questions about the origin and robustness of quantum-driven nonlinearities, but also establishes their potential for practical applications in areas such as imaging, sensing, and quantum photonic technologies.

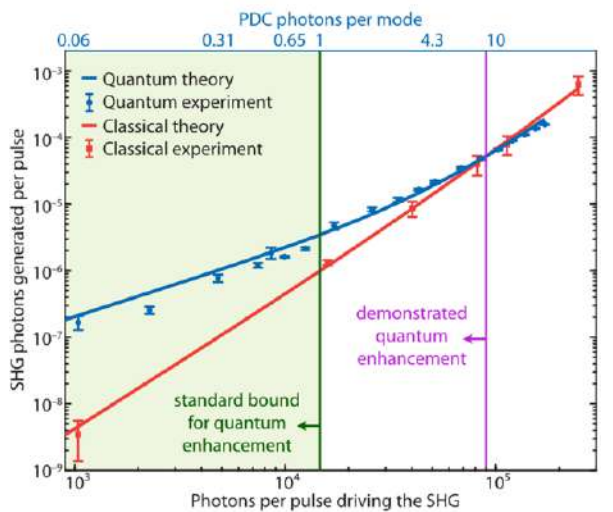


Figure 1: SHG photons per pulse generated by the quantum source (PDC, blue dots) compared to the classical case (standard laser, red squares). The prediction from the theoretical model (solid curves) [6] match well the experiment. The quantum-driven SHG signal outperforms the classical case up to 9.5 PDC photon per mode (purple line).

- [1] J. Javanainen et al., "Phys. Rev. A 41, 5088 (1990). [4] T. Landes et al., Opt. Express 29, 20022 (2021).
- [2] B. Dayan et al., *Phys. Rev. Lett.* **94**, 043602 (2005). [5] T. D
- [5] T. Dickinson et al., Sci. Adv. 11, eadw4820 (2025)
- [3] D. Tabakaev et al., Phys. Rev. Lett. 129, 183601 (2022) [6] A. Gatti et al., "Opt. Quantum 3, 269 (2025).

¹Como Lake Institute of Photonics, Dipartimento di Scienza e Alta Tecnologia, Università dell'Insubria, Via Valleggio 11, 22100 Como, Italy

²Institute of Photonics, Department of Physics, University of Strathclyde, Glasgow G1 1RD, United Kingdom

³James Watt School of Engineering, University of Glasgow, Glasgow G12 8QQ, United Kingdom

⁴School of Physics and Astronomy, University of Glasgow, Glasgow G12 8QQ, United Kingdom

⁵Istituto di Fotonica e Nanotecnologie del CNR, Piazza Leonardo da Vinci 32, 20133 Milano, Italy

^{*}lucia.caspani@uninsubria.it

Air Lasing: from strong-field molecular physics to ultrafast spectroscopy

Jinping Yao

State Key Laboratory of Ultra-intense Laser Science and Technology, Shanghai Institute of Optics and Fine Mechanics, Chinese Academy of Sciences, Shanghai 201800, China *jinpingyao@siom.ac.cn

Abstract

Air lasing, as a novel ultrafast phenomenon, has attracted considerable interests in recent years. Here, we report on enhancement of N_2 ⁺ lasing induced by the synergistic interplay between tunnel ionization and multiphoton resonances, and show basic principle and applications of air-lasing-based coherent Raman spectroscopy.

Air lasing has unveiled new frontiers in strong-field physics by challenging conventional understanding of molecular ionization and excited-state dynamics. Besides, the unique characteristics of air lasing (e.g., high brightness, narrow bandwidth, good directionality) enable it to serve as a probe source for coherent Raman spectroscopy (CRS), opening exciting perspectives in remote sensing. In this talk, we will report our recent progresses in air lasing, including manipulation and enhancement of air lasing, as well as the applications of air-lasing-based coherent Raman spectroscopy in gas sensing, isotopic analysis and temperature measurement.

Firstly, we demonstrate a significant enhancement in multiphoton excitation efficiency when tunneling ionization of neutral molecules and resonant excitation of ions coexist in strong laser fields [1]. It facilitates the population inversion in N_2^+ , resulting in strong N_2^+ lasing radiation around 1000 nm pump wavelength. Our study reveals that the high-efficient photoexcitation is the result of synergistic interplay between tunneling ionization and photoexcitation. The ionization injection at the peaks of the oscillating electric field induces ionic dipoles periodically and endows them with an optimal phase for photoexcitation. At the 1000 nm pump wavelength, the resonance of the pump laser with strong-field-dressed ionic states enables the optimal buildup of ionic coherence due to phase locking and constructive interference of dipoles born at different moments. Therefore, compared with the individual contribution of ionization or multiphoton resonance, the ionic excited-state population is increased by nearly one order of magnitude when two effects coexist. This work provides new insights into the photoexcitation mechanism of ions in strong laser fields and opens up a route for optimizing air lasing radiation.

We also developed coherent Raman spectroscopic technique using air lasing [2,3]. Air-lasing-based Raman spectroscopy shows the advantages of easy implementation and high sensitivity as well as capability for multicomponent detection. Taking advantage of this spectroscopy, we have realized high-sensitivity detection of greenhouse gases [2] and quantitative detection of $^{12}\text{CO}_2$ and $^{13}\text{CO}_2$ [4]. In addition, a single-beam, single-shot coherent Raman thermometry has also been demonstrated by using air lasing [5], which provides an advanced tool for combustion diagnostics in harsh scenarios. Recently, we proposed a cascaded amplification strategy of N_2^+ lasing, yielding the highest output energy of air lasing reported to date [6]. The cascaded scheme allows us to develop a high-sensitivity, single-beam coherent Raman spectroscopy, which enables simultaneous detection of multiple species and exhibits high sensitivity at the parts-per-million level.

These studies not only deepen our understanding of strong-field molecular physics in non-equilibrium quantum systems, but also promote the development of ultrafast spectroscopy.

- [1] Y. Chen et al., "Multiphoton Resonance Meets Tunneling Ionization: High-Efficient Photoexcitation in Strong-Field-Dressed Ions," Phys. Rev. Lett. **133**, 113201 (2024).
- [2] Z. Zhang et al., "High-Sensitivity Gas Detection with Air-Lasing-Assisted Coherent Raman Spectroscopy," Ultrafast Sci. **2022**, 9761458 (2022).
- [3] N. Zhang et al., "Electronic-Resonance-Enhanced Coherent Raman Spectroscopy with a Single Femtosecond Laser Beam," Laser Photonics Rev. 17, 2300020 (2023).
- [4] Y. Wu et al., "Measurement of Carbon Dioxide Isotopes with Air-Lasing-Based Coherent Raman Spectroscopy," J. Phys. Chem. Lett. **15**, 2944-2950 (2024).
- [5] X. Lu et al., "Single-shot single-beam coherent Raman scattering thermometry based on optically induced air lasing," Light Sci. Appl. 13, 315 (2024).
- [6] X. Lu et al., "Cascaded amplification of air lasing," Sci. Adv., in press.

Full characterization of tunable few-fs vacuum ultraviolet pulses

José R. C. Andrade, Martin Kretschmar, Rostyslav Danylo, Stefanos Carlström, Tobias Witting, Alexandre Mermillod-Blondin, Serguei Patchkovskii, Misha Yu Ivanov, Marc J. J. Vrakking, Arnaud Rouzée and Tamas Nagy*

Max Born Institute for Nonlinear Optics and Short Pulse Spectroscopy, Max-Born-Straße 2A, 12489 Berlin, Germany *nagy@mbi-berlin.de

Abstract

We fully characterize above- μJ , sub-3-fs pulses tuned across the vacuum ultraviolet generated by resonant dispersive-wave emission in a stretched capillary. We use the electron-FROG technique for the pulse measurement and for exploring electron dynamics in small molecules, such as ethylene.

The study of ultrafast valence electron dynamics in many atoms and molecules with an adequate time resolution requires few-cycle light pulses tunable across the ultraviolet spectral range. However, in the deep- and vacuum-ultraviolet (DUV and VUV) the generation and handling of such pulses is very challenging and remained impossible for a long time. Recently, tunable few-cycle UV pulses have become available by resonant dispersive-wave (RDW) emission during soliton self-compression in gas-filled hollow waveguides [1]. The first full measurement of the RDW pulses was performed in the DUV by self-diffraction frequency-resolved optical gating (SD-FROG) [2]. However, such an all-optical arrangement can hardly be applied at even shorter wavelengths, i.e. in the VUV due to the excessive material dispersion.

Here we present the first *in-situ* full characterization of VUV pulses tunable between 160 and 190 nm. Instead of using an all-optical arrangement, we use photoionization-based electron FROG [3]. First, we create two pulse replicas by splitting the wavefront by a segmented mirror and then focus the replicas into a noble gas target. We create photoelectrons by two-photon ionization of the gas, and record the kinetic energy spectrum of the electrons as a function of the delay between the two pulse replicas. Unlike optical FROG, the measured traces not only depend on the pulse shape, but also exhibit a fingerprint of the atomic structure of the target. In order to address this complication we developed a retrieval code based on a differential evolution algorithm. We performed a series of checks to validate our method and measured the RDW pulses at four VUV wavelengths revealing sub-3 fs pulse duration. Fig. 1 represents the measurement of an RDW pulse tuned to a central wavelength of 160 nm.

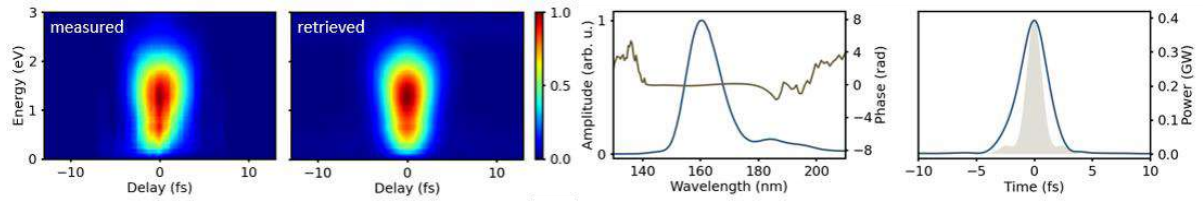


Figure 1: electron FROG measurement of a 2.8 fs pulse centered at 160 nm.

As a first application, we will present a pump-probe measurement of ethylene revealing new details in early-time dynamics of valence electrons.

- [1] J. C. Travers, T. F. Grigorova, C. Brahms, and F. Belli, "High-energy pulse self-compression and ultraviolet generation through soliton dynamics in hollow capillary fibres," Nature Photonics 13, 547-554 (2019).
- [2] M. Reduzzi, M. Pini, L. Mai, F. Cappenberg, L. Colaizzi, F. Vismarra, A. Crego, M. Lucchini, C. Brahms, J. C. Travers, R. Borrego-Varillas, and M. Nisoli, "Direct temporal characterization of sub-3-fs deep UV pulses generated by resonant dispersive wave emission," Optics Express **31**, 26854-26864 (2023).
- [3] T. Sekikawa, T. Katsura, S. Miura, and S. Watanabe, "Measurement of the Intensity-Dependent Atomic Dipole Phase of a High Harmonic by Frequency-Resolved Optical Gating," Physical Review Letters 88, 193902 (2002).
- [4] J. R. C. Andrade, M. Kretschmar, R. Danylo, S. Carlström, T. Witting, A. Mermillod-Blondin, S. Patchkovskii, M. Yu. Ivanov, M. J. J. Vrakking, A. Rouzée and T. Nagy: "High-energy, few-cycle light pulses tunable across the vacuum ultraviolet," under review in Nature Photonics

Bulk self-compression of millijoule 5 μ m pulses to 37 fs in the spatio-temporal soliton regime

Martin Bock, Günter Steinmeyer, and Uwe Griebner*

Max Born Institute, Max-Born-Strasse 2A, 12489 Berlin, Germany *griebner@mbi-berlin.de

Abstract

Temporal soliton self-compression with simultaneous formation of a radial Townes profile is reported in ZnS, leading to the generation of two-cycle pulses at $4.9 \, \mu m$ with $2.0 \, mJ$ energy at 1-kHz repetition rate.

Above 4 μm wavelength, with a large range of materials exhibiting negative GVD, nonlinear bulk compression of ultrashort pulses offers a convenient simplification of dispersion compensation schemes. However, exploitation of self-compression requires the suppression of adverse filamentation effects. Additionally, free-space nonlinear bulk compression schemes typically lead to spatial inhomogeneity of pulse durations across the beam profile. Here we present solitonic self-compression of 2.5 mJ pulses at 5 μ m wavelength in bulk ZnS, yielding compressed pulses with 37 fs duration and 2.0 mJ energy in a 1 kHz pulse train. Excellent spectral homogeneity across the beam profile is demonstrated, which sets our scheme apart from other bulk compression schemes. The high spatio-temporal homogeneity stems from the transformation of a Gaussian input profile into a spatial Townes soliton, leading to a peak power of 45 GW, which constitutes a record value for kHz pulse trains beyond 4 μ m wavelength.

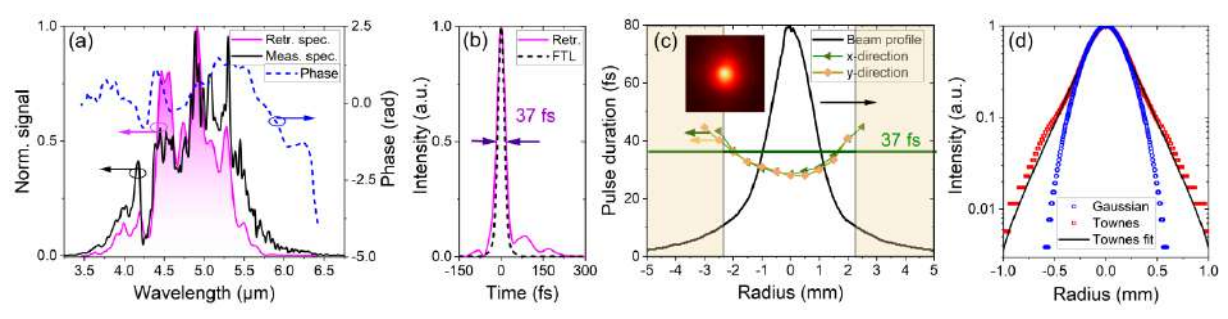


Figure 1: Characterization of self-compressed 5-μm pulses in ZnS. (a) Optical spectrum, (b) temporal shape, (c) spatial-spectral homogeneity, beam profile, (d) transition of Gaussian input beam into Townes profile behind ZnS.

We use idler pulses of a ZGP-based OPCPA at 4.9 µm with 80 fs duration and 2.5 mJ energy as input to the selfcompressor [1]. The scheme is composed of a two-lens telescope and an AR-coated 4-mm thick polycrystalline ZnS plate. The ZnS band gap is at 3.54 eV, and the ZDW is at 3.6 µm. The GVD for the input pulse is -185 fs²/mm. This rather large value is beneficial to enable self-compression. The beam diameter at the sample is 6.5 mm, which translates into an intensity of ~170 GW/cm². The spectrum of the 4.9 µm input pulses are broadened by SPM in ZnS, extending from 3.5 to 6.0 µm (Fig. 1a), which supports FTL pulses of 28 fs. The process is accompanied by a 20% loss, which we chiefly attribute to nonlinear conversion into high harmonics; resulting output pulse energies amount to 2.0 mJ. The input beam profile is dimensioned lest small-scale filamentation appear, resulting in an almost undisturbed beam profile (Inset, Fig. 1c). SH-FROG characterization indicates 37 fs duration (two optical cycles) close to the FTL limit (Fig. 1a,b). The homogeneity of spectral broadening is further analyzed, indicating an energy content of 87% within a 40 fs time window and an averaged pulse duration of 37 fs in the entire beam cross-section (Fig. 1c). The V-parameter is only slightly reduced towards the beam edges, but appears larger than 85% within the 1/e² beam intensity range. Finally, the spatial evolution of the beam profile beyond the ZnS sample is analyzed. This analysis indicates an additional prominent focusing effect due to nonlinear Kerr lensing, leading to the formation of a Townes profile with extended spatial wings after another meter of propagation (Fig. 1d). To substantiate this claim, we numerically solved the eigenvalue problem of the nonlinear paraxial wave equation. Combined action of self-focusing and subsequent diffraction leads to homogenization of spectral content across the beam during formation of the Townes soliton. This selfhomogenizing compression scheme highly simplifies the generation of few-cycle pulses in the mid-infrared.

[1] M. Bock, L. von Grafenstein, U. Griebner, and T. Elsaesser, J. Opt. Soc. Am. B35, C18 (2018).

525-MW peak power, 100-kHz, sub-100 femtosecond Holmium laser at 2.1 µm

Boldizsar Kassai*, Anna Suzuki, Alan Omar, Yicheng Wang, Sergei Tomilov, Martin Hoffmann, and Clara J. Saraceno

Photonics and Ultrafast Laser Science, Ruhr-Universität Bochum, Universitätsstrasse 150, 44801 Bochum, Germany *boldizsar.kassai@ruhr-uni-bochum.de

Abstract

We present a high-peak-power $2.1-\mu m$ laser system consisting of a Ho:CALGO regenerative amplifier and a Herriott-type bulk multi-pass cell (MPC) for external pulse compression. The amplifier generates 9.2-W, 92- μ J, 750-fs pulses at 100-kHz repetition rate, and the MPC provides sub-100-fs pulses with 92% optical transmission, resulting in >500-MW peak power.

High-power ultrafast 2- μ m lasers are attractive for various applications including secondary sources and laser processing among others. While conventional 2- μ m sources typically rely on optical parametric amplifiers (OPAs) pumped by high-power near infrared lasers, direct laser amplification using Tm, Ho lasers is an attractive alternative for efficiency, power and energy scalability. The operation wavelength of Ho-doped solid-state lasers at around 2.1 μ m is in a high atmospheric transparency window, facilitating power and energy scaling and free-space propagation without beam degradation. In this regard, Ho:CALGO is an attractive gain material for amplification due to its combination of broad gain bandwidth and relatively large cross section, enabling femtosecond pulse amplification. This contrasts with most typically used Ho-doped materials, which achieve very high pulse energies well beyond the mJ level but restricted pulse durations to several ps due to strong gain narrowing effects [1]. In this study, we present a 2.1- μ m chirped pulse regenerative amplifier using Ho:CALGO. We achieve 9.2-W average output power with a pulse duration of 750 fs at a 100-kHz repetition rate. Subsequently, a nonlinear pulse compression stage further enhances the peak power to 525 MW with sub-100 fs pulses. This is the highest reported peak power at this repetition rate for 2.1- μ m Ho-doped systems and the first demonstration of a bulk MPC at 2 μ m.

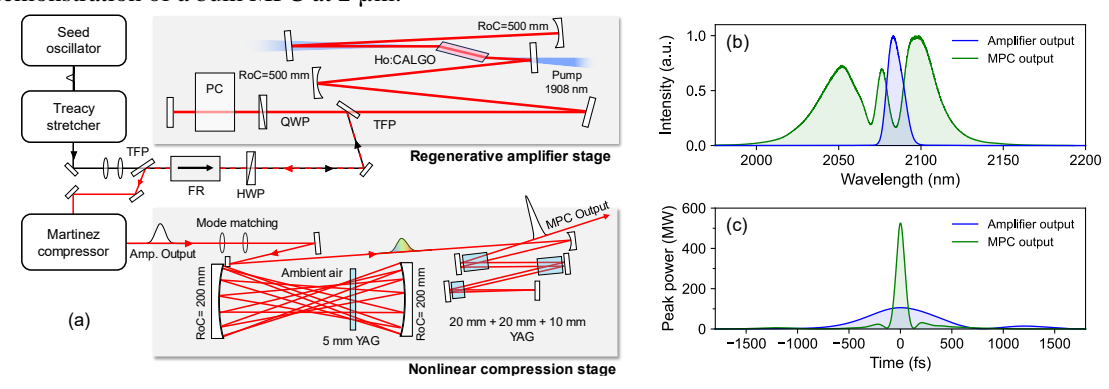


Figure 1: (a) Experimental setup of the Ho:CALGO CPA and nonlinear compression stage. (b) Optical spectra of amplifier output and MPC output at 100 kHz. (c) Temporal pulse profile retrieved from SHG-FROG trace.

Our setup is shown in Fig. 1(a). The Ho:CALGO regenerative amplifier is based on a basic CPA arrangement and the Herriott-type MPC uses YAG as the nonlinear medium followed by three YAG plates which provided the material dispersion for temporal compression. At the CPA stage, we obtain an average power of 9.2 W at 100 kHz. The blue plots in Fig. 1(b, c) show spectra and temporal profile of output pulses from the amplifier. The pulse duration and peak power from the amplifier are 750 fs and 107 MW, respectively. At the nonlinear compression stage, the spectrum of the pulses is broadened by self-phase modulation as shown in the green plot in Fig 1(b), and subsequently compressed to 97 fs, close to the Fourier transform limit of 91 fs. The calculated peak power reached 525 MW, demonstrating an unprecedented combination of high peak power and high repetition rate at this wavelength region. Further pulse energy and peak power scaling is expected in the future.

Generation of 1.5-cycle optical pulses with 60 μJ energy at 3.2 μm

Rajaram Shrestha,¹* Katalin Pirisi,¹ Zoltan Kis,¹ Levente Abrok,¹ Jie Meng,¹ Eric Cormier,¹,² and Bálint Kiss¹

Abstract

We experimentally demonstrated the post-compression of 45 fs, $3.2~\mu m$ laser pulses in mm-thick BaF_2 and Si optical windows followed by recompression in CaF_2/BaF_2 bulk and third-order compensation mirrors resulting in 1.5 optical cycle with 60 μJ of clean compressed pulses with excellent long-term stability, enabling advanced high-intensity applications.

The ELI-ALPS mid-IR OPCPA system provides up to $100~\mu J$, 45 fs phase-stable pulses at 100~kHz repetition rate with a central wavelength of $3.2~\mu m$ [1]. Although such short (four-cycle) pulses allow successful investigations of laser-matter interaction, such as harmonic generation in semiconductor crystals, CEP-sensitive phenomena become more pronounced with shorter pulses [2]. A post-compression system providing 2.3-cycle pulses was implemented before [3], which has been further developed to output 1.5-cycle CEP-stable pulses.

Spectral broadening (covering 1.9-4.2 μm range) is performed in 3-6 mm-thick dielectric (BaF₂) and 1mm semi-conductor (Si) windows in a confocal geometry, followed by recompression in bulk BaF₂ windows combined with dispersive mirrors for third order dispersion (TOD) compensation. We optimized the input intensity for each windows by careful positioning of them along the beam waist in order to balance between broadening factor, stability, laser induced damage and nonlinear absorption. The combination of 5 mm BaF₂ and 1 mm Si window found to be optimal in terms of spectral stability and calculated FTL durations (13 fs) with 6W output (8.2W input) average power. Optimal recompression was achieved in 5 mm CaF₂, 6 mm BaF₂ and 3 reflections on TOD mirrors yielding 14.5 fs pulses with 60 μ J energy, characterized by TIPTOE technique (Figure 1). The long-term stability of power, spectrum, CEP and –most importantly, the generated high harmonics in ZnO bulk crystal– will be discussed.

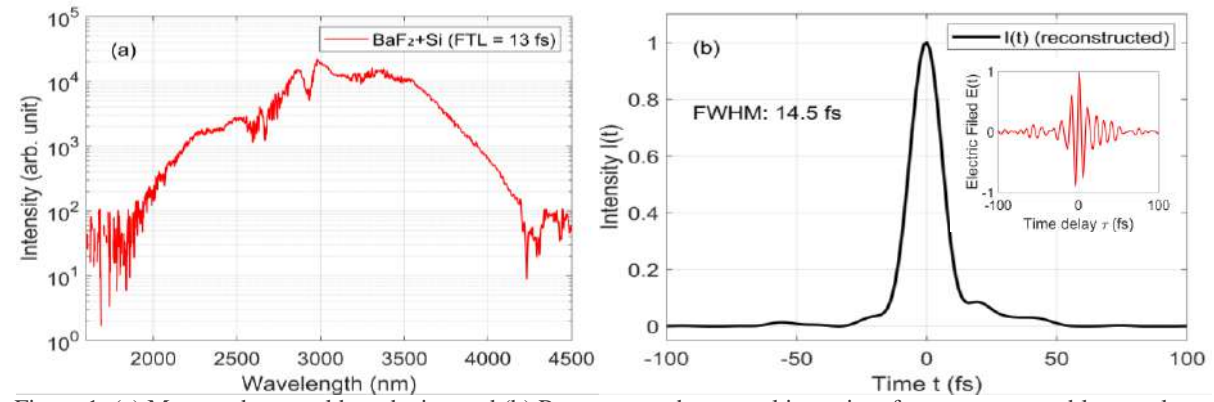


Figure 1: (a) Measured spectral broadening and (b) Reconstructed temporal intensity of post compressed laser pulses with FWHM pulse duration around 15 fs. Inset: Reconstructed electric field versus delay by TIPTOE

[1] N. Thiré, R. Maksimenka, B. Kiss, C. Ferchaud, G. Gitzinger, T. Pinoteau, H. Jousselin, S. Jarosch, P. Bizouard, V. Di Pietro, E. Cormier, K. Osvay, and N. Forget, "Highly stable, 15 W, few-cycle, 65 mrad CEPnoise mid-IR OPCPA for statistical physics," Optics Express **26**, 26907–26915 (2018).

[2] B. Nagyillés, G. N. Nagy, B. Kiss, E. Cormier, P. Földi, K. Varjú, S. Kahaly, M. U. Kahaly, and Z. Diveki, "MIR laser CEP estimation using machine learning concepts in bulk high harmonic generation," Optics Express **32**, 46500–46510 (2024).

[3] M. Kurucz, R. Flender, L. Haizer, R. S. Nagymihaly, W. Cho, K. T. Kim, S. Toth, E. Cormier, and B. Kiss, "2.3-cycle mid-infrared pulses from hybrid thin-plate post-compression at 7 W average power," Optics Communications. **472**, 126035 (2020).

¹ ELI ERIC, ALPS Facility, Wolfgang Sandner u. 3, H-6728 Szeged, Hungary

² Laboratoire Photonique Numérique et Nanosciences (LP2N), UMR 5298, CNRS-IOGS-Université Bordeaux, Bordeaux, France

^{*}rajaram.shrestha@eli-alps.hu

△ UFO XIV Azores 2025

Ytterbium-laser-driven resonant dispersive emission generating wavelength-tuneable few-femtosecond far-ultraviolet pulses

Christian Brahms,^{1,*} Deepjyoti Satpathy,¹ Nikoleta Kotsina,¹ and John C. Travers¹

¹School of Engineering and Physical Sciences, Heriot-Watt University, Edinburgh EH14 4AS, United Kingdom *c.brahms@hw.ac.uk

Abstract

We present a setup to compress laser pulses from an Yb-based laser to 10 fs and to generate few-femtosecond resonant dispersive wave pulses in the far-ultraviolet (100–350 nm) at up to 100 kHz repetition rate. We characterise the far-ultraviolet pulses using in-vacuum transient-grating frequency-resolved optical gating.

Virtually all materials and molecular systems have strong absorption resonances in the far ultraviolet (UV) wavelength region (100–300 nm). Few-femtosecond laser pulses in this region are therefore an important tool for next-generation ultrafast science. Resonant dispersive wave (RDW) emission from higher-order solitons propagating in gas-filled hollow capillary fibres (HCFs) can efficiently generate bright, wavelength-tuneable and extremely short far-UV pulses [1]. For high-sensitivity measurements, it is vital for these sources to operate at much higher repetition rate than in the initial experiments using titanium-doped sapphire amplifiers. We have previously demonstrated far-UV generation above 200 nm at repetition rates up to 50 kHz and average power up to 360 mW with a compact, ytterbium-based drive laser [2]. However, RDW emission below 200 nm, further scaling to Watt-level average power, and the few-femtosecond duration of the pulses [3] have yet to be demonstrated with such a source.

Here we present a three-stage setup (Fig. 1a) to generate few-femtosecond RDW pulses at up to 100 kHz repetition rate. The first two stages of gas-filled, stretched HCF, in combination with two sets of chirped mirrors, compress the pulses from the drive laser (Light Conversion Carbide) from 330 fs to 10 fs. Far UV pulses are generated in the third HCF, which is coupled to a vacuum chamber. So far, we have obtained far UV emission above 200 nm at up to 33 kHz. We have also obtained VUV emission down to 140 nm at lower repetition rate (Fig. 1b). The compressor operates at up to 100 kHz (80 W input power) with an overall efficiency of 66% (Fig. 1c, d). All-in-vacuum transient-grating FROG measurements that the source is capable of generated as for the order for the solution for the capable of the capable of generated as for the order for the solution for the capable of the capable

We are currently working on scaling the system to combine the capabilities demonstrated so far to achieve few-femtosecond vacuum ultraviolet (VUV) generation at $100\,\mathrm{kHz}$.

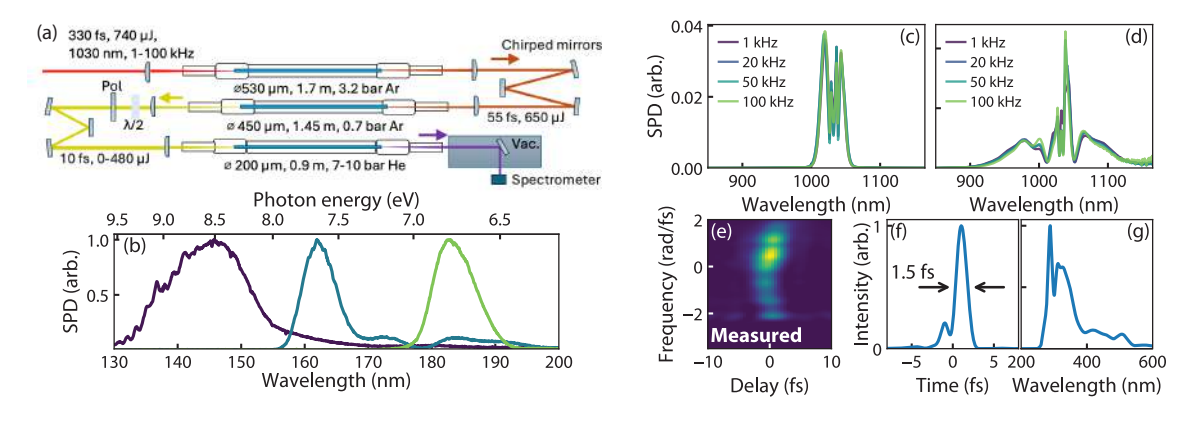


Figure 1: (a) Layout of the light source. (b) Spectral power density (SPD) of VUV RDWs down to 140 nm at 4 kHz. (c, d) Normalised SPD of the two compressor stages. (e-g) TG-FROG measurement of a deep UV RDW at 33 kHz.

- [1] J.C. Travers et al., Nature Photonics 13, 547 (2019).
- [2] C. Brahms and J.C. Travers, Optics Letters 48, 151 (2023).
- [3] M. Reduzzi et al., Opt. Express 32, 31, 26854 (2023).

UV/VIS Frequency Combs for Novel Applications in Dual Comb Spectroscopy

Alexander Eber¹, Lukas Fürst¹, Christoph Gruber¹, Adrian Kirchner¹, Armin Speletz¹, Robert di Vora¹, Emily Hruska¹, Mithun Pal¹, Marcus Ossiander^{1,2} and Birgitta Bernhardt^{1,*}

¹Institute of Experimental Physics, Graz University of Technology, Petersgasse 16, 8010 Graz, Austria ²Harvard John A. Paulson School of Engineering and Applied Sciences, 9 Oxford Street Cambridge, Massachusetts 02138, United States

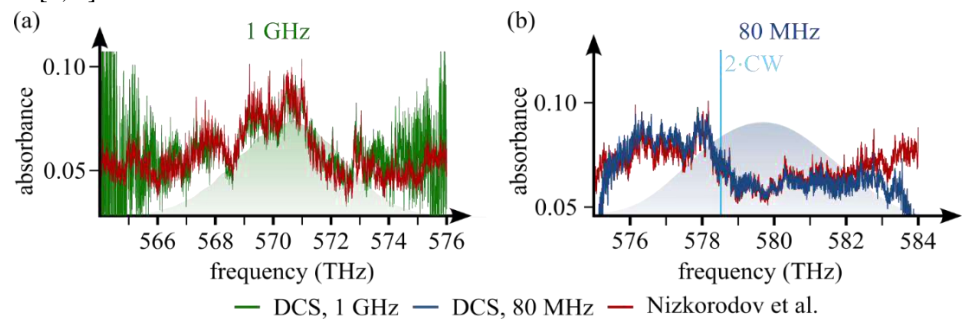
*bernhardt@tugraz.at

Abstract

This contribution demonstrates different UV/VIS laser frequency combs and dual comb spectroscopy's ability to rapidly and precisely study molecular gasses and their dynamics, e.g. providing insights into formaldehyde's optical properties and urban nitrogen dioxide concentration changes, both pollution gasses of high environmental impact.

Although the development of ultraviolet (UV) frequency combs has been accomplished 20 years ago [1, 2], it was only very recently that the ultraviolet spectral region has been conquered by dual comb spectroscopy (DCS) [3-7]. DCS combines broad spectral coverage with frequency comb precision, fast measurement speeds and high spectral resolution. However, as frequency combs mainly emit in the infrared region, frequency up-conversion into the UV is still required for UV DCS. This makes UV DCS challenging: the conversion efficiency scales with pulse energy and hence increases with shrinking pulse repetition rates. On the other hand, DCS favors high repetition rates for stable conditions during the pulse interferometry.

In this conference contribution, the most recent projects of the Coherent Sensing Group at TU Graz aiming at UV/VIS frequency comb generation and DCS will be presented. The efforts advancing dual comb spectroscopy include different comb systems with different repetition rates and the extension into the vacuum ultraviolet via nonlinear methods such as high harmonic generation. Intermediate steps recently enabled dual comb spectroscopy in real time and in the field for atmospheric sensing of nitrogen dioxide with an unprecedented temporal resolution of one second [8, 9].



Nitrogen dioxide absorption spectroscopy with two DCS different systems [10]. The experimental data (green and blue curves, respectively) are compared to Nizkorodov et al. [47] (red curves). (a) Comparison of the 1 GHz system measured with a detuning of 19.8 kHz and a total acquisition time of 500 ms. (b) Measurement with the phase-locked 80 MHz system with 24 Hz detuning and averaged over 2500 interference patterns, resulting in a total acquisition time of 100 s.

- [1] C. Gohle et al., "A frequency comb in the extreme ultraviolet", Nature 436, 234 (2005).
- [2] R. Jason Jones et al., Phys. Rev. Lett. 94, 193201 (2005).
- [3] B. Xu et al., "Near-ultraviolet photon-counting dual-comb spectroscopy". Nature 627, 289 (2024).
- [4] K. F. Chang et al., Multi-harmonic near-infrared-ultraviolet dual-comb spectrometer", Opt Lett 49, 1684 (2024).
- [5] J. J. McCauley et al., "Dual-comb spectroscopy in the deep ultraviolet. Optica 11, 460 (2024).
- [6] A., Muraviev et al., Optica 11, 1486 (2024).
- [7] L., Fürst et al. "Broadband near-ultraviolet dual comb spectroscopy". Optica 11, 471 (2024).
- [8] A. Eber et al., "Streaming self-corrected dual-comb spectrometer", Optics Letters, 33, 35314 (2025)
- [9] A. Eber et al., Coherent field sensing of nitrogen dioxide. Opt Express 32, 6575 (2024).
- [10] A. Eber et al., NIR/VIS DCS comparing high and low repetition rate regimes, arXiv:2509.02159 (2025)

Ultrafast 1-GHz dual-comb optical parametric oscillator from a single cavity

Carolin P. Bauer,^{1,*} Benjamin Willenberg, Justinas Pupeikis, and Ursula Keller²

¹Institute for Quantum Electronics, ETH Zurich, Auguste-Piccard Hof 1, 8093 Zurich, Switzerland

Abstract

We present a femtosecond dual-comb optical parametric oscillator (OPO) at 1 GHz. The singly-resonant single-cavity dual-comb OPO is synchronously pumped by a Yb:CaF $_2$ solid-state single-cavity dual-comb laser. The OPO exhibits high power-per-comb line and an ultra-low timing jitter of 7.1 fs [100 Hz, 10 kHz]; ideal for sensitive open-path spectroscopy.

Results

Dual-comb spectroscopy (DCS) enables rapid high-resolution gas measurements across wide spectral ranges [1]. However, achieving optimal measurement sensitivity remains a challenge. Dual-comb systems at 1-GHz repetition rate provide optimal spectral resolution at ambient pressure and high power-per-comb line, offering a significant sensitivity improvement over conventional ~100-MHz systems. Synchronously pumped optical parametric oscillators (OPOs) are an ideal source to access the longer wavelength regime given their wide tunability, high conversion efficiencies, and the preservation of the low noise performance of the pump.

Here, we demonstrate a powerful, wavelength-tunable, and low-noise synchronously pumped OPO in a single-cavity dual-comb configuration at 1 GHz (Fig. 1a-b). Both the laser and the OPO are based on a spatially multiplexed 15-cm-long linear cavity. An intra-cavity biprism defines two cavity modes in each oscillator, respectively [2]. Due to the ultra-low timing noise of this specific laser implementation and the single-cavity operation, a sub-optical-cycle relative timing jitter (5.6 fs (pump), 7.1 fs (signal) [100 Hz, 10 kHz]) is obtained. Neither f_{rep} , the OPO cavity, nor the carrier-envelope offset frequencies are stabilized. Instead, the system relies on mutual coherence for DCS only. Simultaneous synchronous pumping of both combs is obtained by adjusting the end mirror and biprism position. By adjusting the vertical position of the fan-out 5 mol.% MgO doped periodically-poled LiNbO₃ (PPLN) crystal (HC Photonics) in the OPO cavity, the center wavelength is tunable (Fig. 1c-d) ($\Delta v_{\text{FWHM}} \sim 2 \text{ THz}$). In the present configuration, the pump power is reduced to operate the OPO 2.5x above threshold with a 1.5% output coupler. This is the first ultrafast dual-comb OPO at 1 GHz repetition rate. To demonstrate the suitability of the source for DCS, we will apply it to high-sensitivity open-path DCS.

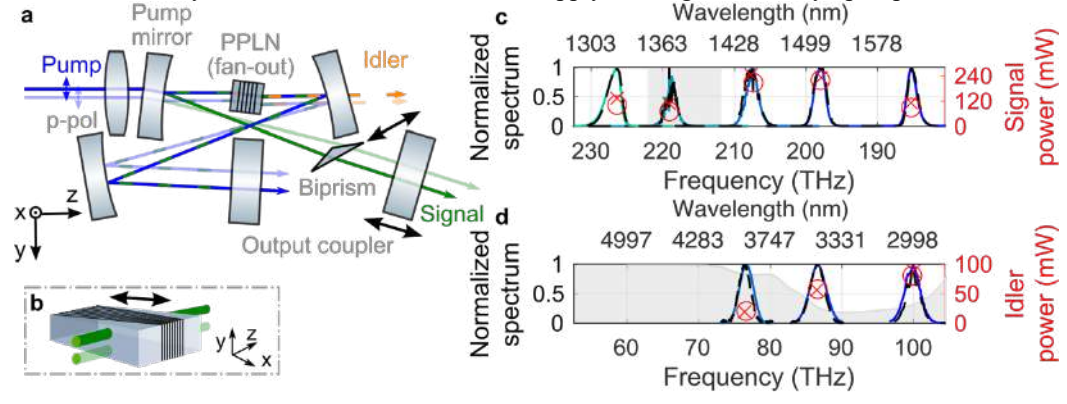


Fig. 1 (a)-(b) Schematic of the experimental implementation of the dual-comb OPO. (c) Optical signal spectra at different tuning points (comb 1 in color, comb 2 in dashed black). Water absorption window (grey shaded). (d) Corresponding idler tuning range. Absorption from idler transmitting dichroic cavity fused silica mirror (grey shaded).

- [1] I. Coddington, N. Newbury, and W. Swann, "Dual-comb spectroscopy," Optica 3, 414-426 (2016).
- [2] J. Pupeikis, B. Willenberg, S. L. Camenzind, A. Benayad, P. Camy, C. R. Phillips, and U. Keller, "Spatially multiplexed single-cavity dual-comb laser," Optica 9, 713-716 (2022).

²Dept. of Information Technology and Electrical Engineering, ETH Zurich, Gloriastrasse 35, 8092 Zurich, Switzerland *cabauer@phys.ethz.ch

Dual-comb Fiber Laser with Dual-phase-biased Nonlinear Amplifying Loop Mirror

Jiayang Chen,1 Yuxuan Ma,1 O. H. Heckl2 and Guanhao Wu1,*

¹Department of Precision Instrument, Tsinghua University, Haidian District, Beijing 100084, China ²Optical Metrology Group, Faculty of Physics, University of Vienna, Boltzmanngasse 5, 1090 Vienna, Austria *guanhaowu@mail.tsinghua.edu.cn

Abstract

We demonstrate a polarization-multiplexed dual-comb fiber laser with a dual-phase-biased nonlinear amplifying loop mirror. The laser generates two orthogonal pulse trains with a tunable repetition rate difference. A proof-of-principle dual-comb ranging experiment using the time-of-flight method achieved micro-level precision in all free-running operation.

A compact and coherent dual optical frequency comb laser source is a powerful tool in optical metrology [1]. Generating two pulse trains within a single laser cavity naturally ensures mutual coherence between the combs while simplifying the laser configurations [2]. We present a configuration that multiplexes polarizations in an all polarization-maintaining (PM) fiber laser [3] using nonlinear amplifying loop mirror (NALM) mode-locking [4]. Figure 1(a) shows the schematic of the fiber laser and the dual-comb ranging experiment. The laser features a dual-phase-bias module that enables mode-locking in both axes of the PM fiber. The output from each axis (Fig. 1(b)) has a broad and nearly identical spectra. The laser has a nominal repetition rate of ~51.52MHz and a difference in repetition rate of ~1.5kHz. By adjusting one of the mirrors in the dual-phase-bias module, the repetition rate difference can be tuned over a flexible range up to 80 kHz. We conducted a dual-comb ranging experiment in a free-running operation, achieving a precision of 1.88 µm in 500 ms acquisition time (Fig. 1(c)). The dual-phase-bias module could be integrated into a monolithic component, paving the way for a more compact dual-comb laser design.

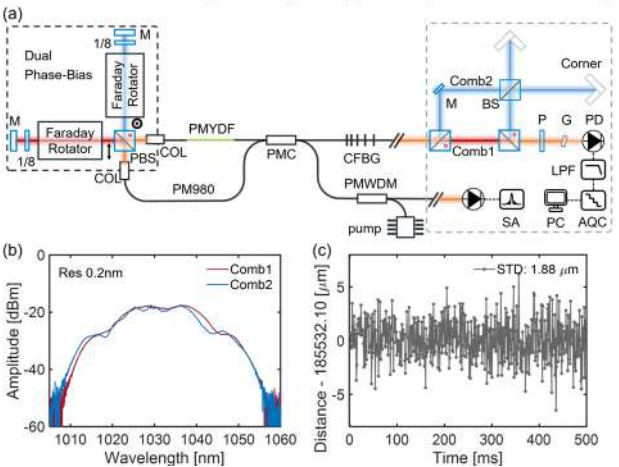


Figure 1: (a) Schematic of the dual-phase-biased NALM fiber laser. M: mirror; 1/8: one-eighth waveplate; COL: collimator; PBS: polarization beam splitter; PMYDF: PM Yb-doped fiber; PMC: PM coupler; CFBG: chirped fiber Bragg grating; PMWDM: PM wavelength-division-multiplexer; BS: beam splitter; P: polarizer; G: grating; PD: photodiode; LPF: low pass filter; AQC: acquisition card; SA: spectrum analyzer. (b) Optical spectra of the two combs. (c) Calculated distance results over a 500 ms acquisition time.

- I. Coddington, W. C. Swann, L. Nenadovic, and N. R. Newbury, "Rapid and precise absolute distance measurements at long range," Nature Photon 3(6), 351–356 (2009).
- 2. J. Yang, X. Zhao, L. Zhang, and Z. Zheng, "Single-cavity dual-comb fiber lasers and their applications," Front. Phys. 10, (2023).
- 3. P. E. C. Aldia, J. Chen, J. K. C. Ballentin, L. W. Perner, and O. H. Heckl, "Detection of carbon monoxide using a polarization-multiplexed erbium dual-comb fiber laser," J. Phys. Photonics **6**(4), 045017 (2024).
- 4. Y. Ma, S. H. Salman, C. Li, C. Mahnke, Y. Hua, S. Droste, J. Fellinger, A. S. Mayer, O. H. Heckl, C. M. Heyl, and I. Hartl, "Compact, All-PM Fiber Integrated and Alignment-Free Ultrafast Yb:Fiber NALM Laser With Sub-Femtosecond Timing Jitter," Journal of Lightwave Technology **39**(13), 4431–4438 (2021).

Dual-comb modelocked Er:Yb:glass oscillator at 500 MHz

Benjamin Willenberg^{1,2}, Justinas Pupeikis^{1,2}, Moritz Seidel¹, Marco Gaulke¹, Matthias Golling¹, and Ursula Keller¹

¹ Department of Physics, ETH Zurich, 8093 Zurich, Switzerland, ² K2 Photonics AG, 8005 Zurich, Switzerland *bwillenb@phys.ethz.ch

Abstract

We demonstrate a spatially multiplexed dual-comb mode-locked Er:Yb:glass solid-state oscillator at 500 MHz. The laser outputs two coherent pulse trains (~40 mW, 230 fs), enabling high-resolution dual-comb spectroscopy without any stabilization.

Results

Dual-comb lasers have emerged as powerful light sources for high-resolution gas spectroscopy and various metrology applications [1]. Among methods to generate dual-comb light, single-cavity dual-comb modelocking is attractive due to its minimal number of required components. Spatial multiplexing using a biprism [2] avoids the crosstalk common in related approaches, provides direct control over the repetition rate difference, and is compatible with high-performance high-repetition-rate lasers, which are advantageous for fast measurements.

A 1550 nm dual-comb light source is appealing for practical applications because of its relative eye safety, proximity to industrially relevant gas absorption lines, availability of mature telecommunication components, and favorable dispersion properties of various waveguide materials. Here, we demonstrate the first single-cavity, dual-comb light source based on an Er:Yb:glass laser using spatial multiplexing. We show sufficient mutual coherence of the source for coherent dual-comb spectroscopy with 487 MHz spectral resolution.

The confocal laser cavity (Fig. 1a) is spatially multiplexed with a biprism in transmission and generates two pulse trains with slightly different repetition rates, tunable within ± 80 kHz around 487 MHz (Fig. 1b). Soliton modelocking is achieved using an InGaAs-based semiconductor saturable absorber mirror (SESAM). Each comb delivers 40 mW of optical power with a spectral bandwidth of ~11 nm centered at 1552 nm (Fig. 1b) and 230 fs pulses. Heterodyning of the two pulse trains reveals the radio-frequency comb lines without postprocessing.

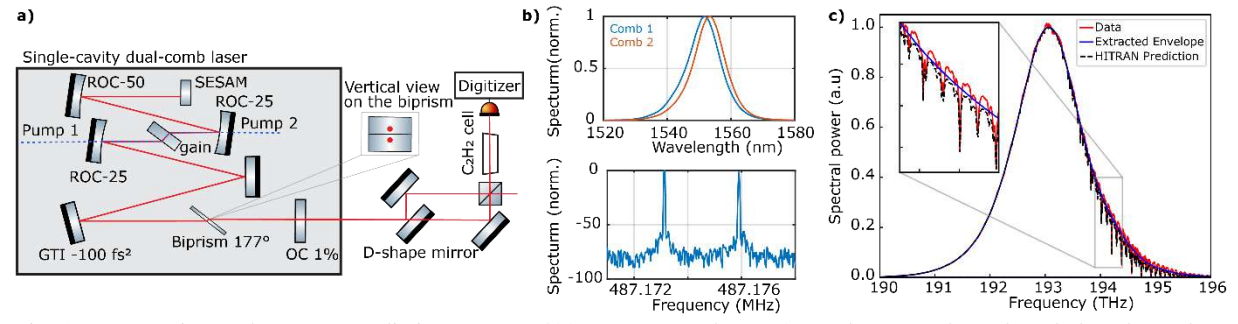


Fig. 1: (a) Experimental setup. Two distinct spots (~400 μm separated) on a 2-mm long Er:Yb co-doped phosphate glass are pumped by two separate 980-nm pumps. A 1-mm thick 177° biprism is used to spatially multiplex the cavity. (b) Optical and microwave spectrum (zoom). (c) Coherently averaged dual-comb measurement of an acetylene gas cell.

To demonstrate the laser's suitability for dual-comb spectroscopy, the interferometrically combined pulse trains (Δf_{rep} around 19 kHz) were passed through an acetylene gas cell (1 bar, 20 cm) and detected on a photodiode. The interferograms were computationally processed [3] and coherently averaged over 1 second of acquisition. The measured absorption features (Fig. 1c) closely match the HITRAN prediction. In this demonstration, the envelope extraction was influenced by the strong acetylene absorption, limiting the accurate estimate of the absorbance.

This work represents a step forward in dual-comb light source development, demonstrating that spatial multiplexing can be successfully applied to Er:Yb:glass solid-state lasers despite the material's challenging thermal properties and significant thermally-induced birefringence. We will discuss how spatial multiplexing counterintuitively overcomes these obstacles, paving the way for a practical dual-comb system at 1550 nm.

- [1] I. Coddington, N. Newbury, and W. Swann, "Dual-comb spectroscopy," Optica 3, 414 (2016).
- [2] J. Pupeikis, B. Willenberg, S. L. Camenzind, A. Benayad, P. Camy, C. R. Phillips, and U. Keller, "Spatially multiplexed single-cavity dual-comb laser," Optica 9, 713–716 (2022).
- [3] C. R. Phillips, B. Willenberg, A. Nussbaum-Lapping, F. Callegari, S. L. Camenzind, J. Pupeikis, and U. Keller, "Coherently averaged dual-comb spectroscopy with a low-noise and high-power free-running gigahertz dual-comb laser," Optics Express 31, 7103 (2022).

Single-Cavity Free-Running Kerr-Lens Mode-Locked Dual-Comb Laser at 2.1 µm

Mykyta Redkin*, Yicheng Wang, Sergei Tomilov and Clara J. Saraceno

Photonics and Ultrafast Laser Science, Ruhr Universität Bochum, Universitätsstraβe 150, 44801 Bochum, Germany *Mykyta.Redkin@ruhr-uni-bochum.de

Abstract

We demonstrate a free-running, soft-aperture Kerr-lens mode-locked dual-comb laser system operating at 2.1 μ m. Utilizing a Ho:CALGO gain medium, it generates sub-100-fs pulses with >(2x)1W output power. The system enables high-speed interferometry, highlighting its potential for precision measurements in the mid-infrared region.

Dual-comb laser systems have gained significant attention for applications in pump-probe sampling, optical ranging, and spectroscopy [1]. Single-cavity designs with spatially multiplexed pulse trains simplify these systems by eliminating complex phase-locking electronics and reducing correlated noise [2]. However, few of such systems have been demonstrated in the 2-µm range, which is crucial for spectroscopic sensing and mid-IR frequency conversion. A Cr:ZnSe-based system at 2.36 µm achieved 200-mW average power, 30-nm spectral bandwidth, and 200-fs pulse durations [3]. Here, we report on a free-running, soft-aperture Kerr-lens mode-locked dual-comb laser at 2.13 µm using a Ho:CALGO gain medium. The system delivers >2 W total output power (1 W per comb) with sub-100-fs pulses at a 96.5 MHz repetition rate. This represents a five-fold average power increase, and a two-fold bandwidth increase over previous systems in this wavelength region, demonstrating its potential for spectroscopic applications in the near future.

The dual-comb laser system, shown in Fig. 1(a), is pumped by a 30-W single-mode 1940-nm Tm-fiber laser. A 50/50 beam splitter divides the pump beam, enabling parallel pumping of two volumes in the 3-at.%-doped Ho:CALGO crystal, separated by ~2 mm to avoid mode competition. The cavity consists of two resonators sharing a pair of 200-mm radius of curvature mirrors and a dispersive mirror introducing -1500 fs² GDD per round trip. Each cavity includes an output coupler (OC) and a high reflective mirror (HR), with one OC on a translation stage for tuning $\Delta f_{rep} = \pm 400$ kHz. Soft-aperture KLM is achieved at 17-W pump power. The laser produces ~90-fs pulses with 50-nm bandwidth at 2133 nm and 2135 nm. With 3% OCs, the system could deliver a maximum average power of 1.17 W and 1.02 W at 96.5 MHz. Figure 1(c) shows a measured interferogram trace at a Δf_{rep} of ~96 Hz. Future works will include improvements in the mechanical stability of the laser, enhancement of the signal-to-noise ratio through averaging, and ultimately the development of spectroscopic applications.

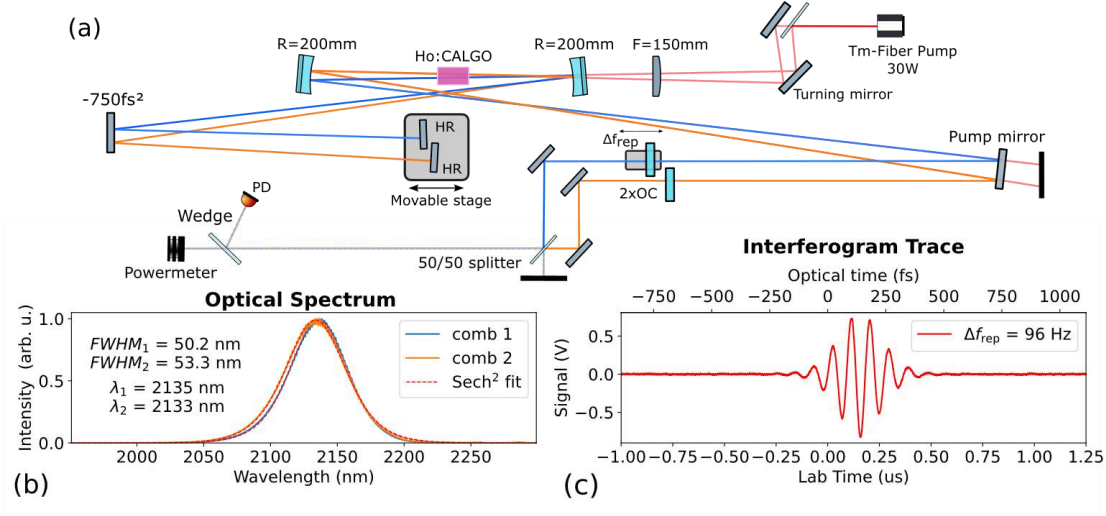


Figure 1: (a) Schematic of the experiment setup, (b) Optical spectra with sech² fit, showing a soliton pulsed with FWHM ~ 50 nm at the center wavelength 2135 nm and 2133 nm, (c) Interferogram example of two collinearly overlapped pulse traces, combined onto one photodiode (PD)

- [1] I. Coddington, et al., "Dual-comb spectroscopy," Optica 3, 414-426 (2016)
- [2] J. Pupeikis, et al., "Spatially multiplexed single-cavity dual-comb laser," Optica 9, 713-716 (2022)
- [3] A. Barh, et al., "Single-cavity dual-modelocked 2.36-µm laser," Optics Express 31, 6475-6483 (2023)

Generation of burst of pulses at 3 µm with widely tunable multi GHz repetition rate

Andrea Monzani^{1,2,*}, Peyo Planche¹, David Horain², Damien Espitallier², Eric Freysz³, Julien Didierjean², Julien Saby², Abdelkrim Bendahmane¹, Giorgio Santarelli¹, Eric Cormier¹

Abstract

We report on the generation and control of high-power trains of pulses with adjustable pulse repetition rates ranging from 1 to 15 GHz at a wavelength around 3 µm.

The recent years have seen growing a sharp interest in sources providing sequences of ultrashort pulses with extreme repetition rates at the GHz level. Beyond obvious telecommunication concerns, micro-machining with NIR bursts of GHz pulses became a hot topic [1]. Converted to UV or DUV, such sources are unavoidable tools in the context of X-band photo-injectors [2]. There is however very little work reporting on GHz sources in the midIR where many applications are also requesting such systems such as for instance pollutant detection or astronomical spectrograph calibration [3]. Here, we report on the generation of Watt-level bursts of pulses whose pulse repetition rate can be freely adjusted from 1 to 18 GHz at a tunable wavelength around 3 µm.

The system consists in an optical parametric amplifier (OPA). The NIR pump is a high-power burst-mode electro-optical comb delivering several W of average power at 1030 nm with 1 ps pulses. The pulse repetition rate, the number of pulses in the burst and the burst repetition rate can be freely adjusted. The signal seeding the OPA is a CW Er-doped fiber laser whose wavelength is tunable around 1550 nm. A 1 cm long periodically poled Lithium Niobate crystal is used to generate an idler wave around 3 μ m by DFG. Thanks to the second-order non-linear process properties, the temporal and spectral structure of the pump are transferred to the idler wave. It results in a midIR train of pulses with the same temporal properties as the pump and in the frequency domain to a transient frequency comb as displayed in figure 1.

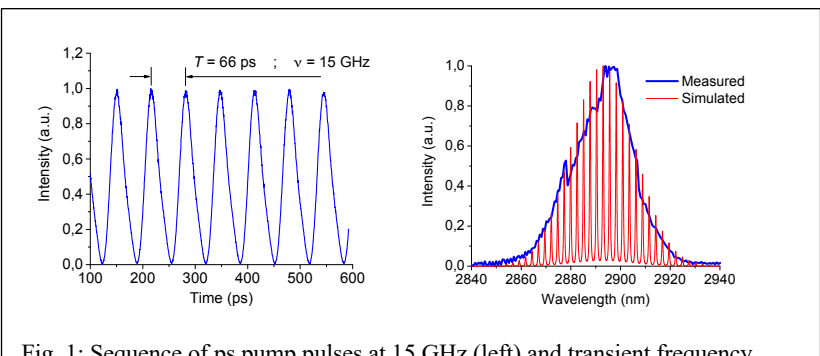


Fig. 1: Sequence of ps pump pulses at 15 GHz (left) and transient frequency comb at the idler wavelength around 3 μ m (right).

The source is tunable in repetition rate between 1 and 15 GHz, as well as adjustable in wavelength between 2.88 to 3.03 μ m. Typical bursts contain 50 to 2000 pulses.

Power scalability is easily achieved by adding non-linear stages and in practice only limited by the available pump amplifier power. The major advantage of the burst mode compare to a continuous emission of GHz pulses, is the ability of achieving

high peak powers and therefore induce strong non-linear effects in either fibers or bulk materials leading to powerful supercontinuum in the midIR.

- 1. C. Kerse, H. Kalaycıoğlu, P. Elahi, B. Çetin, D. K. Kesim, Ö. Akçaalan, S. Yavaş, M. D. Aşık, B. Öktem, H. Hoogland, R. Holzwarth, and F. Ö. Ilday, "Ablation-cooled material removal with ultrafast bursts of pulses," Nature **537**, 84 (2016).
- 2. H. Ye, L. Pontagnier, C. Dixneuf, G. Santarelli, and E. Cormier, "Multi-GHz repetition rate, femtosecond deep ultraviolet source in burst mode derived from an electro-optic comb," Opt. Express, OE **28**, 37209–37217 (2020).
- 3. P. Sekhar, M. K. Kreider, C. Fredrick, J. P. Ninan, C. F. Bender, R. Terrien, S. Mahadevan, and S. A. Diddams, "Tunable 30 GHz laser frequency comb for astronomical spectrograph characterization and calibration," Opt. Lett., OL 49, 6257–6260 (2024).

¹Laboratoire Photonique Numérique et Nanosciences (LP2N), UMR 5298, CNRS-IOGS-Université Bordeaux, 33400 Talence, France

²Bloom Lasers, 11 Avenue de Canteranne, 33600 Pessac

³Laboratoire Ondes et Matiere d'Aquitaine (LOMA), UMR 5798, 351 Crs de la Libération, 33400 Talence *andrea.andrea@u-bordeaux.fr

Attosecond technology deciphering

a chemical reaction

S. Severino¹, K.M. Ziems², M. Reduzzi¹, A. Summers¹, H.-W. Sun¹, Y.-H. Chien¹, S. Gräfe^{2,3,4}, J. Biegert^{1,5,*}

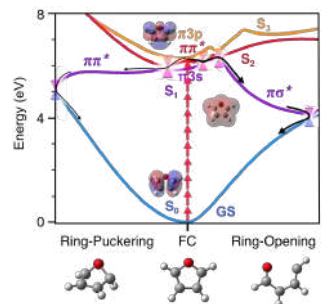
¹ICFO - Institut de Ciencies Fotoniques, The Barcelona Institute of Science and Technology, Castelldefels, Spain ²Institute of Physical Chemistry and Max Planck School of Photonics, Friedrich-Schiller-Universität, Jena, Germany ³ Fraunhofer Institute for Applied Optics and Precision Engineering, Albert-Einstein-Str. 7, 07745 Jena, Germany ⁴Institute of Applied Physics and Abbe Center of Photonics, Friedrich-Schiller-Universität, 07743 Jena, Germany ⁵ ICREA, Pg. Lluís Companys 23, 08010 Barcelona, Spain

*jens.biegert@icfo.eu

Abstract

We use attosecond soft X-ray pulses—the shortest yet achieved—to track many-body interactions among electrons, holes, and nuclei in real time. Core-level spectroscopy disentangles coherent and incoherent processes, revealing ultrafast energy dissipation pathways in furan. This approach opens new opportunities for chemical, material, and non-equilibrium physics.

The performance of materials, devices, and chemical reactions is governed by the microscopic interplay of their fundamental building blocks—electrons, holes, and nuclei. Decoding these many-body interactions is central to advancing basic science and enabling applications. This talk presents how attosecond soft X-ray technology opens an unprecedented window into these dynamics [1]. We report on developing the shortest attosecond soft X-ray pulses to date [2], and their application to directly track many-body interactions in real time via core-level absorption spectroscopy. This approach disentangles contributions from distinct subsystems, captures coherent and incoherent processes, and reveals how coherence evolves and decays. The ultrafast relaxation mechanism of furan (C₄H₄O) is known to be prototypical of the Ring-Opening (RO) and Ring-Puckering (RP) dynamics of cyclic molecules [3]. Despite encouraging results obtained so far [4], experimentally identifying the main relaxation pathways with their electronic and vibrational coherences has been out of reach due to the ultrafast timescales and the involvement of dark states. In this combined experimental and theoretical work [5], we investigate the ultrafast nonadiabatic dynamics of furan and show that core-level x-ray absorption fine structure (XAFS) spectroscopy with attosecond soft x-ray pulses can meet these challenges. We excite furan via multiphoton absorption and follow the subsequent relaxation dynamics, measuring the time-dependent carbon K-edge absorption spectra with an isolated attosecond probe pulse. The data show rich and ultrafast dynamics that follow the photoinduced excitation.



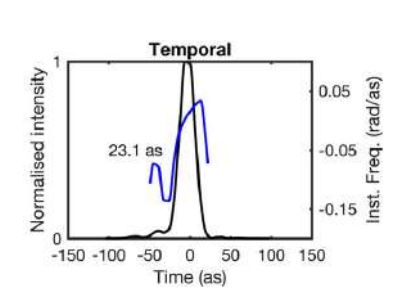


Figure 1: Left: Reaction coordinates for furan, Right: Attosecond SXR pulse.

- [1] J. Biegert, "Attosecond science: a new era for many-body physics", Europhysics News 55/1,12-15 (2024).
- [2] S. L. Cousin et al. "Attosecond Streaking in the Water Window: A New Regime of Attosecond Pulse Characterization", Phys. Rev. X 7, 041030 (2017)
- [3] M. Stenrup and A. Larson, "A computational study of radiation-less deactivation mechanism of furan", Chemical Physics 379, 6-12 (2011).
- [4] E. Wang, et al. "Time-Resolved Coulomb Explosion Imaging Unveils Ultrafast Ring Opening of Furan" arXiv:2311.05099v1 (2023).
- [5] S. Severino, et al. "Attosecond core-level absorption spectroscopy reveals the electronic and nuclear dynamics of molecular ring opening", Nature Photon. 18, 731 (2024).

Multi-Modal X-ray Probing of Catalytic Activity in Photo-driven Nanosystems

Samuel Sahel-Schackis,^{1,2,*} Adam Summers¹, Tom Linker¹, Ritika Dagar¹, Alexandra Feinberg¹, Paul Tuemmler³, Hendrik Tackenberg³, Jeffrey Powell⁴, Martin Grassl¹, Ilana Porter¹, Regina Leiner⁵, Simon Dold⁶, Yevheniy Ovcharenko⁶, Rebecca Boll⁶, Razib Obaid¹, James Cryan¹, Avijit Duley⁷, Chris Aikens⁷, Cesar Costa Vera⁸, Felix Gerke⁹, Markus Gallei⁵, Christian Peltz³, Thomas Fennel³, Daniel Rolles⁷, Artem Rudenko⁷, Eckart Ruehl⁹, Matthias Kling^{1,2}

¹SLAC National Accelerator Laboratory, Menlo Park, CA, USA; ²Stanford University, Stanford, CA, USA; ³Universität Rostock, Rostock, Germany; ⁴Institut national de la recherche scientifique, Montréal, Canada; ⁵Saarland University, Saarbrücken, Germany; ⁶European XFEL, Hamburg, Germany; ⁷Kansas State University, Manhattan, KS, USA; ⁸Escuela Politecnica Nacional, Quito, Ecuador; ⁹Freie Universität Berlin, Berlin, Germany; *samss@slac.stanford.edu

We present a multi-modal method combining single-shot 3D momentum-resolved ion emission spectra, X-ray photoelectron spectroscopy, and coherent diffraction imaging (CDI) to investigate catalytic activity in photo-driven nanosystems. This approach enables simultaneous characterization of charge dynamics, chemical reactions, and nanoparticle morphology, advancing insights into nanoscale photocatalysis.

Nanoparticles are increasingly recognized for their extraordinary catalytic properties, driven by their high surface area, tunable morphology, and unique electronic characteristics. [1] These materials are central to clean energy science, where photoexcitation initiates surface catalytic reactions by generating charge carriers and driving energy migration. [2] To understand the intricate interplay between charge dynamics and chemical reactivity at the nanoscale, we developed a multi-modal experimental approach that integrates ion velocity map imaging (VMI), X-ray photoelectron spectroscopy, and coherent diffraction imaging (CDI).

This method was implemented at the SQS instrument at European XFEL and the Maloja instrument at SwissFEL. The experimental setup (Fig. 1a) involves a nanoparticle injector delivering isolated particles into the interaction region where they intersect with an X-ray beam. VMI enables three-dimensional momentum-resolved ion emission spectroscopy to track ionic fragment distributions, while X-ray photoelectron spectroscopy provides detailed insights into ionization dynamics. Simultaneously, CDI captures far-field diffraction patterns to reconstruct nanoparticle morphology and correlate structural features with catalytic activity.

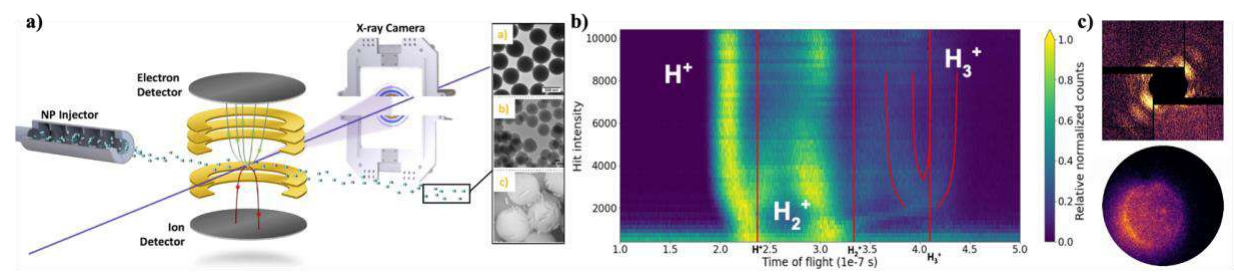


Figure 1: a) Experimental setup. b) Ion time-of flight spectra versus hit intensity demonstrating H⁺, H²⁺ and H³⁺ formation dynamics. c) CDI image of a cubic gold nanoparticle along with the VMI image gated on H⁺ ions

Results from this multi-modal approach reveal distinct regimes of X-ray-induced surface chemistry versus plasma formation at varying fluences. For instance, enhanced formation of H₃⁺ ions on water-decorated nanoparticles was observed under low fluence conditions (Fig. 1b), highlighting the catalytic role of secondary electrons and radicals generated during ionization processes. CDI patterns enabled reconstruction of nanoparticle shapes, such as spherical and cubic gold nanoparticles, revealing orientation-dependent ion momentum distributions (Fig. 1c). High-index facets were found to enhance near-field effects, significantly modulating catalytic activity. Additionally, X-ray photoelectron data provided crucial insights into surface reactions induced by X-ray irradiation, including the active participation of photoelectrons in driving nanoscale catalytic processes.

This multi-modal technique bridges the gap between structural imaging and chemical analysis by simultaneously capturing single-shot data across multiple modalities. It offers unprecedented insights into spatiotemporal reaction dynamics on nanoparticles, advancing our understanding of nanoscale photocatalysis and informing future optimization strategies for clean energy applications.

^[1] N. Narayan, A. Meiyazhagan and R. Vajtai, "Metal Nanoparticles as Green Catalysts", Materials **12**, 3602 (2019). [2] J. Choi *et al.*, "Understanding charge carrier dynamics in organic photocatalysts for hydrogen evolution", Energy & Environmental Science **17**, 7999-8018 (2024).

Ångström-scale surface metrology enabled by a compact milliwatt-class HHG source

Daniel S. Penagos Molina ^{1,2,3,†,*}, Mahmoud Abdelaal ^{1,†}, Wilhelm Eschen ^{1,2,3}, Soo Hoon Chew ⁴, Robert Klas ^{1,2,3,4}, Jens Limpert ^{1,2,3,4}, and Jan Rothhardt ^{1,2,3,4}

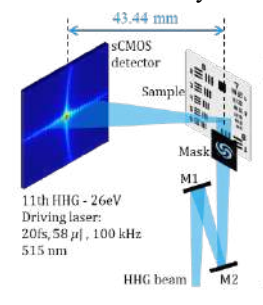
¹Institute of Applied Physics and Abbe Center of Photonics, Friedrich-Schiller-University Jena, Albert-Einstein-Straße 15, 07745 Jena, Germany

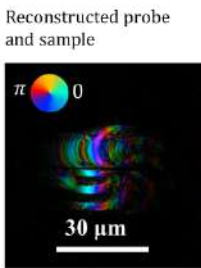
Abstract

Our work demonstrates nearly diffraction-limited lateral resolution, record ~1 Ångström axial resolution and record 10 Mpix/h throughput. This performance is enabled by a milliwatt-class HHG source paired with a high-speed sCMOS detector and a structured illumination, promising the investigation of millimeter-scale samples with sub-100 nm lateral- and sub-Ångström-scale axial resolution.

Recent advancements in laser development have enabled table-top sources with milliwatt-average-power coherent radiation in the extreme ultraviolet (XUV) at ~30 eV through high-order harmonic generation (HHG), achieving synchrotron-like brightness [1]. The generated short-wavelength coherent radiation can be efficiently used by lensless computational imaging techniques, such as ptychography [2], to image samples with diffraction-limited resolution. Such high-flux coherent sources allow conducting experiments on a lab scale with high imaging throughput—a prerequisite for pivoting their use for industrial applications and broadening the accessibility and applicability of high-resolution imaging to large objects, such as precision optics or EUV lithography masks [3]. Combining such sources with ptychography experiments in reflection geometry offers a viable solution to quantitative imaging of large samples, providing sensitive information on the surface profile with Ångström precision. Moreover, the choice of XUV radiation over X-rays or electrons is notably advantageous since almost all elements exhibit electronic resonances in this spectral regime that are detectable upon reflection, enhancing the technique's sensitivity and specificity [4].

In our contribution, we present an XUV ptychography setup operating in reflection geometry (see Fig. 1) that leverages a high-speed detector and a cutting-edge mW-class HHG source [5], doubling the throughput of previous demonstrations [6], and achieving record ~1Å axial resolution. Comparing the reconstructed phase profile from two successive experiments shows an excellent repeatability (standard deviation error < 2Å). At the current energy and a detection NA of 0.25, our lateral resolution is limited to 90 nm. The throughput however, is only limited by the stage overhead time. By advancing our mW-class HHG technology toward 90 eV photon energies, we expect to push the spatial resolution close to 10 nm, while also achieving synchrotron-like imaging throughput of >100 Mpx/h, which would not only advance the capabilities of table-top sources within academic research but also extend their utility into industrial applications, such as optics, wafer or EUV-lithography mask inspection [7].





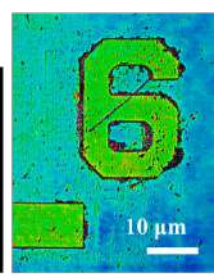


Figure 1: Reflection setup for ptychography. Multilayer mirrors (M1, M2) are used to spectrally filter and focus the HHG beam onto a mask placed $\sim\!\!300~\mu m$ upstream of the sample. A sCMOS detector records the diffracted intensity at 45° with respect to the sample surface normal. The reconstructed beam profile, and a section of the reconstructed sample (USAF Test target) is included.

References

[1] R. Klas et al., PhotoniX 2(1), 1–8 (2021). [2] P. Thibault et al., Science 321(5887), 379–82 (2008)

[3] M. D. Seaberg et al., Optica 1(1), 39 (2014).[4] Henke et al., Atomic Data and Nuclear Data Tables 54 (2), 181-342 (1993). [5] S. Skruszewicz et al., Opt. Express 29, 40333–40344 (2021).

[6] W. Eschen et al., Opt Express 31(9), 14212 (2023).

[7] H. Lu et al., Ultramicroscopy, 249 (2023).

²Helmholtz-Institute Jena, Fröbelstieg 3, 07743 Jena, Germany

³GSI Helmholtzzentrum für Schwerionenforschung, Planckstraße 1, 64291 Darmstadt, Germany

⁴Fraunhofer Institute for Applied Optics and Precision Engineering, Albert-Einstein-Straße 7, 07745 Jena, Germany †Equal contributors

^{*}santiago.penagos@uni-jena.de

Ultrafast Field Sampling Reveals Sub-Cycle Absorption

Václav Hanus, Eszter Papp, Beatrix Fehér, Péter Sándor, Zsuzsanna Pápa, and Péter Dombi^{1,2,*}

Abstract

By simultaneous driving of PHz currents and measuring the light field evolution using TIPTOE field-sampling technique, we extract the temporal evolution of nonlinear polarization and energy absorption of CEP-dependent current-driving process in GaN

To push the operational frequency of computational devices into the petahertz (10^{15} Hz) regime, light-wave field control of charge oscillations in condensed matter is a promising way to increase the processing speeds. Carrier-envelope phase (CEP) stabilization and control is a widely used technique for shaping light fields, enabling steering of currents in matter on sub-cycle timescales. Numerous examples of CEP-based current switching were demonstrated, paving the way towards light-field-driven PHz switches [1,2]. To realize a practical PHz switch, it is essential to understand the energy dynamics of the switching process and minimize energy consumption. While current switching has been achieved with laser energies below the nanojoule (nJ) level [3], its efficiency at sub-nJ energy levels remains unexplored. One potential method for investigating sub-cycle absorption in matter involves reconstructing the nonlinear polarization of the medium from the electric field of the driving light. This method, based on attosecond light-field sampling [4], provides insight into the timing and magnitude of light absorption process in transparent materials.

Here, we generate CEP-dependent PHz currents in GaN using few-cycle laser pulses, while simultaneously measuring the electric field of these pulses using the field-sampling technique known as TIPTOE [5]. By analyzing the waveforms, we extract the temporal evolution of nonlinear polarization and energy absorption. The field sampling setup in Fig. 1(a) operates in two settings: First, an attenuation is behind the target $(E_{J\neq 0})$; second, an attenuation is before the GaN target (E_{ref}) , see Fig. 1(b). The difference of these traces allows to extract the nonlinear polarization $P_{NL}[4]$ and energy transferred to the medium $W(t) = \int_{-\infty}^{t} E(t') \cdot \frac{d}{dt'} P_{NL}(t') dt'$.

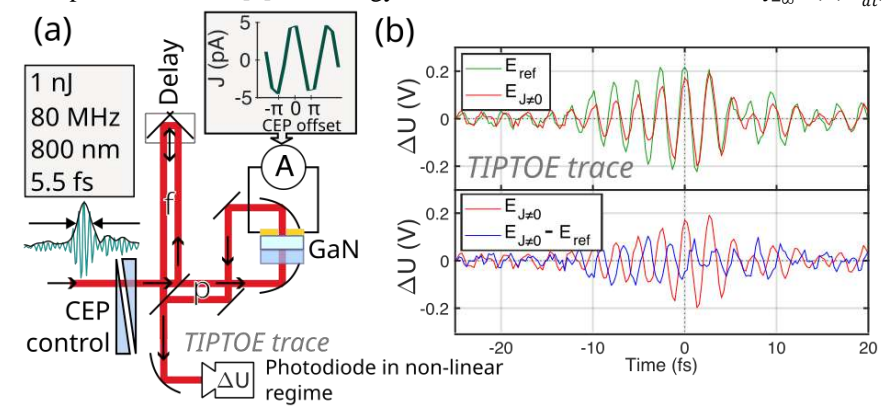


Figure 1: (a) The beam of controlled CEP is split in an interferometer to p-arm and f-arm. The p-arm generates CEP dependent current J in GaN as shown in the inset plot. The two arms overlap in a photodiode, which results in signal ΔU . (b) ΔU as a function of the delay between the two arms, i.e., TIPTOE trace that represents the optical electric field E of the p-arm. (Top) compares the field from linear interaction with GaN (green), E_{ref} , with the field that generates nonzero current (red), $E_{J\neq 0}$. (Bottom) Nonlinear polarization P_{NL} can be derived from measured $E_{J\neq 0}$ - E_{ref} .

- [1] Heide et al., "Petahertz electronics." Nat. Rev. Phys 6. 648–662 (2024)
- [2] Boolakee, T. et al., "Light-field control of real and virtual charge carriers." Nature 605, 251–255 (2022).
- [3] Hanus, V. et al., "Light-field-driven current control in solids with pJ-level ..." Optica 8, 570 (2021).
- [4] Sommer, A. et al., "Attosecond nonlinear polarization and light-matter..." Nature 534, 86–90 (2016).
- [5] Park, S. B. et al., "Direct sampling of a light wave in air." Optica 5, 402 (2018).

¹ HUN-REN Wigner Research Centre for Physics, 1121 Budapest, Hungary

² ELI-ALPS Research Institute, 6728 Szeged, Hungary

^{*}dombi.peter@wigner.hun-ren.hu

Ultrafast valleytronics in bulk crystals

Adam Gindl, Martin Čmel, František Trojánek, Petr Malý, and Martin Kozák,*

¹ Department of Chemical Physics and Optics, Faculty of Mathematics and Physics, Charles University, Ke Karlovu 3, Prague CZ-12116, Czech Republic.

*m.kozak@matfyz.cuni.cz

Abstract

We introduce an ultrafast optical technique allowing to generate and detect valley polarized electron distributions in bulk semiconductor crystals. The principle is based on anisotropic intervalley scattering induced by a strong nonresonant optical fields. We demonstrate its feasibility by generating valley polarization of electrons in silicon and diamond.

Main Text

Apart from charge and spin as the two fundamental degrees of freedom of electrons in solids, electrons in semiconductors with multiple minima (valleys) of the conduction band carry information about which group of equivalent valleys they occupy. Valley quantum number, which corresponds to the electron's wave vector, is a promising candidate for new generation information processing and storage devices and quantum computing. Valleytronics has been widely studied in 2D materials with broken time-reversal symmetry, in which the individual valleys can be addressed directly by coupling to specific helicity of circularly polarized light due to the existence of optical selection rules [1]. However, such selection rules do not exist in technologically important bulk semiconductors, including silicon and diamond.

In this contribution we report on the development of an ultrafast optical technique allowing to generate and read valley polarized populations of electrons in bulk semiconductors on sub-picosecond time scales. The principle of the method is based on unidirectional intervalley scattering of electrons accelerated by oscillating electric field of linearly polarized infrared femtosecond pulses. The induced degree of valley polarization of electrons is measured via polarization anisotropy of transient absorption of a delayed infrared probe pulse allowing us to directly characterize intervalley scattering times in silicon and diamond at different temperatures [2]. These results pave the way towards valleytronic devices working at terahertz frequencies at room temperature that will be compatible with contemporary silicon-based technology.

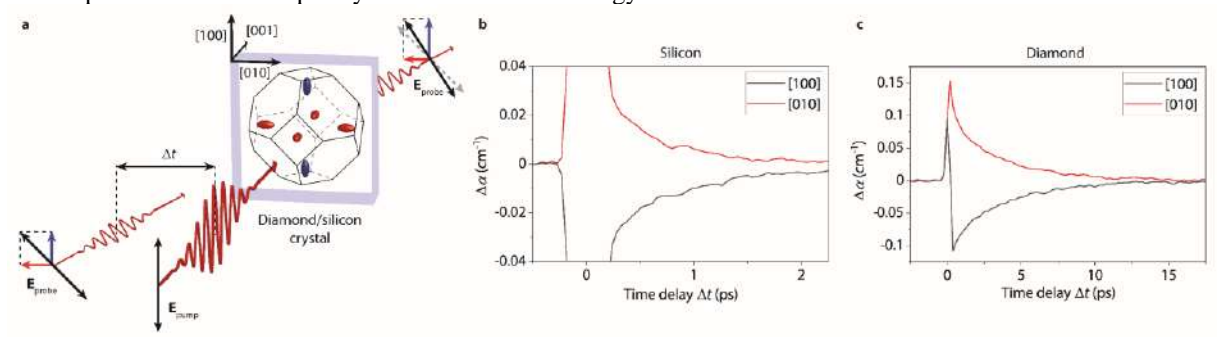


Figure 1: a) Layout of the experimental method for generation and detection of valley polarized electron populations in silicon and diamond. First Brillouin zone of silicon (diamond) crystal is shown together with the six degenerated conduction band minima. Oscillating pump field accelerates the electrons anisotropically in the real space and anisotropic intervalley scattering leads to an increase of population in the blue valleys while depleting the red valleys. b), c) Measured polarization anisotropy of transient absorption induced in silicon (b) and diamond (c) crystals at room temperature by a pump pulse with polarization along [100] (black curves) and [010] (red curves) crystallographic directions.

References

[1] John R. Schaibley, Hongyi Yu, Genevieve Clark, Pasqual Rivera, Jason S. Ross, Kyle L. Seyler, Wang Yao, and Xiaodong Xu, "Valleytronics in 2D materials," Nat. Rev. Mater. 1, 16055 (2016).

[2] Adam Gindl, Martin Čmel, František Trojánek, Petr Malý, and Martin Kozák, "Ultrafast room temperature valleytronics in silicon and diamond", arXiv:2411.11591 (2024).

Quantum-enhanced THz time-domain sensing

Dionysis Adamou,¹ Lennart Hirsch,¹ Taylor Shields,¹ Seungjin Yoon,¹ Adetunmise C. Dada,² Jonathan M.R. Weaver,¹ Daniele Faccio,² Marco Peccianti,³ Lucia Caspani,^{4,5} Matteo Clerici^{1,5,*}

Abstract

We explore time-domain THz spectroscopy using entangled photon probe pulses. Our experiment shows that quantum correlations in the probe allow a marked improvement in the detection sensitivity. We report on the enhancement of detected electric field signal-to-noise ratio and the impact it has on spectroscopy.

Main Text

Time-resolved electric field detection is one of the most insightful techniques for material analysis, spectroscopy, and sensing across a broad range of applications. It has recently demonstrated unparalleled sensitivity in the analysis of human blood [1]. This approach uses electro-optical sampling aided by ultrashort pulses to measure, in the time domain, the electric field of radiation (typically in the far-infrared spectral region) transmitted or reflected by the sample under analysis. Time-domain spectroscopy, one of the most widespread applications of time-resolved electric field detection, is shot-noise-limited in many embodiments. Quantum metrology tools could, therefore, be employed to further enhance its sensitivity [2]. We report here the first experimental demonstration of sensitivity enhancement of this technique enabled by the use of pulsed twin beams [3], i.e., quantum-correlated fields generated by seeded parametric down-conversion. In Fig.1(a) we show the electric field of a THz single-cycle pulse recorded either using classical (blue) or twin-beam (red) probe pulses in the electro-optical sampling. From the electric field standard deviation shown in Fig. 1(b), is clear that the latter provides an enhancement in the field sensitivity. In Fig. 1(c) we show the expected enhancement in spectroscopy enabled by the use of entangled probes. While this is a proof of principle performed in a geometry that does not deliver the highest sensitivity, it paves the way for the development of a novel approach that may transform time-domain metrology and sensing.

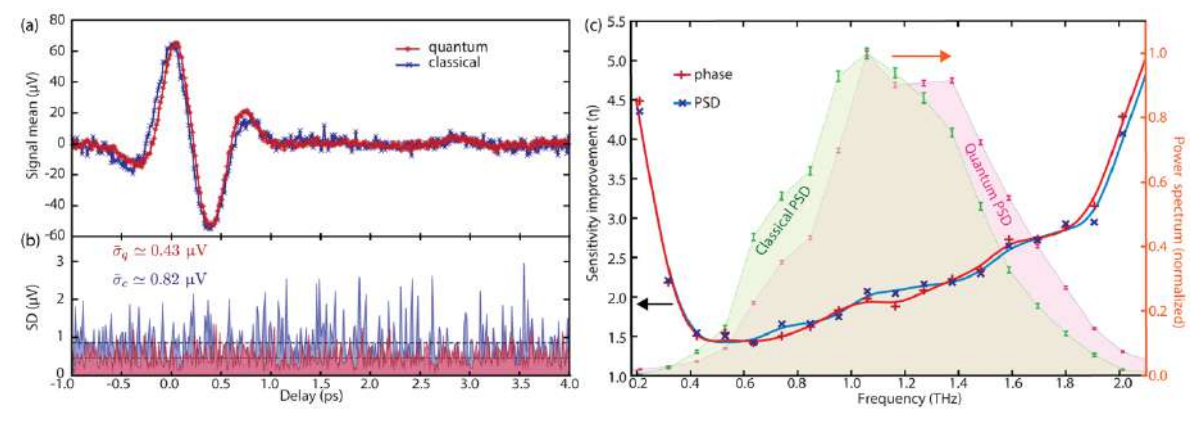


Figure 1: (a) Electric field acquired via electro-optical sampling using classical (blue) and quantum (red) probes. (b) Standard deviation for the data in (a). (c) Calculated sensitivity in the spectral domain.

- [1] I. Pupeza et al., "Field-resolved infrared spectroscopy of biological systems," Nature 577, 52-59 (2020).
- [2] S. Virally, P. Cusson, and D. V. Seletskiy, "Enhanced Electro-optic Sampling with Quantum Probes," Physical Review Letters 127, 270504 (2021).
- [3] D. Adamou, L. Hirsch, T. Shields, S. Yoon, A.C. Dada, J. M.R. Weaver, D. Faccio, M. Peccianti, L. Caspani and M. Clerici, "Quantum-enhanced time-domain spectroscopy," Science Advances 11, eadt2187 (2025).

¹James Watt School of Engineering, University of Glasgow, Glasgow G12 8QQ, UK

²School of Physics and Astronomy, University of Glasgow, Glasgow G12 8QQ, UK

³Emergent Photonics Research Centre, Dep. of Physics, Loughborough University, Loughborough LE11 3TU, UK

⁴Institute of Photonics, Department of Physics, University of Strathclyde, Glasgow G1 1RD, UK

⁵Como Lake Institute of Photonics, Dipartimento di Scienza e Alta Tecnologia, Insubria University, 22100, Como, Italy *matteo.clerici@uninsubria.it

CEP controlled, few-cycle UV pulses

Bruno Schmidt¹

¹few-cycle Inc, 1650 Boul. Lionel-Boulet, J3X 1P7 Varennes, Quebec, Canada

Abstract

We demonstrate that the CEP stability of the driving field is maintained upon soliton driven frequency upconversion. We prove both numerically and experimentally a one-to-one correspondence between the CEP of the IR driving field and the UV output. Unlike in 3 wave parametric processes like SHG or THG, in the case of four wave mixing based frequency up-conversion, the CEP noise does not get multiplied with the factor of wavelength conversion. As a consequence of this phase connection, we achieve very low UV CEP noise: 370 mard (single shot).

Compact hybrid Ho:YLF picosecond amplifier system exceeding 100 mJ pulse energy

Robert Riedel¹

¹CLASS 5 Photonics GmbH, Notkestr. 85 22607 Hamburg, Germany

Abstract

High peak power (tens of GW) lasers in the short-wavelength infrared (SWIR, $1.4-3~\mu m$) region show promising application as secondary sources; generating mid-infrared using OPCPA, terahertz radiation, as well as generating HHG down to the 'water window'. In this talk, we present a compact hybrid Ho:YLF amplifier system, combining a microjoule-level Yb:fiber-driven OPA front-end with a Ho:YLF regenerative amplifier. This hybrid system reduces complexity and optimizes bifurcation dynamics. In the subsequent booster stages, the amplifier geometry and thermal effects are optimized to scale the pulse energy above 100 mJ for MIR OPCPA pumping between $3-11~\mu m$.

Ultrafast tunable solutions from Ekspla

Justas Varpučianskis¹

¹EKSPLA, Savanoriu Ave 237, LT-02300 Vilnius, Lithuania

Abstract

Ekspla's high-intensity laser portfolio spans femtosecond, picosecond, and nanosecond systems for high-field physics. FemtoTune is a compact source delivering sub-50 fs pulses at repetition rates up to 100 kHz with continuous tunability from 650–950 nm. Time-synchronized motor positioning enables full-range scans within seconds or rapid access to specific wavelengths. Gapless mid-IR output (2.5–10 μm) with single polarization improves stability and beam pointing. For narrowband applications (SFG, CARS), channels at 1030 or 515 nm provide <8 cm⁻¹ bandwidth, reducible to <3 cm⁻¹ via optical synchronization. Pumped by FemtoLux industrial lasers, FemtoTune ensures long-term stability, reproducibility, and minimal maintenance for ultrafast spectroscopy and imaging.

High-energy, high-average-power amplifiers at kHz repetition rate and their nonlinear pulse compression

Thomas Metzger¹

¹TRUMPF, Johann-Maus-Strasse 2, 71254 Ditzingen, Germany

Abstract

We report on recent progress in Yb-doped thin-disk amplifiers and nonlinear pulse compression. The Dira 300-1 employs a dual-disk design, providing >300mJ pulse energy at 1kHz with 850fs duration, M² < 1.3, and slope efficiency up to 50%, limited by gain saturation. Using thin-disk systems, such as Dira 1000-5 (200mJ, 5kHz, <500fs) and TruMicro 9000 (10mJ, 100kHz, <1ps), gas-filled and bulk-based multipass cells enable compression below 50fs at kilowatt average power and pulse energies up to 200mJ. These results highlight the potential of the thin-disk technology in combination with multipass cells for realizing next-generation highpeak-power systems at high repetition rates.

Characterizing Pulse Duration at Video-Rate: A Tool for Laser Source Development and Optimization

Vitor Amorim¹

¹Sphere Ultrafast Photonics, Rua do Campo Alegre, 1021, Edificio FC6, 4169-007 Porto

Abstract

We present the developments made in temporal diagnostics at Sphere Ultrafast Photonics, starting from our scanning technique and the optimization path that led to the latest solution, up to its progression into a single-shot technique capable of characterizing the duration of laser pulses in real-time at video-rate.

Towards the future of Ultrafast Ti:sapphire Laser

Ming Yang¹

¹VIULASE GmbH, Liesinger Flur Gasse 3, 1230 Wien, Austria

Abstract

Since the first ultrafast Ti:sapphire laser was realized in 80s, it has become the most powerful laser tool for physicists, chemists and other scientists. However, the bulky volume and the high cost make it not friendly for more variable applications. VIULASE therefore have developed the latest Ti:sapphire ultrafast oscillators with direct diode pumping. This has revolutionarily reduced the cost and volume of the ultrafast oscillators, hence improved the user-friendliness of the used-to-be complex system. VIULASE is glad to take this chance to introduce the latest developments of the direct diode pumping Ti:sapphire ultrafast lasers,.

Towards higher peak powers: Energy scaling of two different multipass cell compressors at sub-10 fs pulse duration and 4 mJ

Kilian Fritsch¹

¹n2 Photonics, Krausestraße 102, 22049 Hamburg, Germany

Abstract

We present two recent developments of our multipass cell pulse compression units: 1) A 400 µJ Pharos laser compressed to 10 fs in a single-stage compressor at 50 kHz repetition rate. The pulses reach a peak power of over 2 GW and a bandwidth of 450 nm, with an excellent transmission efficiency of 83%. 2) The energy scaling of our multipass compressor from 2 mJ to 4 mJ pulse energy. At 5 kHz repetition rate, the output pulses exceed 100 GW peak power with excellent pulse and beam shape.

High-dynamic range pulse-contrast measurements for wide use in scientific applications and laser development

Matthias Baudisch¹

¹APE, Plauener Strasse 163-165, Haus N, 13053 Berlin, Germany

Abstract

Ultrashort pulses from femtosecond laser sources can feature considerable energy at the picosecond time scale beneath the main femtosecond peak, which only partially contributes to peak power driven applications. We propose Type-II SHG-autocorrelation as a simple and robust tool for high-dynamic range pulse-contrast measurements of sub-µJ energy, high-repetition rate pulses. We demonstrate dynamic ranges of the autocorrelation of over 107 with input energies of 55 nJ at 1 MHz repetition rate. The technique provides the perfect tool for wide use pulse-contrast measurement and laser optimization, possibly enabling a more effective use of pulse energy in peak power driven scientific applications.

UFI developments and updates 2025

Alexander Guggenmos¹

¹UltraFast Innovations GmbH, Dieselstr. 5, 85748 Garching (Munich), Germany

Abstract

This year, UltraFast Innovations introduced several key advances in nonlinear optical technology, enabling new frontiers for scientific and industrial applications. The commercial table-top XUV beamline was upgraded with compatibility to SWIR drivers, repetition rates beyond 50 kHz, and an extended spectrum reaching into the soft X-ray region. A compact cascaded post-compression system (40 × 300 cm) achieved a compression factor of ~35, delivering few-cycle pulses directly from industrial-grade Yb-lasers. In addition, novel use of multipass cells enabled controlled spectral red-shift and efficient contrast cleaning. Together, these innovations mark significant progress in commercialization of cutting-edge technologies.

High-Energy and -Peak-Power Yb Lasers

Valdas Maslinskas¹

¹Light Conversion, Keramiku St. 2B, LT-10233 Vilnius, Lithuania

Abstract

Ytterbium (Yb) 1030 nm femtosecond lasers have secured their ground in both scientific and industrial areas thanks to their high average power, high repetition rate and industrial-grade stability. In this talk we will present our capabilities to scale the Yb laser pulse energy up to 5 mJ, while keeping a pulse duration of 250 fs or less. Furthermore, we will showcase the results of coupling the laser to an optical parametric amplifier (OPA). Finally, we will discuss coupling Yb lasers to optical parametric chirped-pulse amplification (OPCPA) systems or different pulse compression techniques to obtain few-cycle pulses.

High-Performance 2 µm Lasers Venturing into Novel Scientific and Industrial Fields

Christian Gaida¹

¹Active Fiber Systems GmbH, Ernst-Ruska-Ring 17, 07745 Jena Germany

Abstract

Laser systems at 2µm wavelength are able to revolutionize several industrial, scientific and medical applications due to their unique absorption properties. We present recent progress in thulium-doped fiber-laser technology allowing for record laser parameters. We discuss promising applications such as ultrashort-pulse silicon processing, high-harmonic generation into the water-window or the use of 2µm-lasers as secondary-source drive

Optical parametric amplifier and integrated broadband pulses characterization

Antoine Dubrouil¹

¹Femto Easy – SAS, 23 avenue Léonard de Vinci, 33600 Pessac, France

Abstract

Femto Easy developed an OPA with output wavelength flexibility from 640 nm to 2.6 μm, as well as Fourier transform limited pulse duration tuning (via spectral bandwidth adjustment), from an input pump laser at 1 μm up to 50 W. It is a compact and easy to use design, offering hands-free operation. In particular, this OPA system integrates advanced online monitoring capabilities, such as beam profile, spectrum and pulse duration measurements. Also a new technique that uses the signal and idler as a pump-probe set up to characterize the output of the OPA is presented.

Wednesday

October 8th

Spatio-temporal control and characterization for ultrafast nonlinear interactions

Charles G. Durfee, 1,* Nathaniel Westlake, 1 Patrick Hunt1, Cameron Clarke1 and Dan Adams1

¹Department of Physics, Colorado School of Mines, 1523 Illinois St, Golden, CO 80401 USA *cdurfee@mines.edu

Abstract

Full spatio-temporal characterization is increasingly important both for minimizing and exploiting nonlinear effects. In this talk, we will describe our strategies for spatio-spectral and spatio-temporal characterization. We will show examples of linear and nonlinear spatio-temporal control in the areas of direct laser ponderomotive acceleration and high-order harmonic generation.

The importance of understanding, controlling and characterizing the coupling of the spatial and temporal properties of ultrafast pulses is gaining increasing attention. Whether the spatio-temporal coupling is intended or not, the time-dependence of the beam properties can dramatically affect experimental results in nonlinear interactions. When the field of the pulse-beam is not-separable in the spatial and temporal domains, i.e. $E(r,t) \neq f(r)g(t)$, it is not sufficient to make separate measurements of the beam (profile and wavefront) and the pulse (amplitude and phase). Moreover, the structure of any beam with spatio-temporal coupling will evolve with propagation, so it is critical to collect information sufficient to numerically calculate the downstream field. Rather than make a set of spatially-resolved temporal measurements, our approach is to combine full spatio-spectral measurements with a single measurement of the time-domain amplitude and phase at one well-defined point in the beam. This approach takes advantage of the fact that linear free-space propagation is separable in the spatio-spectral domain: each frequency component can be thought of as a beamlet that propagates independently from the rest [1].

Spatially-chirped beams are an important category of spatio-temporal shaped pulses. Pulse front tilt can be obtained by introducing angular spatial chirp on the beam. For pure angular chirp, where the spectral components are fully overlapped at the focus the pulse front tilt angle is proportional to the angular chirp rate. We have implemented this on the 3J beamline for the Aleph laser at Colorado State University, using the tilted pulse to ponderomotively accelerate electrons [2]. A very useful tool to characterize the alignment of such a system is a spectrally-resolved knife-edge scan that tracks the beamlet centerline and divergence as a function of wavelength through the focus. For imprinting spatial chirp on the fully-compressed output of systems (e.g. after harmonic conversion or an optical parametric amplifier), we have developed a zero-dispersion spatial stretcher that separates the spectral components of a pulse in the transverse direction without greatly affecting the pulse spectral phase.

For more general full-field spatio-temporal characterization we have implemented two approaches. In FISH-FROG (Fourier Interferometric Shack-Hartmann – Frequency-Resolved Optical Gating), the Shack-Hartmann shifted dot pattern is spectrally-resolved with Fourier-transform spectroscopy. In the other approach, we use broadband ptychography to characterize the spatio-spectral beam in a single shot [3]. For each of these, full pulse characterization is applied at a known position in the same plane as the spatio-spectral measurement.

Finally, we illustrate methods for nonlinear spatio-temporal beam shaping through high-order harmonic generation. In one experiment, we use crossed-beam mixing of matched tilted pulse fronts with opposite circular polarization and orbital angular momentum to produce attosecond pulse trains [4]. In another, we create a high-order Hermite-Gauss beam to drive the harmonics, creating a phase-locked array of harmonic beamlets that could be used for single-shot EUV ptychographic imaging [5].

- [1] C. G. Durfee, M. Greco, E. Block, D. Vitek, and J. A. Squier, Intuitive analysis of space-time focusing with double-ABCD calculation, Optics Express **20**, 14244 (2012).
- [2] P. Hunt et al., Ponderomotive snowplow electron acceleration with high energy tilted ultrafast laser pulses, *in review*, Nature Communications (2024).
- [3] D. Goldberger, J. Barolak, D. Schmidt, B. Ivanic, C. A. M. Schrama, C. Car, R. Larsen, C. G. Durfee, and D. E. Adams, Single-pulse, reference-free, spatiotemporal characterization of ultrafast laser pulse beams via broadband ptychography, Opt. Lett. 48, 3455 (2023).
- [4] A. de las Heras et al., Attosecond vortex pulse trains, Optica 11, 1085 (2024).
- [5] D. D. Schmidt et al., Self-interfering high harmonic beam arrays driven by Hermite–Gaussian beams, APL Photonics 10, 060801 (2025).

△ UFO XIV Azores 2025

Spatially-dependent group delay dispersion from a grating and its application for single-shot d-scan

Daniel Díaz Rivas^{1,*}, Cristian Barbero², Chen Guo¹, Marzo C. López Cerón¹, Miguel Canhota¹, Ivan Sytcevich¹, Saga Westerberg¹, Gaspard Beaufort¹, Miguel Miranda³, Helder Crespo^{3,4}, Rosa Romero³, Anne-Lise Viotti¹ and Cord L. Arnold¹

Abstract

We demonstrate that angular dispersion from a diffraction grating can lead to a spatially-dependent group delay dispersion. We use this effect to implement a novel single-shot d-scan, more suitable for longer pulse durations compared to approaches based on material dispersion.

When a laser beam is diffracted by a grating [1], it acquires a non-trivial spatially-dependent spectral phase. Expressing the diffracted beam as a sum of plane waves of different frequencies, we obtain an expression for the second order derivative of the spectral phase against angular frequency (ω) , also known as the group delay dispersion (GDD):

$$GDD(x_2, z_2, \omega_0) = z_2 \left(-\frac{\omega_0}{c} (\theta'(\omega_0))^2 \right) + x_2 \left(\frac{\omega_0}{c} \tan(\theta_0) (\theta'(\omega_0))^2 \right)$$
 (1) (See Fig. 1a for illustration of the relevant axes). The variation of GDD results in a non-uniform pulse duration in

(See Fig. 1a for illustration of the relevant axes). The variation of GDD results in a non-uniform pulse duration in any direction not parallel to the grating. Using a combination of two lenses in 4f-configuration (Fig. 1b), we can access a plane crossing the grating, in which there is minimum spatial chirp and zero dispersion offset, but with a spatially varying GDD. We used this arrangement to realize a new implementation of the single-shot dispersion-scan technique [2] and demonstrate a measurement of 170 fs pulses at 1030 nm (Fig. 1c). Our results (Figs. 1d, 1e) serve as a first demonstration of this new d-scan, which we referred to as g-shot. Although there are discrepancies between the single-shot and scanning measurements, probably due to the limited resolution of our imaging spectrometer and aberrations of the imaging system, this does not result in significant differences in the temporal profile of the pulse.

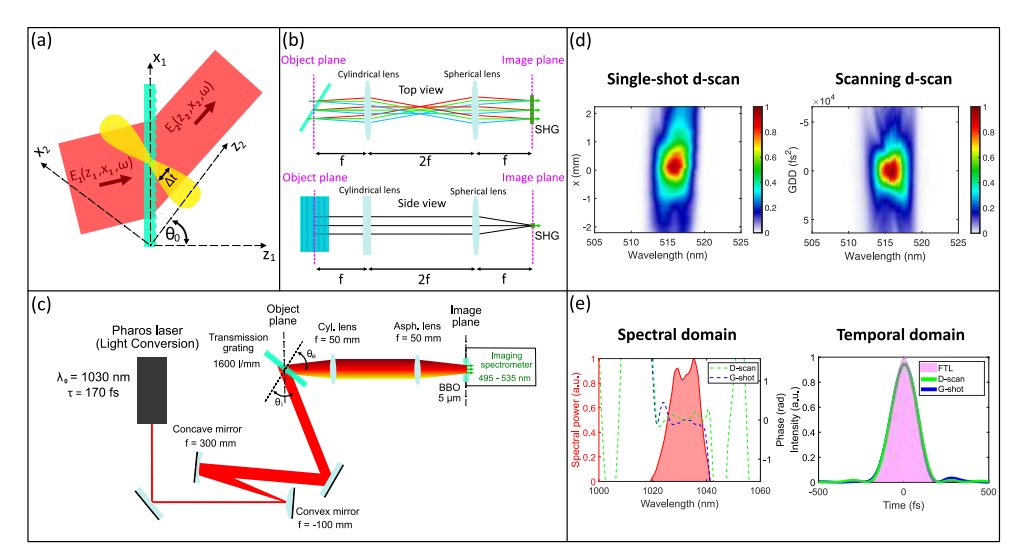


Figure 1: (a) Angular dispersion from a grating; (b) 4-f setup; (c-e) New single-shot d-scan.

This previously overlooked effect of angular dispersion allows us to introduce a large spatially-dependent GDD on the pulse. We believe that applications using gratings for pulse shaping will benefit from its understanding.

- [1] O. E. Martinez, J. Opt. Soc. Am. B, JOSAB 3, 929 (1986).
- [2] I. Sytcevich et al, J. Opt. Soc. Am. B 38, 1546 (2021).

¹Department of Physics, Lund University, P.O. Box 118, SE-22100, Lund, Sweden

²Grupo de Investigación en Aplicaciones del Láser y Fotónica (ALF), Universidad de Salamanca, Spain

³Sphere Ultrafast Photonics, Rua do Campo Alegre, 1021, Edificio FC6, 4169-007 Porto, Portugal

⁴Central Laser Facility, STFC, Rutherford Appleton Laboratory, Didcot OX11 0QX, United Kingdom

 $^{^*}$ daniel.diaz $_$ rivas@fysik.lth.se

△ UFO XIV Azores 2025

Generation and characterisation of TW-scale sub-fs optical pulses

Joleik Nordmann^{1,*}, Nikoleta Kotsina¹, Michael Heynck¹, Martin Gebhardt¹, Teodora Grigorova¹, Christian Brahms¹, and John C Travers¹

Abstract

Optical attosecond pulses can be directly generated through soliton self-compression. Here we describe the generation and characterisation of TW-scale sub-femtosecond pulses using our high-energy XSOL (Extreme Soliton) beamline and an in-vacuum dispersion-free TIPTOE apparatus. We obtain multi-mJ pulses with an envelope full-width at half-maximum duration of 0.77 fs.

Optical attosecond pulses—pulses with sub-femtosecond duration but with a spectrum in the near-ultraviolet to infrared spectral range—have only been generated through two techniques: light-field synthesis [1] and soliton self-compression [2]. Such pulses are both hard to create and hard to measure. So far, they have also only been achieved with relatively low peak power: sufficient for ultra-high time resolution measurements in the perturbative regime but insufficient for driving relativistic intensity strong-field physics.

In this work, we describe the generation and characterisation of sub-femtosecond pulses with terawatt-class peak power using our high-energy XSOL (Extreme Soltion) beamline and an in-vacuum dispersion-free TIPTOE (tunneling ionization with a perturbation for the time-domain observation of an electric field) apparatus [3, 4]. The full XSOL beamline is described in a separate submission and represents a ten-fold energy up-scaling compared to our previous soliton source [2]. The soliton-compression stage consists of a 4 m long, 530 μ m core diameter hollow capillary fibre, pumped with 5.5 fs, ~ 3 mJ pulses. The input and output of the fibre are in vacuum, while helium gas is fed into the centre of the fibre with the pressure tuned to obtain soliton self-compression at the output. For temporal characterisation, we constructed a custom in-vacuum TIPTOE apparatus, similar to refs. [3, 4]. The output of the fibre and the entire TIPTOE apparatus are contained within a single large vacuum system. The characterisation chambers are filled with a few mbar of helium to act as the gas medium for the TIPTOE measurement. Figure 1(a) shows the measured pulse envelope and the square of the electric field. We obtained a full-width at half maximum envelope duration of 0.77 fs for multi-mJ self-compressed pulse energy. The squared electric field transient has a duration of just 313 attoseconds, which represents, to our knowledge, the shortest ever generated and characterised optical pulse. Figure 1(b) compares the spectrum of these pulses obtained from TIPTOE to that measured with an independent spectrometer, confirming the fidelity of our measurement.

Our next goal is to tightly focus these pulses and use them to drive relativistic nonlinear optics in the sub-cycle regime for the first time.

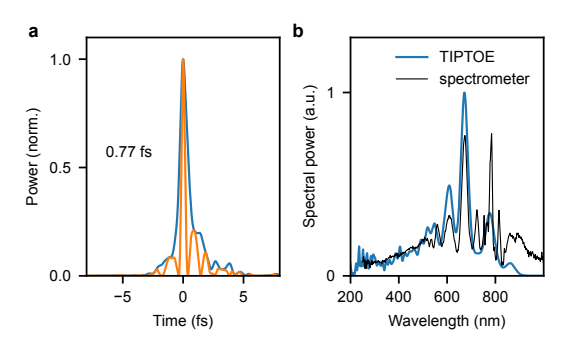


Figure 1: (a) Retrieved pulse envelope (blue) and absolute square of the electric field transient (orange). (b) Corresponding spectra.

- [1] Hassan et al., Nature 530, 66 (2016).
- [2] Travers et al., Nat. Phot. 13, 547 (2019).
- [3] Parket al., Optica 5, 402 (2018).
- [4] Cho et al., Sci Rep 9 16067, (2019).

¹School of Engineering and Physical Sciences, Heriot-Watt University, Edinburgh, EH14 4AS, United Kingdom

^{*}jmn2000@hw.ac.uk

Advanced Laser Pulse Metrology through 2D Self-Referenced Spectral Interferometry

Stefan Bock^{1,*}, Thomas Oksenhendler², Jörn Dreyer¹, René Gebhardt¹, Uwe Helbig¹, Toma Toncian¹ and Ulrich Schramm^{1,3}

Abstract

High intensity lasers with high temporal intensity contrast require the ability to measure this property comprehensively. The 2D self-referenced spectral interferometry method represents one solution to this need, with the capability of spatial, spectral and temporal high-dynamic field measurements in single-shot.

The latest generation of high intensity short-pulse laser systems are generating peak powers in the range of $10\,\mathrm{PW}$. Their application for relativistic laser plasma experiments with intensities of up to $10^{23}\,\mathrm{W/cm^2}$ in focus require contrast ratios of 10^{-12} or better and corresponding on-shot metrology. Typical temporal intensity contrast metrology relies on third-order correlators. Such devices are scanning and require a huge number of shots, and are limited in their capability to completely measure the laser pulse characteristics [1]. As an alternative the single-shot 2D SRSI technique has been introduced [2] and successfully applied, e.g. for plasma mirror contrast enhancement characterization [3]. We will report on the latest generation of the technique allowing for measurements of intensity contrast with up to 90 dB in single shot, together with spatial-temporal and spatial-spectral measurement capabilities [4], allowing for an enhanced understanding of the laser pulse performance enabling the improvement of high-intensity laser systems. The capabilities of 2D SRSI make this method an essential tool in particular to continue the quest for more powerful and temporally cleaner pulses of modern high intensity ultra-short pulse laser systems.

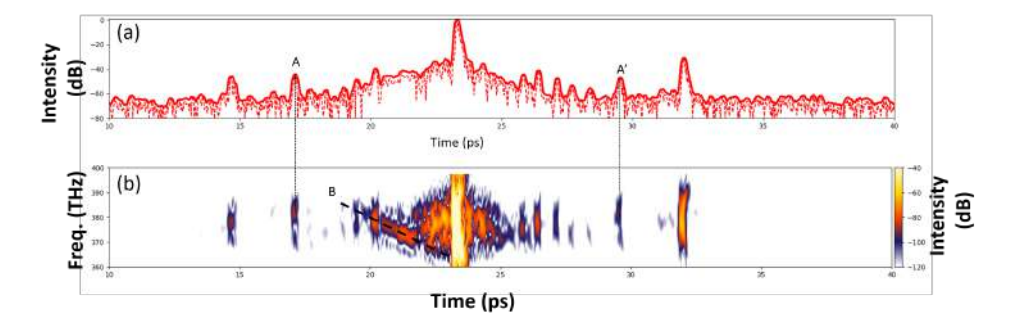


Figure 1: (a) contrast trace as measured by 2D SRSI. (b) corresponding spectrogram. A and A' represent a post-pulse and the corresponding generated and blue shifted pre-pulse [5]. B represents a strongly chirped pre-pulse pedestal.

- [1] S. Bock, T. Oksenhendler, et.al., "Spectral-temporal Measurement Capabilities of Third-order Correlators," Optics Express **31**, 9923-9934 (2023).
- [2] T. Oksenhendler, S. Bock, et. al., "High dynamic, high resolution and wide range single shot temporal pulse contrast measurement", Optics Express 25, 12588-12600 (2017).
- [3] L. Obst, S. Bock, et.al., "On-shot characterization of single plasma mirror temporal contrast improvement," Plasma Physics and Controlled Fusion **60**, 054007 (2018).
- [4] T. Oksenhendler, S. Bock, et.al., "Advanced Laser Pulse Metrology through 2D Self-Referenced Spectral Interferometry", Scientific Reports, submitted (2025).
- [5] T. Oksenhendler, S. Bock, et.al., "Instantaneous Frequency Representation Used for CPA Laser Simulation", Applied Sciences 11, 8934 (2021).

¹Helmoltz-Zentrum Dresden-Rossendorf (HZDR), Bautzner Landstr. 400, Dresden, 01328, Germany

²iTEOX, Gometz-le-châtel, 91940, France

³Technische Universität Dresden, 01062, Dresden, Germany

 $[{]m ^*s.bock@hzdr.de}$

Visible and NIR optical vortices measured in space-time with BLASHI

Benjamín Alonso^{1,2}, Miguel López-Ripa¹, and Íñigo Sola^{1,2}

¹Grupo de Investigación en Aplicaciones del Láser y Fotónica (ALF), Universidad de Salamanca, Spain

Abstract

We generate NIR and visible ultrashort optical vortices from vector beams combined with second harmonic and characterize their spatiotemporal properties using Bulk LAteral SHearing Interferometry (BLASHI).

Ultrashort laser pulses are some of the shortest controllable events in nature, with time evolution in the femtosecond scale. Often, space-time couplings require devoted characterization [1]. In previous works [2,3], the STARFISH technique [4] has been used to measure the beam. In the case of optical vortices, the use of BLASHI [5] allows retrieving the wavefront with precision, thanks to using a compact and ultra-stable bulk interferometer.

Here, we first generate the vortices in the near infrared from Ti:sapphire laser pulses by means of structured waveplates and beam manipulation [3]. Then, we produce the visible vortices through second-harmonic generation in a nonlinear crystal. The reference pulse is temporally characterized with a-swing [6]. The spatiotemporal phase profiles showed that the orbital angular momentum (OAM) has doubled for the visible vortices (Fig. 1) [7].

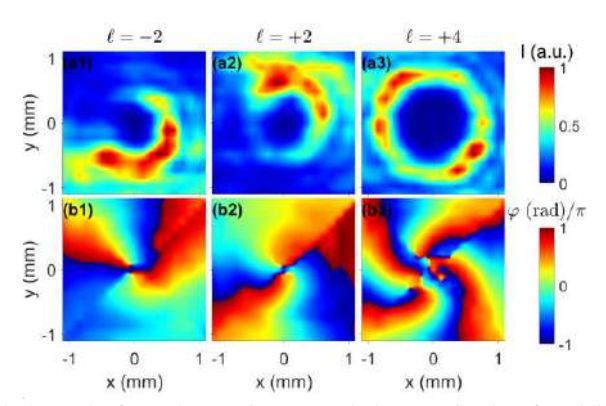


Figure 1: Intensity (a) and phase (b) from the spatio-spectral characterization for visible vortices for the central wavelength ($\lambda = 396.7 \text{ nm}$) with OAM: $\ell = -2 \text{ (1st column)}$, $\ell = +2 \text{ (2nd column)}$ and $\ell = +4 \text{ (3rd column)}$.

We have demonstrated that bulk lateral shearing interferometry can be used for pulsed beams across widely different spectral regions with the same setup (as is the case for the in-line interferometer in a-swing [8]), which is significant for future applications of the technique with various sources.

- [1] B. Alonso, A. Döpp, and S. W. Jolly, "Space-time characterization of ultrashort laser pulses: A perspective," APL Photonics 9, 070901 (2024).
- [2] B. Alonso, I. Lopez-Quintas, W. Holgado, R. Drevinskas, P. G. Kazansky, C. Hernández-García, and Í. J. Sola, "Complete spatiotemporal and polarization characterization of ultrafast vector beams," Commun Phys 3, 151 (2020).
- [3] I. Lopez-Quintas, W. Holgado, R. Drevinskas, P. Kazansky, I. Sola, and B. Alonso, "Optical vortex production mediated by azimuthal index of radial polarization," Journal of Optics **22**, 095402 (2020).
- [4] B. Alonso, I. J. Sola, O. Varela, J. Hernández-Toro, C. Méndez, J. Román, A. Zaïr, and L. Roso, "Spatiotemporal amplitude-and-phase reconstruction by Fourier-transform of interference spectra of high-complex-beams," J Opt Soc Am B **27**, 933 (2010). [5] M. López-Ripa, Í. J. Sola, and B. Alonso, "Bulk lateral shearing interferometry for spatiotemporal study of time-varying ultrashort optical vortices," Photonics Res **10**, 922–931 (2022).
- [6] B. Alonso, W. Holgado, and Í. J. Sola, "Compact in-line temporal measurement of laser pulses with amplitude swing," Opt. Express 28, 15625–15640 (2020).
- [7] M. López-Ripa, Í. J. Sola, and B. Alonso, "Visible optical vortices measured with bulk lateral shearing interferometry," arXiv:2503.24218 (2025).
- [8] M. López-Ripa, Í. J. Sola, and B. Alonso, "Amplitude swing ultrashort pulse characterization across visible to near-infrared," Opt. Laser Technol **164**, 109492 (2023).

²Unidad de Excelencia en Luz y Materia Estructuradas (LUMES), Universidad de Salamanca, Spain

^{*} b.alonso@usal.es

Analytically describing and analyzing spatiotemporal couplings in focusing laser pulses

K. Steiniger^{1,2*}, F. Dietrich^{1,3}, D. Albach¹, M. Bussmann^{1,2}, A. Irman¹, M. Loeser¹, R. Pausch¹, T. Püschel¹, R. Sauerbrey¹, S. Schöbel^{1,3}, U. Schramm^{1,3}, M. Siebold¹, K. Zeil¹, A. Debus¹

¹Helmholtz-Zentrum Dresden-Rossendorf, Dresden, Germany

²CASUS - Center for Advanced Systems Understanding, Görlitz, Germany

³Technische Universität Dresden, Dresden, Germany

*k.steiniger@hzdr.de

Abstract

Analytic expressions for duration, tilt, and other pulse properties are presented, being valid along the entire distance between the focusing mirror and focus. In contrast to previous work, these account for the impact of spatial dispersion during propagation and explain observed pulse-front tilts of several ten degrees near the focus.

In ultra-short laser pulses, small changes in dispersion properties before the final focusing mirror can lead to severe pulse distortions near the focus and therefore to very different pulse properties at the point of laser-matter interaction yielding unexpected interaction results. The mapping between far and near-field pulse properties intricately depends on the pulse's spatial and angular dispersion properties as well as the focal geometry.

For a focusing Gaussian laser pulse under the influence of angular, spatial, and group delay dispersion, we present analytical expressions for its pulse-front tilt, duration, width, group-delay dispersion, and third-order dispersion. In contrast to earlier work [1], these new expressions are valid along the entire propagation distance between the focusing mirror and focus. Consequently, they display previously unknown terms which have a significant impact on the pulse's properties in the vicinity of the focus. These are derived from a fully analytic expression for the laser pulse's electric field in time-space domain, which we obtained utilizing scalar diffraction theory and presented for the first time in ref. [2]. Additionally, expressions relating angular, spatial, group-delay dispersion, and third-order dispersion before focusing at an off-axis parabola, where they are well measurable, to their in-focus values are obtained by a ray-tracing approach and presented, too. Together with the analytic expressions for their evolution during propagation, these enable the evaluation of a pulse's properties between the focusing mirror and focus.

Exemplary real-world setups show that pulses with small initial dispersion can develop pulse-front tilts of several ten degrees in the vicinity of the focus while having negligible pulse-front tilt directly in the focus. While this has been observed in numerical experiments previously, the appearance of these large pulse-front tilts can be linked to a combined effect of spatial dispersion and phase-front curvature only now. The presented formulas are further verified by comparison to a numerical propagation simulation of a Gaussian pulse over distances of several Rayleigh lengths from the focus.

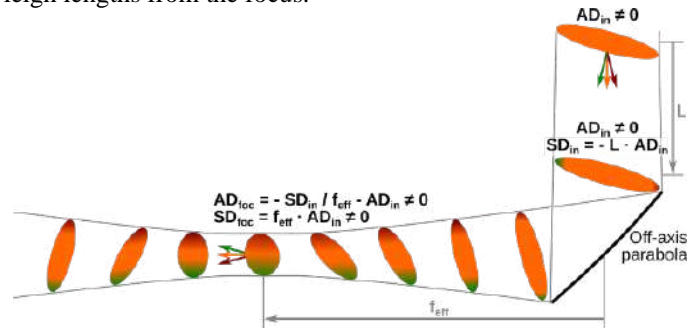


Figure 1: Envelope of a focusing laser pulse with angular dispersion (AD) at different points in time along its path. It develops spatial dispersion and a large pulse-front tilt while propagating.

References

[1] S. Akturk et al., "The general theory of first-order spatio-temporal distortions of Gaussian pulses and beams," Opt. Express 13, 8642-8661 (2005). doi:10.1364/OPEX.13.008642

[2] K. Steiniger et al., "Distortions in focusing laser pulses due to spatio-temporal couplings—An analytic description," High Power Laser Science and Engineering 12, e25 (2024). doi:10.1017/hpl.2023.96

Advancing the next generation of photonic measurement systems using machine learning

Darko Zibar

. DTU Electro, Technical University of Denmark, Ørsteds plads, Building 343, DK-2800, Kgs. Lyngby *author@institution.edu

Abstract

.

The 2024 Nobel Prize in Physics underscores the growing influence of machine learning in diverse areas of physical science. In the field of photonics, machine learning is proving invaluable for tasks such as optimizing and designing fiber-optical communication systems, optical amplifiers, noise characterization of frequency combs, inverse design of photonic components, and quantum-noise-limited signal detection. In this talk, I will review notable applications of machine learning in photonics and explore future directions in this emerging field. Specifically, I will highlight its role in phase noise characterization of optical frequency combs, end-to-end learning for fiber-optic communication, and realization of programmable ultra-wideband Raman amplifiers. Lastly, I will introduce an exciting new application of machine learning: controlling nonlinear interactions in highly nonlinear waveguides

Machine learning for the control of ultrafast nonlinear spectral broadening processes

Yassin Boussafa¹, Lynn Sader¹, Bruno P. Chaves¹, Van Thuy Hoang¹, Manal Arbati¹, Alexis Bougaud¹, Jérémy Saucourt¹, Marc Fabert¹, Alessandro Tonello¹, Vincent Couderc¹, John M. Dudley^{2,3}, Michael Kues⁴, Benjamin Wetzel¹*

Abstract

We review recent experiments using machine learning to control ultrafast nonlinear dynamics. After covering multidimensional control and optimization of nonlinear broadening, we focus on modulation instability, highlighting how advanced characterization and machine learning strategies enable gaining insight and tailoring optical wavepackets, even in noise-driven regimes.

Machine learning (ML) has recently driven major advances in ultrafast and nonlinear photonics by combining efficient characterization techniques with advanced pulse-shaping capabilities, thus enabling precise control of nonlinear fibre dynamics. Within this context, we review recent experimental progresses where ML proves relevant: We briefly highlight the spectro-temporal optimization of coherent supercontinuum and frequency combs using reconfigurable optical pulse patterns [1,2]. Such approaches demonstrate control over nonlinear propagation with potential for advanced microscopy and imaging through tailored focusing and temporal shaping [3,4].

We then address the control of incoherent signals generated by noise-driven modulation instability (MI). Weak coherent seeding can alter spontaneous MI, while dispersive Fourier transform (DFT) techniques provide real-time access to spectral fluctuations [5,6]. ML approaches—including evolutionary algorithms [7] and ANNs [8]—can optimize seed parameters to tailor incoherent broadening, predict statistical correlations, and even retrieve hidden input information from noisy outputs. These examples highlight how combining advanced diagnostics, optical shaping, and ML inference paves the way for scalable and smart ultrafast nonlinear photonics [9].

- [1] B. P. Chaves, et al., "Leveraging Machine Learning and a Photonic Integrated Chip for the Spectro-Temporal Tailoring of Supercontinuum Generation," in CLEO/Europe-EQEC (2025). 10.1109/CLEO/Europe-EQEC65582.2025.11111412.
- [2] M. Arbati, et al. "Harnessing Electro-Optic Modulation and On-Chip Temporal Interleaving Towards Versatile Frequency Comb Generation," in CLEO/Europe-EQEC (2025). 10.1109/CLEO/Europe-EQEC65582.2025.11109983
- [3] V. T. Hoang, et al., "Optimizing supercontinuum spectro-temporal properties by leveraging machine learning towards multi-photon microscopy," Front. Photon. **3**, 940902 (2022).
- [4] T. Mansuryan, et al., "Nonlinear flying focus pulses for ultrafast 3D nonlinear microscopy," Optica 12, 1192 (2025).
- [5] T. Godin, et al. "Recent advances on time-stretch dispersive Fourier transform and its applications," Advances in Physics X 7, 2067487 (2022).
- [6] L. Sader et al., "Single-photon level dispersive Fourier transform: ultrasensitive characterization of noise-driven nonlinear dynamics," ACS Photonics 10, 3915 (2023).
- [7] L. Sader et al., "Modulation instability control via evolutionarily optimized optical seeding," Nanophotonics 14, 2821 (2025).
- [8] Y. Boussafa et al., "Deep learning prediction of noise-driven nonlinear instabilities in fibre optics," Nature Communications 16, 7800 (2025).
- [9] This project has received funding from the European Research Council (ERC) under the European Union's Horizon 2020 research and innovation programme under GA No. 950618 (STREAMLINE), the French ANR through the OPTIMAL project (ANR-20-CE30-0004) and the Région Nouvelle-Aquitaine (SCIR & SPINAL).

¹XLIM Institute, CNRS UMR7252, Université de Limoges, 87060 Limoges, France

²Université Marie et Louis Pasteur, CNRS Institut FEMTO-ST, 25030 Besançon, France

³Institut Universitaire de France, Paris, France

⁴Institute of Photonics & Cluster of Excellence PhoenixD, Leibniz University Hannover, 30167 Hannover, Germany *benjamin.wetzel@xlim.fr



AI-Driven Design of Ultra-Broadband Dispersive Mirrors

Utsa Chattopadhyay,^{1,2,*} Florian Carstens,⁵, Andreas Wienke,⁵ Ingmar Hartl,² Nihat Ay,¹ Christoph M. Heyl, ^{2,3,4} and Henrik Tünnermann²

Abstract

We present a machine-learning framework for optical thin-film coating design that accelerates the design process while achieving excellent performance characteristics without expert intervention. To demonstrate its capabilities, we design a broadband high-reflectivity mirror with state-of-the-art performance, including a $-200 \, \mathrm{fs}^2$ GDD covering a spectral range from 940 nm to 1120 nm.

Ultrafast laser systems rely on optical thin-film coatings to control dispersion and precisely manipulate ultrashort pulses. Designing these coatings is a complex inverse problem, traditionally solved using computationally intensive methods like the Needle Algorithm [1], often requiring expert intervention [2]. Here, we propose a physics-informed machine learning framework based on an autoencoder to efficiently design optical thin film coatings.

Our approach takes desired optical properties (e.g., reflectivity, group delay dispersion) as input and directly predicts an optimized layer structure. By integrating a physics-based transfer matrix model [3] and a physics-informed loss function into the neural network, we ensure physically consistent coating designs.

We validate our framework by designing an ultra-broadband dispersive mirror without expert input or prior knowledge of existing designs. The resulting mirror design achieves state-of-the-art performance, with reflectivity exceeding 99.99% and a flat group delay dispersion of $-200\,\mathrm{fs^2}$ across a broad spectral range (940–1120 nm). To assess performance, we compare our numerical results with standard industry-grade coating designs for similar target specifications, as shown in Figure 1. Our results show that AI-driven approaches have the potential to rival or even surpass classical optimization techniques for optical coating design. By enabling greater automation and exploration of unexplored design spaces, they have the potential to accelerate the development of high-performance coatings and advance applications e.g. in ultrafast optics and nonlinear light-matter interactions.

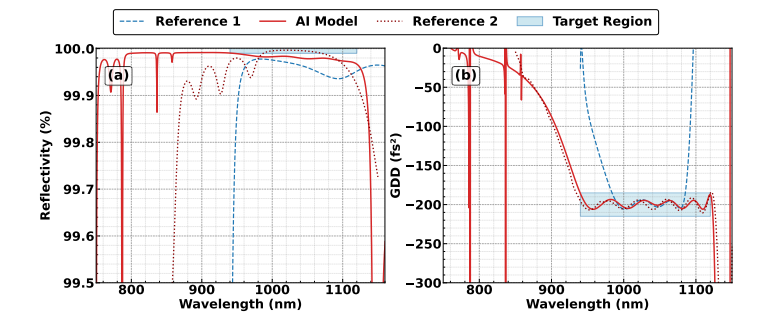


Figure 1: Comparison of AI-designed coating (solid lines) with state-of-the-art industrial designs (dashed lines) for reflectivity (a) and group delay dispersion (GDD) (b). The target reflectivity (>99.99 %) and GDD $(-200 \pm 5\,\mathrm{fs^2})$ used as input for our AI model are indicated by the shaded regions in (a) and (b) respectively. The simulation includes material absorption by incorporating extinction coefficients into the refractive index during the forward model calculations.

- [1] Alexander V. Tikhonravov, Michael K. Trubetskov, and Gary W. DeBell. Application of the needle optimization technique to the design of optical coatings. *Appl. Opt.*, 35(28):5493–5508, Oct 1996.
- [2] N. Kaiser. Old rules useful to the designer of optical coatings. https://doi.org/10.1002/vipr.200890042, 2008.
- [3] Alexander Luce, Ali Mahdavi, Florian Marquardt, and Heribert Wankerl. Tmm-fast, a transfer matrix computation package for multilayer thin-film optimization: tutorial. J. Opt. Soc. Am. A, 39(6):1007–1013, Jun 2022.

¹Institute for Data Science Foundations, Technical University of Hamburg, Blohmstraße 15, 21079, Hamburg, Germany

²Deutsches Elektronen-Synchrotron, Notkestraße 85, 22607, Hamburg, Germany

³Helmholtz Institute Jena, Fröbelstieg 3, 07743, Jena, Germany

⁴GSI Helmholtz Centre for Heavy Ion Research, Planckstrasse 1, 64291, Darmstadt, Hamburg

⁵Laser Zentrum Hannover e.V., Hollerithallee 8, 30419, Hannover, Germany

 $^{^*}$ utsa.chattopadhyay@tuhh.de

High Harmonic Generation driven Extreme Ultraviolet 0^{th} order Scatterometry for Nanostructure Characterization

Francesco Corazza^{1,*}, Emmanouil Kachaoglou¹, Maximillian Lipp¹, Leo Guery¹, Zhonghui Nie¹, Lyuba Amitonova^{1,2} and Peter M. Kraus^{1,2}

Abstract

We introduce a tabletop high harmonic generation (HHG) scatterometry technique to extract structural and material characteristics of periodic nanostructures. Grazing incidence reflection scatterometry enables fast and robust measurements of linewidth and groove height with 20 nm and 2 nm precision respectively, paving the way for ultrafast spectroscopy on layered heterostructures.

We present a novel approach based on a table-top HHG setup for the evaluation and extraction of the structural and material-related characteristics of nanostructures. Our focus is on grazing incidence scatterometry, a non-imaging metrology method for periodic nanostructures, operating in the extreme ultraviolet (XUV) spectral region (10-30 nm) in reflection geometry. By collecting and spectrally resolving only the 0^{th} diffraction order, we can precisely reconstruct structural parameters of nanostructures with far below the illumination wavelength accuracy. Although this method inherently provides limited information compared to the full diffraction pattern, it leverages the brightest diffraction order and reduces the impact of local defects. We prove our measurements to be rapid due to an enhanced signal-to-noise ratio and resilient against distortions from non-uniform sample contamination. Experiments were performed on pairs of orthogonal gratings with the goal of retrieving morphological parameters such as linewidth and groove height.

Morphological parameters are extracted solving the scatterometry inverse problem, framed as an optimization task. This task involves comparing the measured diffraction efficiencies to specialized libraries of simulated datasets computed via the Rigorous Coupled-Wave Analysis (RCWA) method [1]. More in the detail, reconstruction is realized using Maximum Likelihood Estimation regression (MLEr) algorithms, to correctly account for the different uncertainty sources. We have contextually developed a Simulation Based Inference approach that exploits machine learning to further improve the reconstructed parameters accuracy. Our initial experimental campaign has demonstrated groove height reconstruction accuracy below 2 nm and linewidth reconstruction accuracy of about 20 nm. A primary aim of this work is to exploit material-specific near-edge absorption dynamics for observing ultrafast carrier processes in complex heterostructures and simultaneously monitoring diffraction changes upon photoexcitation. To achieve this, we integrated an ultrafast time-resolved spectroscopy scheme within our scatterometer to inspect charge injection phenomena within these layered structures, as described in [2]. In conclusion, we present a scatterometry approach based on HHG, capable of rapidly and reliably inspecting nanostructures with a reconstruction precision of approximately 2 nm. With the aim of combining material-specific and morphological characterization, we devote our efforts to merging the capabilities of XUV scatterometry with ultrafast spectroscopy, pushing the boundaries of functional metrology.

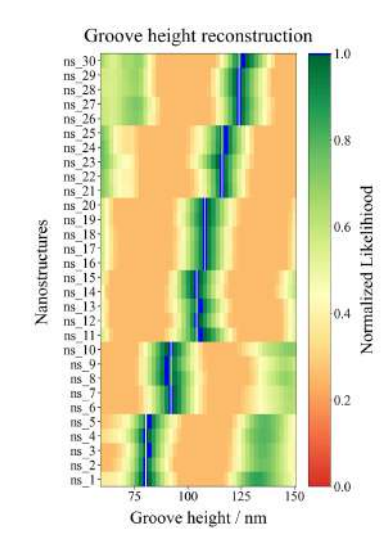


Figure 1: Morphology reconstruction result using a Maximum Likelihood regression compared to an independent AFM characterization (white lines).

- [1] P. Lalanne, "Improved formulation of the coupled-wave method for two-dimensional gratings", JOSA A, vol. 14, no. 7, pp. 1592–1598, 1997.
- [2] S. K. Cushing, et al., "Layer-resolved ultrafast extreme ultraviolet measurement of hole transport in a ni-tio2-si photoanode", Science advances, vol. 6, no. 14, p. eaay6650, 2020.
- [3] Y. S. Ku, et al. "EUV scatterometer with a high-harmonic-generation EUV source", Optics express 24.24 (2016): 28014-28025.

¹Advanced Research Center for Nanolithography, Science Park 106, 1098XG, Amsterdam, NL

²Department of Physics and Astronomy & LaserLaB, Vrije Universiteit, De Boelelaan 110, 1081HV Amsterdam, NL

^{*}f.corazza@arcnl.nl

i²PIE for broadband pulse measurement and compression

Pieter H Neethling^{1,2,*}, Eugene E Fouché¹, and Gurthwin W Bosman^{1,2}

¹ Stellenbosch Photonics Institute (SPI), Stellenbosch University, Private Bag X1, Stellenbosch 7599, South Africa

Abstract

i²PIE is an implementation of time-domain ptychography which allows for the accurate measurement of the spectral phase of a broadband laser pulse, including higher order phase terms. This paper shows the implementation of this pulse compression scheme and highlights some applications and extensions.

Recently time-domain ptychography[1] was generalised to utilize phase-only transfer functions, simplifying its implementation and making it more applicable in most ultrafast laboratories. This generalisation was termed i²PIE, referring to the fact that the square of the signal is measured and that a set of known transfer functions (*intrinsic knowledge*) is used[2]. This co-linear scheme simplifies pulse characterization as no probe pulse is required. Furthermore, it can be applied to any temporal signal, not only laser pulses. Since then we have demonstrated a number of different implementations, highlighting its broad applicability and the advantage offered in pulse compression. These studies include applications in non-linear microscopy[3], single-beam CARS[4] and non-linear light sheet microscopy[5]. Fig.1a shows the reconstruction (amplitude and phase), of a broadband pulse generated in an all-normal-dispersion photonic crystal fibre (ANDi-PCF), while Fig.1b shows the same pulse, after compression using i²PIE. Fig.1c compares the temporal profile of the compressed pulse to that of the Fourier limit, highlighting the quality of compression, and the ability of i²PIE to not only compensate for quadratic phase but also higher order chirp.

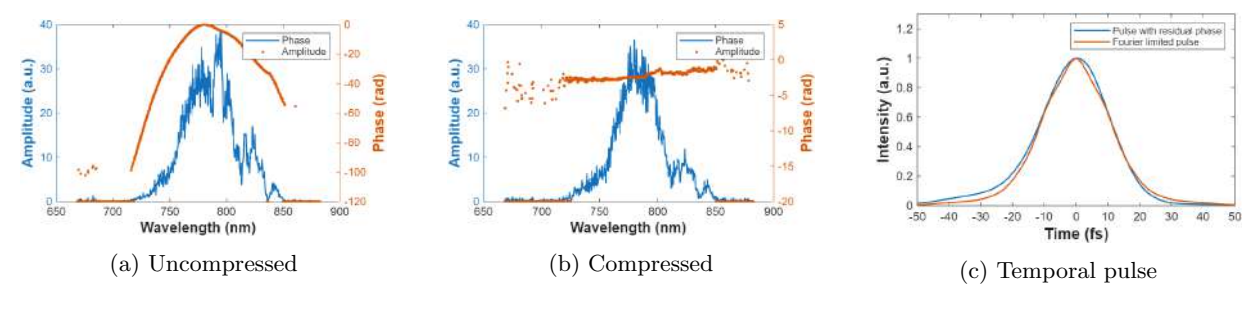


Figure 1: (a) Reconstructed amplitude and phase using i²PIE. (b) Reconstructed amplitude and phase after pulse compression. (c) Temporal comparison of compressed pulse to that of the Fourier limit.

- [1] Dirk Spangenberg, Pieter Neethling, Erich Rohwer, Michael H. Brügmann, and Thomas Feurer. Time-domain ptychography. *Phys. Rev. A*, 91:021803, Feb 2015.
- [2] Dirk-Mathys Spangenberg, Erich Rohwer, Michael Brügmann, and Thomas Feurer. Extending time-domain ptychography to generalized phase-only transfer functions. *Opt. Lett.*, 45(2):300–303, Jan 2020.
- [3] George Dwapanyin, Dirk Spangenberg, Alexander Heidt, Thomas Feurer, Gurthwin Bosman, Pieter Neethling, and Erich Rohwer. Generalized spectral phase-only time-domain ptychographic phase reconstruction applied in nonlinear microscopy. J. Opt. Soc. Am. B, 37(11):A285–A292, Nov 2020.
- [4] Ruan Viljoen, Pieter Neethling, Dirk Spangenberg, Alexander Heidt, Hans-Martin Frey, Thomas Feurer, and Erich Rohwer. Implementation of temporal ptychography algorithm, i2pie, for improved single-beam coherent anti-stokes raman scattering measurements. J. Opt. Soc. Am. B, 37(11):A259–A265, Nov 2020.
- [5] Imraan Badrodien, Pieter H Neethling, and Gurthwin W Bosman. Improved image contrast in nonlinear light-sheet fluorescence microscopy using i^2 PIE pulse compression. *Scientific Reports*, 14:12770, 2024.

² National Institute for Theoretical and Computational Sciences (NITheCS), Private Bag X1, Stellenbosch 7599, South Africa

^{*}pietern@sun.ac.za

PI-FROSt to reveal driving mechanisms in harmonic generation from solid-state media

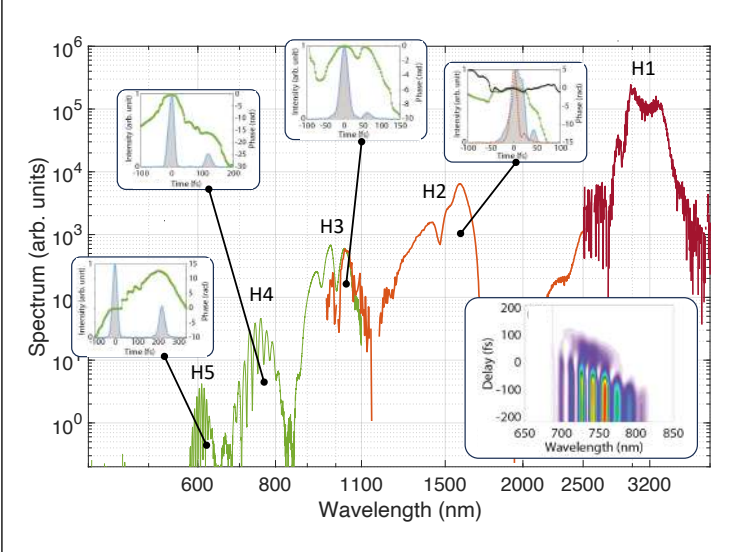
P. Béjot¹, B. Kiss², R. Shrestha², L. Àbrók², Z. Kis², K. Pirisi², B. Bagó², O. Faucher¹, F. Billard¹, E. Cormier^{2,3,*}, E. Hertz¹

Abstract

The novel PI-FROSt method has been applied to synchronously characterize all harmonics generated in a semiconductor crystal by midIR ultrashort pulses enabling to retrieve processes at play during the interaction.

We report on the detailed characterization of ultrashort harmonic pulses produced in a solid-state target by a few-cycle driving pulse (3.2 µm, 100 kHz). In this experiment, conducted at ELI-ALPS in the frame of the "3rd Joint ELI Call for Users", harmonic fields, generated in a ZnO crystal, are fully characterized by the newly developed Plasma-Induced Frequency Resolved Optical Switching (PI-FROSt) method [1,2]. This approach is

straightforward to implement, free from phase-matching constraints, capable of operating at ultra-high repetition rates, with no damage threshold. We demonstrate the ability of PI-FROSt to characterize, without any reconfiguration of the setup, the MIR driving field with all (odd and even) harmonics up to the fifth order. The resulting spectrum spans a remakable bandwidth of 2.6 octaves across the visible mid-infrared spectral region (0.59–3.6) μm) and all assessments confirm PI-FROSt as a highly effective metrology tool for unconventional secondary sources. Beyond demonstrating the metrology capabilities, the comprehensive characterization provides valuable insights driving the mechanisms harmonicgeneration. Notably, measurements highlight the consistent production of bi-pulses across



PI-FROSt full characterization of several harmonics from ZnO driven by a 3 μ m few cycle pulses.

harmonics corroborated by numerical simulations. This effect stems from the combined contributions of large phase and group velocity mismatches, emphasizing the limitation of "point-model responses" to capture the key features of harmonics and the critical importance of propagation and cascading effects in the harmonic build-up.

¹Laboratoire Interdisciplinaire Carnot de Bourgogne, UMR CNRS 6303 - Université Bourgogne Europe, Dijon, 21078, France

²ELI-ALPS, ELI-HU Non-Profit Ltd., Dugonics tér 13, Szeged, 6720, Hungary

³Laboratoire Photonique Numérique et Nanosciences (LP2N), UMR 5298, CNRS-IOGS-Université Bordeaux, Talence, 33400, France

^{*}eric.cormier@u-bordeaux.fr

^[1] R. K. Bhalavi, P. Béjot, A. Leblanc, A. Dubrouil, F. Billard, O. Faucher, E. Hertz, "Phase-matching-free ultrashort laser pulse characterization from a transient plasma lens", Opt. Lett. **49** (2024) 1321.

^[2] P. Béjot, R. Kumar Bhalavi, A. Leblanc, A. Dubrouil, F. Billard, O. Faucher, E. Hertz, Temporal characterization of laser pulses using an air-based knife-edge technique, Adv. Photonics Res., 6, (2024).

Detection of pulse-duration fluctuations and drifts with attosecond precision

Arno Klenke, ^{1,2,3,4,*}, Maximilian Benner, ¹ Jonas Margraf¹, Mats Segbers¹, Tino Eidam⁵ and Jens Limpert^{1,2,3,4}

¹Institute of Applied Physics, Abbe Center of Photonics, Friedrich-Schiller-Universität Jena, Albert-Einstein-Straße 15, 07745 Jena, Germany

Abstract

We present the detection of dispersion-related pulse-duration fluctuations in an ultrafast laser with attosecond precision. By pre-chirping the pulses in combination with spectral-broadening, a per-pulse measurement signal can be generated that allows to detect these changes with precision down to 20 as and use it as a feedback for stabilization.

Today, femtosecond lasers based on chirped-pulse-amplification (CPA) drive a wide variety of applications. Many of the involved processes are of highly non-linear nature, such as non-linear pulse compression or the generation of higher harmonics. Thus, they are very sensitive to the peak-power of the laser pulses. In large-scale CPA systems, beam-pointing or temperature changes can result in pulse duration changes that affect the peak-power stability. Here we present a concept to measure these fluctuations that is based on prechirping a fraction of the laser output pulses, followed by spectral broadening in a single-mode fiber and detection of the output bandwidth [1], which then acts as the measurement signal (see Fig. 1 a)). Applying this pre-chirp allows for a significantly increased precision for the measurement of the pulse duration fluctuations (which result in spectral bandwidth changes), reaching attosecond precision.

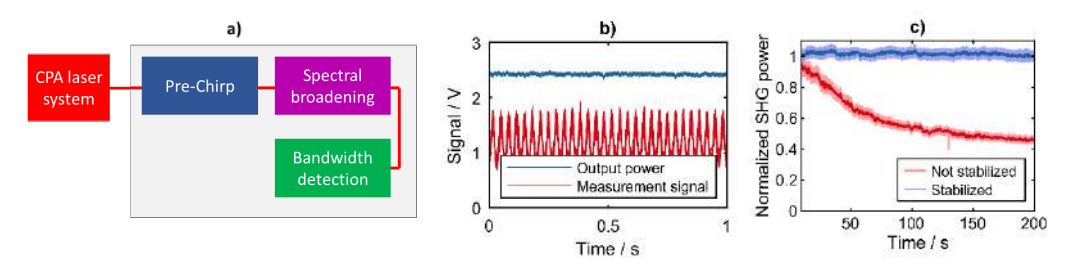


Figure 1: a): Schematic setup. b): Per-pulse signals of the output power and the pulse duration measurement signal if the pulse duration is modulated. c): Second harmonic power if the stabilization is turned off and on during startup.

In Fig. 1 b), the per-pulse measurement signal over a timescale of 1 second is shown if the pulse duration of a 100 kHz repetition rate fiber laser system emitting pulses with 280 fs duration is intentionally modulated with an amplitude of 2 fs. A strong modulation of the measurement signal is visible, while the output power of the system stays constant. Without this modulation, we determined pulse-to-pulse fluctuations of the pulse duration of around 80 as (RMS), with a measurement sensitivity of 20 as. The frequency dependency of the signal follows residual energy fluctuations of the pulses, as predicted in the literature [2]. We also used this signal to stabilize the pulse duration of a high-power CPA system by driving a thermally tunable pulse stretcher. In Fig. 1 c), the power of out-of-loop second-harmonic generation (SHG) is shown during start-up (thermalization of the laser) with the feedback system enabled and disabled. As can be seen, a drastic improvement of the stability of the generated SHG power due to the stabilization of the pulse duration is observed, with the residual fluctuations being similar to the case of a completely thermalized system.

- [1] T. Eidam, S. Hädrich, and F. Stutzki, "System for detecting pulse duration fluctuations of laser pulses and method for generating laser pulses," Patent application WO2022171675A1 (2022).
- [2] R. Paschotta, "Noise of mode-locked lasers (Part II): Timing jitter and other fluctuations," Appl. Phys. B Lasers Opt. **79**, 163–173 (2004).

²Helmholtz-Institute Jena, Froebelstieg 3, 07743 Jena, Germany

³GSI Helmholtzzentrum for heavy ion research, Planckstraße 1, 64291 Darmstadt, Germany

⁴Fraunhofer IOF, Albert-Einstein-Straße 7, 07745 Jena, Germany

⁵Active Fiber Systems GmbH, Ernst-Ruska-Ring 17, 07745 Jena, Germany

^{*}a.klenke@hi-jena.gsi.de

Shaping Exciton Polarization Dynamics in 2D Semiconductors by Tailored Ultrafast Pulses

Omri Meron,^{1,2*} Uri Arieli,^{1,2} Eyal Bahar, ^{1,2} Swarup Deb1, ¹ Moshe Ben-Shalom1, ¹ Haim Suchowski^{1,2}

¹Condensed Matter Physics Department, School of Physics and Astronomy, Faculty of Exact Sciences, Tel Aviv University, Tel-Aviv, 6997801, Israel

²Center for Light-Matter Interaction, Tel Aviv University, Tel-Aviv, 6997801, Israel *omrimeron@tauex.tau.ac.il

Abstract

We demonstrate precise temporal control of coherent exciton polarization dynamics in monolayer WSe2 using a single sub-10 fs shaped pulse. By tuning multiphoton pathway interference, we selectively tune and enhance four-wave mixing (FWM) generated by distinct excitonic states, identifying exciton-exciton interactions as the predominant FWM mechanism.

Strongly bound excitons in two-dimensional transition metal dichalcogenides offer an exceptional platform for studying fundamental light-matter interactions and developing novel optoelectronic applications. While excitonic many-body interactions and their nonlinear properties have been extensively studied, the potential to study these phenomena by directly controlling the underlying coherent polarization dynamics has not been fully realized. In this work, we employ an ultrabroadband pulse shaper to precisely control coherent exciton polarization in monolayer WSe2 under ambient conditions. As shown in Figure 1, by applying arctangent spectral phase functions with varying linewidths to our sub-10 fs pulses, we systematically tune the temporal profile of excitation pulses interacting with the sample. Our approach enables manipulation of multiphoton pathway interference from destructive to constructive, resulting in a 2.6-fold enhancement of FWM yield compared to transform-limited pulses. This demonstrates how tailored ultrafast pulses can counteract temporal dispersion during resonant lightmatter interactions to compress the transient exciton polarization and maximize nonlinear responses. Significantly, our method allows selective excitation of both 1s and 2s excitonic states, providing state-specific control over nonlinear processes. By comparing experimental results with theoretical models incorporating different nonlinear contributions, we conclusively identify exciton-exciton (X-X) interactions as the predominant mechanism driving the observed FWM, rather than Pauli blocking (PB). This capability opens new possibilities for precise optical control in future quantum optoelectronic devices. [1]

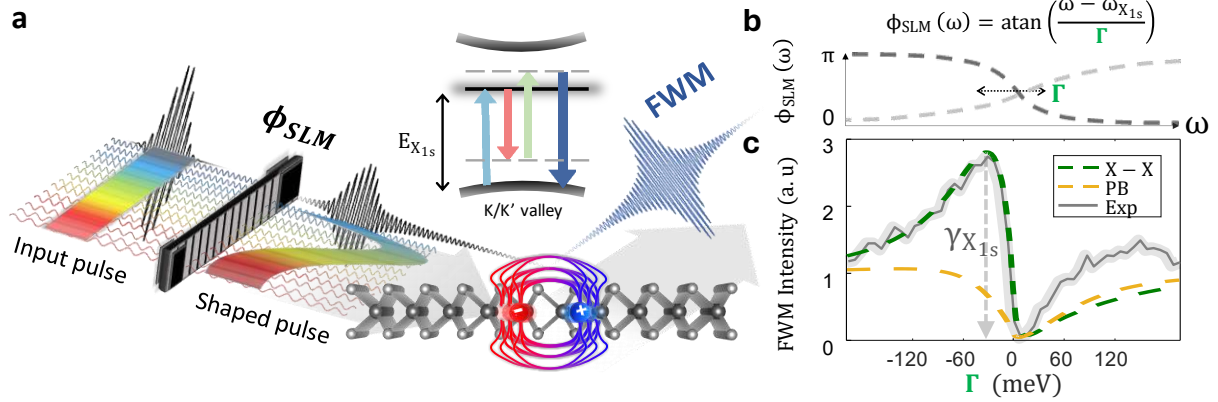


Figure 1: FWM intensity induced by temporally shaped pulses with varying arctangent phase functions. (a) left: an ultrabroadband sub-10fs pulse (690-1030nm) propagates through a spatial light modulator (SLM). Schematic illustration describing how a negative arctangent spectral phase applied by the SLM, affects the group delay of the pulse. Right: The shaped pulse then interacts with the sample, generating a FWM signal. Illustration of an intra-pulse FWM process in which spectral counterparts interact nonlinearly with the A1s exciton. (b) Illustration of an arctangent phase function with a varying linewidth Γ applied to the SLM. (c) Experimental results plotted against the theoretical model: TMD Bloch equations of motion including two theoretical nonlinear contributions, PB and X-X interactions, plotted separately.

References

[1] O. Meron, et al. "Shaping exciton polarization dynamics in 2D semiconductors by tailored ultrafast pulses" Light Sci Appl 14, 80 (2025).

Single-Shot Carrier-Envelope Phase Measurement at 586 kHz Using Optical Fourier-Transform Interferometry

C Guo,^{1,*} M Miranda,^{2,3} A-K Raab,¹ A-L Viotti,¹ P Tiago Guerreiro,^{2,3} V Amorim,^{2,3} P Matyba,⁴ R Romero,^{2,3} H Crespo,^{3,5} A L'Huillier,¹ C L Arnold¹

Abstract

In this work, we demonstrate single-shot and every-shot measurements of the carrier-envelope phase (CEP) of ultrashort pulses at a repetition rate of 586 kHz. Synchronous measurements using a commercial CEP detector, operating at a lower sampling rate (117 kHz), show excellent agreement, validating the accuracy and reliability of our approach.

In the few-cycle regime, the absolute phase of ultrashort light pulses, known as the carrier-envelope phase (CEP), plays a crucial role in controlling light-matter interactions, such as the generation of isolated attosecond pulses [1]. Precise, single-shot CEP detection is therefore essential, but particularly difficult at high repetition rate. We have recently demonstrated a novel, all-optical, single-shot (and every shot) method to measure the CEP of ultrashort laser pulses at a repetition rate of $200\,\mathrm{kHz}$ [2]. In the present work, we extend the measurement speed to a repetition rate of $586\,\mathrm{kHz}$, which to our knowledge is the fastest reported CEP measurement in single-shot.

CEP is commonly encoded in the form of spectral fringes in f:2f spectra (Fig. 1a, left panel). Our technique employs optical Fourier transform, implemented via filtering the f:2f spectrum with optical elements that have a spectrally periodic transmission function (Fig. 1a, middle panel). The CEP is then simply determined as the arctan of two photodiode signals (Fig. 1a, right panel), a measurement that can in principle be performed at many MHz repetition rate up to the speed of common ultrafast oscillators. Our approach effectively circumvents bottlenecks limiting conventional CEP detectors, such as the need for high-speed spectrometers and the time required for numerical Fourier transform operations [2].

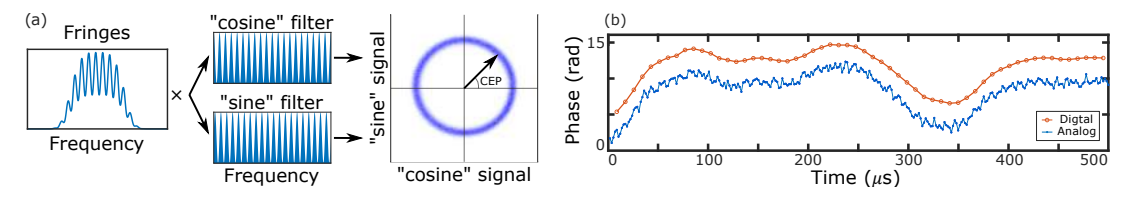


Figure 1: (a) Principle of obtaining the phase of f:2f spectral fringes via optical Fourier transform. (b) Comparison with the commercial CEP detector.

We also have performed synchronized measurements with a commercial, high-speed CEP detector (Sphere Ultrafast Photonics), based on a fast CMOS linear sensor for measuring the f:2f spectra and numerical FFT to calculate the phase of the fringes. A CEP-stable Pharos laser (Light Conversion), was measured at the full repetition rate of 586 kHz with the high speed detector (indicated as "analog" in Fig. 1b), while every fifth pulse (117 kHz) was sampled with the commercial detector (indicated as "digital" in Fig. 1b). Unlike previous correlation measurements [2], here two completely independent CEP detectors, each with its own white-light generation and f:2f stages, were used. Fig. 1b shows a time interval of 500 µs of the two synchronized detectors with an arbitrary CEP offset between them (f:2f is not sensitive to absolute phase). The agreement is excellent, indicating at least similar performance as compared to conventional CEP detectors.

- [1] J Schoetz et al., ACS Photonics 6, 3057 (2019).
- [2] C Guo et al., Opt. Lett. 48, 5431-5434 (2023).

¹Department of Physics, Lund University, P. O. Box 118, SE-22100 Lund, Sweden

²IFÍMUP-IN and Departamento de Física e Astronomia, Universidade do Porto, Rua do Campo Alegre 687, 4169-007 Porto, Portugal

³Sphere Ultrafast Photonics, Rua do Campo Alegre, 1021, Edifício FC6, 4169-007 Porto, Portugal

⁴Department of Physics, Umeå University, Umeå, 90187, Sweden

⁵Central Laser Facility, STFC, Rutherford Appleton Laboratory, Didcot OX11 0QX, United Kingdom

^{*}Chen.Guo@fysik.lth.se

d-scan ultrashort pulse characterization implemented with a 4-f pulse stretcher/compressor

Miguel Miranda, 1,2,* Chen Guo, Paulo T. Guerreiro, 1,2 Cord L. Arnold, Vitor Amorim, 1,2 and Rosa Romero 1,2

Abstract

We present an implementation of the d-scan technique using a variable grating-based 4f stretcher/compressor arrangement. This allows us to continuously scan from negative to positive dispersion over a large range. We demonstrate this implementation by measuring sub 8 fs to 100 fs pulses with the same setup.

The d-scan technique [1] is often implemented as a part of the compression system itself. Typically, chirped mirrors introduce a fixed amount of negative dispersion, and glass wedges introduce variable positive dispersion. By measuring the nonlinear spectrum as a function of glass insertion, a d-scan trace is built, and an iterative algorithm is used to retrieve the pulse's spectrum.

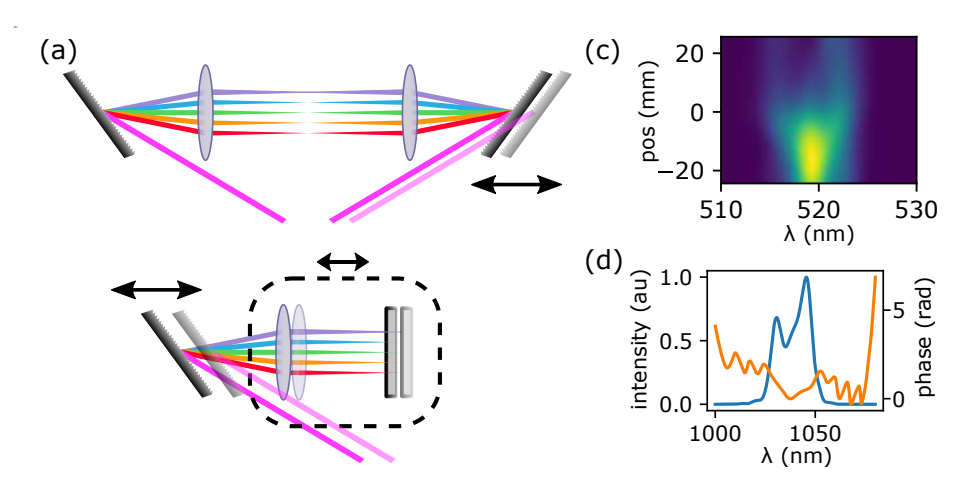


Figure 1: (a) Illustration of the concept and (b) simplified schematic of the implementation of a folded 4f pulse stretcher/compressor. (c) d-scan trace and (d) retrieved spectrum and phase of a ~ 100 fs pulse at 1 µm wavelength.

In this work, we use a grating-based pulse stretcher/compressor to implement d-scan as a standalone device, without the need for dispsersion pre-compensation (Fig.1a and 1b). Using (for example) a 4f geometry, one can create a zero-dispersion system by having the image of the first grating on the second grating [2]. By moving one of the gratings, we can introduce negative or positive dispersion at will, with much higher dispersion ranges than typically achievable with glasses. As a demonstration, we measured pulses with about 100 fs FWHM (Fig 1 c and 1 d). The same system is capable of measuring pulses below 8 fs.

- [1] M. Miranda, T. Fordell, C. Arnold, A. L'Huillier, and H. Crespo, "Simultaneous compression and characterization of ultrashort laser pulses using chirped mirrors and glass wedges," *Opt. Express*, vol. 20, pp. 688–697, Jan 2012.
- [2] O. E. Martinez, J. P. Gordon, and R. L. Fork, "Negative group-velocity dispersion using refraction," J. Opt. Soc. Am. B, vol. 1, p. 1003, 1984.

¹Sphere Ultrafast Photonics, Rua do Campo Alegre 1021, Edifício FC6, 4169-007 Porto, Portugal

²IFIMUP-IN and DFA, Universidade do Porto, Rua do Campo Alegre 687, 4169-007 Porto, Portugal

 $^{^3\}mathrm{Department}$ of Physics, Lund University, P.O. Box 118, SE-22100 Lund, Sweden

^{*}mmiranda@sphere-photonics.com

Progress on the commissioning of 10 Hz Petawatt beamline at the Extreme Photonics Applications Centre

Cristina Hernandez-Gomez ¹, Veselin Aleksandrov ¹, Chris Armstrong ¹, Samuel Buck, Thomas Butcher ¹, Danielle Clarke ¹, Rob Clarke ¹, Stephen Dann ¹, Tiago Faria Pinto ¹, Chris Gregory ¹, James Green ¹, Robert Heathcote ¹, Paul Mason ¹, Luke McHugh ¹, Rajeev Pattathil ¹, Gary Quinn ¹, Chris Spindloe ¹, Jorge Suarez-Merchan ¹, Nicholas Stuart ¹, Dan Symes ¹, Agnieska Wojtusiak ¹ and John Collier ¹

¹Central Laser Facility, STFC Rutherford Appleton Laboratory, Harwell Campus, Didcot, Oxfordshire, OX11 0QX, United Kingdom

*corresponding author: Cristina.hernandez-gomez@stfc.ac.uk

Abstract

In this paper we present the current status of the Extreme Photonics Applications Centre (EPAC). This new facility will deliver 1 PW laser operating 10 Hz into two versatile experimental areas. EPAC has been designed to further the development and application of laser-driven accelerators in academic, industrial, and medical spheres.

The EPAC facility at the Central Laser Facility (UK) is currently being commissioned and operations are expected in the summer of 2026. The 1PW laser system is diode pumped, it has been built with an all-OPCPA joule-class front end, the output of which is amplified in a high energy gas cooled multi- slab titanium-sapphire (Ti:Sa) amplifier. The Ti:Sa amplifier will be pumped by the frequency-doubled output of a DiPOLE 150J diode pumped cryogenic gas cooled Yb:YAG slab laser[1]. The output from the Ti:Sa amplifier will be compressed to 30 fs pulses, delivering a peak power of one petawatt to the experimental areas. The facility has been designed to incorporate additional laser beams at a later stage. A second 150J DiPOLE is also being constructed for either "long pulse" ns interactions or as a pump for a second PW beamline. We report on progress with commissioning the petawatt laser. EPAC will initially operate a single PW beam into two versatile experimental areas and will support a multi-disciplinary community of users. The first experimental area (EA1) will be specifically designed for laser wakefield acceleration (LWFA), where multi-GeV electron beams, x-ray and g-Ray beams can be generated in 2 dedicated synchrotron style beamlines. The second flexible experimental area (EA2) will deliver fundamental science and applications, enabling the generation of electron, proton, neutron, muon beams, x-rays and g-ray beams simply by swapping out the target and altering the laser focusing geometry.



Figure 1: EPAC Building

References

[1] [P. D. Mason et al, "Development of a 100 J, 10 Hz laser for compression experiments at the High Energy Density instrument at the European XFEL," High Power Laser Science and Engineering, 6, e65 (2018).

Picosecond contrast improvement for PW class lasers based on modified stretcher design

Chalus O.^{1*}, Papadopoulos D.², Mathieu F.², Audebert P.², Lebas N.², Charbonneau M.¹, Pasternak S.¹, C. Derycke¹, Ferhat S.¹, Pellegrina A.¹ Ricaud S.¹, LeGarrec B.^{2,3}, Gaul E.⁴, Cojocaru G.⁵, Toma A.⁵, Norbaev S.⁵, Dancus I.⁵

¹Thales LAS France, Elancourt, France; ²Laboratoire pour l'Utilisation des Lasers Intenses, CNRS, Ecole Polytechnique, CEA, Sorbonne Université, France, France; ³LASYEX, Prague, Czech Republic; ⁴MARVEL Fusion, Munich, Germany; ⁵ELI-NP Magurele, Romania *corresponding author: <u>olivier.chalus@fr.thalesgroup.com</u>

Abstract: To improve picosecond contrast within mulit-petawatt laser system a stretcher without convex mirror is proposed, designed and implemented to demonstrate the gain of contrast of several order of magnitude on hundred picosecond time-scale pedestal.

The picosecond contrast is an outmost parameter for multi-PW laser systems. The presence of tens of picosecond pedestal prior to the main pulse in multi-PW class laser system could lead to damage of the target as it can reach intensity on target higher than 10^{14} W/cm². It has been demonstrated that the convex mirror within the Offner stretcher of those laser systems is the main contributor to this pedestal [1]. To reduce this effect, ultralow roughness mirrors have been implemented in some laser systems [2].

To reduce even more this pedestal, a stretcher without a convex mirror has been developed. A complete simulation of this stretcher demonstrates its compatibility with the requirements of PW class lasers..

A version of this stretcher has been recently implemented on the 10 PW beamline of the ELI-NP [3,4] HPLS further improving the contrast ratio. It is designed to match perfectly the stretching factor of the existing Offner stretcher as the existing 10PW compressor presents a fixed configuration, and to minimize aberrations and spatial chirp.

Implementing the ultralow roughness mirrors (with the RMS of 0.2 nm) in the ELI-NP Offner-type stretcher improved the temporal contrast at 10 ps from the main pulse by about three orders of magnitude in comparison with the "regular" roughness mirror (with the RMS of 3.5 nm). Implementing the new stretcher led to a further improvement of about one order of magnitude. After these optimisations, we achieved a contrast of about 10 orders of magnitude at 10 ps from the main pulse, further going to 11 orders of magnitude at 50 ps (Fig. 1) [5]

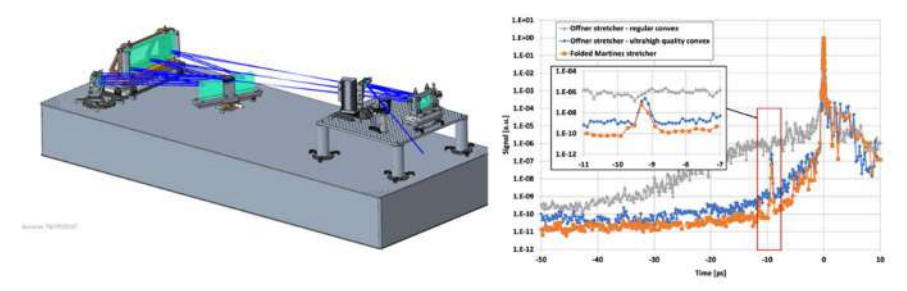


Figure 1: Contrast measurement curves for the three cases: grey curve, Offner-type stretcher using a regular convex mirror; blue curve, Offner stretcher using an ultrahigh-quality convex mirror; orange curve, reflective Martinez-type stretcher. The peak at approximately 9 ps is generated by a bulk dispersion compensator. The inset provides a clearer representation of the position of the approximately 9 ps pre-pulses, thereby revealing the sampling rate of the measuring device and the peaks with similar relative positions.

A Martinez type stretcher with all reflective optical components allows an improvement of several orders of magnitude in the pedestal contrast of multi-PW laser systems. It generates minimum spatial chirp and chromatic aberrations while inducing a stretching factor of more than 14ps/nm on a bandwidth larger than 120nm in order to accommodate sub-22fs pulse duration at 10PW.

Experimental results showing performance of better than 10^{10} contrast on the pedestal at 10ps prior to the main pulse for a 10PW laser have been demonstrated and will be presented.

- [1] Bromage et al., "Temporal contrast degradation at the focus of ultrafast pulses from high-frequency spectral phase modulation" J. Opt. Soc. Am. B 29, 1125 2012
- [2] Ranc et al., "Improvement in the temporal contrast in the tens of ps range of the multi-PW Apollon laser front-end" Opt. Letters 4600 Vol. 45, No. 16, 2020
- [3] Lureau et al., "High-energy hybrid femtosecond system demonstrating 2x10PW capability", HPLSE Vol. 8, 2020
- [4] Radier et al., "10 PW peak power femtosecond laser pulses at ELI-NP", HPLSE Vol. 10, 2022
- [5] Chalus et al., "High-contrast 10 PW laser system at the Extreme Light Infrastructure Nuclear Physics facility", HPLSE, Vol. 12, 2025

Advancing Short-Pulse Laser Drivers for Fusion Applications

E. W. Gaul¹, P. Fischer¹, G. Bodini¹, J. Jung¹, F. Buckstegge², C. Aleshire², P. Jhetre², O. Naranjo², A. Schmalz², M. Krüger¹, J. H. Buss^{1*}, M. Schollmeier¹, H. Ruhl¹, and G. Korn¹

¹ Marvel Fusion GmbH, Theresienhöhe 12, 80339 Munich, Germany

*heye.buss@marvelfusion.com

Abstract

We develop a diode-pumped solid-state Petawatt laser (>100 J, <100 fs, 10 Hz, 527nm) with up to 10% wall-plug efficiency. Optimized for high temporal pre-pulse contrast (>10 $^{-10}$:1), it efficiently couples laser energy to ions via ponderomotive electron expulsion and Coulomb acceleration, reaching MeV energies in a compact design.

Introduction

Marvel Fusion is advancing laser-based inertial fusion energy (IFE) [1] to provide a carbon-free power source. In the context Marvel Fusion explores nanostructures for efficient laser energy absorption. High contrast Petawatt pulses, ideal for this method, achieve near-total absorption, ensuring rapid laser energy deposition in the target.

To enable this ultrafast energy transfer, Marvel Fusion is developing high-efficiency laser systems combining optical parametric chirped pulse amplification (OPCPA) with broadband amplification in Neodymium-doped glass [2]. Nd:glass provides sufficient bandwidth for sub-100 fs pulses while maintaining energy levels. Ytterbium-doped materials offer high power but require cryogenic cooling, which narrows gain bandwidth. To mitigate pulse degradation, power amplifier gain is limited to 20-30 dB [2]. High-power diode pumping (>10 kW/cm²) enhances gain while enabling compact designs, reducing nonlinear phase accumulation, and improving system efficiency in comparison to traditional flashlamp pumped high energy systems.

A key focus is optimizing wall-plug efficiency through enhanced diode laser performance, energy delivery, and minimal losses in amplification and beam transport. Dielectric gratings with high damage thresholds achieve 90-95% compression efficiency [3]. Additionally, second harmonic generation (SHG) enhances temporal contrast (>10¹⁰:1), ensuring clean interactions with nanostructured targets. Initial SHG tests demonstrate >60% conversion efficiency, with further improvements underway [4].

Marvel Fusion's collaboration [5] with Pulsed Light Technology and Colorado State University is driving advancements in compact, high-performance laser systems for fusion energy. By optimizing energy deposition and contrast, these innovations are shaping the future of fusion research.

- [1] see for example Zylstra, A.B., Hurricane, O.A., Callahan, D.A. et al. Burning plasma achieved in inertial fusion. Nature 601, 542–548 (2022). https://doi.org/10.1038/s41586-021-04281-w
- [2] E. Gaul, et al, "Demonstration of a 1.1 petawatt laser based on a hybrid optical parametric chirped pulse amplification/mixed Nd:glass amplifier," Appl. Opt. 49, 1676-1681 (2010)
- [3] H. T. Nguyen, et al "Advancements in High Fluence Meter-Size Multilayer Dielectric Gratings for Ultrafast Lasers," in Optical Interference Coatings (OIC), (2022), paper ThE.1.
- [4] P. Fischer, B. Gonzalez-Izquierdo, V. Scutelnic, et al (2023). Second Harmonic Generation in a 140 fs Petawatt Laser System. 1-1. 10.1109/CLEO/Europe-EQEC57999.2023.10231686.
- [5] see https://source.colostate.edu/csu-marvel-fusion-groundbreaking-laser-facility/

² Pulsed Light Technology GmbH, Lagerhofstraße 4, 04103 Leipzig

Multilayer dielectric coatings for ultrahigh intensity lasers and their challenges to achieve long term operation without damage

Carmen S. Menoni, 1,2

¹ RISE, DOE IFE-STAR Inertial Fusion Energy hub and Department of Electrical & Computer Engineering, Colorado State University, Fort Collins, CO 80523, USA

*carmen.menoni@colostate.edu

² XUV Lasers, Inc. Fort Collins, CO 80523

csmenoni@xuvlasers.com

Abstract

Amorphous oxide coatings, a ubiquitous laser technology, are being challenged by premature damage at ultra-high intensities and ultra-high energy. This talk will describe efforts in improving the materials' morphology, and how it can be exploited to engineer novel multilayer dielectric coatings with high resilience to laser damage.

The 2023 DOE/NSF Basic Research Needs (BRN) workshop report and subsequent publication [1,2] identified ultra-high intensity laser platforms that are needed to advance the science frontiers in areas such as the generation of secondary photon and particle sources, the sensing of fundamental atomic process in matter and the exploration of the physics of high energy density plasmas [1,2]. Among the priority research directions for basic research in laser science and technology, the BRN identified laser materials and, in particular, interference coatings as a critical technology to enable advances in ultrahigh intensity solid state lasers operating from the ultraviolet to the mid-infrared.

There have been enormous advances in MLD coatings for lasers operating from the near infrared to the ultraviolet in continuous wave mode or producing pulses of nanosecond pulse duration. However, similar advances in MLD coatings for ultrashort pulse lasers have been slower, to the point that this critical laser technology is the limiting factor for scaling solid state lasers in pulse energy and repetition rate. This talk will summarize the state-of-the-art in MLD coatings for high intensity lasers operating from the UV to the near infrared, and discuss the challenges for MLD coatings to achieve long term operation without damage. Results will be presented on the use of novel amorphous metal-oxide mixtures that when incorporated into MLD coatings show promising results in terms of laser damage performance. Specific examples of MLD coatings designed for specific applications, such as phase shifting, will also be presented.

Work supported by: the U.S. Department of Energy (DOE), Office of Science, Fusion Energy Sciences, under Awards No. DE-SC0024882: IFE-STAR, DE-SC0023237, DE-SC0024882 and DE-SC0019900.

References

[1] Report Of The Basic Research Needs Workshop On Laser Technology, US Department of Energy, Office of Science,https://science.osti.gov/-/media/ardap/pdf/2024/Laser-Technology-Workshop-Report 20240105 final.pdf

[2] Matthias F Kling, et al, J. Optics, vol. 27, Issue 1, Art. No.: 013002, 2024,

Toward 100Hz Joule class ultra-short pulses TiSa laser

Pellegrina A.¹; Kabacinski A.¹; Jeandet A.¹; Leroux V.¹; Lavenu L.¹; Chalus O.¹; Casagrande O.¹; Ricaud S.¹; Simon-Boisson C.¹

¹ Thales LAS France., 2 avenue Gay-Lussac, 78995 Elancourt Cedex, France

Abstract: Joule class lasers at 100Hz with ultra-short pulse involve a lot of challenges to manage thermal issues in the amplifiers as well as in the compressors. Recent results achieved in this direction are presented.

Acceleration experiments have been performed at limited repetition rate ranging from 1 Hz for PetaWatt class lasers to 10 Hz for 100 TeraWatt class lasers [1]. Higher repetition rate is required to generate the particle or radiation flux necessary for applications in different fields of industry and medicine. In this goal, we report on the way to amplify laser light in TiSa at average power levels exceeding 100 Watts while managing the induced thermal issues. Compression of those pulses under vacuum presents also a challenge in order to manage the heat load in the gratings and prevent degradation of the wavefront due to thermal deformation.

We present here an OPCPA frontend amplified in a multi-stage TiSa to reach more than 850mJ at 100Hz (Fig. 1).

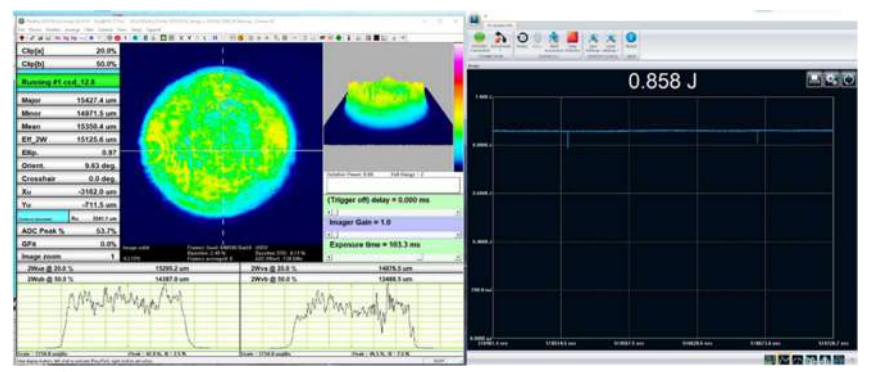


Figure 1: >850mJ at 100Hz beam profile and energy stability

The amplifiers are pumped by a THEIA laser (Thales catalog product) which is a nanosecond diode-pumped frequency doubled Nd:YAG laser delivering more than 750 mJ of green light pulses at a repetition rate of 100 Hz. The pump beams can make 4 passes within the TiSa disks whereas the number of passes of the 800 nm beam to amplify can be adjusted.

First amplifier is pumped by a single THEIA and can deliver up to 300 mJ whereas the second amplifier is pumped by 2 THEIA pump lasers in order to obtain 850 mJ at amplifier output and will be further upgraded to 4 THEIA to achieve 1.5J.

For the compression, gold gratings are required to support sub-25fs pulses spectral bandwidth but suffer from absorption and grating over-heating could lead to wavefront deformation [2]. This phenomena has been modelled and experimental tests have been performed in order to validate the results. With a properly designed thermal management of the grating, the surface temperature could be reduced by more than a factor of 3 from more than 120°C to just 46°C.

We have demonstrated amplification at room temperature within TiSa crystals up to 850 mJ energy per pulse at a repetition rate of 100 Hz, a record average power value for this material. We expect to produce soon a 1 J - 25 fs - 100 Hz TiSa CPA laser system paving the way for introduction of laser technology in many societal applications needing laser-based particle acceleration and secondary radiation sources.

- [1]: "Laser Electron Accelerator", T. Tajima, J. Dawson, Physical Review Letters, vol 43, p267 (1979)
- [2]: "Wavefront degradation of a 200 TW laser from heat-induced deformation of in-vacuum compressor gratings" V. Leroux et al. Optics Express, vol 26, Issue 10, pp 13061-13071 (2018)

Towards a sub-10 fs hybrid frontend with $>10^{14}$ temporal contrast for high intensity lasers

Roland S. Nagymihály, Mikhail Kalashnikov, Levente Lehotai, Viktor Pajer, János Bohus, Nóra Csernus-Lukács, Szabolcs Tóth, János Csontos, Balázs Tari, Ignas Balciunas, Ernestas Kucinskas, Tomas Stanislauskas, and Ádám Börzsönyi

¹ELI ALPS Research Institute, Wolfgang Sandner u. 3, H-6728 Szeged, Hungary

Abstract

Performance of an OPCPA seeded Ti:Sa-based 7 mJ 100 Hz frontend is presented with an ultrahigh temporal contrast of >10¹² in combination with sub-15 fs pulse duration. Investigation of further temporal cleaning in a multipass cell is in progress to obtain sub-10 fs with a contrast reaching the 10¹⁴ level.

Introduction

Next generation high intensity lasers based on Ti:Sa gain medium require reliable frontends with ultrabroad spectral bandwidth and temporal contrast of extreme values in the range of >10¹³. Multi-PW lasers currently use Ti:Sa-based chirped pulse amplification (CPA) combined with cross-polarized wave generation and picosecond parametric amplifiers before as a frontend before their main stretcher [1]. Seeders based on optical parametric CPAs (OPCPA) are now emerging as they can produce intrinsically very high contrast and high bandwidth [2,3].

Results

Here we present results on the development of a hybrid OPCPA-Ti:Sa-based frontend architecture. The system starts with an industrial grade OPCPA (ORPHEUS, Light Conversion) pumped by an ultrastable Pharos laser. Seed pulses with $100~\mu J$ energy and 8 fs transform limited spectrum are stretched negatively, spectrally shaped, amplified in a two-stage Ti:Sa amplifier scheme, and finally compressed via positive dispersion. After the second amplifier, an energy of 13~mJ is reached at 100~Hz repetition rate with a spectrum corresponding to 14.4~fs transform limited duration (Fig. 1).

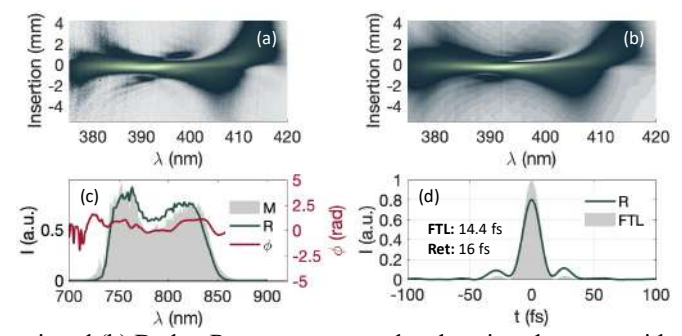


Fig. 1. Measured (a) and retrieved (b) D-shot R traces, measured and retrieved spectra with spectral phase (c), and the retrieved temporal profile (d).

By compressing 1 mJ from the amplified 13 mJ in air, we measured the spatio-spectral quality, pulse duration, and the high dynamic intensity contrast. We confirmed, that the output pulses are free of spatio-spectral couplings, while a temporal contrast $>10^{12}$ was measured at -15 ps before the main pulse. Implementation of a multipass cell is in progress to perform nonlinear temporal cleaning in combination with spectral broadening to further improve temporal characteristics with mJ-level output and an intensity contrast reaching 10^{14} .

- [1] F. Lureau et al, High Power Laser Science and Engineering, 8, 43 (2020).
- [2] R. S. Nagymihály et al, Opt. Express 31, 44160-44176 (2023).
- [3] R. Maksimenka et al, EPJ Web Conf., 309, 07003 (2024).

²Light Conversion Ltd., Keramiku str. 2b, LT-10233 Vilnius, Lithuania

^{*}roland.nagymihaly@eli-alps.hu

Thursday

October 9th

Innovative Microfluidic Sources for XUV and Soft-X Ray Generation

Caterina Vozzi

CNR Istituto di Fotonica e Nanotecnologie, Milano, 20133, Italy caterina.vozzi@cnr.it

Abstract

We present recent experimental advances in using an efficient microfluidic HHG-based XUV source, developed for studying ultrafast electron dynamics in materials and complex molecules.

Main Text

Molecular dynamics play a key role in ultrafast spectroscopy, impacting physics, biochemistry, and quantum technologies. High Harmonic Generation (HHG) with femtosecond lasers and noble gases produces coherent EUV pulses, enabling attosecond resolution for probing electronic dynamics, though challenges remain regarding complexity and efficiency at higher photon energies.

Here, we introduce recent developments of microfluidic devices with hollow core channels for efficient HHG generation and manipulation, achieving high photon flux and phase matching up to 200 eV [1,2] and HHG in the water window. Our microfluidic approach enables precise control over the properties of the HHG beam, enabling structured EUV and soft-X light for ultrafast spectroscopy and high-resolution imaging. Furthermore, this integrated microfluidic approach allows controlling the spatial properties of the HHG beam through the direct manipulation of the waveguide's modes, making it possible to generate high-brightness attosecond XUV and soft-X ray pulses with unique polarization properties.

The XUV source based on microfluidic device is coupled to a versatile beamline for EUV and soft-X-ray spectroscopy, designed for time-resolved experiments and supporting Transient Absorption (TA) and reflectivity measurements, featuring a high-resolution spectrometer and polarimeter.

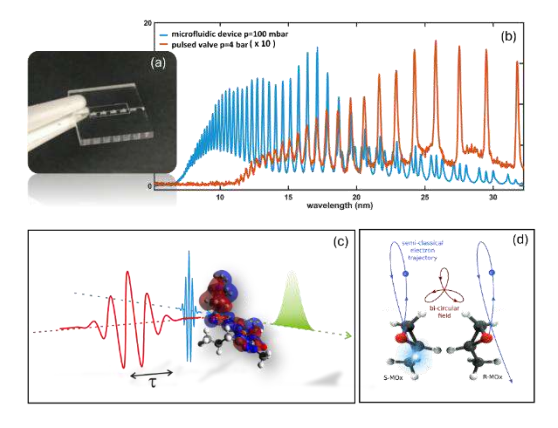


Figure 1: a microfluidic device used for HHG. b HHG spectrum generated with the microfluidic approach (blue) compared with the spectrum generated by gas-jet valve (red). c and d provide a concept-frame of TA and HHG spectroscopy in complex molecules.

- [1] A. G. Ciriolo et al., Journal of Physics: Photonics 2 024005 (2020)
- [2] A G Ciriolo et al 2022 APL Photonics 7, 110801

Intrinsic Limits to Achieving Application-Relevant Soft X-ray Flux in High Harmonic Generation

Robert Klas, 1,2,3* Martin Gebhardt, 1,2+ Jan Rothhardt, 1,2,3 and Jens Limpert 1,2,3

Abstract

This contribution reveals the fundamental limitations of achieving application-relevant flux in high harmonic generation (HHG) at high photon energies due to CEP walk-off effects. The dephasing caused by differing phase and group velocities results in a limited effective coherence length, preventing efficient high harmonic generation beyond 0.5 keV.

High harmonic generation (HHG) is a cornerstone technology for a wide range of applications in physics, chemistry, biology, and material sciences. The increasing availability of photon flux in the XUV to soft X-ray spectral regions enables laboratory experiments that were previously only possible at large-scale facilities. At low photon energies (<50 eV), the demonstrated photon flux is already comparable to that of 3rd generation synchrotrons [1]. However, the gap in available photon flux widens with increasing photon energy. To maximize yield, it is crucial to achieve coherent build-up of the generated high harmonics over a sufficiently long medium length, ideally leading to absorption-limited HHG [2]. To push the phase-matching cutoff to higher photon energies, longer driving wavelengths and ever shorter pulse durations have been proposed and applied for HHG [3,4].

Here, we uncover a fundamental limitation to this approach. Our simulations and experiments show that the intrinsic carrier-envelope walk-off hinders the effective coherent build up particularly when targeting the soft X-ray region using long driving laser wavelengths and ultrashort driving pulses. This limitation arises from the different phase and group velocities of the driving laser, resulting in dephasing of the generated HHG radiation due to a changing intrinsic phase [5]. This dephasing leads to a limited effective coherence length, $L_{\text{walk-off}}^{\Delta\Phi=\pi}$, which can be much shorter than the absorption length. Figure 1 exemplifies this effect with HHG driven by a wavelength of 1900 nm in neon and helium. The color bar shows the ratio, x, of the effective coherence length to the absorption length, indicating that absorption-limited HHG ($L_{\text{coh}} > 5 L_{\text{abs}}$) is only possible up to approximately 300 eV.

This contribution will highlight the fundamental processes responsible for this effect. Finally, it will be shown that it is fundamentally impossible to design efficient HHG-based soft X-ray sources with application-relevant coherent flux at photon energies above 0.5 keV in this framework. Alternative approaches will be presented and discussed.

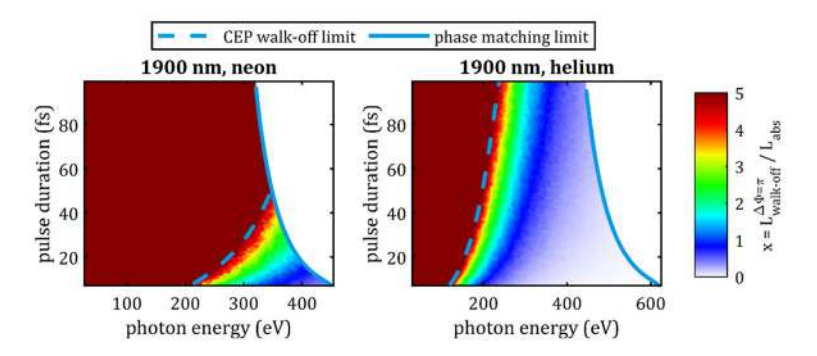


Figure 1: Ratio of the walk-off and absorption length for 1900 nm driven HHG in Neon and Helium. The dashed blue line indicates the CEP walk-off limit. The solid blue lines show the phase matching cutoff.

- [1] W. Eschen, et al. APL Photonics, submitted (2025)
- [2] E. Constant, et al. Phys. Rev. Lett. 82 (1999).
- [3] T. Popmintchev, et al. Nature Photon 4 (2010).
- [4] S. Hädrich, et al. J. Phys. B: At. Mol. Opt. Phys. **49** (2016).
- [5] C. Hernández-García, et al. New J. Phys. 18 (2016).

¹Institute of Applied Physics, Friedrich-Schiller-Universität Jena, Albert-Einstein-Str. 15, 07745 Jena, Germany ²Helmholtz-Institute Jena, Fröbelstieg 3, 07743 Jena, Germany

³Fraunhofer Institute for Applied Optics and Precision Engineering, Albert-Einstein-Str. 7, 07745 Jena, Germany ⁺now with: School of Engineering and Physical Sciences, Heriot-Watt University, Edinburgh, EH14 4AS, UK *robert.klas@iof.fraunhofer.de

Continuous Relativistic High-Harmonic Generation from a Liquid-Leaf Plasma Mirror at kHz Repetition Rate

Antoine Cavagna,^{1,*} Milo Eder,² Jaismeen Kaur¹, André Kalouguine¹, Stefan Haessler¹, Enam Chowdhury³ and Rodrigo Lopez-Martens¹

¹Laboratoire d'Optique Appliquée, Institut Polytechnique de Paris, ENSTA Paris, Ecole polytechnique, CNRS, 91120 Palaiseau, France

²Department of Physics, The Ohio State University, Columbus, OH 43210, USA

³Department of Materials Science and Engineering, Fontana Laboratories, The Ohio State University, Columbus, OH, 43210. USA

*antoine.cavagna@ensta.fr

Abstract

We demonstrate, for the first time, continuous relativistic high-harmonic generation (RHHG) at 1 kHz using an ethylene glycol liquid-leaf plasma mirror driven by waveform-controlled 1.5-cycle laser pulses.

Main Text

RHHG from plasma mirrors is a promising way of producing intense attosecond pulses by converting the large number of photons contained within an ultra-intense near-single-cycle laser pulse into an isolated sub-cycle burst of coherent XUV and soft X-ray light [1, 2]. Until now, this process has mostly been driven on solid targets with limited lifetime at high repetition rates. Self-replenishing liquid-leaf targets solve this problem by enabling continuous operation at kHz rates with optical surface quality [3]. Liquid plasma mirrors have recently been used for high-harmonic generation in the sub-relativistic regime at 1 kHz and for RHHG in single-shot mode [4].

In this work, we demonstrate continuous RHHG at 1 kHz for the first time from a liquid-leaf plasma mirror driven by waveform-controlled 1.5-cycle pulses [5]. A 2.4-micron thick sheet of ethylene glycol with out-of-plane motion below 200 nm RMS enables stable and repeatable RHHG. By adjusting the waveform of a 1.5-cycle laser pulse and controlling the plasma gradient at the liquid surface [6], we can switch between modulated and quasi-continuum XUV spectra on demand, as shown in Fig. 1., which should in principle correspond to the generation of stable trains of isolated attosecond pulses at 1 kHz. Liquid-leaf targets pave the way towards high-power attosecond light sources from plasma mirrors.

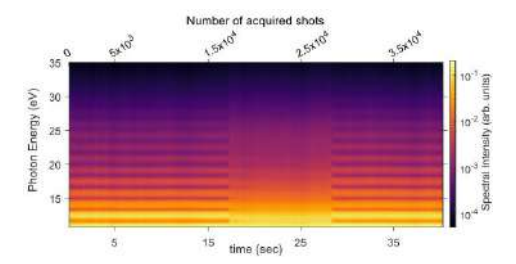


Fig. 1: RHHG spectra recorded at 1 kHz from an ethylene glycol leaf target driven by CEP-controlled 1.5-cycle pulses with locked CEP (545 frames made up of a 75-shot average recorded every 75 ms). The relative CEP was offset by π between 18 s and 29 s, showing the repeatable generation of XUV quasi-continua, which should correspond to a stable train of isolated attosecond pulses in the time domain.

- [1] G.D. Tsakiris et al., New J. Phys. 261, 19 (2006)
- [2] J. M. Mikhailova et al., Phys. Rev. Lett. 109, 245005 (2012).
- [3] J.T. Morrison et al., New J. Phys., 20 022001 (2018)
- [4] Y.H. Kim et al., Nat Commun. 14, 2328 (2023).
- [5] A. Cavagna et al., Opt. Lett. 50,165-168 (2025)
- [6] M. Ouillé et al., Light: Sci. Appl. (2020) 9:47

Bright Isolated Attosecond Pulses from Post-Compressed Yb Laser Filaments

Ming-Chang Chen1*

¹Institute of Photonics and Technologies, National Tsing Hua University, Hsinchu 30013, Taiwan *mingchang@mx.nthu.edu.tw

Abstract

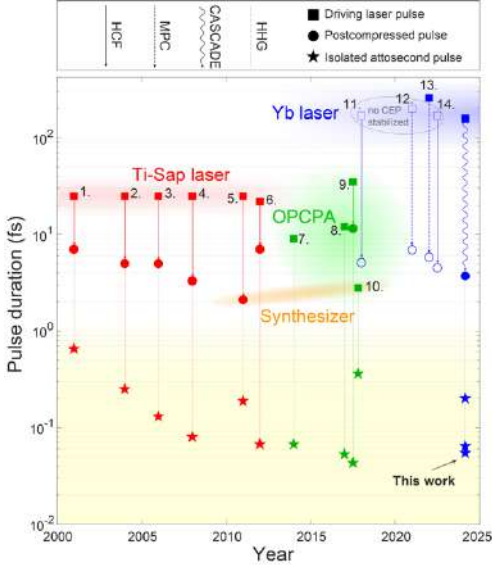
We demonstrate robust isolated attosecond pulse generation using post-compressed Yb laser filaments in a semi-infinite gas cell. Filamentation induces self-compression and phase-matching, enabling bright 200-as pulses in Ar and sub-70-as pulses in Ne and He, establishing a universal route toward high-contrast attosecond sources.

Isolated attosecond pulses (IAPs) are essential for resolving ultrafast electronic processes in atoms, molecules, and solids. While Ti:Sapphire and OPCPA systems have enabled major advances, they remain maintenance-demanding. Commercial Yb lasers are attractive for their robustness and high power but are typically limited by long pulse durations (>150 fs), restricting direct use in attosecond applications (see Fig. 1).

We introduce a hybrid strategy combining CASCADE post-compression [1] with filamentation-assisted shaping in a semi-infinite gas cell (SIGC) [2]. The CASCADE scheme spectrally broadens and compresses 170-fs Yb:KGW laser pulses to the few-cycle regime (~4.7 fs). When launched into the SIGC near the critical power ($P_{peak}/P_{cr} \approx 1$), the pulses undergo filamentation, which provides self-guiding, spatial cleaning, and further temporal self-compression to ~3.5 fs. This nonlinear propagation not only improves pulse quality but also establishes favorable phase-matching conditions for high-harmonic generation (HHG). Importantly, the SIGC simultaneously serves as the final compression stage and the IAP generation medium, producing high-contrast attosecond pulses.

In argon, we obtained bright 200-as pulses at 70 eV with excellent temporal contrast and spatial homogeneity. Extending the approach to neon and helium produced even shorter IAPs: 69 as at 100 eV and 65 as at 135 eV. Attosecond streaking measurements confirmed the high stability and reproducibility of the pulses. Compared with conventional short gas cells, the SIGC significantly improved IAP brightness and beam quality, underscoring the importance of filamentation-induced self-cleaning and self-compression.

In summary, we demonstrate for the first time bright IAPs directly from post-compressed Yb laser filaments. The combination of commercially available Yb technology, CASCADE post-compression, and filamentation-assisted self-guiding provides a simple and robust route to stable attosecond sources, opening new opportunities for widespread use in attosecond science.



- 1. Nature 414, 509-513 (2001).
- 2. Nature 427, 817-821 (2004).
- 3. Science 314, 443-446 (2006).
- 4. Science 320, 1614-1617 (2008).
- 5. Science 334, 195-200 (2011).
- 6. Opt. Lett. 37, 3891-3893 (2012).
- 7. Nat. Commun. 5, 3331 (2014).
- 8. Nat. Commun. 8, 186 (2017).
- 9. Opt. Express 25, 27506-27518 (2017).
- 10. Nat. Photon. 14, 629-635 (2020).
- 11. Sci. Rep. 8, 1-6 (2018).
- 12. Opt. Lett. 46, 2678-2681 (2021).
- 13. Opt. Lett. 47, 1537-1540 (2022).
- International Conference on Ultrafast Phenomena, Tu2B-4 (2022).

Figure 1: Laser sources and associated post-compression techniques demonstrated so far for generating IAPs.

- [1] M.-S. Tsai, A.-Y. Liang, C.-L. Tsai, P.-W. Lai, M.-W. Lin, and M.-C. Chen, "Nonlinear compression toward high-energy single-cycle pulses by cascaded focus and compression," Sci. Adv. 8, eabo1945 (2022).
- [2] Y.-E. Chien, M. Fernández-Galán, M.-S. Tsai, A.-Y. Liang, E. Conejero-Jarque, J. Serrano, J. S. Román, C. Hernández-García, and M.-C. Chen, "Filamentation-Assisted Isolated Attosecond Pulse Generation," under review; 10.48550/arXiv.2412.06339 (2024).

Low-Divergence Harmonic Generation with Hollow Gaussian Beams for Compact, High-Intensity Attosecond Sources

Melvin Redon,^{1,*} Rodrigo Martín-Hernández,² Ann-Kathrin Raab¹, Saga Westerberg¹, Victor Koltalo¹, Chen Guo¹, Luis Plaja^{2,3}, Julio San Román^{2,3}, Anne-Lise Viotti¹, Anne L'Huillier¹, Carlos Hernández-García^{2,3} and Cord Louis Arnold¹

Abstract

We use Hollow Gaussian Beams (HGBs) produced with a spatial light modulator to generate high-order harmonics in an argon gas jet. As opposed to conventional Gaussian beams, HGB-driven harmonics exhibit decreasing divergence with increasing harmonic order. This could be a recipe for more compact attosecond beamlines with higher refocused intensity.

High harmonic generation (HHG) occurs when an intense laser pulse interacts with a gas target, producing coherent radiation at multiples of the driving laser frequency. This converts visible or near-infrared pulses into extreme-ultraviolet (XUV) radiation, enabling ultrafast pulses from femtoseconds to attoseconds timescales [1]. Precise control over harmonic beam divergence and spot size is crucial for maximizing the refocused intensity. Gaussian laser beams generate harmonics with minimal divergence when the gas target is placed slightly before the beam's geometric focal point. However, all harmonic orders have different real or virtual longitudinal source points and cannot be refocused to the same position [2]. Alternative profiles, such as flat-top beams with uniform central intensity, reduce the divergence and chromatic aberrations [3].

In this study, we propose and demonstrate the use of Hollow Gaussian Beams (HGBs), a beam featuring a ring-shaped intensity distribution with a central intensity minimum and a flat phase over the ring [5]. As shown in Figure 1 a), harmonics generated with HGBs exhibit decreasing divergence with increasing harmonic order, in contrast to the increasing divergence typically observed for generation at focus with Gaussian beams (Figure 1 b)). Quantum and macroscopic simulations [4] reveal that the HGB's intensity profile and flat phase distribution effectively suppress the harmonic dipole phase contribution. Despite originating from a ring-shaped intensity pattern, the generated harmonics can be refocused into a restricted longitudinal spread focal spot with minimal chromatic aberrations (Figure 1 c)), making HGB-driven HHG advantageous for compact, high-intensity attosecond sources.

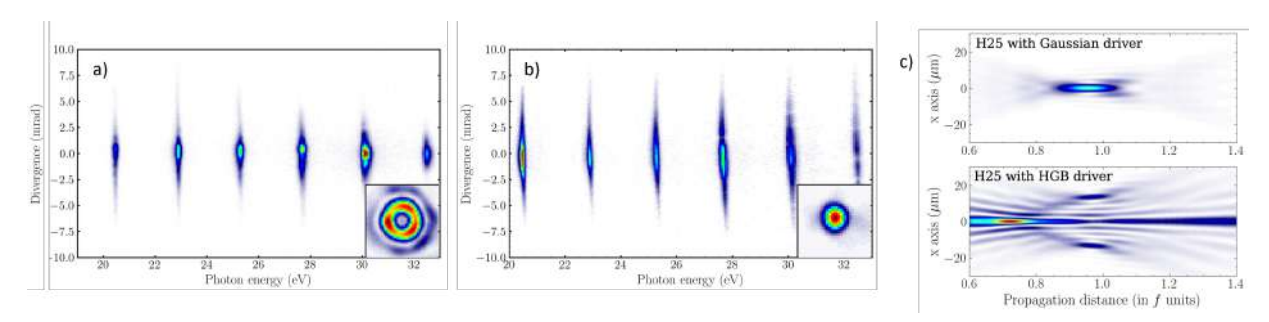


Figure 1: Comparison of experimental harmonic spectra for a Gaussian beam (a)) and a HGB (b)). The insets show the experimentally measured beam profiles. Panel c) illustrates the focusing dynamics for the 25th harmonic order generated with a Gaussian (top) and a HGB driver (bottom).

- [1] F. Krausz et al., Rev. Mod. Phys. 81, 163 (2009).
- [2] H. Wikmark et al., PNAS 116, 4779 (2019).
- [3] K. Veyrinas et al., New J. Phys. 25, 023017 (2023).
- $[4]\ {\rm C.}$ Hernández-García et al., Phys. Rev. A ${\bf 82},\,033432$ (2010).
- [5] Y. Cai, X. Lu, and Q. Lin, Opt. Lett. 28, 1084 (2003).

¹Department of Physics, Lund University, P.O. Box 118, 22100, Lund, Sweden

²Grupo de Investigación en Aplicaciones del Láser y Fotónica, Departamento de Física Aplicada, Universidad de Salamanca, Salamanca, Spain

³Unidad de Excelencia en Luz y Materia Estructuradas (LUMES), Universidad de Salamanca, Salamanca, Spain

 $^{^*}$ melvin.redon@fysik.lth.se

Synthesis of isolated attosecond extreme-ultraviolet spatiotemporal optical vortices via high-order harmonic generation

Rodrigo Martín-Hernández, ^{1,2,*} Guan Gui, ³ Henry C. Kapteyn, ³ Margaret M. Murnane, ³ Chen-Ting Liao, ^{3, 4} Luis Plaja, ^{1,2} Miguel A. Porras, ⁵ Carlos Hernández-García ^{1,2}

- $^{\rm 1}$ Grupo de Investigación en Aplicaciones del Láser y Fotónica, Universidad de Salamanca, 37008, Salamanca, Spain
- ² Unidad de Excelencia en Luz y Materia Estructuradas (LUMES), Universidad de Salamanca, Salamanca, Spain
- ³ JILA and Department of Physics, University of Colorado and NIST, Boulder, CO 80309, United States of America
- ⁴ Department of Physics, Indiana University, Bloomington, IN 47405, United States of America
- ⁵ Grupo de Sistemas Complejos, ETSIME, Universidad Politécnica de Madrid, Ríos Rosas 21, 28003 Madrid, Spain *rodrigomh@usal.es

Abstract

Spatiotemporal optical vortices (STOVs) are structured light fields strongly coupled in space and time. We demonstrate, for the first time, that extreme-ultraviolet harmonic STOVs can be synthesized into an isolated attosecond STOV. This is achieved through advantageous nonlinear up-conversion of infrared spatiospectral optical vortices via high-order harmonic generation.

The generation of STOVs—with intensity and phase distributions coupled in space and time—has been limited to the infrared (IR) and visible regimes with pulse durations as short as hundreds of femtoseconds [1]. In this work we first demonstrate that in high-order harmonic generation (HHG), IR STOVs can be up-converted into extreme-ultraviolet (EUV) harmonic STOVs, with topological charges that increase with the harmonic order [2]. This scaling prevents their synthesization into attosecond STOVs. However, we further demonstrate that harmonic STOVs with the same topological charge can be obtained if driving the HHG process with spatiospectral optical vortices (SSOVs) [3], the spectral counterparts of STOVs[4]. In addition, combined with spatial chirp—as that used in the attosecond lighthouse effect [5]—, we demonstrate that an isolated attosecond STOV can be synthesized (Fig. 1).

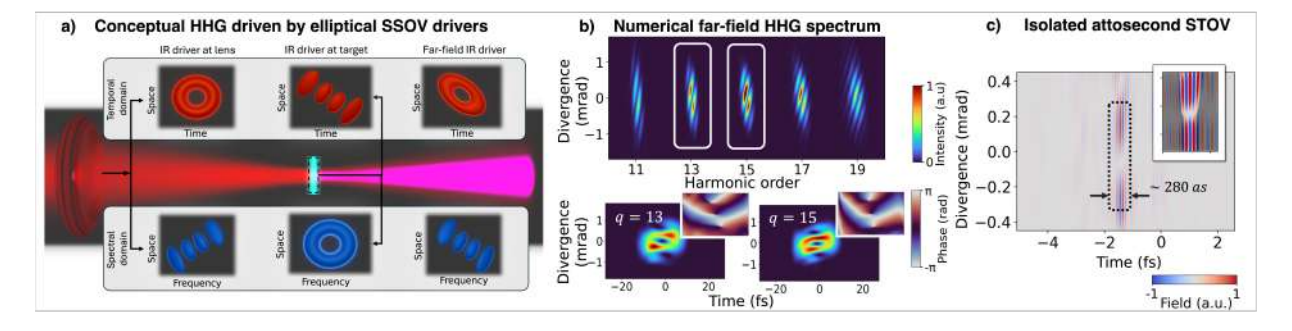


Figure 1: High-order harmonic generation results driven by SSOVs. a) Schematic representation of the IR driving field dynamics in the HHG process. b) Simulated far-field spatially-resolved spectrum (top) and spatiotemporal intensity and phase distribution of the 13th and 15th harmonic orders. (c) Isolated attosecond STOV electric field distribution obtained from overlapping harmonic orders from 13th to 19th.

- [1] G. Gui, et al. Second-harmonic generation and the conservation of spatiotemporal orbital angular momentum of light, Nature Photonics 15, 608-613, (2021).
- [2] R. Martín-Hernández et al. Extreme-ultraviolet spatiotemporal vortices via high harmonic generation, arXiv:2412.01716 [physics.optics] Accepted in Nature Photonics.
- [3] R. Martín-Hernández et al. Isolated, attosecond spatio-temporal vortices from high-order harmonics excited by spatio-spectral optical vortices, in preparation.
- [4] M.A. Porras, Optics of spatiotemporal optical vortices for atto-and nano-photonics, Nanophotonics 14, 845 (2025).
- [5] H. Vincenti, F. Quéré, Attosecond lighthouses: how to use spatiotemporally coupled light fields to generate isolated attosecond pulses, Physical Review Letters 108, 113904 (2012).

On-demand isolated attosecond pulses: the optimal in-situ and in silico tailored waveforms

Rafael de Q. Garcia*^{1,2}, Fabian Scheiba^{1,2,3}, Maximilian Kubullek^{1,2}, Roland E. Mainz^{2,3}, Miguel A. Silva Toledo^{1,2}, Giulio Maria Rossi², Franz X. Kärtner^{1,2,3}

¹ Department of Physics, University of Hamburg, 20355 Hamburg

Abstract

We experimentally demonstrate an 8-fold efficiency enhancement and extreme tunability of attosecond pulse generation in the water window by employing a two-channel infrared waveform synthesizer. The waveforms that optimize emission from 200 to 450 eV are obtained via a field characterization technique and the gating mechanisms are understood via simulations.

The optimization of the high harmonic generation (HHG) process with the aim of producing isolated attosecond pulses (IAPs) from the XUV to soft X-rays is essential for its establishment as a widespread tool for time-resolved spectroscopy. As multi-octave ultrashort pulses are now available at single and sub-cycle durations, tailoring the electric field shape becomes central for optimizing specific aspects of the HHG.

In this work, we show experimentally how two-color waveform synthesis at sub-cycle durations is a robust tool for increasing IAP generation efficiency in the water window. In the experiment, we achieve an 8-fold increase in the efficiency compared to a 1.5-cycle 8 fs IR driver over the 200-450 eV photon energy range under the same macroscopic conditions (Fig. 1 (a)). This is done with the combination of the IR driver (centered at 1.8 µm) and a 7 fs NIR pulse (centered at 800 nm) by changing the carrier envelope phase (CEP) and the relative delay in time. With these two synthesis parameters, it is possible to optimize the IAP generation above 200 eV on the microscopic level while also maintaining macroscopic phase matching. In particular, we are now able to determine what are the best waveforms for producing higher flux IAPs and to explain the gating mechanisms (Fig. 1 (b)). This is accomplished via a combined effort of thorough in-situ experimental characterization [1] of the synthesized pulses and a simulation code that uses the characterized fields as an input and computes the macroscopic HHG. Figure 1 shows how just a slight modulation of the waveform's left and central half cycles allows us to switch the optimal emission from 225 eV to 350 eV. With the benchmarked code, we are also able to predict the case of other two-and three-color driving fields which would further improve the flux by another order of magnitude.

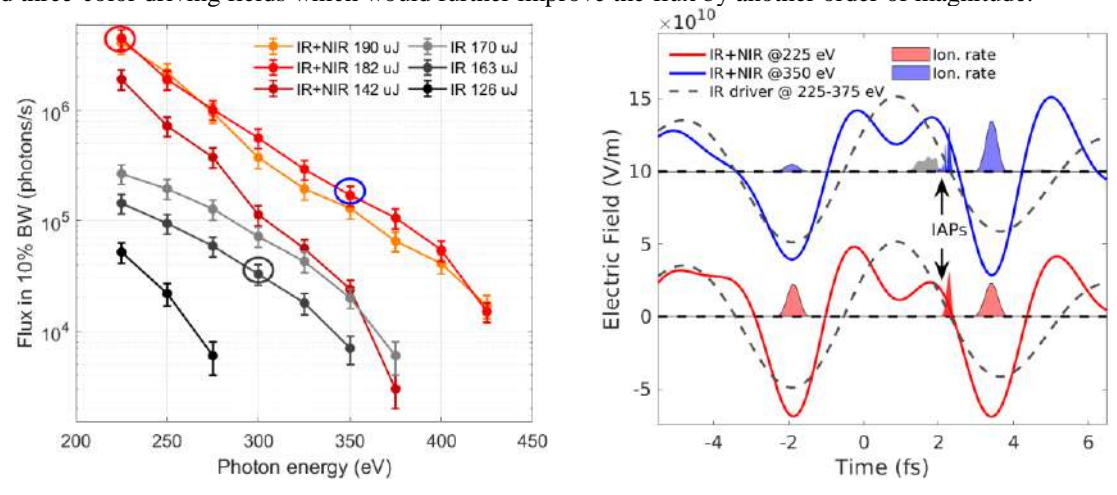


Figure 1: Scanning all CEPs and delays, the maximum photon flux within 10% bandwidth at a certain photon energy is plotted for the synthesized (IR+NIR) and single-color field cases (a). In (b), the waveforms in the focus responsible for the maximum photon flux at a certain photon energy are plotted together with the ionization rates and the output IAPs.

References

[1] M. Kubullek, *et al*, "Complete electric field characterization of ultrashort multi-colour pulses", Ultrafast Science 5, 0081 (2025).

² Center for Free-Electron Laser Science (CFEL), Deutsches Elektronen-Synchroton (DESY), 22607 Hamburg, Germany

³ The Hamburg Centre for Ultrafast Imaging (CUI), University of Hamburg, 22761 Hamburg Germany *rafael.garcia@desy.de

All-attosecond transient reflection spectroscopy

LB Drescher^{1*}, A de las Heras², R Sharma¹, N Mutz¹, MJJ Vrakking¹, SA Sato^{2,3}, A Rubio², and B Schütte¹

¹Max-Born-Institut für Nichtlineare Optik und Kurzzeitspektroskopie, Max-Born-Straße 2A, 12489 Berlin, Germany ²Max Planck Institute for the Structure and Dynamics of Matter and Center for Free Electron Laser Science, 22761 Hamburg, Germany

The large configuration space and interaction strength of solids presents challenges for time-resolved spectroscopy and require attosecond temporal resolution. We introduce all-attosecond transient reflection spectroscopy, enabling core excitation in both the pump and the probe steps. We present results on XUV-excited ionic crystal insulators, shining light on the quasi-particle dynamics of core-excitons.

Solid state materials are true many-body systems, often reaching electron densities beyond 10^{20} cm⁻³. In the temporal domain, this large interaction space can present itself as a variety of ultrafast dynamics following interaction with light that lie beyond the PHz barrier. Previously, transient absorption and reflection spectroscopy using attosecond XUV pulses have been shown to be an insightful tool in understanding these dynamics, such as photoinjection [1] and thermalization of carriers [2], charge localization [3] and exciton decoherence [4]. These experiments combine the high spectral resolution and core-level sensitivity of XUV transient spectroscopy with excellent temporal resolution. The latter so far has been limited by requiring a strong low-frequency pulse (UV to THz range) to accompany the relatively weak attosecond XUV pulse to provide the transient signal.

A longstanding ambition in attosecond science has been to perform all-attosecond pump-probe spectroscopy, eliminating the need for strong laser fields while enabling specific excitation of valence and/or core levels in both the pump and the probe steps. Recently, we have conducted the first all-attosecond transient absorption spectroscopy experiments in atoms using a table-top HHG source [5, 6].

Here we present the first demonstration of all-attosecond transient reflection spectroscopy (AATRS), with results obtained for ionic crystals. An AATRS map recorded in BaF2 is shown in Fig. 1. Preliminary analysis suggests a shift in energy of core-exciton quasi-particle resonances following one-photon interband transition across the insulator's bandgap (~10eV) and reshaping of the exciton resonance during overlap of pump and probe, revealing the attosecond duration of the pulses.

Our results demonstrate that all-attosecond pump-probe spectroscopy can be transferred to solids without significant sample degradation. This opens the door to study electron dynamics in a wide range of materials from a core-level perspective and across large bandwidths on the attosecond domain. For instance, it may be possible to observe core-hole decay and charge transfer processes in solids directly in the time domain.

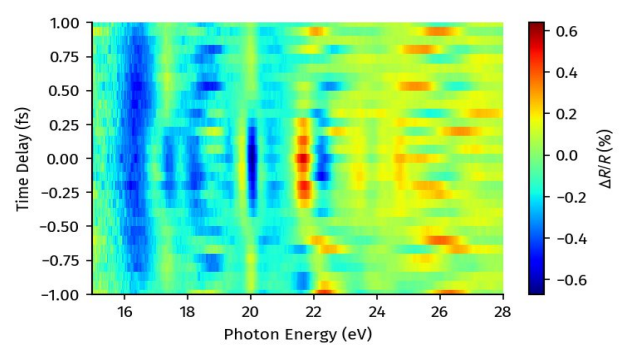


Figure 1: All-attosecond transient reflection spectrum of BaF2 in the Ba⁺⁺ 5p core-excited region, showing strong shifts in the core-exciton resonance reflectivity due to carrier excitation by the XUV pump

- [1] G Inzani et al., Nature Photonics 17, 1059 (2023)
- [2] BR de Roulet et al., PRB 110, 174301 (2024)
- [3] Z Schumacher et al., PNAS 120, e2221725120 (2023)
- [4] A Moulet et al., Science 357, 1134–1138 (2017)
- [5] E Sobolev et al., Opt. Express 32, 46251 (2024),
- [6] M Volkov, E Svirplys et al., in preparation.

³Department of Physics, Tohoku University, Sendai 980-8578, Japan

^{*}lauren.drescher@mbi-berlin.de

Sub-20-fs UV Pump – XUV Probe Beamline for Ultrafast Molecular Spectroscopy

Marta Arias-Velasco,^{1,3} Aurora Crego,^{1,2,*} Stefano Severino,³ Fabio Medeghini,³ Lorenzo Mai,³ Fabio Frassetto,⁴ Luca Poletto,⁴ Matteo Lucchini,^{1,3} Maurizio Reduzzi,³ Mauro Nisoli^{1,3} and Rocío Borrego-Varillas¹

Abstract

We present a UV pump - XUV probe setup with sub-20 fs resolution, enabling the first direct measurement of the ultrafast $S_2 \rightarrow S_1$ transition in acetylacetone. Using in-situ photoelectron cross-correlation, we track excited-state dynamics with unprecedented precision, demonstrating the potential of UV-XUV spectroscopy for ultrafast photochemical process investigations.

Time-resolved photoelectron spectroscopy is essential for studying ultrafast molecular dynamics. Understanding these processes requires generating and optimizing ultrashort ultraviolet (UV) and extreme-ultraviolet (XUV) pulses. We present a UV pump - XUV probe setup with sub-20 fs resolution [1], characterized via in-situ photoelectron cross-correlation, enabling precise tracking of excited-state dynamics in acetylacetone (AcAc).

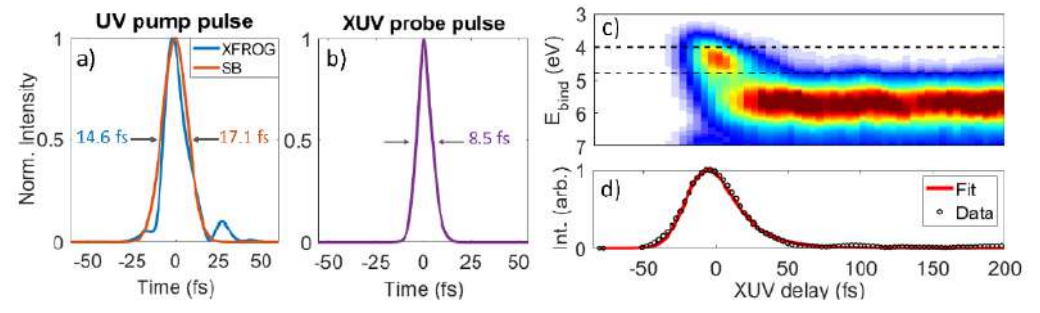


Figure 1: (a) Temporal profiles of the UV pump pulse (blue: XFROG, orange: sideband reconstruction). (b) XUV probe pulse. (c) Experimental photoelectron spectrogram of acetylacetone excited with a UV pulse and probed with an XUV pulse. (d) Ultrafast decay dynamics of the S₂ state (open dots: data, red line: fit). The black dashed lines in (c) show the energy region in (d).

The UV pump pulses (270 nm, \sim 17 fs, μ J-level energy) are generated by frequency up-conversion [2]. In contrast, XUV probe pulses (\sim 8.5 fs) are generated through high-harmonic generation and filtered spectrally using a time-delay compensated monochromator (TDCM) [3]. Temporal characterization of both UV and XUV pulses was performed by a two-color photoelectron cross-correlation measurement in argon. The resulting sideband (SB) signal provides information on the spectral phases of both pulses, which can be retrieved by a proper algorithm [4].

By applying this technique to AcAc, we resolve the ultrafast $S_2 \rightarrow S_1$ transition with unprecedented precision. The experimental spectrogram effectively maps this process, showing excellent agreement with previous studies and revealing, for the first time, the S_2 state lifetime. Our findings highlight the potential of UV-XUV spectroscopy for probing ultrafast photochemical processes.

- [1] A. Crego et al., "Sub-20-fs UV-XUV beamline for ultrafast molecular spectroscopy," Sci. Rep. 14, 26016 (2024). [2] R. Borrego-Varillas et al., "Microjoule-level, tunable sub-10 fs UV pulses by broadband sum-frequency generation," Opt. Lett. 39, 3849-3852 (2014).
- [3] L. Poletto et al., "Time-delay compensated monochromator for the spectral selection of extreme-ultraviolet high-order laser harmonics," Rev. Sci. Instrum. 80, 123109 (2009).
- [4] G. Dolso et al., "Versatile and robust reconstruction of extreme-ultraviolet pulses down to the attosecond regime", APL Photonics 8, 076101 (2023).

¹Institute for Photonics and Nanotechnologies, IFN-CNR, Piazza Leonardo da Vinci 32, 20133 Milano, Italy ²Grupo de Investigación en Aplicaciones del Láser y Fotónica, Departamento de Física Aplicada, Universidad de

Salamanca E-37008 Salamanca, Spain,

³Dipartimento di Fisica, Politecnico di Milano, Piazza Leonardo da Vinci 32, 20133 Milano, Italy

⁴Institute for Photonics and Nanotechnologies, IFN-CNR, via Trasea 7, 35131 Padova, Italy *acrego@usal.es

FridayOctober 10th



Compact yet mighty: tapered double-clad amplifiers for picosecond pulses

Regina Gumenyuk

Laboratory of Photonics, Tampere University, Korkeakoulunkatu 3, Tampere 33720, Finland regina.gumenyuk@tuni.fi

Abstract

In this presentation, I will focus on our effort in realizing high power/energy laser systems based on active double-clad tapered fiber amplifiers. Owning to the special longitudinal profile, these fiber amplifiers are capable of directly amplifying picosecond pulses, delivering excellent beam profile and high polarization stability in a compact footprint.

In the era of high-power laser systems, there is a constant demand for compact and efficient short-pulsed amplifiers boosting the power/energy level with excellent output parameters, where the active tapered double-clad fibers (T-DCF) offer a number of distinguished advantages. Owning to the special longitudinal profile, T-DCF enables efficient amplification of the short-pulsed signal and leads to the elevation of thresholds for nonlinear effects in a very compact setup (Figure 1a) [1, 2]. The typical laser system consists of a seed with a single-mode pre-amplifier elevating the average power up to 100 mW level and a T-DCF amplifier boosting the average power beyond half-kW level. Recently, we demonstrated the dramatic progress of the T-DCF technology by a number of records in single-channel laser systems. The 50 ps pulses at 20 MHz were directly amplified from 50 mW up to 625 W with the excellent beam profile and polarization stability (Figure b-e). By decreasing the repetition rate down to 1 MHz the same laser system delivered over 2 MW peak power. T-DCF -based amplifier is also capable of achieving over 1 mJ energy by amplifying 8 ns pulses at 100 kHz repetition rate from 1 µJ level (Figure 1f).

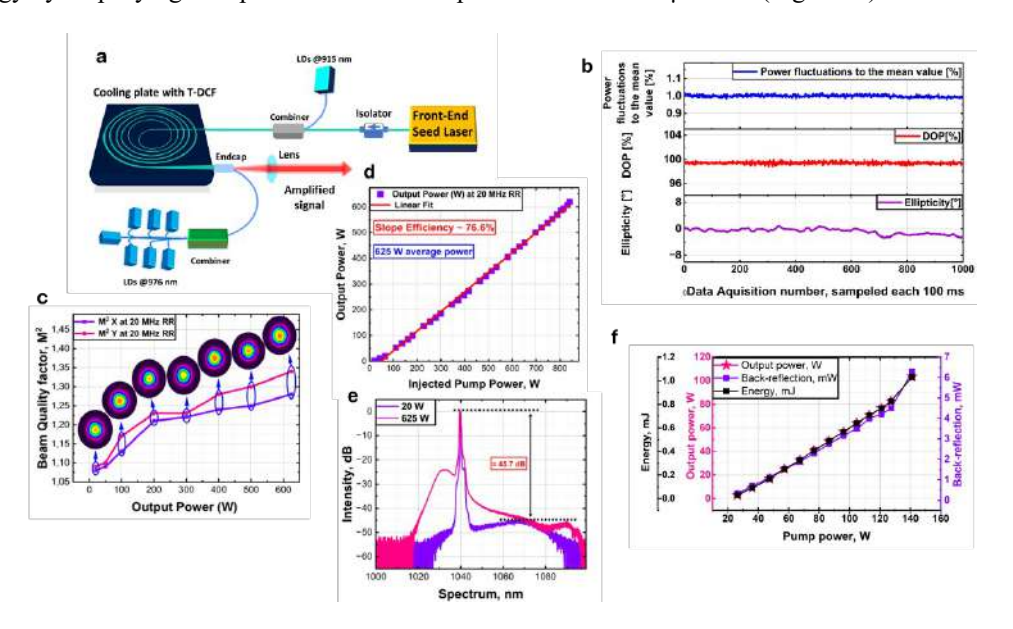


Figure 1: a – a typical laser system setup based on a tapered fiber amplifier, b – typical polarization stability measurements, c – beam quality evolution with output power, d – slope efficiency for 50ps/20MHz/625W laser system, e – output spectra for 50 ps pulsed signal at the 20W and 625 W power levels, f – slope efficiency for 8ns/100kHz/1mJ pulsed laser system.

References

[1] Fedotov A., et al., "Active tapered double-clad fiber with low birefringence.", Optics Express, Vol. 29, No. 11, p. 16506-16519, 2021.

[2] Fathi, H., et al., "Yb-doped tapered double-clad fibers with polarization maintenance for half-kW power amplifiers," Optics Express, Vol. 32, No. 19, p. 33064-33074, 2024.

△ UFO XIV Azores 2025

44 W, 100 kHz, 2.5-cycle pulses from a flat-top pumped OPCPA

H. Kassab, ¹ L. Oppermann, ¹ V. Fortin, ² M. Lavastre, ² S. Petit, ² T. Witting, ¹ M. J. J. Vrakking, ¹ and F. J. Furch ^{1,*}

¹Max-Born-Institut für Nichtlineare Optik und Kurzzeitspektroskopie, Max-Born-Strasse 2A, 12489 Berlin, Germany
²Centre Lasers Intenses et Applications, UMR5107, CNRS-Université de Bordeaux-CEA, 33400 Talence, France

Abstract

We present a two-stage OPCPA delivering sub-7 fs pulses around 800 nm with 44 W average power at 100 kHz. The pump beam of the second stage is shaped utilizing a holographic high reflectance mirror to provide a flat-top shape at the OPCPA crystal plane.

Ultrashort laser pulses with high power and high repetition rate are very attractive for applications in attosecond

Introduction and results

science, surface science, or as complementary sources at Free Electron Laser facilities. Here we present a two-stage OPCPA delivering 55 W at 100 kHz before compression and sub-7 fs at 800 nm with 44 W after compression. The architecture of the OPCPA follows our previous work [1]. To achieve higher pulse energy, a booster thin-disk multi-pass amplifier has been added to the CPA that pumps the OPCPA stages. The amplifier can deliver more than 1 kW, 100 kHz at 1030 nm with a beam characterized by an M² below 1.3. Currently 0.5 kW are compressed, limited by the size of the gratings in the compressor. The pump line of the second OPCPA stage incorporates a holographic high reflector mirror at 1030 nm [2] that introduces a structured spatial phase before second harmonic generation (SHG). Upon SHG and propagation to the OPCPA crystal, the pump beam at 515 nm is re-shaped from a nearly Gaussian to a flat-top shape for reduced spatio-temporal couplings during amplification [3]. Seed pulses are amplified to 0.55 mJ (55 W) in two noncollinear OPCPA stages. The amplified pulses are compressed with 10 pair of bounces in dispersive

mirrors, thin fused-silica wedges and a 4-f pulse shaper (located before the amplification stages) [1]. Characterization with the SEA-F-SPIDER technique [4] shows a pulse duration of 6.6 fs for 10 consecutive measurements (Fig. 1) corresponding to 2.5 cycles at the carrier frequency. After a waveplate and two thin-film polarizers that control the

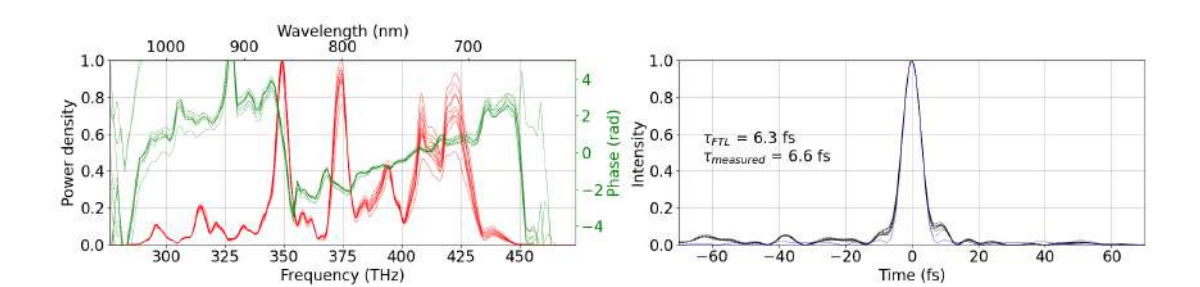


Figure 1: SEA-F-SPIDER measurements after spatial integration. Left: Spectral power density (red) and retrieved spectral phase (green). Right: Pulse reconstructions (black) and Fourier Transform limit (blue).

References

[1] T. Witting, F. J. Furch and M. J. J. Vrakking, J. Opt. 20, 044003 (2018).

power into experiments the compressed output power is 44 W.

- [2] V. Fortin, M. Nadeau, and S. Petit, in Optica Advanced Photonics Congress 2022, Technical Digest Series (Optica Publishing Group, 2022), paper JTu6A.17.
- [3] A. Giree, M. Mero, G. Arisholm, M. J. J. Vrakking, and F. J. Furch, Opt. Express 25, 3104-3121 (2017).
- [4] T. Witting, F. Frank, C. Arrell, W. Okell, J. Marangos, and J. Tisch, Opt. Lett. 36, 1680–1682 (2011).

^{*}furch@mbi-berlin.de

Pulse compression of 300W, 12mJ with 83% transmission in hollow-core fiber

Maksym Ivanov,^{1,2*} Etienne Doiron,¹ Marco Scalia,¹ Gabriel Tempea,¹ Pedram Abdolghader¹, Kevin Watson,³ Tobias Saule,³ Carlos Trallero³, and Bruno E Schmidt¹

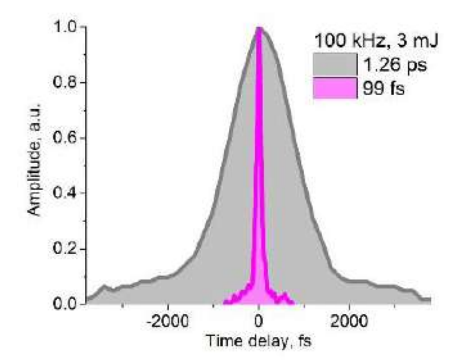
Abstract

We demonstrate power scaling of pulse post-compression using an air-cooled hollow-core fiber, achieving pulse compression from 1.3 ps to 100 fs at 300 W of average power. Supporting 25–100 kHz (12–3 mJ) at constant 300 W average power, the system operates with noble or molecular gases, highlighting its scalability and versatility.

Main Text

Narrowband Ytterbium-doped laser technology has driven advances in pulse post-compression. Building on our previous 80 W, 2 mJ, 6 fs demonstration [1] using a hollow-core fiber (HCF) setup, we now show scalability of the HCF compression technique for input average power of up to 300 W with energy of up to 12 mJ using hardware similar to that in the low power case. An Yb:YAG InnoSlab laser delivers 1.26 ps pulses with 3–12 mJ at 100–25 kHz, while maintaining 300 W average power. At the HCF output we achieved 250 W and 10 mJ. This denotes to date the highest energy pulse compression in HCFs filled with atomic gases at the multi-hundred-Watt level, with comparable results using molecular gases (N₂, O₂, N₂O) [2].

We used a 3.1 m long, 1 mm core diameter HCF filled with krypton. The relative pressure of krypton varies with input energy (0.17 bar with 12 mJ and 1.5 bar with 3 mJ). However, input coupling conditions remain the same with no need in realignment of the setup highlighting its versatility. Compression involved 36 chirped mirror bounces (–500 fs² at 1010–1060 nm, few-cycle Inc), yielding 103 fs pulses (99 fs at 3 mJ), a 12-fold compression. Beam quality was confirmed by a symmetric beam refocusing, with a stable 1-hour long power measurement demonstrating a remarkably low standard deviation of 0.58% at 250 W of average power with 10mJ.



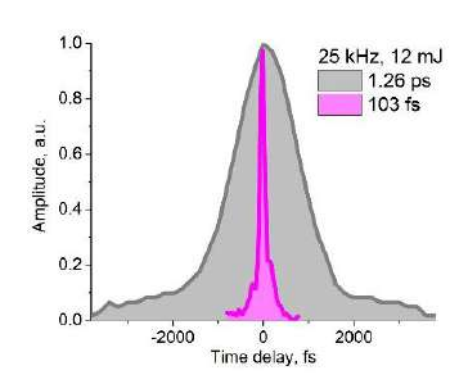


Figure 1: Left and central image: Autocorrelation showing compressed pulse duration after the HCF, 99 and 103 fs (magenta), versus input pulse duration of 1.26 ps (gray) at 100 and 25 kHz, respectively.

References

[1] M. Ivanov *et al.*, "Advancing High-Power Hollow-Core Fiber Pulse Compression," in IEEE Journal of Selected Topics in Quantum Electronics, vol. **30**, no. 6, Art no. 5100310 (2024).

[2] K Watson *et al.*, "High-power femtosecond molecular broadening and the effects of ro-vibrational coupling," Optica **12**, 5-10 (2025).

¹few-cycle Inc, J3X 1P7 Varennes, Canada

²Institut national de la recherche scientifique, Varennes, J3X 1P7, Canada

³Physics Department, University of Connecticut, Storrs, 06269, USA

^{*}ivanov@few-cycle.com

△ UFO XIV Azores 2025

Tailored Ultrashort Pulse Bursts in a Gain-Managed Nonlinear Fiber Amplifier for Coherent 50fs Pulse Stacking at mJ Energies

Lauren Cooper,^{1,*} Siyun Chen,^{1,2}, Pavel Sidorenko,^{3,4}, Frank Wise,³, and Almantas Galvanauskas¹

- ¹ College of Engineering, University of Michigan, Ann Arbor, Michigan 48109, USA
- 2 Currently with Lawrence Berkeley National Laboratory, Berkeley, California 94720, USA
- 3 School of Applied and Engineering Physics, Cornell University, Ithaca, New York 14853, USA
- ⁴ Currently with the Department of Electrical and Computer Engineering, Technion-IIT, Haifa, 3200002, Israel

Abstract

We propose a method of scaling gain-managed nonlinear amplifiers (GMNA) to mJ energies using tailored pulse bursts that can be time-combined into a single 50fs output pulse using coherent pulse stacking.

Gain-managed nonlinear amplification (GMNAs) offers a simple approach to generating high-energy femtosecond pulses, with $2.9\mu J$, 50fs pulses demonstrated recently using $50\mu m$ low-NA LMA fibers [1]. Here we propose a new method to scale such GMNA pulses to mJ levels, by amplifying specially-tailored pulse bursts suitable for efficient coherent pulse stacking (CPS) into a single pulse [2] and subsequent compression to $\sim 50 fs$. Theoretical analysis indicates that GMNA of an equal-amplitude burst would lead to varying pulse-chirp characteristics along the burst, preventing efficient stacking and compression to bandwidth-limit. Here we show theoretically that pulse bursts can be pre-shaped to produce identically-chirped picosecond pulses at GMNA output, stackable and compressible to a single $\sim 50 fs$, 0.989mJ pulse. Figure 1 illustrates the conceptual CPS-GMNA system layout. Figure 2 (top) shows simulated pulses and spectra of 729 pulses (each $1.3\mu J$) in a pre-compensated output burst from a 2.5 m $50\mu m$ core fiber GMNA amplifier, each compressible to $\sim 50 fs$ bandwidth-limit (bottom). This result shows a pathway to temporally-combined GMNA systems producing 50 fs-scale mJ pulses without using chirped pulse amplification.

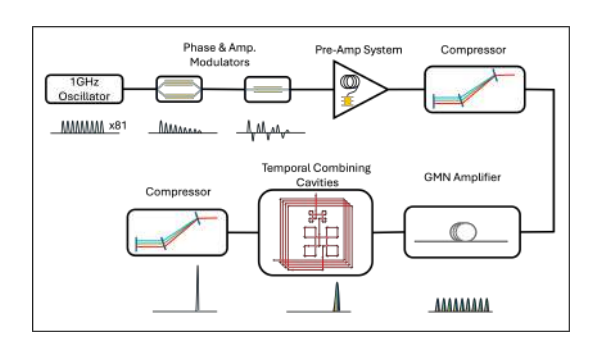


Figure 1: Pulses from a multi-GHz oscillator are amplitude and phase modulated using electro-optic modulators. After pre-amplification and compression back to bandwidth-limit, pulses are amplified and spectally-broadened in a GMNA amplifier to $>1\mu J/{\rm pulse}$, and then stacked using Gires-Tournois Interferometers into a single output pulse, with subsequent compression to the bandwidth-limit.

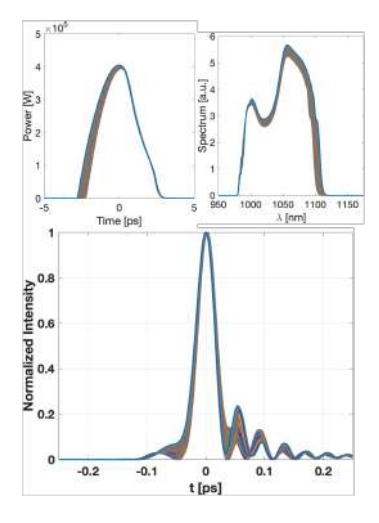


Figure 2: Top: all individual pulses and spectra in the pre-compensated 729-pulse burst from GMN amplifier. Bottom: corresponding $\sim 50 \,\mathrm{fs}$ compressed pulses.

- [1] L. Cooper, M. Chen, S. Chen, P. Sidorenko, F. Wise, T. W. Hawkins, L. Dong, A. Galvanauskas, "53fs, $2.9\mu J$ Pulses from Gain-Managed Nonlinear Amplifier Using A 50 μm Core Low-NA LMA Fiber," CLEO Conference Proceedings (2025).
- [2] A. Rainville, M. Whittlesey, C. Pasquale, Y. Jing, M. Chen, S. Chen, H. Pei, J. Ruppe, T. Zhou, Q. Du, Z. Zhang, G. Chang, F. X. Kärtner, A. Galvanauskas, "Near-Complete Extraction of Maximum Stored Energy from Large-Core Fibers Using Coherent Pulse Stacking Amplification of Femtosecond Pulses," Optica 11, 1540-1548 (2024).

^{*}lacoop@umich.edu

Energy Scaling of Kerr-Lens Modelocked Ho:YAG Thin-Disk Oscillators to the Microjoule Level

Sergei Tomilov^{1,*}, Mykyta Redkin¹, Yicheng Wang¹, Anna Suzuki¹, Martin Hoffmann¹, Clara J. Saraceno¹

¹Photonics and Ultrafast Laser Science, Ruhr-Universität Bochum, Universitätsstraβe 150, 44801 Bochum, Germany *Sergei.Tomilov@ruhr-uni-bochum.de*

Abstract

We demonstrate high-energy Kerr-lens modelocked (KLM) Ho:YAG thin-disk laser (TDL) emitting at 2.1- μ m wavelength. We compare different laser configurations to reach a maximum pulse energy of 1.7μ J at an output power of 29 W with a pulse duration of 434 fs, corresponding to a peak power of $3.7 \, \text{MW}$.

The short-wave infrared (SWIR) wavelength region is in growing demand for various applications in science and technology. More specifically, the 2-µm to 3-µm wavelength range can be covered by ultrafast lasers emitting directly in this wavelength region, based, for example, on transition-metal (Cr²⁺) and lanthanide (Tm³⁺, Ho³⁺ and Er³⁺) dopants, offering enormous potential for extending the performance of modern laser systems to this wavelength region. Although powerful laser systems operating in this wavelength region have made significant progress over the last two decades, their state-of-the-art specifications in terms of average output power, pulse energy, and peak intensity are still behind those of modern 1-µm systems, with numerous research efforts still to be undertaken. In this context, TDLs are well-known to be very promising for the average power scaling of high-repetition-rate oscillators, and for future energy scaling of amplifiers. However, the implementation of the thin-disk geometry for active gain media emitting in the SWIR region is typically not straightforward, and so far, only a few 2-µm ultrafast TDLs have been demonstrated. In [1] a KLM oscillator based on Ho:YAG was demonstrated featuring an average output power of 25 W and a pulse energy of 0.325 µJ. More recently, using Semiconductor Saturable Absorber Mirror (SESAM) mode-locking, average power and energy scaling of a Ho:YAG TDL was demonstrated, reaching an average power of 50 W and a pulse energy of 2.11 µJ [2]. Despite the record performance, this system exhibits a rather long pulse duration of 1.13 ps and a moderate peak power of 1.6 MW, due to the limited modulation depth of the available SESAMs. In this work, we demonstrate further scaling of Ho:YAG KLM TDLs reaching an output power of 29 W with a pulse duration of 434 fs, corresponding to a pulse energy of 1.7 µJ and a peak power of 3.7 MW. This is, to our knowledge, the highest peak power reported from 2-µm oscillators to date.

Fig. 1a) depicts the experimental setup of the KLM TDL oscillator. It features two TDL pump modules used to split the pump between two Ho:YAG disks with doping concentrations of 2 and 2.5 at.% to mitigate the thermal damage of the disks under the maximum pump power of 200 W at 1908 nm. Stable modelocking was achieved in the range of output couplers (OCs) from 1% to 10%. Fig. 1b) and c) demonstrate the measured laser spectrum and autocorrelation (AC) trace at maximum output power of 29 W and 16.7-MHz repetition rate. The demonstrated laser oscillator operated in a non-hermetic, nitrogen-purged environment with robust and heat-resistant intracavity components capable of withstanding intracavity powers of nearly 1 kW. Further power scaling of the laser system output was limited by the available pump power and the rising temperature of the active media, which can be optimized by changing the disk thickness. The developed system showcases the technological maturity of 2-μm laser components, demonstrating an open path towards 100-W and 10-μJ-class single-oscillator systems.

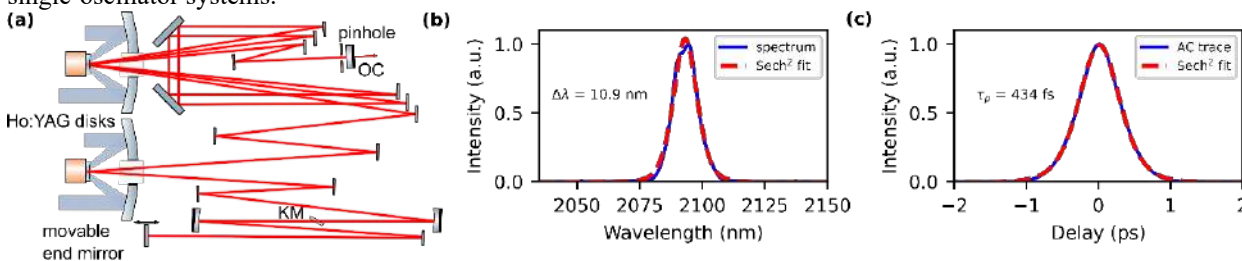


Figure 1: (a) Ho:YAG KLM TDL cavity; (b) Laser spectrum and (c) AC trace at the maximum power.

- [1] J. Zhang, K. F. Mak, and O. Pronin, "Kerr-Lens Mode-Locked 2-μm Thin-Disk Lasers," IEEE J. Select. Topics Quantum Electron. **24**, 1–11, (2018);
- [2] S. Tomilov *et al.*, "50-W average power Ho:YAG SESAM-modelocked thin-disk oscillator at 2.1 μm," Opt. Express **30**, 27662–27673, (2022).

High Power Kilohertz Thin Disk Amplifier with 600mJ Pulse Energy Developed for OPCPA

Huang Zhou,^{1*} Renchong Lv,^{1,2} Lei Feng,¹ Sen Tian,¹ Jiangfan Pan,¹ Yong Zhen,^{1,3} Peng He,¹ Wenlong Tian,³ Jiangfeng Zhu,³ Xinkui He,^{1,2} and Zhiyi Wei^{1,2}

¹Songshan Lake Materials Laboratory, No.333, Pingdong Road, Dalang Town, Dongguan City, China ²Institute of Physics, Chinese Academy of Sciences, No. 8, 3rd South Street, Beijing 100190, China ³School of Optoelectronic Engineering, Xidian University, Xi'an 710071, Shaanxi, China *huang-zhou@outlook.com

Abstract

Addressing OPCPA's demand for high-energy pump sources, we are developing a kHz thin-disk Yb:YAG amplifier system. The broadband seed laser integrating a solid-state oscillator and a spectrum-shaped Yb:CALGO pre-amplifier (>5 nm BW) feeds sequential amplification stages: a regenerative amplifier and three multi-pass amplifiers, achieving pulse energy of >600 mJ. Grating compression (1740 l/mm, 93% throughput) yields 600-fs pulse length with PW-scale applicability.

Significant progress of optical parametric chirped pulse amplification (OPCPA) [1] technologies has driven an increasing demand for high-energy, high-repetition-rate pump lasers to achieve ultra-intense and ultra-short pulse outputs. We developed a high-energy kHz-repetition-rate thin disk laser system, which delivers ultrafast laser pulse with energy of >600 mJ at the pulse length of <600 fs at 1 kHz repetition rate. The diagram of the thin disk amplifier is shown in Figure 1. A solid-state oscillator is used as the seed pulse due to its excellent spectrum without spectrum modulation. The seed pulse is stretched by the CFBG with a chirp rate of 750ps/nm and amplified by fiber pre-amplifiers. To suppress the gain narrowing in the following thin disk amplifiers, broad spectrum and high pulse energy of the seed laser is required. A broad-spectrum high-energy dual-Yb:CALGO regenerative amplifier is designed to amplifier the seed pulse energy up to 2 mJ while keeping the bandwidth >5 nm (FWHM). The pulse energy is amplified by a thin disk regenerative amplifier up to 100 mJ before injecting to the cascaded multi-pass thin disk amplifiers, which boosts the pulse energy >760 mJ before compression. A Treacy type compressor with two deflective gratings is used to compress the laser pulse length to <600 fs with an output energy of >600 mJ.

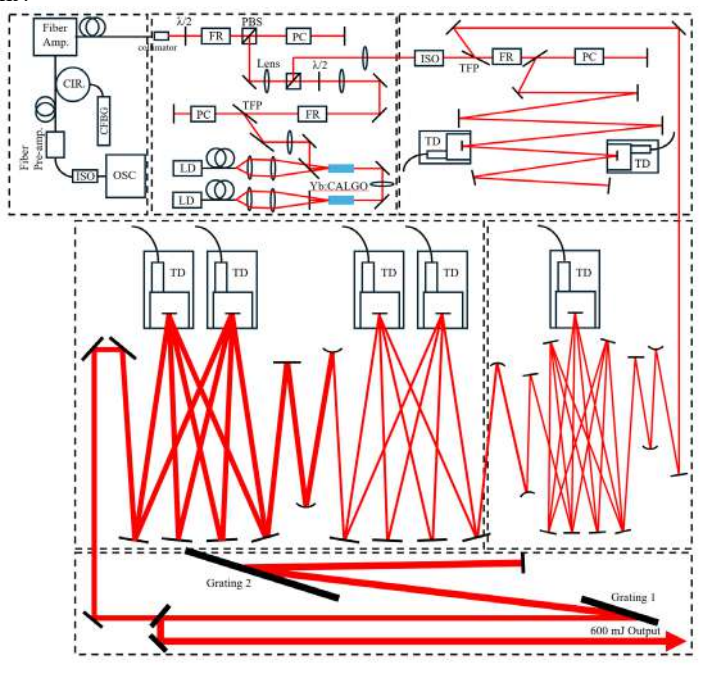


Figure 1: The diagram of the thin disk amplifier system.

References

[1] Dubietis, A.; Jonušauskas, G.; Piskarskas, A. Powerful femtosecond pulse generation by chirped and stretched pulse parametric amplification in BBO crystal. *Opt. Commun.* **1992**, *88*, 437–440.

High average power THz-time domain systems

Robin Löscher, Tim Vogel¹, Samira Mansourzadeh¹, Mohsen Khalili¹, and Clara Saraceno^{1,*}

¹Photonics and Ultrafast Laser Science, Ruhr University Bochum, Universitätsstraße 150, 44801, Bochum, Germany *clara.saraceno@ruhr-uni-bochum.de

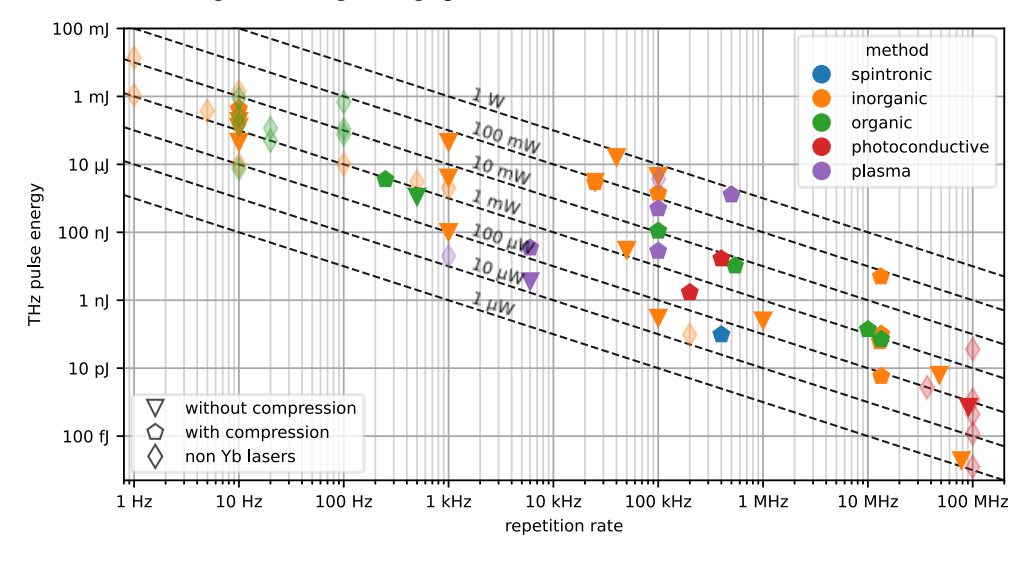
Abstract

We present recent advancements in broadband terahertz sources utilizing high-power Yb-based ultrafast lasers as drivers, which are nearing watt-level average power. We discuss various approaches explored thus far, current challenges, prospects for scaling, and future research areas that will accelerate their implementation in applications.

Coherent sources producing ultrashort, few-cycle pulses of terahertz (THz) radiation have become well-established in an immense variety of scientific fields, spanning physics, chemistry, material science, engineering, biology, and medicine. They allow for steering and probing the dynamics of a variety of low-energy phenomena in condensed matter, ranging from ultrafast dynamics of charge carriers, phonons and spins, conductivity to intermolecular dynamics of liquids in biological systems. Furthermore, ultrafast laser-driven THz sources are powerful tools for material identification and imaging and are starting to be increasingly deployed in industrial inspection scenarios, for quality control of layered materials.

The most commonly used techniques to generate ultra-broadband THz pulses using ultrafast lasers are down conversion in materials with $\chi^{(2)}$ nonlinearity using intra-pulse difference frequency generation (optical rectification), photocurrents in biased semiconductors and ionized gaseous media, and more recently, spintronic THz emitters; all these techniques have seen spectacular progress in terms of pulse strength, bandwidth, polarization control among others; however their average power has remained low. In the last few years however, the rapid advancement of high-power ultrafast laser technologies based on ytterbium (Yb)-doped solid-state lasers has enabled us to make significant progress in reaching higher powers. Ultrafast laser systems with tens to hundreds of watts of average power are now commercially available with industrial-grade stability, and pulse compression methods are transforming these lasers into the new workhorse of broadband THz science.

In this new context, we summarize most recent findings in applying these laser systems to generate high-average-power broadband THz radiation. We discuss various challenges and differences that arise in the generation mechanisms when increasing the driving average power.



Overview of current progress made with Yb laser drivers in the generation of high-power THz broadband radiation

References

[1] R, Löscher et al, "Laser-driven few-cycle Terahertz sources with high average power" Arxiv https://doi.org/10.48550/arXiv.2507.11501 (2025)

Extended Length Femtosecond Laser Filamentation via High Repetition Rate Effects

Malte C. Schroeder*, Robin Löscher, Alan Omar, and Clara J. Saraceno

Photonics and Ultrafast Laser Science, Ruhr-Universität Bochum, Universitätsstr. 150, 44801 Bochum, Germany *malte.schroeder-w9x@ruhr-uni-bochum.de

Abstract

Femtosecond laser filamentation has numerous applications that benefit from an extended filament range, such as cloud clearing or lightning guiding. We demonstrate a novel approach to extend filamentation based on cumulative gas hydrodynamics at high laser repetition rates which induce a "leapfrog" effect without requiring additional optics or beam shaping. © 2025 The Author(s)

There are many practical applications of femtosecond laser filamentation, for example, drilling holes in clouds for optical telecommunication, generating air or plasma waveguides for optical or microwave radiation, as well as

guiding lightning strikes and electrical discharges [1], among others. In this context, most practical applications of filamentation benefit from increased filament lengths. Several approaches have been employed in the past to achieve this, for example, multifocal phase masks or lens arrays for a broken-wire approach [2]. However, these techniques require additional optics, which are highly specialized and require costly custom manufacturing. Here, we propose and show experimental proof of a new technique to increase filament length significantly based on increasing the repetition rate of the driving laser and the use of pre-formed channels of reduced air density [3]. Recent advances in ytterbium (Yb)-based high-power ultrafast laser systems have opened the door to new high-repetition-rate filamentation regimes at tens to hundreds of kHz, where the resultant inter-pulse time is too small for complete diffusion of the residual heat left after the plasma recombination. This leads to cumulative effects in the gas hydrodynamics [4], which can alter many of the previously well-known filament formation mechanisms. In the case studied here, using a 500 W ultrafast laser system running at 10 to 100 kHz, the short inter-pulse times and high pulse energies drive cumulative effects in the gas hydrodynamics, which result in spatially varying gas densities along the filament, thereby varying the nonlinear refractive index resulting in a dynamic change of the position where filamentation occurs. We propose to coin this effect as "leapfrog" extended filamentation.

We show this effect experimentally, by studying the beam profiles after filamentation, the onset of filamentation by recording the spatially resolved plasma fluorescence, and the air density evolution along the channel via interferometry, that with increasing repetition rates filaments do not occur at the same position, but instead "leapfrog" over the previously heated air channel. In Figure 1, a transversal cross-section of the recovering gas density along the propagation axis is shown. At 1 kHz within 1 ms the depleted air density recovers fully, while at 100 kHz the following pulse will pass through the changed density profile left from the previous filament. Since consecutive pulses arrive before the depleted volume recovers, they experience a lowered nonlinear refractive index along the depleted channels, and thus a delayed onset of filamentation, which leads to this "leapfrog" effect, effectively extending the filamentation range without the need for additional optics or beam shaping.

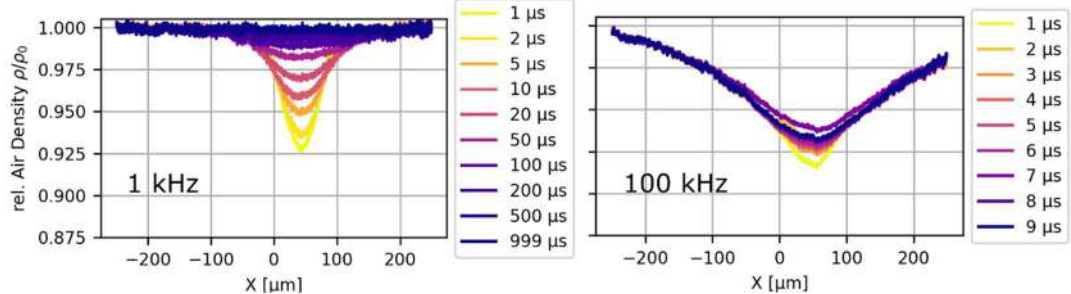


Figure 1: Temporal evolution of the cross-section of the relative change in air density at repetition rates of 1 kHz and 100 kHz. At 1 kHz, the air achieves complete recovery, while at 100 kHz, the depletion does not recover before the following pulse arrives.

- J. P. Wolf, "Short-pulse lasers for weather control," Rep. Prog. Phys., vol. 81, no. 2, p. 026001, Feb. 2018, doi: 10.1088/1361-6633/aa8488.
- [2] S. Fu, A. Mysyrowicz, L. Arantchouk, M. Lozano, and A. Houard, "Extending femtosecond laser superfilamentation in air with a multifocal phase mask," *Appl. Phys. Lett.*, vol. 125, no. 1, p. 011103, Jul. 2024, doi: 10.1063/5.0203415.
- [3] J. Chang, D. Li, L. Xu, L. Zhang, T. Xi, and Z. Hao, "Elongation of filamentation and enhancement of supercontinuum generation by a preformed air density hole," *Opt. Express*, vol. 30, no. 10, p. 16987, May 2022, doi: 10.1364/OE.458128.
- [4] R. Löscher, M. C. Schroeder, A. Omar, and C. J. Saraceno, "Time-Resolved Measurements of Cumulative Effects in Gas Dynamics Induced by High-Repetition-Rate Femtosecond Laser Filamentation," ArXiv Prepr. ArXiv250110198, 2025.

Two-Photon Dual-Comb LiDAR Imaging

Alexander J. M. Nelmes,¹ Hollie Wright,^{1,*} Simon Fletcher,² Andrew P. Longstaff,² and Derryck T. Reid¹

¹ School of Engineering and Physical Sciences, Heriot-Watt University, Edinburgh, EH14 4AS, UK.

² School of Computing and Engineering, the University of Huddersfield, Huddersfield, UK.

*H.Wright@hw.ac.uk

Abstract

Two-photon dual-comb LiDAR replaces data intensive acquisition with time-tagged cross correlations to achieve precision metrology without the need for phase-stabilized ultrafast lasers. With amplified detection, extend the technique to non-cooperative targets, allowing LiDAR point-cloud imaging at precisions orders of magnitude higher than conventional LiDAR.

Dual-comb ranging employs one laser frequency comb to probe distances to target and reference surfaces, and a second local-oscillator (LO) comb to time-gate the resulting probe reflections. In the conventional implementation, coherent gating yields interferograms which are digitized at sampling rates >100 MSa/s [1]. Conversely, two-photon dual-comb LiDAR acquires intensity cross-correlations which can be time-tagged by a microcontroller to enable precision metrology with a minimal data burden [2,3]. By using an active detection scheme in which probe pulses scattered from non-cooperative metal surfaces are amplified in an Erbium-doped fiber amplifier prior to local-oscillator time-gating, ranging is possible with precisions comparable to those obtained with perfectly reflecting optical targets [4]. This capability opens a route to obtaining point-cloud images of the kind familiar in conventional LiDAR but with the precision of dual-comb ranging. Here, we present the first demonstration of two-photon dual-comb LiDAR imaging, applying it to an aluminum test object fabricated on a multi-axis milling machine, showing the ability to resolve even challenging features like thin shoulders and edges woth an average surface finish between $0.5~\mu m$ and $1.5~\mu m$.

Figure 1 compares the original object (Fig. 1(a)) with the measured point-cloud representation (Fig. 1(b)), which clearly shows the six distinct surface heights present in the design (Fig. 1(c)). The measurement precision was determined by localizing the point cloud data associated with each surface then fitting a plane to each dataset to account for any tilt. This process yielded fitting residuals of between 71 μ m and 86 μ m, representing the instantaneous surface measurement precision. Allan deviation measurements made at a single point on the object show that this precision can be improved to 4 μ m after 2 seconds of averaging, allowing a precise comparison of the test-object feature heights with the original mechanical design. In future work we will seek to improve signal return, minimize the scan time and further improve the precision.

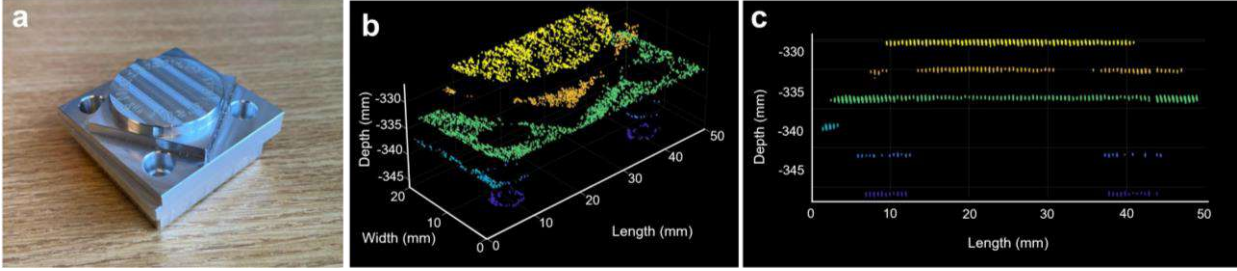


Figure 1 (a) Original test object, compared with (b) two-photon dual-comb LiDAR point-cloud image. (c) Side projection of the point-cloud dataset, showing six different surface heights, including (below -346 mm) wide and narrow shoulders around a through-hole. The height values are absolute distances from a reference reflector situated close to the common transmit / receive aperture of the imager.

- [1] I. Coddington, W. C. Swann, L. Nenadovic and N. R. Newbury, Nature Photonics 3, 351 (2009).
- [2] H. Wright, J. Sun, D. McKendrick, N. Weston and D. T. Reid, Optics Express 29, 37037 (2021).
- [3] H. Wright, A. J. M. Nelmes and D. T. Reid, Optics Express 31, 22497 (2023).
- [4] H. Wright, A. J. M. Nelmes, N. J. Weston and D. T. Reid, CLEO: Science and Innovations. Optica (2024).

Offset tunable 650–1050 nm astrocomb

Yuk Shan Cheng,^{1,*} Kamalesh Dadi,¹ William Newman,¹ Jake M. Charsley,¹ Richard A. McCracken¹ and Derryck T. Reid¹

¹ School of Engineering and Physical Sciences, Heriot-Watt University, Edinburgh, EH14 4AS, UK. *y.cheng@hw.ac.uk

Abstract

By using a feed-forward technique, we integrate a cw laser into a 650–1050 nm supercontinuum from a 1-GHz laser frequency comb. Transmitting the supercontinuum through a Fabry-Pérot filter cavity locked to the cw laser produces a 16-GHz astrocomb, whose offset frequency is fully tunable in 1-GHz intervals.

Laser frequency combs (LFCs) from modelocked ultrafast oscillators are ideal calibration sources for astronomical spectrographs due to their atomically-referenced and evenly-spaced spectral lines [1]. However, the typical comb-mode spacing (f_{rep}) of 100–1000 MHz is not resolvable and must be increased by using a Fabry-Pérot (FP) filter cavity to select a subset of modes with a spacing of mf_{rep} , introducing an ambiguity over which of the m primary LFC subsets has been filtered. Here, we present a broadband (650–1050 nm) astrocomb integrating a cw laser via a feed-forward technique [2], which not only allows the cw laser to serve as a fiducial marker of the astrocomb but also enables control over the astrocomb offset, facilitating comb-mode sweeping across the spectrograph detector pixels to enable instrument-function mapping that can be used to reveal camera inhomogeneities [3].

To integrate the cw laser, a heterodyne beat with the LFC was obtained using a beat-detection unit (BDU, Fig. 1a) and amplified to drive an acousto-optic frequency shifter (AOFS) applied to the cw laser. We pre-conditioned the cw laser frequency with a software feedback loop to match the beat to the AOFS operating frequency (150±10 MHz), and in this way overlapped the cw laser frequency onto a comb mode. A wavemeter was used to confirm the cw-laser frequency before and after shifting (Fig. 1b), showing a consistent +150 MHz shift, along with noise reduction. The 650–1050 nm LFC supercontinuum and cw laser were polarization-multiplexed into the FP cavity, which could be scanned to confirm the coincidence of the cw and comb-mode transmissions (Fig. 1c, arrows). After locking the FP cavity to the AOFS-shifted cw laser via Pound-Drever-Hall stabilization, a portion of the filtered LFC was observed on an echelle spectrograph, showing that by stepping the cw laser frequency in 1 GHz intervals the astrocomb offset frequency could be tuned over the full FP free-spectral range of 16 GHz (Fig. 1d).

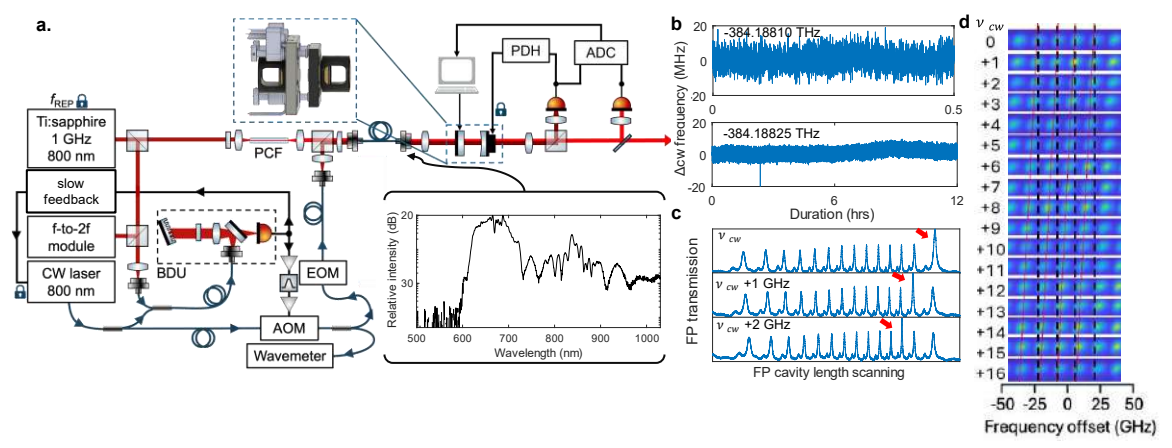


Figure 1: (a) Overview of the astrocomb and spectrum of the LFC supercontinuum. (b) cw laser frequency before and after frequency shifting. (c) FP transmission showing the overlap between the supercontinuum LFC fringes and the cw laser (red arrows) as the offset of the astrocomb was stepped. (d) Astrocomb tuning in 1 GHz steps across the full 16 GHz Fabry-Pérot free-spectral range, observed on an echelle spectrograph.

References

[1] R. A. McCracken, J. M. Charsley, and D. T. Reid, "A decade of astrocombs: recent advances in frequency combs for astronomy [Invited]," Opt. Express 25, 15058 (2017).

[2] Y. S. Cheng, B. Szutor, and D. T. Reid, "Feed-forward stabilization of a single-frequency, diode-pumped Pr:YLF-Cr:LiCAF laser operating at 813.42 nm," Opt. Express **30**, 42902 (2022).

[3] T. M. Schmidt, F. Bouchy, "Characterization of the ESPRESSO line-spread function and improvement of the wavelength calibration accuracy," Monthly Notices of the Royal Astronomical Society **530**, 1252 (2024).



A Simple, Multi-Channel Architecture for 10-fs Spectroscopy Covering Visible to Mid-IR

Connor Davis,1* Dylan Heberle,1 Noah Flemens,1,2 and Jeffrey Moses1

¹School of Applied and Engineering Physics, Cornell University, Ithaca, New York 14853, USA ²Department of Applied Physics, Stanford University, Palo Alto, California 94305, USA *ctd55@cornell.edu

Abstract

We present the architecture and experimental progress of the 10-fs Hyperspectral Stroboscope, a device to generate synchronized sub-10 fs pulses spanning the visible to mid-infrared. Using nonlinear-optical stages employing adiabatic frequency conversion with intrinsic dispersion management, we can greatly simplify the architecture for multi-channel, ultrafast spectroscopy covering several octaves.

Mapping electronic energy landscapes near nonadiabatic transitions in photoexcited systems require pump-probe experiments utilizing ultrafast pulses in the mid-IR, near-IR, and/or visible. The dynamics of interest often occur in tens of femtoseconds, requiring compressed pulses at a desired spectral range. We present our progress towards the 10-fs Hyperspectral Stroboscope, a device designed to produce synchronized ~10-fs pulses spanning the visible to mid-IR. The device utilizes a new and simple architecture based on a NOPA front-end with modular frequency translation stages employing adiabatic frequency conversion (AFC) with intrinsic dispersion management.

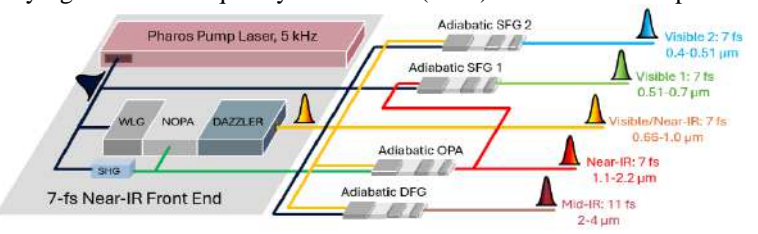


Figure 1: Hyperspectral Stroboscope architecture under development.

The Hyperspectral Stroboscope is designed to create five synchronized pulses with ~10 fs duration (Fig. 1). These pulses are generated from an Yb-amplifier-pumped NOPA front-end, which produces a 7-fs Vis/Near-IR pulse. This seeds four nonlinear-optical conversion stages that up- or down-convert the NOPA pulse to a specified frequency range while imparting zero group delay dispersion. Since frequency conversion and dispersion management occur in a single device, the multi-channel pump-probe system has a flexible, modular architecture, and can be constructed in a small space that minimizes uncommon beam paths.

Typically, a sub-10-fs beamline requires its own complex dispersion management scheme. Synthesizing several beamlines in a single device is a complex, often infeasible task. To solve this issue, we developed a variant [1] of AFC [2] in which a single aperiodically poled, quasi phase-matched crystal can convert an octave-spanning bandwidth while intrinsically compensating for its material dispersion. By utilizing the frequency-dependent and localized conversion of AFC with a tailored nonlinear poling function, we ensure that each frequency has the same total group delay. This enables a monolithic device that realizes the concept in Fig. 2 (left): it accepts a 10-fs near-IR pulse and emits a frequency-translated copy as a compressed 10-fs pulse. Fig. 2 (right) illustrates a first experimental realization: a 2-cm-long LiNbO₃ crystal transfers compressed 11.1-fs pulses from the near-IR (680–820 nm) to compressed 11.6-fs pulses covering an octave in the mid-IR ($2-4\mu m$) [2]. The three other crystals have been designed (and fabricated, in the case of the adiabatic OPA) and show similar promise through simulations.

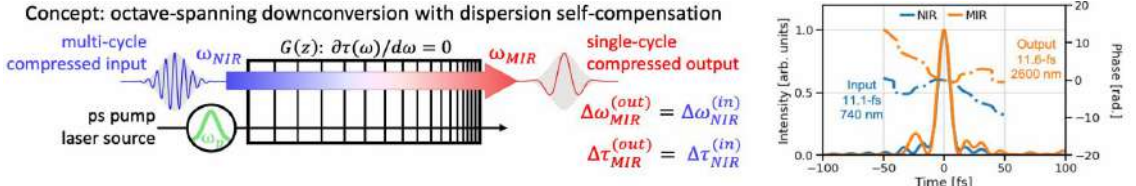


Figure 2: (left) Concept of AFC with intrinsic dispersion management. (right) Experimental demonstration: an 11.1-fs compressed input (680-820 nm) is converted to an 11.6 fs compressed output pulse (2000-4000 nm). (From [1].)

- [1] D. Heberle, et al., "Self-dispersion-managed adiabatic frequency conversion," arXiv:2405.17679 (2024).
- [2] P. Margules, et al., "Ultrafast Adiabatic Frequency Conversion," J. Phys. Photonics 3, 022011 (2021).

Chiral optical tweezers – efficient enantioseparation of molecules

R. M. Jones, N. Mayer, S. Patchkovskii, E. Pisanty, and M. Khokhlova, **

Abstract

We present an experimentally realisable scheme for all-electric dipole trapping of chiral molecules in an enantioselective fashion. Our theory shows that light with chirality structured in time induces a chiral Stark shift resulting in trapping of the chosen enantiomer in the laser beam, while the other enantiomer is shaken away.

Optical tweezers have proven to be an extremely powerful and versatile tool for trapping and manipulating matter from atoms to micron-scale objects. One long-lasting dream, which has yet to be realised, is the enantiosensitive trapping of chiral objects in an optical tweezer: an optical trap which will keep, say, the right-handed version of a molecule, but will reject (and, indeed, eject) its left-handed mirror version, providing an optical solution to an essential task of the chemical and pharmaceutical industries over the past 200 years.

A chiral optical trap, however, has remained elusive to standard methods, as linear chiroptical phenomena rely on magnetic-dipole and electric-quadrupole interactions, and these are dominated by the much stronger electric-dipole contribution.

Here we leverage recent developments in chiral nonlinear optics, direct brainchildren of attosecond and ultrafast science, which permit pure electric-dipole interactions in the ultrafast regime, built around synthetic chiral light (SCL) [1] as the main tool: a multicolour light field, which couples to a multi-photon chiral molecular pseudoscalar [2], that exhibits its chirality over time. We construct a tightly-focused tricolour chiral (TRICC) beam, designed to be globally chiral [3]. We demonstrate how this leads to the highly efficient enantioseparation of small molecules using only electric-dipole transitions that give rise to a nonlinear (three-photon) chiral Stark shift.

This chiral Stark shift, the product of a molecular and a light-field pseudoscalar, which is tuned through the relative phases and frequencies of the TRICC field, permits the enantiosensitive optical trapping of a specific enantiomer – i.e., a "Chiral Optical Tweezer" – in the same way that the linear achiral Stark shift enables standard optical tweezers [4].

We analyse the nonlinear susceptibility of the molecule of choice to optimise the TRICC-beam frequencies, and h⁽³⁾

Figure 1: Cartoon for chiral optical tweezers catching D-methyloxirane, while L-enantiomer is sent off the laser TRICC beam with the nonlinear correlation function $h^{(3)}$ responsible for trapping.

we show that results in a realistic trap in the presence of a cold buffer gas.

- [1] D. Ayuso, O. Neufeld, A. Ordonez et al., "Synthetic chiral light for efficient control of chiral light–matter interaction", Nat. Photon. 13, 866 (2019).
- [2] S. Beaulieu, A. Comby, D. Descampset al., "Photoexcitation circular dichroism in chiral molecules", Nat. Phys. 14, 484 (2018).
- [3] M. Khokhlova, E. Pisanty, S. Patchkovskii et al., "Enantiosensitive steering of free-induction decay", Sci. Adv. 8, eabq1962 (2022).
- [4] R. M. Jones, N. Mayer, S. Patchkovskii et al., "Chiral optical tweezers efficient enantioseparation of molecules", in preparation.

 $^{^{1}\}mathrm{Department}$ of Physics, King's College London, WC2R 2LS London, UK

²Max-Born-Institute, 12489 Berlin, Germany

 $^{^*}$ margarita.khokhlova@kcl.ac.uk

HHG-Based Lensless Imaging: Unique Insights into Material and Life Sciences

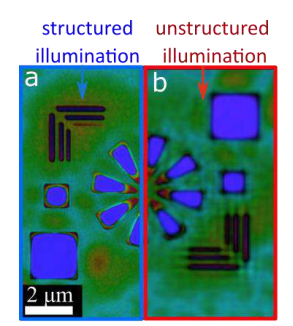
Leona Licht^{1,2,3*}, Wilhelm Eschen,^{1,2,3}, Chang Liu^{1,2,3}, Daniel S. Penagos M.,^{1,2,3}, Johannes Reents,¹ Robert Klas,^{1,2,3} Jens Limpert^{1,2,3,4} and Jan Rothhardt^{1,2,3,4}

¹Institute of Applied Physics, Abbe Center of Photonics, Friedrich-Schiller-University Jena, Albert-Einstein-Straße 15, 07745 Jena, Germany

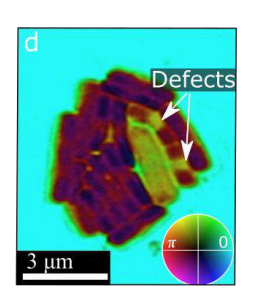
Abstract

We present a table-top, extreme ultraviolet ptychography microscope at 13.5 nm. Structured illumination improves resolution and image quality, enabling the investigation of nanoscale structure and composition of microorganisms and battery electrodes. Additionally, we demonstrate a novel method for quantitative single-shot EUV imaging, paving the way for imaging of ultrafast dynamics.

High power ultrafast lasers can generate coherent and high photon-flux extreme ultraviolet (EUV) radiation via high harmonic generation (HHG) [1], [2], rendering this spectral region that was once exclusive to large-scale facilities broadly accessible. Combined with imaging experiments, EUV radiation provides high resolution, high penetration depth and excellent, label-free element-contrast [3]. By combining a high photon flux EUV source and ptychography [4], a lenses imaging technique, we obtain quantitative amplitude and phase images with sub-20 nm resolution. Here we show, that a structured illumination, particularly a diffuse pattern, is especially suited for EUV ptychography (see Fig 1a) [5]. Utilizing this state-of-the art EUV-Microscope, *Bacillus subtilities* Bacteria and the effect of the antibiotic monazomycin were studied. For the first time defects in the treated bacteria could be visualized, employing a novel self-calibration technique, suited for soft tissue (see Fig 1d) [6]. Additionally, a thin lamella of a silicon anode from an all-solid-state battery was investigated, highlighting the enhanced penetration depth and material contrast in the EUV, compared to electron microscopy (see Fig 1. e/f). Moreover, the structured EUV beam enables quantitative single-shot imaging through novel reconstruction algorithms [7], which we demonstrated here for the first time on a table-top EUV setup. Thus, our work opens novel opportunities for ultrafast physics, as well as material and life sciences.



single shot EUV image



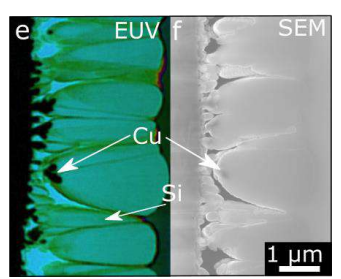


Fig.1: **a, b:** Image reconstruction with structured/unstructured illumination. **c:** Single shot EUV image using RPI. **d:** Antibiotic treated *B. subtilis* Bacteria. **e/f:** EUV and electron microscopy (SEM) image of a columnar silicon anode lamella.

- [1] M. Ferray et al., J. of Phys. B: 21(3) L31–L35 (1988)
- [2] S. Hädrich, et al. J. Phys. B: At. Mol. Opt. Phys. 49 (2016)
- [3] W. Eschen, et al. Light Sci Appl 11, 117 (2022).
- [4] P. Thibault et al., Science 321(5887), 379–82 (2008)
- [5] W. Eschen, et al., Opt. Exp. 32, 3480-3491 (2024)
- [6] C. Liu, et al., Opt. Letters 50, 1581-1584 (2025)
- [7] A. Levitan, et al., Opt. Exp. 28, 37103–37117 (2020)

²Helmholtz-Institute Jena, Fröbelstieg 3, 07743 Jena, Germany

³GSI Helmholtzzentrum für Schwerionenforschung, Planckstraße 1, 64291 Darmstadt, Germany

⁴Fraunhofer Institute for Applied Optics and Precision Engineering, Albert-Einstein-Str. 7, 07745 Jena, Germany *leona.licht@uni-jena.de

Ultrafast Imaging Below the Diffraction Limit with High Harmonic Deactivation Microscopy

K Murzyn 1*, T van Horen¹, P van Essen¹, Z Nie¹, L Guery¹, M v. d. Geest¹, S Witte¹, P Kraus¹

¹Advanced Research Center for Nanolithography, Science Park 106,1098XG Amsterdam, The Netherlands

* k.murzyn@arcnl.nl

Abstract

We harness attosecond waveform and coherence control in multicolor laser fields to spatially deactivate solid-state high-harmonic generation below the diffraction limit. This harmonic deactivation microscopy (HADES) enables label-free super-resolution microscopy. We demonstrate imaging of nanostructures via HADES and describe its prospects for (sub-)-femtosecond nanoscopy.

Nonlinear optical microscopy provides elegant means for label-free imaging of biological samples and condensed matter systems. The widespread areas of application could even be increased if resolution were improved, which the famous Abbe diffraction limit now restrains. Super-resolution techniques can break the diffraction limit, but most rely on fluorescent labeling. This makes them incompatible with (sub)femtosecond temporal resolution and applications that demand the absence of labeling. In a recent study, we introduced harmonic deactivation microscopy (HADES) for breaking the diffraction limit in nonfluorescent samples [1].

This technique generates high harmonics in a sample (Fig. 1A) by tightly focusing near-infrared light. A donut-shaped beam with radially varying fluence deactivates the harmonics spatially (Fig. 1B). HADES reduces the harmonic point-spread function (PSF) noticeably. For third harmonic generation (THG) microscopy, four-fold reduction of the PSF compared to the Abbe limit has been demonstrated, which thus represents a lower limit for potential resolution improvement. Experiments showed that deactivation scales with harmonic order (Fig. 1B inset), leading to increased resolution gains: For fifth harmonic microscopy, we thus expect sub-100 nm resolution. We deactivate high-harmonic generation (HHG) by overlapping two incommensurate electric fields. The new waveform synthesized by both fields reduces HHG efficiency during overlap. After pulse overlap increased scattering due to photoexcited carriers leads to an overall amplitude suppression [2,3]. HADES utilizes these effects and increases the resolution of an existing third-harmonic generation (THG) microscope (Fig. 1C, D).

Combining HADES with higher harmonic orders enables nanoscale resolutions. The general nature of harmonic deactivation allows for translating the results to a variety of materials subject to current research, e.g., 2D materials, or topological insulators [2]. The intrinsic attosecond nature of HHG yields the potential of unveiling subfemtosecond processes on a nanoscale [4], such as the resolution of insulator-to-metal phase transitions in strongly correlated materials, which HADES may resolve at the most extreme attosecond time and nanometer length scales.

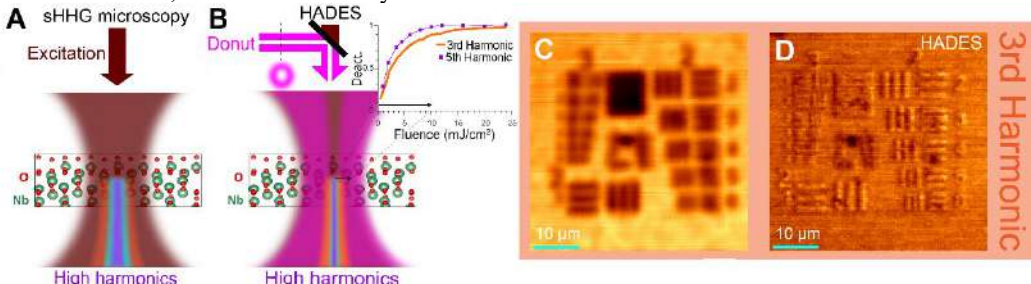


Figure 1: A: Tightly focused NIR beam excites HHG in a sample for imaging. B: A donut-shaped beam reduces the spatial extent of HHG. The deactivation curve for higher orders (inset, purple) is steeper than for lower harmonics (orange), further increasing the resolution with harmonic order. C-D: Harmonic deactivation microscopy (HADES) improves the resolution of a THG microscope visibly in a NbO2 sample.

- [1] K. Murzyn, et al., "Breaking Abbe's diffraction limit with harmonic deactivation microscopy", Sci adv. 10, (2024). [2] P.J. van Essen, et al., "Toward Complete All-Optical Intensity Modulation of High-Harmonic Generation from Solids", ACS photonics 11.5, 1832-1843 (2024).
- [3] B. de Keijzer, et al., "Effect of photoexcitation on high-harmonic generation in semiconductors", J. Opt. Soc. Am. B 41.8, 1754-1763 (2024).
- [4] M. Garg, et al., "Multi-petahertz electronic metrology", Nature 538, 359-363 (2016).

Tunable Femtosecond Source Based on Spatiotemporal Nonlinear Enhancement

Bahareh Hosseini Fakhar,^{1,*} Zeinab Norouzinik,¹ Kourosh Zarekarizi,¹ François Légaré,¹ Reza Safaei¹

¹Institut national de la recherche scientifique, Centre Énergie Matériaux Télécommunications, Varennes, QC J3X 1S2, Canada

*Bahareh.Hosseini.Fakhar@inrs.ca

Abstract

This study presents a wavelength-tunable, multi-megawatt pulse source using N₂O-filled hollow-core Kagome photonic crystal fibers (PCFs) for nonlinear microscopy. Starting with a Ytterbium laser, we achieved 50% efficiency at 1300 nm, essential for three-photon fluorescence microscopy, enabled by spatiotemporal nonlinear enhancement in the Raman-active medium.

Methodology and Results

Three-photon fluorescence microscopy requires ultrashort pulses with an intensity of over 1 MW and a wavelength of \sim 1300 nm for deep-tissue imaging. Gas-filled Kagome PCFs offer tunable dispersion, nonlinearity, and low loss (\sim 0.1 dB/m) broadband guidance. Raman-active gases enable redshift spectral broadening via stimulated Raman scattering (SRS). An 82 μ m core Raman-active gas-filled Kagome PCF with weak anomalous group velocity dispersion (GVD) and controlled modal dispersion enables 1300 nm generation via multidimensional solitary states (MDSS)[1].

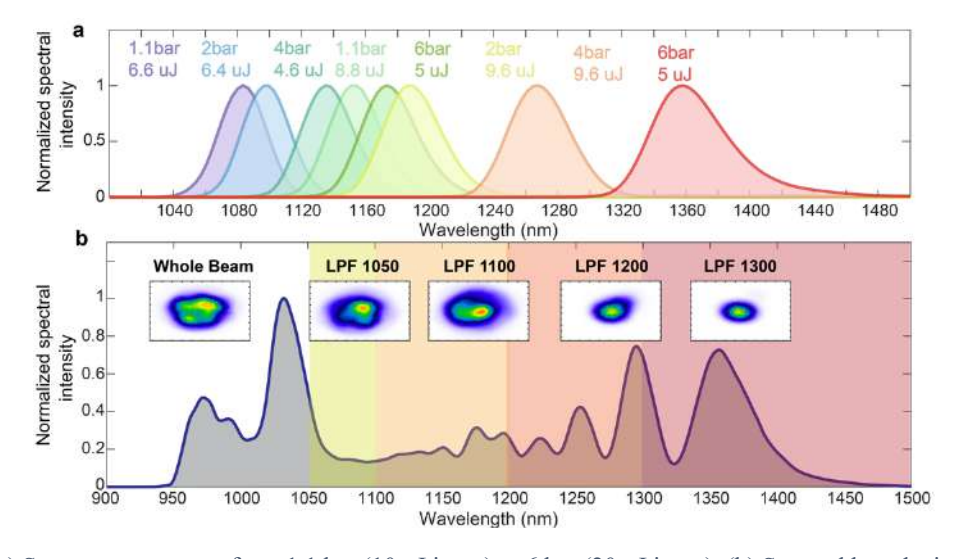


Figure 1: a) Spectra at pressures from 1.1 bar (10 μ J input) to 6 bar (20 μ J input). (b) Spectral broadening and beam profile at 6 bars with 20 μ J input, the full beam, and the beam after long-pass filters (LPFs) at 1050-1300 nm.

In our experiment, 130-fs, 20- μ J pulses at 1030 nm from a Yb-doped fiber amplifier were coupled into a 1-m N₂O-filled Kagome PCF with an 82- μ m core. Figure 1a illustrates a cascaded SRS redshift from 1080 to 1360 nm by adjusting the N₂O pressure and input energy, resulting in a conversion efficiency of ~50% (compared to 10% in previous 1D studies). Mode profiles reveal nonlinear interactions and higher-order mode competition. LPF spatial profiles at 1050–1300 nm show high beam quality, especially at 1300 nm (Figure 1b). The generated multi-megawatt pulses redshift to 1.36 μ m via Raman-enhanced intermodal interactions, offering a promising source for nonlinear microscopy.

References

[1] R. Safaei *et al.*, 'High-energy multidimensional solitary states in hollow-core fibres', *Nat Photonics*, vol. 14, no. 12, pp. 733–739, Dec. 2020, doi: 10.1038/s41566-020-00699-2.

Distributed Charge Compton Sources & Applications

C. P. J. Barty^{1,2}

¹Department of Physics & Astronomy, University of California, Irvine, 4162 Frederick Reines Hall, Irvine, CA 92697 ²Lumitron Technologies, Inc. 5201 California Avenue, Irvine, CA 92617 *cbarty@uci.edu, cto@lumitronxrays.com

Abstract

This presentation reviews the motivation, design, performance, and applications of laser-Compton x-ray & gamma-ray sources based on the collision of high-frequency trains of high-brightness electron bunches and trains of ultrashort duration laser pulses created via multi-GHz pulse synthesis.

Main Text

For nearly 130 years, x-ray systems used in clinical and industrial settings have been based on the n x-ray tube. Laser-Compton sources, which produce x-rays via the interaction of energetic laser pulses with highly relativistic electrons, can produce low-divergence beams of nearly mono-energetic x-rays or gamma-rays. In this presentation, a unique, distributed charge Compton scattering (DCCS) architecture is presented that optimizes source performance and in doing so creates both clinically and industrially-relevant beams of x-rays. Underpinning this architecture is a novel laser pulse synthesis technology which utilizes the x-band (11.424 GHz) RF clock of a compact, high-gradient accelerator and telecom-quality amplitude and phase modulators to create a high-repetition laser with a macro/micro pulse structure consisting of up to 1000 micro-pulses repeated at a macro-pulse rate of up to 400 Hz. This approach significantly improves electron beam emittance, maximizes the electron beam current, reduces x-ray bandwidth, inherently creates synchronization between the laser and electron beam subsystems, and maximizes the average x-ray brilliance. At MeV energies, DCCS systems can exceed the average brilliance of even the world's largest synchrotrons by many orders of magnitude. Applications span detection & treatment of cancer, industrial NDE, and nuclear photonics.



Figure 1: Operational, high-brilliance, distributed charge Compton x-ray source in Irvine, California

References

[1] C P J Barty et al., Design, construction, and test of compact, distributed-charge, X-band accelerator systems that enable image-guided, VHEE FLASH radiotherapy, 2025 Frontiers in Physics, DOI=10.3389/fphy.2024.1472759

High flux femtosecond fiber laser driven hard X-ray source

Maximilian Benner,^{1*} Mohammed Almassarani,¹ Robert Klas,² Maximilian Karst,^{1,3,4} Lucas Eisenbach,^{1,2,3,4} Philipp Gierschke,^{1,2} Warunya Röder,² Arno Klenke,^{1,2,3,4} Jan Rothhardt^{1,2,3,4}, and Jens Limpert^{1,2,3,4}

Abstract

We present a high-flux, continuously operated femtosecond hard X-ray source by tightly focusing short laser pulses on a regenerative liquid metal jet. The photon flux is the highest ever reported at photon energies above 10keV, moreover it scales linearly with laser power, enabling scalable X-ray generation with great application potential.

New table-top laser-driven X-ray sources are being developed for their ultrashort pulse capabilities, enabling femtosecond X-ray pump-probe experiments and atomic-scale structural dynamics studies [1,2] that demand high photon flux and a small source size. We report a high-photon-flux, scalable X-ray source at energies >10 keV from a liquid metal jet of bismuth-indium alloy. The measured photon flux is 2×10^8 photons/s/sr at 10.8 keV (Bi La) and $\sim 1 \times 10^8$ photons/s/sr at 24.2 keV (In Ka), representing record flux values for laser driven X-ray sources above 10keV. An X-ray spectrum measured at 5 kHz repetition rate is shown in figure 1.

The laser driver is a 1 kW all-fiber laser system operating at 1.03 μ m [3] with an adjustable repetition rate of up to 100 kHz. The pulse duration was compressed to 32 fs using a multipass cell, with 5 mJ pulse energy on target and a 6.4 μ m (1/e²) focal spot size, yielding a peak intensity of ~4 × 10¹⁷ W/cm². A key result of the experiment is the linear scalability of the total X-ray photon count with laser average power. In this initial run, scaling was only limited by the liquid jet speed, which will be enhanced in future iterations. These findings highlight the potential of a continuous regenerative liquid metal jet combined with a high-average-power laser system to generate tabletop, high-flux hard X-ray pulses at photon energies above 10 keV.

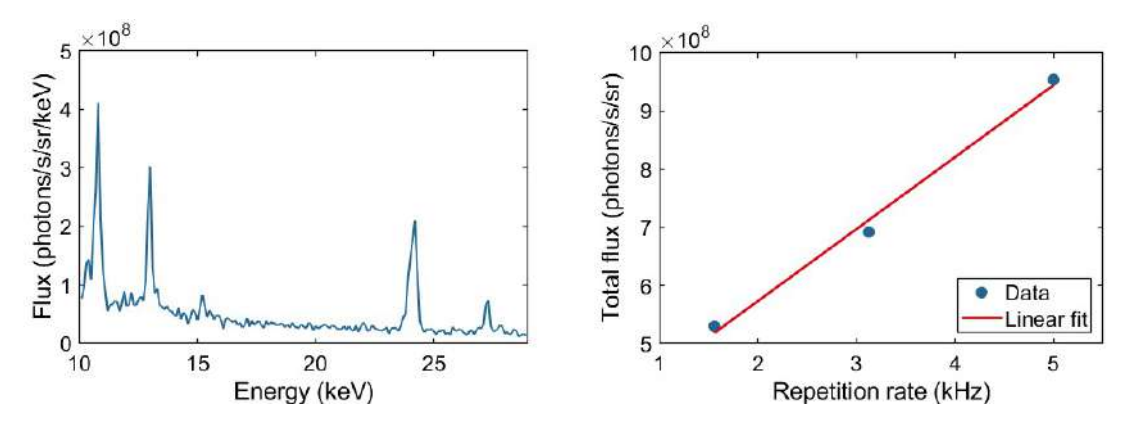


Figure 1: (left) measured X-ray spectrum with characteristic emission peaks; (right) measured total X-ray flux for different repetition rates.

- [1] T. Elsaesser and M. Woerner, J. Chem. Phys. 140, 020901 (2014).
- [2] A. Rousse, C. Rischel, and J.-C. Gauthier, Rev. Mod. Phys. 73, 17 (2001).
- [3] H. Stark, J. Buldt, M. Müller, A. Klenke, and J. Limpert, Opt. Lett. 46, 969 (2021).

¹Friedrich-Schiller University Jena, Institute of Applied Physics, Albert-Einstein-Str. 15, 07745 Jena, Germany

²Fraunhofer Institute for Applied Optics and Precision Engineering, Albert-Einstein-Str. 7, 07745 Jena, Germany

³Helmholtz-Institute Jena, Fröbelstieg 3, 07743 Jena, Germany

⁴GSI Helmholtz Centre for Heavy Ion Research, Planckstraße 1, 64291 Darmstadt, Germany

^{*}maximilian.benner@uni-jena.de

Optical control of electrons in a Floquet topological insulator

Daniel M. B. Lesko, ^{1,2,*} Tobias Weitz, ^{1,2} Simon Wittigschlager, ¹ Weizhe Li, ^{1,2} Christian Heide, ¹ Ofer Neufeld, ³ and Peter Hommelhoff^{1,2}

Abstract

We demonstrate optical control of electrons in light-dressed graphene using bi-chromatic electric fields. Circularly polarized femtosecond laser pulses at 1550 nm generate a Floquet topological insulator (FTI). A phase-locked second harmonic controls electrons within the FTI. We observe photocurrent circular dichroism, the all-optical anomalous Hall effect, and attosecond FTI micromotion.

Light interaction with materials can modify their electronic band structure, creating light-dressed Floquet states with new quantum and topological properties. Trivial materials can be transformed by periodic driving into topologically nontrivial periodic states, known as Floquet topological insulators (FTIs), and have been previously observed in photonic waveguides [1] and cold atom systems [2]. While theory suggests that Floquet dressing can synthesize almost arbitrary material band structures with varying topological phenomena [3], FTI states in real materials have yet to be directly observed and controlled. Here we demonstrate a new method for generating and probing these phenomena by harmonically related optical fields. The circularly polarized fundamental frequency laser pulse dresses bare graphene (ω , 1550 nm, Fig. 1), a topologically trivial material, into an FTI. Our FTI is unique in that the circular dressing breaks only time-reversal symmetry, not inversion symmetry, allowing us to directly probe the topological properties of the transient state. We probe topological bands of the strongly driven FTI using a second harmonic pulse (2ω , 775 nm). For the first time we measure photocurrent circular dichroism, the optical anomalous Hall effect, and observe the FTI state's attosecond micromotion [4]. This directly connects the traditionally steady-state Floquet picture with attosecond phenomena probed by optical fields. By understanding how to optically modify and control materials, we can dynamically change material properties and engineer quantum and topological phenomena into trivial materials on the femtosecond timescale.

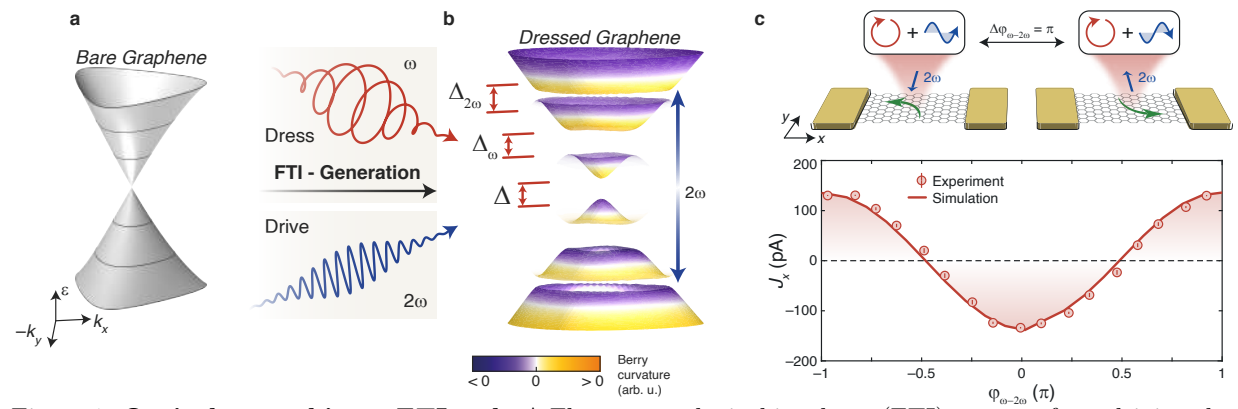


Figure 1: **Optical control in an FTI. a**–b, A Floquet topological insulator (FTI) emerges from driving the gapless, topologically trivial band structure of graphene (a) by irradiation with a circularly-polarized fundamental laser field (red waveform, dress). Broken time-reversal symmetry gives rise to a nonzero gap Δ and same signed Berry curvature (colorbar, a), resulting in a non-zero Chern number. This topological insulating phase exhibits avoided crossings at resonant energies ($\Delta_{n\omega}$), which we probe with a second harmonic pulse (blue waveform). c, All-optical anomalous Hall currents (green arrows) emerge from excitation FTI with 2ω polarized perpendicularly to the electrode axis. Shifting $\varphi_{\omega-2\omega}$ by π effectively results in a reversal of the 2ω deflection and consequently also the Hall current direction.

- [1] Rechtsman, M. C. et al. "Photonic Floquet topological insulators." Nature 496, 196-200 (2013).
- [2] Jotzu, G. et al. "Experimental realization of the topological Haldane model with ultracold fermions." Nature **515**, 237-240 (2014).
- [3] Rudner, M. S., Lindner, N. H. "Band structure engineering and non-equilibrium dynamics in Floquet topological insulators." Nature Reviews Physics **2**, 229-244 (2020).
- [4] Lesko, D. M. B. et. al. "Optical control of electrons in a Floquet topological insulator." arXiv:2407.17917.

¹Department of Physics, Friedrich-Alexander-Universität Erlangen-Nürnberg (FAU), Erlangen, Germany

²Fakultät für Physik, Ludwig-Maximilians-Universität, München, Germany

³Schulich Faculty of Chemistry, Technion - Israel Institute of Technology, Haifa, Israel

^{*}Daniel.Lesko@fau.de

A soft X-ray timing tool based on spintronic THz emission

Robert Carley^{1,*}, Laurent Mercadier^{1,*}, Luigi Adriano¹, Benjamin van Kuiken¹, Loïc Le Guyader¹, Yi-Ping Chang¹, Carsten Broers¹, Le Phuong Hoang¹, Jan Torben Delitz¹, Natalia Gerasimova¹, Zhong Yin³, Giuseppe Mercurio¹, Giacomo Merzoni^{2,1}, Teguh Citra Asmara¹, Sergii Parchenko¹, Alexander Reich¹, Justine Schlappa¹, Martin Teichmann¹, Andreas Scherz¹

¹European X-Ray Free Electron Laser Facility GmbH, Holzkoppel 4, 22869 Schenefeld, Germany

Abstract

THz single cycle pulses emitted from a spintronic thin film illuminated by X-ray free electron laser pulses are detected by spectrally-encoded single-shot electro-optic sampling to parasitically measure and correct the arrival time variation in pump-probe experiments in condensed matter

The time resolution of pump-probe experiments at X-ray free electron lasers (XFEL) based on self-amplified spontaneous emission is limited by the arrival time jitter of the of X-ray pulses in combination with drifts arising from the scale of the such facilities. Many approaches to mitigate these problems have been developed, including transient optical reflectivity or transmission of an X-ray pumped semiconductor [1], THz streaking [2], as well as synchronization systems with few femtosecond stability [3]. Nevertheless, condensed matter experiments with soft X-rays present a particular set of challenges for pulse arrival diagnostics that limit their applicability. The pulse energy incident on the sample is often low, limiting the fluence available for timing diagnostics. The transmitted beam often forms part of the measurement, so is not available for downstream use. Bulk samples typically absorb the whole pulse, again ruling out downstream measurements. Beam splitting techniques can be used upstream of the sample but may negatively impact beam quality.

We have developed a novel X-ray pulse arrival time diagnostic based on detecting terahertz (THz) radiation emitted by a ferromagnetic spintronic sample irradiated by the X-ray pulses from the FEL. We demonstrated this technique first in the extreme UV at the seeded Fermi FEL [4] and have now implemented it at the soft X-ray Spectroscopy and Coherent Scattering (SCS) Instrument of the European X-ray Free Electron Laser (European XFEL).

Spintronic THz emitters (STE) are thin-film nanostructures comprising a ferromagnetic material sandwiched between two non-magnetic heavy metals [5]. For use in soft X-rays, the STE is grown on a thin, X-ray transparent membrane of silicon, silicon nitride or silicon carbide, and held in an in-plane magnetic field. The femtosecond X-ray pulse excites a spin current in the ferromagnetic layer that is converted into a charge current in the two heavy metal layer via the inverse spin Hall effect. The THz pulse is detected using spatially-encoded single-shot electro-optical sampling with the same infrared laser pulse as used for pump-probe experiments, providing a measurement of the relative arrival time of the X-ray and optical laser pulses.

The pulse arrival diagnostic tool is located a few meters upstream of the user experimental station to reduce relative jitter between them arising from their different laser paths. The STE sample absorbs only a small fraction of the X-ray pulse energy and does not cut the beam spatially and survives large X-ray fluence, so the pulse arrival diagnostic can be run in parallel to user experiments without disturbing them.

- [1] Gahl, C. et al., Nature Photonics 2, 165 (2008)
- [2] U. Frühling, et al., J. Phys. B 44, 243001 (2011)
- [3] Schulz, S. et al., Proceedings, 39th International Free Electron Laser Conference (FEL2019)
- [4] Ilyakov, I. et al., Optica 9, 545 (2022)
- [5] Seifert, T. et al., Nature Photonics 10, 483 (2016)

²Dipartimento di Fisica, Politecnico di Milano, 20133, Milano, Italy

³SRIS, Tohoku University, Japan

^{*}robert.carley@xfel.eu, laurent.mercadier@xfel.eu



Linking Adaptable and Optimized Ultrafast Photoemission to Brighter X-rays

Jack Hirschman, 1,2,* Randy Lemons, Hao Zhang, 2,3 Mat Briton, Razib Obaid, Agostino Marinelli,² Ryan Coffee,² and Sergio Carbajo^{2,3}

Abstract

We present a versatile framework enabling spectral and temporal shaping of the photoinjector laser pulses through programmable infrared modulation and innovative nonlinear upconversion techniques. Demonstrating temporally-tailored UV pulses, this approach provides an avenue for enhanced control over electron-emission, targeting order-of-magnitude increase in XFEL brightness and applications of attosecond pulse production.

SLAC's LCLS-II is undergoing major upgrades aimed at boosting X-ray brightness, increasing repetition rates, and enhancing control over X-ray temporal profiles. Achieving the full benefit of these improvements requires coordinated optimization across every stage of the X-ray generation process—starting with the UV photoinjector laser, which initiates electron emission via cathode photoemission and ultimately defines the X-ray beam characteristics [1]. The next-generation laser system introduces programmable IR spectral shaping and advanced upconversion methods to produce tunable, ultrafast photoemission (Fig. 1a). One such method, dispersion-controlled nonlinear synthesis (DCNS), employs noncollinear sum-frequency generation driven by oppositely chirped pulses to generate diverse, static UV pulse shapes on picosecond timescales (Fig. 1c). When combined with upstream IR pulse shaping (Fig. 1b), this architecture provides a powerful lever for tailoring UV pulses. These shaped UV pulses induce controlled electron emission at the cathode, generating electron bunches that traverse undulators producing coherent X-ray light. Downstream diagnostics measure X-ray pulses and depleted electron bunches (Fig. 1d), correlating these outcomes to the UV pulse shaping.

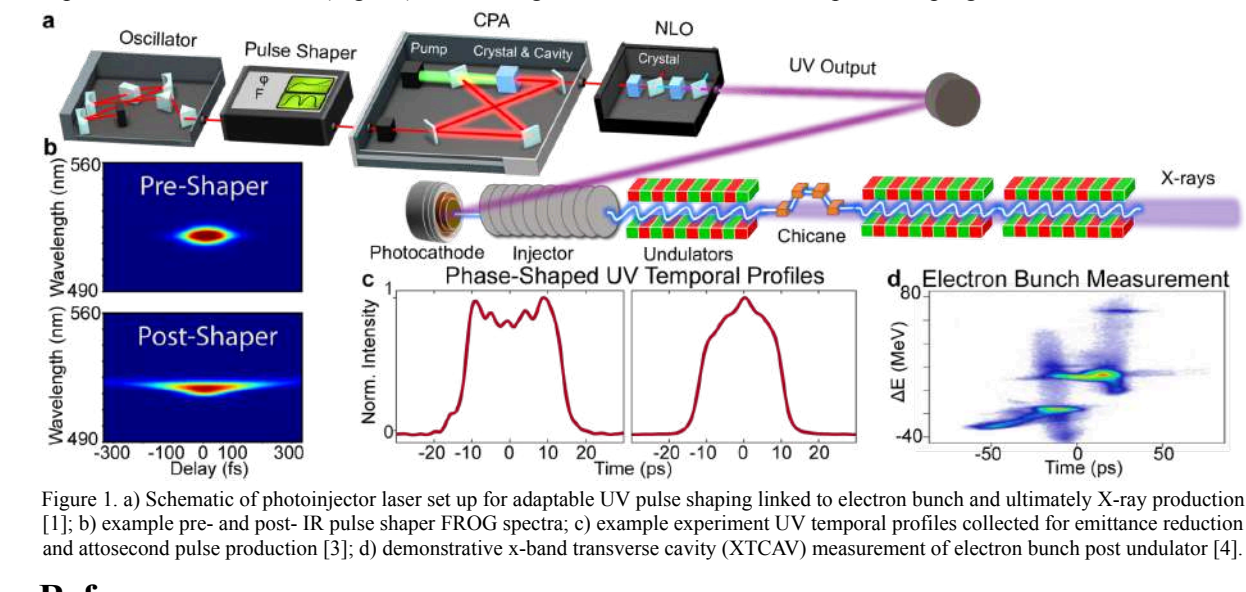


Figure 1. a) Schematic of photoinjector laser set up for adaptable UV pulse shaping linked to electron bunch and ultimately X-ray production [1]; b) example pre- and post- IR pulse shaper FROG spectra; c) example experiment UV temporal profiles collected for emittance reduction and attosecond pulse production [3]; d) demonstrative x-band transverse cavity (XTCAV) measurement of electron bunch post undulator [4].

- [1] H. Zhang, et al., "The Linac Coherent Light Source II photoinjector laser infrastructure," HPLSE 12, e51 (2024).
- [2] J. Hirschman, et al., "Design, tuning, and blackbox optimization of laser systems", Opt. Express 32, 15610–22
- [3] R. Lemons, et al., "Nonlinear shaping in the picosecond gap", ArXiv Preprint ArXiv:2410.19926 (2024)
- [4] P. Franz, et al., "Terawatt-scale attosecond X-ray pulses from a cascaded superradiant free-electron laser", Nat. Photonics 18, 698–703 (2024)

¹Department of Applied Physics, Stanford University, Stanford, CA 94305, USA

²SLAC National Accelerator Laboratory, Menlo Park, CA 94025, USA

³Department of ECE & Physics and Astronomy Department, UCLA, Los Angeles, CA 90095, USA *ihirschm@stanford.edu

Poster Session 1

High-order frequency mixing: harvesting bright XUV from propagation

M. Khokhlova^{1,*}

¹Department of Physics, King's College London, WC2R 2LS London, UK *margarita.khokhlova@kcl.ac.uk

Abstract

High-harmonic generation (HHG) in gases became our trusty source of coherent XUV, however it is affected by the media photoionisation, causing the blue shift of the driver and disturbing the XUV growth with propagation. We show that high-order frequency mixing produces much brighter XUV than HHG, gaining from the blue-shift compensation.

The generation of bright, coherent XUV light via frequency conversion of intense laser drivers is a problem of both fundamental and technological importance. Increasing the intensity of the generated high harmonics by raising the intensity of the driving field only works up to a point: at high intensities, rapid ionisation of the medium limits the conversion efficiency.

We identify the dominant limiting mechanism – the combined effect of phase matching and the blue shift of the driving field during its propagation through a rapidly ionising medium [1, 2]. We introduce the blue-shift length, which sets the upper bound for the quadratic intensity growth of the harmonics.

We study analytically and numerically (solving the propagation equation coupled with the TDSE) the behaviour of the macroscopic HHG signal with propagation distance. We show that its quadratic growth is limited by the shortest of three lengths: absorption, coherence, or blue-shift length. Thus, we define three regimes of HHG, corresponding to the dominant limiting mechanisms (see Fig.1(a)).

Moreover, we show that this seemingly fundamental restriction can be overcome by using an additional generating weak mid-IR field. For suitable combinations of frequencies of the generating fields, the corresponding high-order frequency-mixing (HFM) process does not suffer from the blue shift of the drivers and phase mismatch [1], and thus its efficiency grows quadratically with propagation (see Fig.1(b)).

Our results open a new route for highly efficient generation of XUV light, the first step of which has been taken already via an observation of high-order parametric generation [3]. Moreover, HFM offers new handles for XUV control such as the control of the carrier envelope phase of the emitted attosecond XUV pulses [4, 5]. This work is done in tight collaboration with Vasily Strelkov.

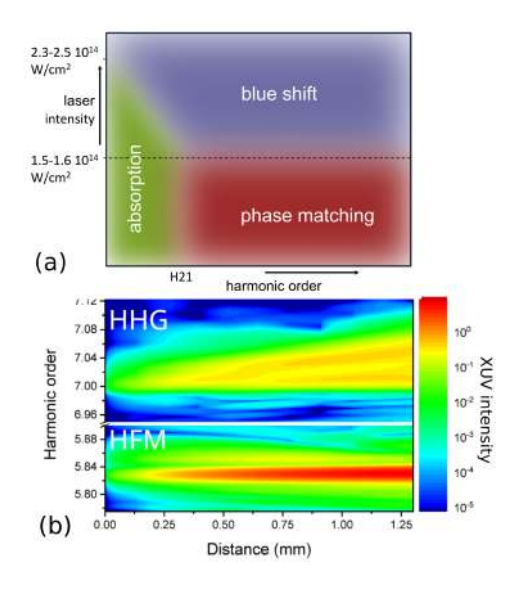


Figure 1: (a) Diagram showing dominant mechanisms for HHG in argon. (b) TDSE calculation for the propagation of HHG and HFM in argon for $2 \cdot 10^{14} \mathrm{W/cm^2}$ of 330nm driver with weak 1980nm.

- [1] M. Khokhlova, V. Strelkov, "Highly efficient XUV generation via high-order frequency mixing", New J. Phys. 22, 093030 (2020).
- [2] M. Khokhlova, V. Strelkov, "Role of blue-shift length in macroscopic properties of high-harmonic generation", New J. Phys. 26, 073013 (2024).
- [3] O. Hort et al., "High-order parametric generation of coherent XUV radiation", Opt. Express 29, 5982 (2021).
- [4] V. Birulia et al., "Generation of attosecond pulses with a controllable carrier-envelope phase via high-order frequency mixing", Phys. Rev. A 106, 023514 (2022).
- [5] V. Birulia et al., "Macroscopic effects in generation of attosecond XUV pulses via high-order frequency mixing in gases and plasma", New J. Phys. 26, 023005 (2024).

18 20

△ UFO XIV Azores 2025

Femtosecond pulse replication via phase-only shaping and RandoMICS algorithm

Konstantin B. Yushkov,^{1,*} Mikhail A. Martyanov,² and Vladimir Ya. Molchanov¹

¹National University of Science and Technology MISIS, 4 Leninsky Prospekt, 119049 Moscow, Russia

Abstract

We experimentally demonstrate a phase-only technique for programmable ultrashort laser pulse replication based on stochastic interleaved combs in frequency domain. For generating two femtosecond pulse replicas, we use quasi-random binning of spatial light modulator pixels with different phase modulation slopes for two pixel subsets.

We demonstrate a new technique for phase-only femtosecond laser pulse shaping using a 4F pulse shaper with a liquid-crystal spatial light modulator (SLM). The technique is based on Randomized Multiple Indepenent Comb Shaping (RandoMICS) with irregular binning of adjacent pixels has been developed to suppress undesired satellite pulses resulting from intrapulse interference [?]. For this purpose, stochastic aperiodic assignment of the spectral pixels to different subsets is applied. Thus, satellite-free generation of multiple pulse replicas is achieved and the full delay range of the pulse shaper can be utilized.

The RandoMICS algorithm was experimentally validated with an Yb-doped fiber laser emitting 250-fs pulses with 8 nm FWHM spectrum and a 4F pulse shaper based on an 800-pixel phase-only SLM. Two pixel subsets of the SLM corresponding to the pulse replicas were generated with a binary random number generator in MATLAB, see Fig. 1(a). One subset had no phase modulation ($\Phi=0$) while the other subset had a linear phase delay $\Phi(\Delta f)=2\pi\Delta fT$, where optical frequency offset Δf is linearly mapped to the SLM pixel number in the 4F pulse shaper. One replica of the pulse is at t=0, while the second replica is set at variable delay T ranging from -20 to 20 ps. We experimentally compare RandoMICS and regular MICS pulse replication algorithms with smooth phase modulation. The experimental results are cross-correlation traces at variable delays of the second pulse replica shown in Fig. 1(b). A series of 10 sequential measurements for each delay preset is demonstrated. Measured delay of the replicas obtained by the RandoMICS algorithm is within 0.2% of preset delay T and the RMS measurement jitter is below 60 fs. The decrease of the replica intensity at |T| > 10 ps is explained by wavefront tilt in the pulse shaper and resulting reduced efficiency of laser beam coupling into the fiber.

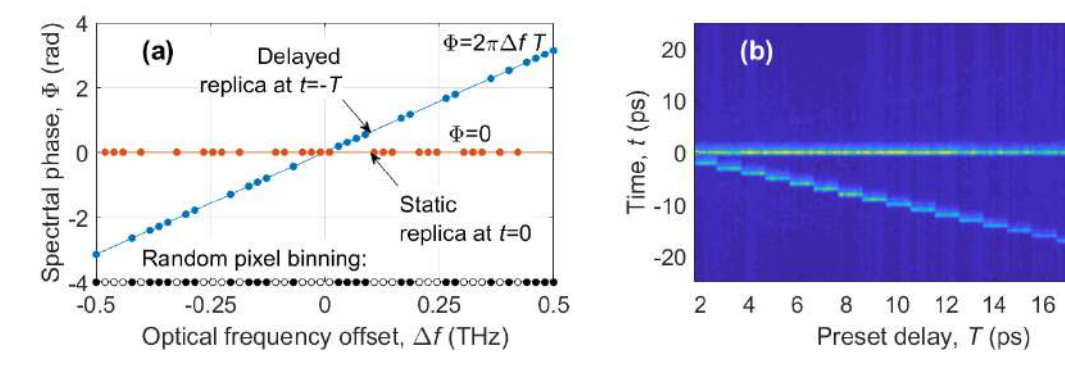


Figure 1: Implementation of the RandoMICS algorithm for the case of two replicas at t=0 and T: (a) phase modulation pattern with randomized pixel binning; (b) measured cross correlation functions at various preset delays T.

References

[1] K.B. Yushkov and V.Ya. Molchanov, "Randomly spaced phase-only transmission combs for femtosecond pulse shaping", in IEEE Journal of Selected Topics in Quantum Electronics 26, 8700108 (2020).

² A.V. Gaponov-Grekhov Institute of Applied Physics, Russian Academy of Sciences, 46, Ulyanova str., 603950 Nizhny Novgorod, Russia

^{*}konstantin.yushkov@misis.ru



Uncertainty relations in femtosecond laser pulse shaping

Konstantin B. Yushkov,^{1,*} Vladimir Ya. Molchanov,¹ and Efim A. Khazanov²

¹National University of Science and Technology MISIS, 4 Leninsky Prospekt, 119049 Moscow, Russia

Abstract

Spectral modulation of chirped femtosecond pulses is an effective method for obtaining arbitrary timedomain waveforms. We analyze chirped pulse modulation in terms of information theory and demonstrate that modulation contrast and resolution satisfy uncertainty relations. Performance is maximized when the shaper's bandwidth equals twofold bandwidth of laser radiation.

Consider a chirped laser pulse with the carrier frequency modulation bandwidth $\Delta\omega$ processed with a pulse shaper having the full transmission bandwidth B_{ω} . Gabor's uncertainty principle implies that the bandwidth necessary for transmitting an element with duration τ is $\delta\omega=2\pi/\tau$. To ensure that this condition is satisfied for all spectral components of the chirped pulse, we restrict the transmission bandwidth as $B_{\omega} \geqslant \Delta\omega + 2\pi/\tau$. On the other hand, duration of a linearly chirped laser pulse is $T=2b_2\Delta\omega$, where b_2 is the second order dispersion coefficient. Thus, we can estimate the number of resolvable spots as

$$N = T/\tau = b_2 \Delta \omega (B_\omega - \Delta \omega)/\pi. \tag{1}$$

Equation (1) allows for explicit optimization of the modulation resolution:

$$\max N = \frac{b_2}{4\pi} B_{\omega}^2 \quad \text{at} \quad B_{\omega} = 2\Delta\omega. \tag{2}$$

Figure 1 demonstates up to 5 dB enhancement in spectral contrast for 167-bits meander modulation over 80-nm bandwidth. In the experiment, 12-fs pulses from a Ti:sapphire master oscillator were processed with a high-resolution AOPDF designed and fabricated in-house. Control RF waveform was generated by the Dispersive Fourier Synthesis (DFS) software package in MATLAB [2]. The case in Fig. 1(a) was obtained at $B_{\omega} = \Delta \omega$ resulting in contrast decay near the pulse spectrum borders. The optimal case $B_{\omega} = 2\Delta \omega$ is shown Fig. 1(b) that demonstrates maximized contrast of spectral modulation.

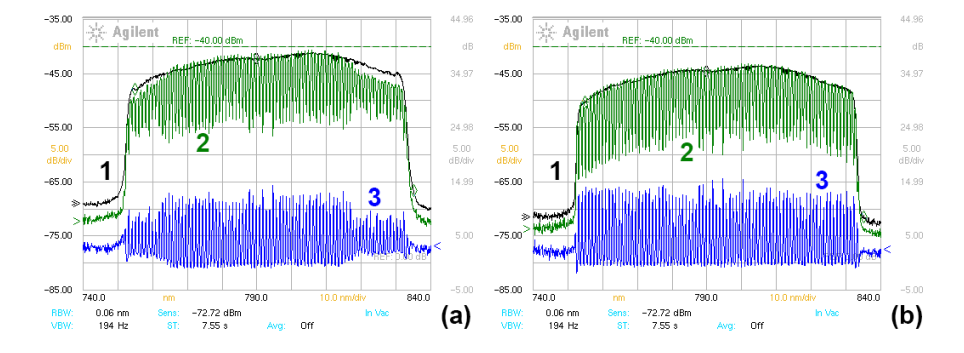


Figure 1: 167-bit periodic binary modulation of 12-fs pulse spectrum: (a) minimum modulation bandwidth $B_{\omega}=\Delta\omega$; (b) optimal modulation bandwidth $B_{\omega}=2\Delta\omega$. 1 — reference spectrum without modulation, AOPDF transmission window $\Delta\lambda=80$ nm; 2 — output spectrum with the modulation pitch of $\delta\lambda=0.48$ nm; 3 — modulation depth.

- [1] K.B. Yushkov, V.Ya. Molchanov, and E.A. Khazanov "Uncertainty relation in broadband laser pulse shaping", in Physics-Uspekhi 64, 828–835 (2021).
- [2] K.B. Yushkov, et al. "Dispersive Fourier Synthesis: Universal method and MATLAB tool for acousto-optic arbitrary femtosecond laser pulse shaping", in Optics and Laser Technology, preprint (2025).

²A.V. Gaponov-Grekhov Institute of Applied Physics, Russian Academy of Sciences, 46, Ulyanova str., 603950 Nizhny Novgorod, Russia

^{*}konstantin.yushkov@misis.ru

Towards energetic single-cycle pulses with postcompression of the SYLOS lasers

Szabolcs Tóth,¹ Roland S. Nagymihály,¹ János Csontos,¹ Levente Lehotai,¹ Imre Seres,¹ Viktor Pajer¹, Károly Osvay,² and Ádám Börzsönyi¹

¹ELI ALPS Research Institute, Wolfgang Sandner u. 3, H-6728 Szeged, Hungary

Abstract

Results on the post-compression studies performed on the SEA, SYLOS2 and SYLOS3 lasers of ELI ALPS are presented at energy levels ranging from 12 to 100 mJ with input pulse durations around 10 fs and repetition rates of 10 Hz and 1 kHz.

Introduction

Generation of energetic isolated attosecond pulses from surface high harmonics requires well controlled single-cycle pulses with reasonably high energies in the range of tens of millijoules. Reaching such laser pulses is possible through post-compression of already sub-15 fs pulses with well controlled spectral phase at the input using a single thin dielectric plate as the nonlinear medium [1]. Modulations in the spatial intensity distribution are critical to avoid for controlled utilization of self-phase modulation along the beam cross-section. The SYLOS lasers, all based on noncollinear optical parametric chirped pulse amplification (OPCPA), are in the forefront of few-cycle generation technology [2], and are ideal candidates for reaching the single-cycle duration with multi-TW peak power at the output via post-compression.

Results

Here we present results on the spectral broadening of the SEA and SYLOS2 lasers by using the single thin plate concept, through which spectra corresponding to sub-4 and sub-5 fs Fourier transform limited (FTL) duration were achieved. The effect of spatial filtering was also investigated before the nonlinear interaction, which led to high quality 3.9 fs pulses in the case of the SEA laser after compression in combination with an energy of 15 mJ.

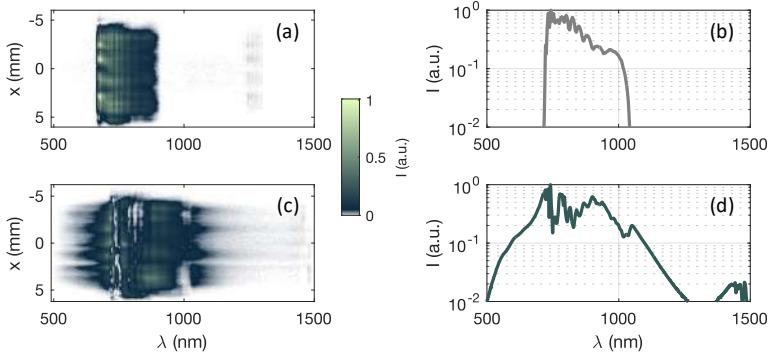


Fig. 1. Spatially resolved spectrum without (a) and with broadening (c) in a single fused silica plate at 100 mJ energy. The corresponding spatially integrated spectra are shown in (b) and (d).

Recently, the output pulses of SYLOS3 were also spectrally broadened in different nonlinear media. We tested the single thin plate concept here, as well, on top of which we also investigated the application of a gas cell with helium, and also broadening in air. The effects of spatial inhomogeneities were investigated by measuring the spatially resolved spectrum for the different nonlinear media. Our results are paving the way towards 10 TW single-cycle pulse generation via post-compression at 1 kHz repetition rate.

- [1] Sz. Toth et al, Opt. Lett. 48, 57-60 (2023).
- [2] Sz. Toth et al, J. Phys. Photonics 2 (2020) 045003.

²National Laser-initiated Transmutation Laboratory, University of Szeged, Dugonics tér 13, 6720 Szeged, Hungary *roland.nagymihaly@eli-alps.hu

Spatio-spectral characterization of few-cycle lasers from visible to mid-infrared

Roland S. Nagymihály,¹ Levente Lehotai,¹ Miguel Miranda,² Bálint Kiss,¹ Rajaram Shrestha,¹ Viktor Pajer¹, János Csontos,¹ Szabolcs Tóth,¹ Imre Seres,¹ Péter Jójárt,¹ Paulo T. Guerreiro,² Matias Charrut,² Eric Cormier,^{1,3} Rosa Romero,² and Ádám Börzsönyi¹

Abstract

We present results on measuring the spatio-spectral structure of the few-cycle pulses generated by Ti:Sa and OPCPA-based laser systems of ELI ALPS, where spatially resolved Fourier transform spectroscopy was extensively utilized in spectral ranges from 650 to 4000 nm.

Introduction

Proper control of few-cycle pulses for experiments with any type of target requires the knowledge on the behavior of the different frequency components within their extensive spectral bandwidth. Furthermore, tracing back distortions to any part of the laser system is not enough to accomplish in the spectral or temporal domain, but it must be spatially resolved, as well. Spatially resolved Fourier transform spectroscopy has the advantage, that the pulses do not have to be compressed for the measurement of the complete spatio-spectral characteristics, thus it can be applied in practically any part of the laser system. Several different implementations have been introduced on this technique in the last decade in the near infrared spectral region [1-3]. Here we present a comprehensive analysis on different laser systems with the ICE [1] and the INSIGHT [3] methods.

Results

Ultrabroadband pulses from the ORPHEUS optical parametric chirped pulse amplification (OPCPA) frontend, furthermore the SYLOS2 and SYLOS3 OPCPA systems were measured by both ICE and INSIGHT methods, where the spatio-spectral optimization for seeding a Ti:Sa amplifier chain, and for experiments were achieved successfully, in the spectral ranges of 680-1050 nm and 740-1100 nm, respectively. By using a mid-infrared CCD detector, we were also able to utilize the ICE technique to characterize four-cycle pulses of our mid-infrared OPCPA system around the central wavelength of 3200 nm (Fig. 1).

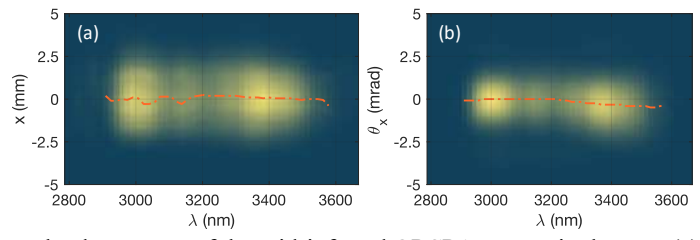


Fig. 1. Spatially resolved spectrum of the mid-infrared OPCPA system in the near (a) and far field (b).

Implementing a SWIR CCD as a detector in the ICE device is also in progress, by which pulses of the HR laser systems after multiple stages of post-compression will be investigated in the spectral range of 600 and 1300 nm.

This work paves the way towards the general understanding of spatio-spectral optimization of different few-cycle laser systems, while the experimental specific effects are also addressed.

- [1] M. Miranda et al, Opt. Lett. 39, 5142-5145 (2014).
- [2] G. Pariente et al, Nat. Photon. 10, 547-53 (2016).
- [3] A. Borot et al, Opt. Express 26, 26444-26461 (2018).

¹ELI ALPS Research Institute, Wolfgang Sandner u. 3, H-6728 Szeged, Hungary

²Sphere Ultrafast Photonics, Rua do Campo Alegre, n.º 1021, Edificio FC6 4169-007 Porto, Portugal

³Laboratoire Photonique Numérique et Nanosciences (LP2N), UMR 5298, CNRS-IOGS-Université Bordeaux, 33400 Talence, France

^{*}roland.nagymihaly@eli-alps.hu

Dielectric grating technology for high power ultrashort laser source

Samy Ferhat¹, Doriane Jussey², Guillaume Croizier¹, Justin Rouxel², Raphael Guillemet², Sandrine Ricaud¹, Olivier Chalus¹, Mane-Si Laure Lee², Brigitte Loiseaux²

1. Thales LAS France, 2 Avenue Gay-Lussac, 78990 Elancourt, France

2. Thales Research & Technology, 1 Avenue Augustin Fresnel, 91767 Palaiseau, France

Abstract: High peak power lasers require compression under vacuum. Combined with high average power, a thermal issue arose from the absorption of gold gratings. In order to limit this absorption and conserve ultrashort pulses we propose a new dielectric gratings type allowing in the plane compressor design.

High-power lasers operating at high operation rates based on gold-coated grating compressors are limited by the absorption of the gold coating [1,2] that leads to heating and deformation of gratings under vacuum. An alternative to decrease absorption is the use of all-dielectric gratings that consists in dielectric ridges on a reflective dielectric multilayer stack. Such approach enables broadband acceptance for the compression step of the chirp pulse amplification [3] of high power femtosecond pulses. Dielectric gratings have been reported but can have a limited spectral bandwidth and requires an out-of-the plane layout for the associated pulse compressor design, resulting into a more complex and higher volume architecture as compared to in-plane layout. In this paper, we propose all-dielectric compressors for high power ultrashort laser source, enabling both high broadband efficiency (> 90% efficiency on spectral bandwidth>100nm centered at 800nm) and high laser induced damage threshold (LIDT). Two architectures have been proposed with grating periods of 610nm and 560nm, enabling operation at 36° and 55° incidence angle in TE polarization. As an example, the theoretical efficiency of the -1st diffraction order of the designed 560nm-period grating, given in Fig. 1a, shows a bandwidth larger than 100nm for 90% efficiency computed by RCWA (Rigorous Coupled Wave Analysis). Several components with different ridge profiles and reflective stacks are simulated in terms of efficiency and electric field intensity distribution, and manufactured by nanoimprint lithography and high-density plasma etching on a multilayer dielectric reflective stack. A picture of the 15mm x 15mm gratings manufactured on a 2 inch wafer is given in Fig. 1b. On Fig. 1c, the Scanning Electron Microscope (SEM) image of a FIB (Focused Ion Beam) cut of the grating shows the multilayer dielectric stack and the ridges of the gratings.

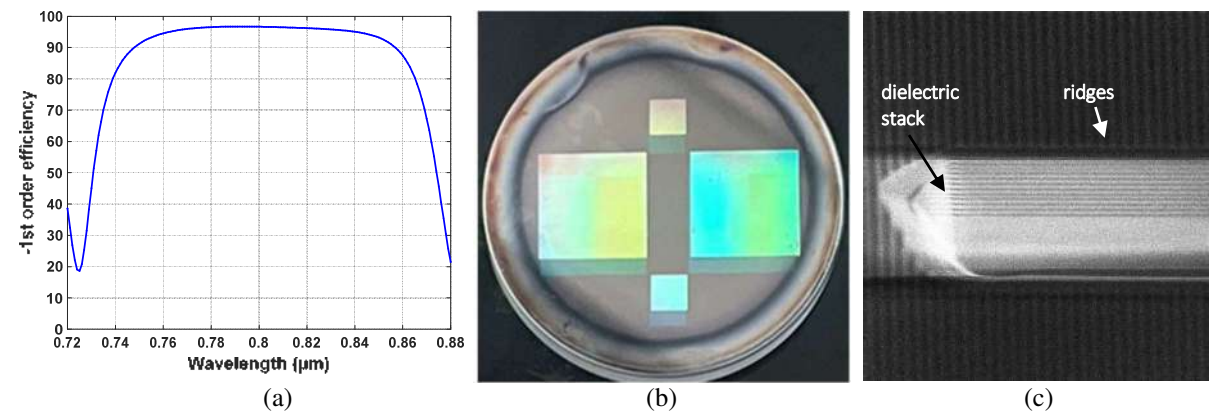


Fig. 1 a) Simulated -1st order diffraction efficiency for a large spectral bandwidth of dielectric grating with a 560nm period, under TE polarisation. b) Picture of one of the manufactured dielectric Grating, c) SEM image of the FIB cut of the grating.

Spectral measurement of -1st order efficiency at various grating angle of incidence and losses caused by scattering have been experimentally measured using a broadband source (GECCO Oscillator) with a pulse duration of 15 fs in the nanojoule range at 800nm at a repetition rate of 80 MHz. In plane configuration at 36° for a period of 610 nm and 55° for a period of 560nm (which allows the closest configuration to standard gold grating compressor layout) can be used for compressor alignment. Efficiencies in between 88% and 91% have been measured for the different gratings geometries. The best diffraction efficiency is 91% based on a 97% reflectivity dielectric stack for a large spectral acceptance bandwidth of 110nm (FWHM). A laser damage threshold of 200 mJ/cm² have been estimated with 15 mJ, 30fs 10Hz compressed pulses. We can expect to reach at least 94% by improving the reflective stack and fine-tuning the ridges profile.

References

[1] O. Loebich, "The optical properties of gold," Gold Bull. 5, 2–10 (1972).

[2] V. Leroux, S.W. Jolly, M. Schnepp, T. Eichner, S. Jalas, M. Kirchen, P. Messner, C. Werle, P. Winkler, A.R. Maier,. "Wavefront degradation of a 200 TW laser from heat-induced deformation of in-vacuum compressor gratings," Opt. Express 26, 13061-13071 (2018). [3] D. Strickland, G. Mourou, "Compression of amplified chirped optical pulses", Optics Communications, vol. 56, no. 3, pp. 219–221 (1985).

Compact 60 mJ Ho:YLF amplifier system seeded with a robust Yb:fiber-driven OPA

S. Reuter, P. Merkl, J. Schauss, S. Starosielec, M. J. Prandolini, M. Schulz, M. Bock, U. Griebner, and R. Riedel,*

¹Class 5 Photonics GmbH, Notkestrasse 85, D-22607 Hamburg, Germany

²Max-Born-Institut für Nichtlineare Optik und Kurzzeitspektrosophie, Max-Born-Str. 2A, 12489 Berlin, Germany *robert.riedel@class5photonics.com

Abstract

A compact Ho:YLF amplifier system delivering 60 mJ pulse energy for pumping MID-IR OPCPAs between $3-11~\mu m$ is presented, implementing a microjoule-level Yb:fiber-driven OPA as a front-end reducing the footprint, complexity and optimizing bifurcation dynamics.

A high-energy, kHz-repetition rate amplifier with picosecond pulses at 2 μm is ideal for efficiently pumping optical parametric chirped-pulse amplifiers (OPCPAs) with multi-millijoule pulse energies in the 3 –11 μm range. Such drivers allow the generation of table-top, high-flux femtosecond X-ray pulses at photon energies around 8 keV [1]. Recently, a 22 mJ regenerative amplifier has been demonstrated, using an Yb:KGW regenerative amplifier with 2.05 μJ DFG and OPA as front-end [2]. Despite the relatively compact architecture of the Ho:YLF amplifiers, all systems realized to date depend on highly complex front-end seed designs, involving, for example, either Er:fiber and supercontinuum [1] or 3-stage parametric amplifiers driven by Yb:KGW regenerative amplifiers [2]. We present a compact high-energy picosecond Ho:YLF amplifier system designed to efficiently pump MID-IR OPCPA stages at 5 μm . Our system achieves pulse energies exceeding 60 mJ, and is seeded by a robust OPA driven by an Yb:fiber laser (Fig. 1), allowing the reduction of the overall system to a footprint of < 2m².

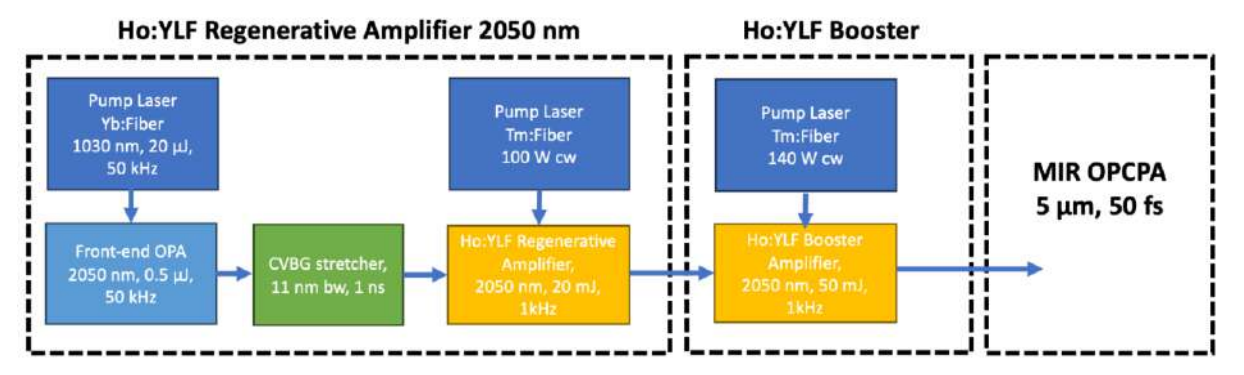


Figure 1: Schematic of the compact Ho:YLF amplifier system.

As a front-end, the system uses a compact medical-grade Yb:fiber laser operating at 1030 nm, 20 μ J and 50 kHz. It pumps a single-stage OPA system delivering 2.7 μ J at 2050 nm. The front-end operates robustly with a power instability below 0.6%. The seed pulses are stretched to 1 ns in a chirped volume Bragg grating (CVBG) with 11 nm spectral bandwidth, resulting in 0.5 μ J in-band seed energy. The regenerative amplifier follows the ring cavity architecture of [1], pumped by a 100 W continuous-wave (cw) Tm:fiber laser. We were able to achieve a pulse energy of 18.5 mJ with an excellent pulse-to-pulse instability of 0.3%. The spectral bandwidth of 2.8 nm supports a Fourier-limited pulse duration of 1.9 ps, and the beam quality is $M^2 < 1.15$ in both axes. Further power scaling is achieved via additional booster amplifier stages. Adding two booster stages, pumped by 135 W from Tm:fiber pump lasers, we could achieve more than 60 mJ pulse energy at 1 kHz repetition rate. Our laser system aims for exceeding 20 GW peak power, approaching the self-focusing limit, which would also allow for air filamentation studies and related atmospheric phenomena.

- [1] Koç, A., et al. Compact high-flux hard X-ray source driven by femtosecond mid-infrared pulses at a 1 kHz repetition rate. Opt. Lett. 46(2), 210–213 (2021).
- [2] Bock, M., et al., Ho:YLF regenerative amplifier delivering 22 mJ, 2.0 ps pulses at a 1 kHz repetition rate. Opt. Express 32, 23499-23509 (2024).

High-Contrast Broadband Seed Generation for Vulcan 20-20

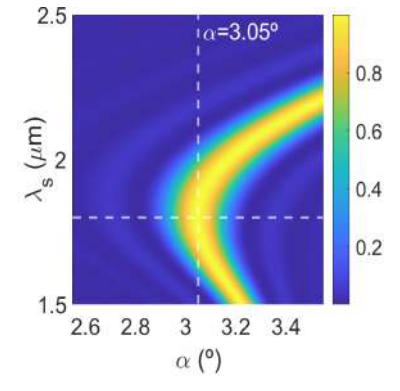
Gonçalo A. L. Vaz,^{1,*}, Pedro B. M. A. Oliveira,^{2,*}, Helder M. Crespo,² and Hugo F. A. Pires,¹

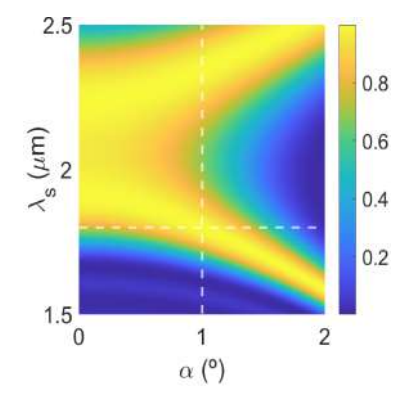
Abstract

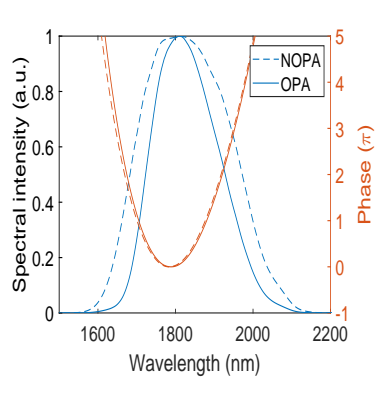
We conducted simulations of a novel approach for the generation of a broadband seed for the upcoming Vulcan 20 PW (400 J, 20 fs) beamline based on amplification in the mid-infrared region followed by second-harmonic generation for improved contrast, while retaining a relatively simple and compact setup.

For several decades, the Vulcan laser at the Rutherford Appleton laboratory in the United Kingdom stood as a vital tool for international users, supporting experimental endeavors in fields such as astrophysics, fast electron generation and transport, and particle acceleration. In 2023, an ambitious upgrade project was formally announced - Vulcan 20-20 - aiming to reach 20 PW (400 J, 20 fs)[1]. To seed the main 20 PW beamline of Vulcan 20-20, we require a very high-contrast broadband (within 850-1050 nm) pulse capable of supporting sub-20 fs durations.

We propose an approach for the front-end of Vulcan 20-20 starting with a laser delivering 2 mJ, 500 fs pulses at 1030 nm, where a fraction is used for supercontinuum (SC) generation down to 1700-2100 nm. Due to the intrinsic low energy of SC generation, the pulses are amplified by optical parametric amplification (OPA) in a mid-infrared nonlinear crystal (HGS), followed by second-harmonic (SH) generation to obtain the intended bandwidth. We performed simulations with the Chi23D code[2] to evaluate the performance of the system. Figure 1 depicts the phase matching curves and the resulting simulated bandwidth from the amplification stages, consisting of a noncollinear OPA (NOPA) followed by a quasi-collinear OPA. The chained stages (NOPA+OPA+SH) contribute to a higher pulse contrast, as the conversion efficiency of the pre- and post-pulses will be significantly lower than that of the main pulse due to the χ^2 nature of these processes. Additionally, it allows pumping with the driver rather than its SH, as is common in many facilities using BBO-based OPAs, making it more efficient. This approach avoids reliance on the idler, preventing spatial chirp.







- (a) Phase matching of the NOPA in a 1.5 mm HGS crystal.
- (b) Phase matching of the OPA in a 0.6 mm HGS crystal.
- (c) Simulated amplification bandwidth

Figure 1: Simulation of chained amplification stages in HGS.

- [1] Buck, S., Oliveira, P., Angelides, T., & Galimberti, M. (2024). A Review of Optical Parametric Amplification at the Vulcan Laser Facility. Photonics, 11(6), 495.
- [2] Lang, T., Harth, A., Matyschok, J., Binhammer, T., Schultze, M., & Morgner, U. (2013). Impact of temporal, spatial and cascaded effects on the pulse formation in ultra-broadband parametric amplifiers. Optics Express, 21(1), 949.

Group of Lasers and Plasmas/Instituto de Plasmas e Fusão Nuclear, Instituto Superior Técnico da Universidade de Lisboa, Av. Rovisco Pais 1049-001 Lisboa, Portugal

² Central Laser Facility, Science and Technology Facilities Council, Rutherford Appleton Laboratory, Harwell Science and Innovation Campus, OX11 0QX Didcot, United Kingdom

goncalovaz98@tecnico.ulisboa.pt

Few-cycle, mJ-level 3 µm source driven by 1030 nm pulses

Gonçalo A. L. Vaz,^{1,*} Hugo F. A. Pires,¹ and Gonçalo N. M. F. Figueira¹

¹Group of Lasers and Plasmas/Instituto de Plasmas e Fusão Nuclear, Instituto Superior Técnico, Universidade de Lisboa, Av. Rovisco Pais 1049-001 Lisbon, Portugal

Abstract

We describe the ongoing development of a high-energy, ultrafast mid-infrared laser, designed for 5 mJ, 85 fs operation at 3 μ m. This system is based on multi-stage parametric amplification seeded by a 100 kHz, 1030 nm Yb-based system.

Mid-infrared ultrafast lasers play a crucial role in modern science, as they provide access to molecular vibrational and rotational modes. The emergence of high-energy ultrafast sources drove the growth of applications such as harmonic generation and attosecond pulse generation[1]. One of the most well established methods of producing high-energy, mJ-level mid-infrared sources is Optical Parametric Chirped Pulse Amplification (OPCPA) [2, 3, 4, 5].

We present the current stage of such a source, driven by a high-repetition-rate Yb system. Our Yb driver seeds a comercial OPCPA enclosure generating CEP stable 65 μ J, 40 fs, 3 μ m pulses. The output will then be amplified up to 5 mJ, 85 fs, 10 Hz in a custom OPCPA consisting of three parametric amplifiers pumped by a home-built Chirped Pulse Amplification (CPA) system, seeded by the Yb driver, see Fig.1. We lower the repetition rate of the driver to 10 Hz due to limitations on our CPA system. Operation > kHz is feasible with thin-disk laser technologies, however, our approach allows the implementation of a pre-existing CPA system.

We discuss the architecture of this source and its potential for driving next generation mid-infrared applications such as high harmonic generation, attosecond science and particle acceleration.

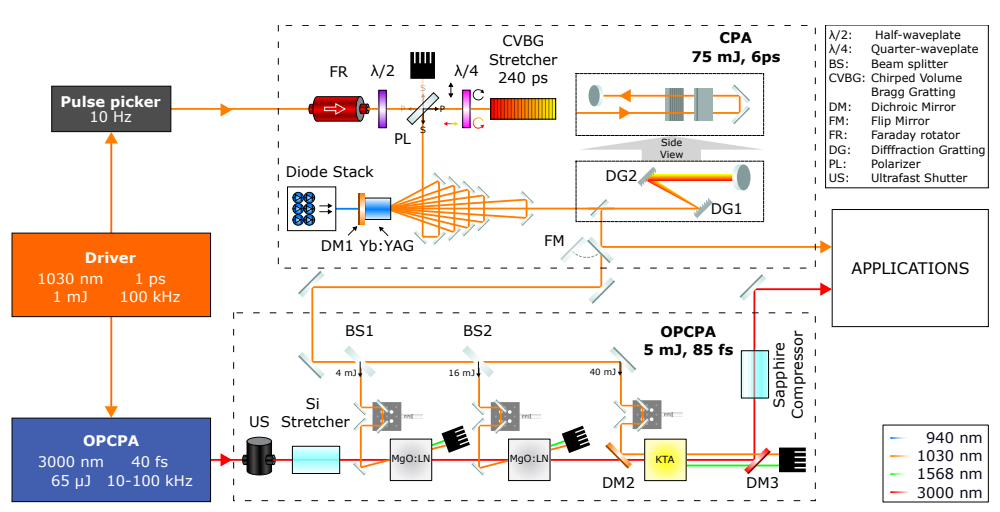


Figure 1: Design of the mJ-level 3 µm amplifier.

- [1] Pires, H., et al., "Ultrashort pulse generation in the mid-IR", Progress in Quantum Electronics 43, 1–30 (2015).
- [2] Andriukaitis, G. et al., "90 GW peak power few-cycle mid-infrared pulses from an optical parametric amplifier", Optics Letters 36, 2755 (2011).
- [3] T. Popmintchev *et al.*, "Bright coherent ultrahigh harmonics in the keV x-ray regime from mid-infrared femtosecond lasers", Science 336, 1287–1291 (2012).
- [4] J. Alves et al., "Multi-mJ scaling of 5-optical cycle, 3 µm OPCPA", Photonics 8, 503 (2021).
- [5] J. H. Buss *et al.*, "Mid-infrared optical parametric chirped-pulse amplifier at 50 W and 38 fs pumped by a high-power Yb-InnoSlab platform," Opt. Express 32, 36185-36192 (2024).

 $^{^*}$ goncalovaz98@tecnico.ulisboa.pt

Effect of Plasma Mirror Substrate and Coating Material on the Resultant Temporal Contrast of the Astra-Gemini Laser

E. Asquith^{1,*}, G.G. Scott¹, M. Savage¹, C. Baird¹, N. Bourgeois¹, Y. Tang¹, O. Chekhlov ¹, R. Timmis², H. Huddleston³, B. Dromey³, M. Yeung³, R. Pattathil¹ and S. Hawkes¹

- 1 Central Laser Facility, STFC, Rutherford Appleton Laboratory, Harwell Campus, Didcot
- ² Department of Physics, University of Oxford | ³ School of Mathematics and Physics, Queens University Belfast
- *eleanor.asquith@stfc.ac.uk

Abstract

The effect of a double plasma mirror system (DPM) on the temporal contrast of the Astra-Gemini laser is investigated. Variations in DPM coatings affected the temporal profile, revealing distinct regions of performance. Dependence of the temporal profile on coating configuration in high-intensity regions is noted, implying PM coating degradation.

Diagnosing the temporal contrast of short pulse laser systems is crucial for conducting well understood and controlled laser-plasma interactions. While multiple methods exist for temporal cleaning, plasma mirrors (PMs) remain popular due to their versatility and capacity to suppress amplified spontaneous emission and pre-pulses from the temporal profile. It is therefore essential to identify how PM coating and substrate type impact the quality of temporal cleaning. This work explores a DPM configuration on the Astra-Gemini laser, a petawatt-class Ti:S laser at the CLF [1]. A Sequoia autocorrelator [2] measured the temporal contrast for various DPM configurations, investigating BK7 and Fused Silica substrates with uncoated and anti-reflective (AR) coatings. No significant difference in performance was found between substrate types. However, different coating configurations showed distinct behavior, with two identifiable regions (Fig. 1). At t < -4 ps, the configuration with two AR mirrors (AR/AR) exhibits a contrast that is an order of magnitude higher than for uncoated/AR. As the laser intensity on the PM increases, a step-like change in the AR/AR contrast profile is observed, occurring at $t \approx -4$ ps. After this point, AR/AR and uncoated/AR have similar profiles, implying a degradation of the first AR coating in the AR/AR set up. This has widespread implications for facilities fielding PMs for temporal cleaning, but more data is needed to explore additional features in detail. Further characterisation of the rising edge contrast will be presented, following a scheduled Astra-Gemini experiment in July, where single shot contrast diagnostics will be exploited to gain deeper insight into these features.

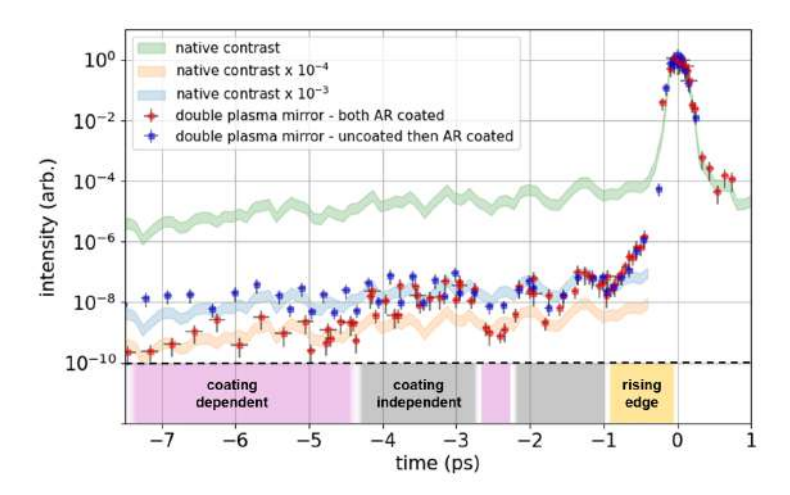


Figure 1: Temporal contrast of the Astra-Gemini laser [1] using DPMs as diagnosed by a Sequoia autocorrelator [2]. (Green) The native Gemini temporal contrast. (Blue, Orange) The native contrast multiplied by a constant $(10^{-3}$ and 10^{-4} respectively) to aid in presenting PM measurements. (Dark blue) DPM set up where both mirrors have an AR coating. (Red) DPMs where the first is uncoated and the second is AR coated. (Bottom) Different operating regimes of the PMs. (Pink) Coating dependent. (Grey) Coating independent. (Yellow) Rising edge.

- [1] CLF Astra-Gemini, [Online]. Available: https://www.clf.stfc.ac.uk/Pages/The-Astra-Gemini-Facility.aspx
- [2] Amplitude Technologies, "Sequoia: Third-order autocorrelator", Amplitude Technologies, [Online]. Available: [https://amplitude-laser.com/products/femtosecond-lasers/instrumentation-lasers-femtosecondes/sequoia/]

Spatiotemporal characterization of ultrafast pulses using a dispersive interferometer

Yeong Gyu Kim^{1,*}, Byungjoo Kim¹, Dohyun Kim¹, Jiyeon Choi¹, and Sanghoon Ahn¹

¹Department of Laser & Electron Beam, Korea Institute of Machinery & Materials, 34103, 156 Gajeongbuk-Ro, Yuseong-Gu, Daejeon, Korea *ygkim@kimm.re.kr

Abstract

This paper presents a method for measuring spatiotemporal profiles of ultrafast pulses. By introducing a dispersive material in one arm of an interferometer, frequency-resolved wavefront and intensity are measured. To validate the proposed method, radial group delay, induced by two spherical singlets, was experimentally measured, showing excellent agreement with theory.

Introduction and Method

Spatiotemporal couplings of ultrafast pulses result in enlarged focal spot sizes, extended pulse durations, and distorted wavefronts, ultimately reducing the spatiotemporal peak intensities. Accurate characterization of spatiotemporal couplings is therefore essential for optimizing ultrafast laser applications. Existing measurement methods often face difficulties when handling pulses with relatively narrow spectrums and long pulse durations [1-3]. To address this, we propose a high-resolution spatiospectral measurement method utilizing a Michelson interferometer with dispersive material placed in one arm. The dispersive material temporally elongates the laser pulses, causing only specific wavelengths, determined by the length difference between the dispersive arm and the reference arm, to temporally overlap at the camera. Consequently, interference fringes for these matched wavelengths can be precisely measured, yielding frequency-resolved wavefront and intensity information. By systematically varying the length difference between two arms, spatiospectral properties of laser pulses is obtained. Finally, performing an inverse Fourier transform along the frequency axis at each spatial position then successfully reconstructs the spatiotemporal profile of laser pulses.

Experimental Results and Validation

To experimentally validate the proposed method, radial group delay was induced using two plano-convex singlet lenses. Since the radial group delay induced by the lenses can be theoretically calculated [4], we compared these calculations with our experimental measurements to assess accuracy. We used a BK-7 material as the dispersive material and determined the appropriate wavelengths by calculating arrival times based on wavelength-dependent group velocities. By adjusting the path length of the dispersive arm, the wavelengths matching the reference arm were systematically varied. The measured radial group delay closely matched the theoretical predictions. Additionally, integrating the frequency-resolved intensity spatially yielded a spectral profile in excellent agreement with independent measurements obtained using a spectrometer. Furthermore, the spatial beam profiles obtained by integrating frequency-resolved intensities along the frequency axis agreed well with beam profiles directly measured by a camera. These results confirm that our proposed measurement method accurately characterizes ultrafast pulses, even those with narrow spectral bandwidths.

- [1] P. Gabolde and R. Trebino "Single-shot measurement of the full spatio-temporal field of ultrashort pulses with multispectral digital holography," Opt. Express 14, 11460-11467 (2006).
- [2] A. Jeandet, A. Borot, K. Nakamura, S. W. Jolly, A. J. Gonsalves, C. Tóth, C. H. Mao, W. P. Leemans, and F. Quéré, "Spatio-temporal structure of a petawatt femtosecond laser beam," J. Phys. Photonics 1, 035001 (2019).
- [3] Y. G. Kim, J. I. Kim, J. W. Yoon, J. H. Sung, S. K. Lee, and C. H. Nam, "Single-shot spatiotemporal characterization of a multi-PW laser using a multispectral wavefront sensing method," Opt. Express **29**, 19506-19514 (2021).
- [4] J.-C. Diels and W. Rudolph, Ultrashort Laser Pulse Phenomena, 2nd ed. (Science Direct, 2006).

Impact of imperfect surface and imperfect groove pattern of compressor diffraction gratings on laser pulse focal intensity

Efim Khazanov

Gaponov-Grekhov Institute of Applied Physics of the Russian Academy of Sciences, 46 Ulyanov St, N.Novgorod, Russia

efimkhazanov@gmail.com

Abstract

For plane and out-of-plane compressors, analytical expressions for the focal intensity are derived for arbitrary surface profiles and arbitrary groove patterns of all gratings. Quality requirements for the surface of the optics used to write the grating are several times higher than quality requirements for the surface of the grating.

Compressor diffraction gratings introduce two types of space-time coupling: amplitude and phase ones. The amplitude coupling is related to the spatial dependence of the reflection coefficient, as well as to beam clipping on the gratings, if any. In this paper, we will limit our study to the phase space-time coupling caused by two reasons. The first one is an imperfectly flat grating surface. The second, much less studied reason for the phase space-time coupling is the groove pattern imperfection: non-equidistance and non-parallelism. We will restrict ourselves to four most interesting cases – plane Treacy compressors with four or two gratings (4TC and 2TC) and out-of-plane Littrow compressor with four or two gratings (4LC and 2LC). In the Littrow compressor incident angle equals the Littrow angle.

The focal intensity (Strehl ratio St) is product of two multipliers: $St = St_{gr}St_{wr}$, where St_{gr} depends on the grating surface profile and St_{wr} depends on the groove pattern imperfection, which origins from nonperfect optics used for grating writing. In most cases, the degradation of St_{gr} is much more than St_{gr} , i.e. the requirements for the quality of the surface of the optics used for the gratings writing are several times higher than the requirements for the quality of the grating surface, see Fig.1. Note the difference between rms of grating surface H on Fig.1a and rms of surface of optics used for gratings writing h on Fig.1b. By rotating the gratings by 180 degrees around the normal and exchanging them it is possible to find an optimal variant maximizing St.

The influence of all imperfections of all compressor gratings on St is described by one function $\Psi(x,y)$ that has the sense of the effective wavefront. The decrease in St is proportional to the squared rms of this function. The $\Psi(x,y)$ function is determined by the total distortions of gratings G2 and G3 for the four-grating compressor and of G1 for the two-grating compressor, with the St decrease in the latter being much smaller, which is its undoubted advantage. In all cases the reduction of the pulse spectrum width $\Delta\omega$ proportionally reduces the requirements for the rms of both the surface of the gratings and the surface of the optics used for their writing.

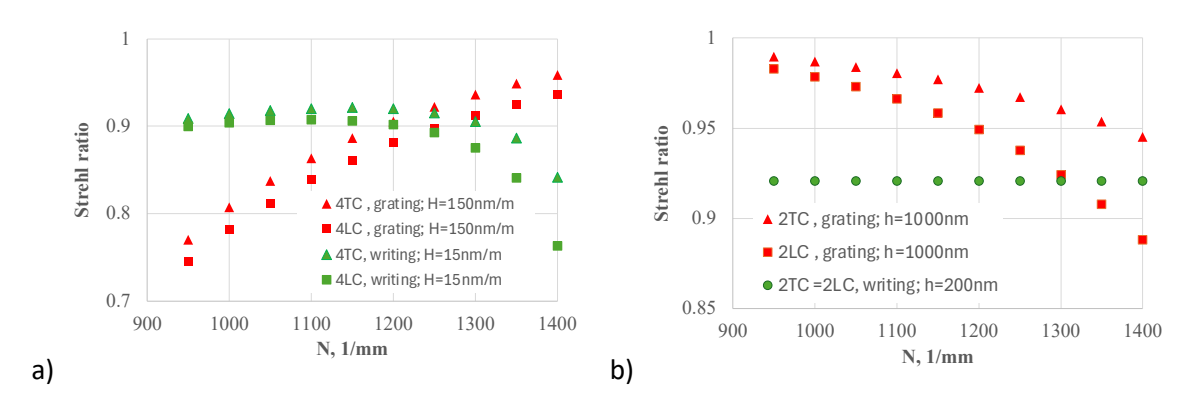


Fig. 1. Strehl ratio St vs groove density N. $St_{gr}(N)$ (red) and $St_{wr}(N)$ (green) for 4TC and 4LC (a) and for 4TC, 2TC and 2LC (b). For clarity, curves for $St_{gr}(N)$ are plotted for larger values of distortion than for $St_{wr}(N)$: a factor of 10 for (a) and a factor of 5 for (b).

Impact of Vacuum Conditions on Wavefront Stability in the SYLOS2 Laser System

J. CSONTOS,^{1,*} Sz. Toth¹, L. Toth¹, I. Dora¹, D. Abt¹, P. Prasannan Geetha¹, B. Kovalovszki¹, T. Somoskoi¹, B. Nagyilles¹, B. Farkas¹, Z. Diveki¹, A. Körmöczi¹ and A. Börzsönyi¹

¹ELI ALPS, Wolfgang Sandner utca 3., H-6728 Szeged, Hungary *janos.csontos@eli-alsp.hu

Abstract

We investigated the impact of vacuum conditions on the SYLOS2 laser system's. Placing the beam expansion and pre-compression stages in vacuum significantly improved wavefront quality by reducing air-induced instabilities. These findings support the development of a dedicated vacuum chamber with enhanced vibration isolation, optimizing beamline performance for ultrafast applications.

Introduction

The Extreme Light Infrastructure – Attosecond Light Pulse Source (ELI ALPS) is one of the three ELI pillars, located in Szeged, Hungary. A key component of ELI ALPS is the SYLOS system [1, 2], a NOPCPA-based single-cycle laser system that serves as the primary driver for six secondary sources, all connected via a vacuum beam transport system. These secondary sources, powered by the SYLOS systems, generate attosecond pulses and laser-accelerated particles, including electrons, protons, deuterons, and neutrons.

At the end of the laser system, the beam is expanded by a telescope operating under atmospheric conditions to mitigate nonlinear effects. This section of the system is enclosed to minimize airflow; however, residual heat still induces air movement under the covers. Despite extensive efforts over the past five years to minimize the impact of airflow, its effects on wavefront stability and pointing fluctuations remain noticeable.

Results

A recent experiment was conducted to evaluate the effects of placing the back-end section, including the beam expansion telescope and pre-compressor of SYLOS2, in a vacuum environment. The vacuum chamber was connected to the beam transport system to maintain vacuum integrity during laser beam propagation. The output beam was directed into the SYLOS Long Beamline, where its wavefront parameters were analyzed. Two sets of measurements were performed to assess the influence of air on beam quality. The first dataset was collected under the original configuration, where beam expansion and pre-compression occurred under atmospheric conditions. The second dataset was obtained with the back-end section placed in vacuum. The results, shown in Figure 1, illustrate the comparison of wavefront parameters under air and vacuum conditions, represented by two key Zernike polynomials.

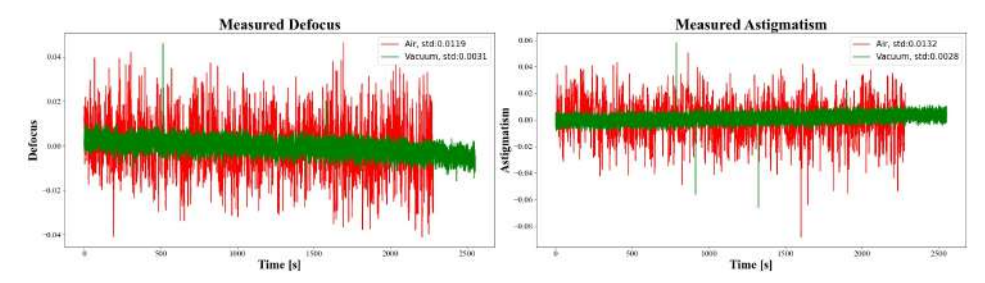


Figure 1. Measured defocus and 0° astigmatism under air (red) and vacuum (green) conditions

Our findings indicate that placing the large-beam-size section of the system under vacuum one can achieve more than one order of improvement in the defocus and astigmatism quality while higher order Zernike polynomials were improved by a factor of two due to the lack of refractive index changes by the air turbulence under vacuum.

- [1] R. Budriunas et al., "53 W average power CEP-stabilized OPCPA system delivering 5.5 TW few cycle pulses at 1 kHz repetition rate", Opt. Express 25(5), 5797-5806 (2017)
- [2] S. Toth et al., "SYLOS lasers the frontier of few-cycle, multi-TW, kHz lasers for ultrafast applications at extreme light infrastructure attosecond light pulse source", J. Phys. Photonics 2 045003 (2020)

Tunable sub-2 fs ultraviolet pulse generation

M. F. Galán, 1,2,* E. C. Jarque, 1,2 J. San Roman, 1,2 C. Brahms, 3 and J. C. Travers 3

¹Grupo de Investigación en Aplicaciones del Láser y Fotónica, Universidad de Salamanca, Salamanca 37008, Spain ²Unidad de Excelencia en Luz y Materia Estructuradas (LUMES), Universidad de Salamanca, Salamanca 37008, Spain ³School of Engineering and Physical Sciences, Heriot-Watt University, Edinburgh EH14 4AS, United Kingdom *marinafergal@usal.es

Abstract

We demonstrate the generation of microjoule-level and widely tunable sub-2 fs ultraviolet pulses through resonant dispersive wave acceleration in capillary fibres with individually placed pressure control points.

Bright, wavelength-tunable few-cycle ultraviolet pulses promise to break new ground in ultrafast science, but their generation is still extremely challenging. Resonant dispersive wave (RDW) emission in gas-filled capillary fibres offers great potential to generate continuously tunable pulses from the deep to the vacuum ultraviolet [1], with microjoule-level energies, and few-femtosecond durations [2]. However, the resonant nature of the emission process limits the spectral bandwidth of the RDW, hindering the generation of pulses shorter than 2-3 fs. In this work, we numerically demonstrate a novel concept for the generation of clean sub-2 fs RDWs which relies on precise dispersion engineering through an intermediate pressure control point along the capillary. Inspired by earlier studies in tapered fibres [3,4], the creation of a double decreasing pressure gradient inside the fibre (Fig. la) produces an acceleration of the RDW and allows a re-collision with its parent self-compressing soliton. The strong nonlinear interaction between both pulses through cross-phase modulation results in extreme spectral broadening of the RDW towards higher frequencies (Fig. 1b). The final decreasing pressure enables dispersionfree delivery of the RDW directly to vacuum as a clean pulse with record ultrashort duration of ~1 fs (Fig. 1c). In addition, the central wavelength of the RDW can be continuously tuned by simply changing the input pulse energy and gas pressure in a given configuration, resulting in the generation of sub-2 fs pulses across the whole deep and vacuum ultraviolet (Fig. 1d). Overall, our concept, which is currently under experimental construction, represents a major step forward to the generation of few- and even sub-cycle ultraviolet pulses, with great prospects for the investigation of photoinduced electronic processes with unprecedented temporal resolution.

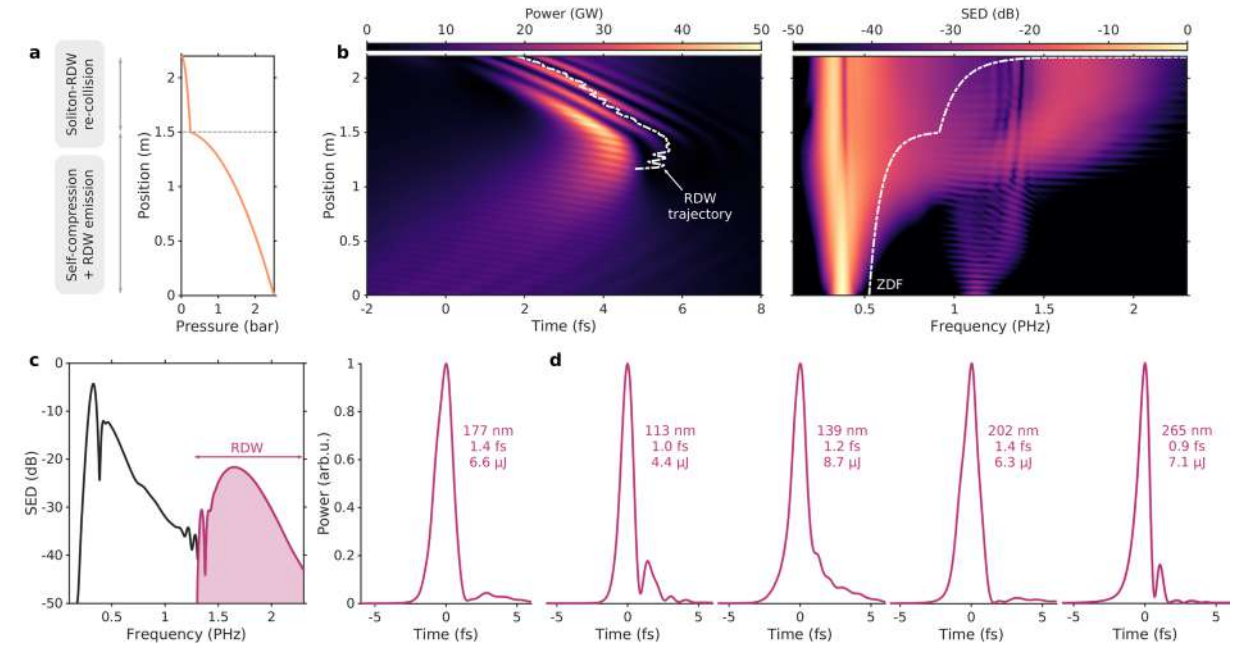


Fig. 1: (a) Double decreasing pressure gradient design in a HCF with an intermediate gas control point. (b) Modelled propagation of a self-compressing soliton showing re-collision with its RDW. (c) Output spectrum and corresponding RDW as directly delivered to vacuum. (d) Microjoule-level, sub-2 fs pulses generated at different central wavelengths.

- [1] J. C. Travers et al., Nat. Photon. 13, 547-554 (2019).
- [2] M. Reduzzi et al., Opt. Express 31, 26854-26864 (2023).
- [3] J. C. Travers and J. R. Taylor, Opt. Lett. 34, 115-117 (2009).
- [4] S. F. Wang et al., Phys. Rev. A 92, 023837 (2015).

High-Power 930-nm Femtosecond Fiber Laser based on Frequency Doubling

Siying Wang,¹ Yizhou Liu,^{2,3} and Aimin Wang^{1,*}

- ¹ State Key Laboratory of Photonics and Communications, School of Electronics, Peking University, Beijing, 100871, China
- ² Key Laboratory of Laser & Infrared System, Ministry of Education, School of Information Science and Engineering Shandong University, Qingdao 266237, China
- ³ Beijing Fatonics Technology Co., Ltd., Beijing, 100094, China

Abstract

We demonstrated a 79-MHz high-power femtosecond laser at 930-nm based on a frequency doubled 1860-nm fiber laser. The corresponding delivered pulse duration was 138 fs under the output power of 1.8 W. This laser source was further integrated into a two-photon imaging system.

Introduction

High-power femtosecond fiber lasers contribute significantly in the applications of terahertz-wave generation, biomedical imaging, and materials science [1-2]. In biomedical imaging, 930-nm femtosecond fiber lasers can be utilized to effectively excite fluorescent proteins labeled in the mouse cerebral cortex and hippocampus, enabling Ca²+ imaging with single dendritic spine resolution [3]. One sufficient approach in generating 930-nm femtosecond pulses is the nonlinear frequency conversion [4]. We report on a high-power, 79-MHz, 930-nm femtosecond laser generated by second harmonic generation (SHG) of an all-fiber mode-locked 1860-nm laser in a Periodically Poled Lithium Niobate (MgO: PPLN) crystal .

Experimental Results

The schematic design of the high-power 930-nm fiber laser was illustrated in Fig. 1(a), comprising a mode-locked erbium-doped fiber oscillator, a nonlinear erbium-doped fiber amplifier as the pre-amplifier, a thulium-doped chirped pulse amplifier (CPA), and the SHG stage.

Fig. 1(c-f) illustrated the optical characteristics of the delivered 930-nm femtosecond laser. A 4-W, 1860-nm fiber laser with the pulse duration of 198 fs can be realized by the thulium-doped fiber CPA. After carefully optimizing the nonlinear phase-matching condition, the 1.8-W, 930-nm laser pulses with the pulse duration of 138 fs based on the Sech² assumption can be generated.

This high-power, 930-nm femtosecond laser was further integrated into a two-photon microscopy system, and the imaging of mouse brain slices was demonstrated. The imaging validation showed a clearly visible neuronal structure, confirming the perfect effectiveness of this 930-nm laser for the high-resolution two-photon microscopy applications.

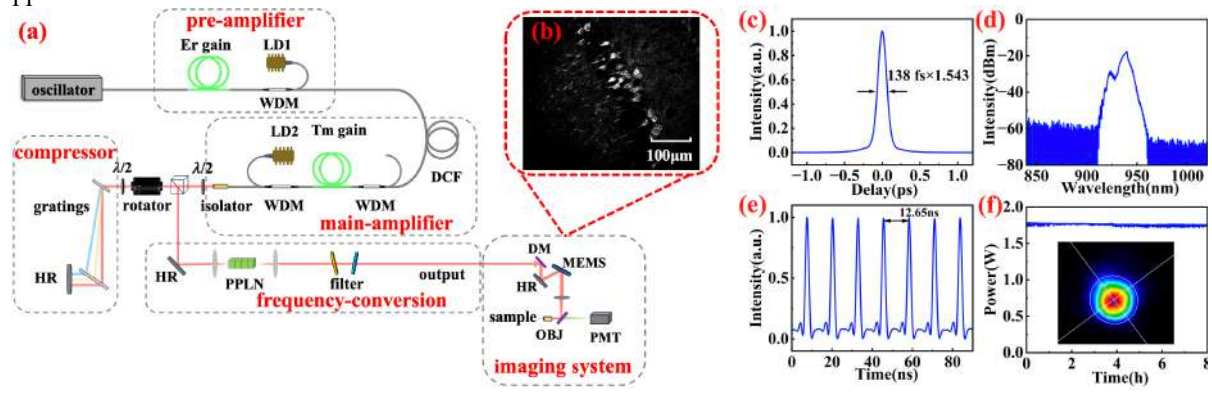


Fig. 1. (a) Schematic design of the 930-nm fiber laser; (b) two-photon imaging results; (c) optical pulse duration, (d) spectrum, (e) temporal performance of the pulse train, and (f) output power stability, inset: 930-nm laser beam profile. LD: laser diode; DCF: dispersion compensation fiber; WDM: wave length division multiplexer; DM: dichroic mirror; OBJ, objective; PMT, photomultiplier tube; HR: high reflection mirror.

- [1] Takayanagi J, "High-resolution time-of-flight terahertz tomography using a femtosecond fiber laser", Optics express, 17(9): 7533-7539(2009).
- [2] Sugioka K," Ultrafast lasers—reliable tools for advanced materials processing", Light: Science & Applications, 3(4): e149-e149(2014).
- [3] J. Nakai, M. Ohkura, and K. Imoto, A high signal-to-noise Ca(2+) probe composed of a single green fluorescent protein, Nat. Biotechnol 19(2), 137–141 (2001).
- [4] B. LI, M. Wang, K. Charan, M. Li and C. Xu, Investigation of the long wavelength limit of soliton self-frequency shift in a silica fiber, Opt. Express 26(15), 19637-19647 (2018).

^{*} wangaimin@pku.edu.cn

Single-shot a-swing pulse characterization

Cristian Barbero,1,* Íñigo J. Sola,1,2 and Benjamín Alonso1,2

¹Grupo de Investigación en Aplicaciones del Láser y Fotónica (ALF), Universidad de Salamanca, Spain ²Unidad de Excelencia en Luz y Materia Estructuradas (LUMES), Universidad de Salamanca, Spain *cristianbp@usal.es

Abstract

In this work, we present a single-shot implementation of the amplitude swing technique, where the amplitude modulation is applied using a pair of uniaxial wedges to obtain a spatially resolved trace. This compact inline setup allows versatile and robust characterization of single ultrashort pulses.

Temporal characterization of single pulses is necessary when dealing with shot-to-shot pulse-shape fluctuations, as usual in high-power and low repetition rate lasers. Amplitude swing (a-swing) [1,2] involves scanning the relative amplitude of two delayed replicas of the pulse to be measured, using a bulk inline interferometer that confers stability and compactness to the system. Here, we replace the rotating waveplate of the scanning configurations [3] with a pair of uniaxial wedges with their optical axes perpendicular between them (Fig. 1a), which introduce a relative phase $\delta(y,\omega)$ between the horizontal and vertical projections of the input pulse. This way, by means of a quarter waveplate, the amplitude modulation is imparted along a spatial coordinate (y-axis in this case), allowing us to measure the a-swing trace in a single acquisition using an imaging spectrometer [4]. From this trace, the pulse is retrieved by using a fast iterative ptychographic algorithm recently introduced [5]. We show an example of an a-swing single-shot measurement and reconstruction, validated by comparing it with the corresponding scanning retrieval (Fig. 1b and 1c).

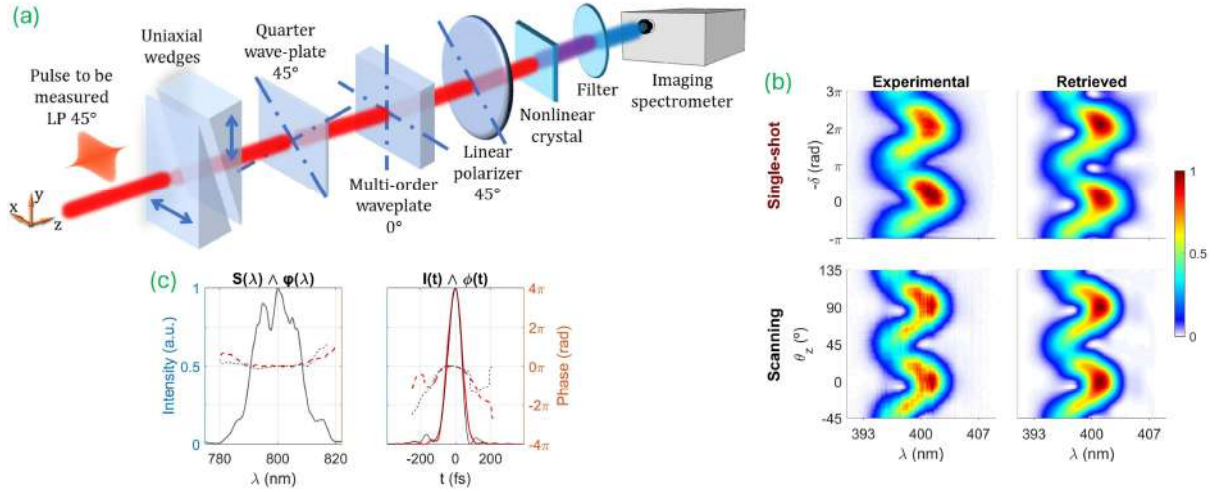


Figure 1: (a) Single-shot a-swing setup. (b) Measured and retrieved scanning and single-shot a-swing traces, (c) retrieved pulses in spectral and temporal domains. Gray: measured spectrum; red: single-shot; black: scanning.

In conclusion, we present a single-shot a-swing setup for ultrafast characterization, retaining the key advantages of the scanning a-swing versions: simplicity, resilience to noise and clipping, and versatility in spectral bandwidth (including few-cycle regime), chirp, and central frequency [6].

- [1] B. Alonso, W. Holgado, and Í. J. Sola, "Compact in-line temporal measurement of laser pulses with amplitude swing", Opt Express 28, 15625-15640 (2020).
- [2] Í. J. Sola, and B. Alonso "Robustness and capabilities of ultrashort laser pulses characterization with amplitude swing", Sci Rep 10, 18364 (2020).
- [3] M. López-Ripa, Í. J. Sola, and B. Alonso, "Generalizing amplitude swing modulation for versatile ultrashort pulse measurement", Opt Express **31**, 34428–34442 (2023).
- [4] C. Barbero, Í. J. Sola, and B. Alonso, "Measuring ultrafast laser pulses using a single-shot amplitude swing implementation", arXiv:2503.08824 (2025).
- [5] C. Barbero, Í. J. Sola, and B. Alonso, "Ptychographic retrieval for complete ultrashort pulse amplitude swing reconstruction", Opt Laser Technol 188, 112939 (2025).
- [6] M. López-Ripa, Í. J. Sola, and B. Alonso, "Amplitude swing ultrashort pulse characterization across visible to near-infrared," Opt Laser Technol **164**, 109492 (2023).

Compact Tunable Sub-20 fs Visible Pulses via Fiber Laser-Driven Resonant Dispersive-Wave Emission

Mohammed Sabbah,¹ Robbie Mears,² Leah R. Murphy,¹ Kerrianne Harrington,² James M. Stone,² Tim A. Birks,² and John C. Travers^{1,*}

¹School of Engineering and Physical Sciences, Heriot-Watt University, Edinburgh, EH14 4AS, United Kingdom
²Centre for Photonics and Photonic Materials, Department of Physics, University of Bath, Claverton Down, Bath, BA2 7AY, United Kingdom

Abstract

We demonstrate a compact fiber-laser-based source of tunable sub-20 fs pulses spanning 400-700 nm at 4.8 MHz. Using gain-managed nonlinear amplification and resonant dispersive-wave emission, we achieve pulse energies up to 39 nJ and durations as short as 13 fs.

Tunable ultrashort laser pulses across the near-ultraviolet to near-infrared with high peak power are crucial for wideranging applications in science and industry. Resonant dispersive-wave (RDW) emission in gas-filled hollow-core fibers is a well-established technique for generating tunable ultrashort pulses from the vacuum ultraviolet to the near-infrared [1]. However, previous demonstrations have relied on complex and expensive laser systems to provide the necessary energetic ultrashort pump pulses. Recent advances in fiber laser technology, particularly gain-managed nonlinear amplification [2], offer a promising alternative pump source. Here, we combine gain-managed nonlinear amplification with resonant dispersive-wave emission to demonstrate a compact and tunable source of sub-20 fs pulses at 4.8 MHz. We achieve a tunable output spanning from 400 nm to beyond 700 nm (Figure 1(a)), with energy up to 39 nJ, pulse duration down to 13 fs (Figure 1(b) and (c)), and peak power exceeding 2 MW. Further experimental details are available in Ref. [3]. This compact and efficient laser source opens new avenues for deploying resonant dispersive-wave-based technologies for broader scientific and industrial applications.

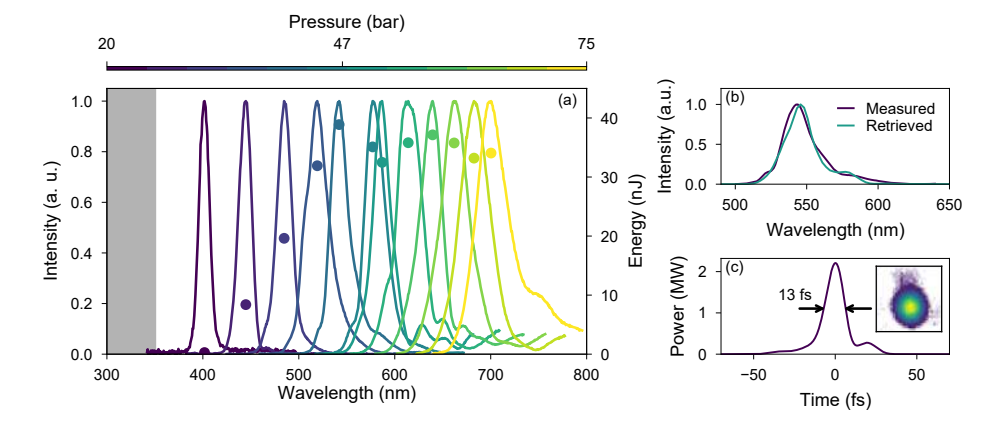


Figure 1: (a) Tunable RDW generation (left axis) in a 36 µm core diameter antiresonant fiber as the argon filling pressure is varied from 20 to 75 bar. The scattered dots (right axis) represent the energy of the corresponding RDWs at the fiber output. (b) The measured and retrieved spectrum of the RDW generated at 550 nm. (c) Retrieved temporal profile of the pulse. The inset in (c) shows the near-field beam profile of the RDW.

- [1] Joly, Nicolas Y. et al., Phys. Rev. Lett. 106, 203901.
- [2] Pavel Sidorenko et al., Optica 6, 1328-1333 (2019).
- [3] Sabbah, Mohammed et al., arXiv preprint arXiv:2502.01322 (2025).

j.travers@hw.ac.uk

A high-repetition rate, table-top coherent soft x-ray source

Azize Koç,1,* Daniel Walke,1 Minjie Zhan,2 and Iain Wilkinson1

 1 Helmholtz-Zentrum Berlin für Materialien und Energie GmbH, Hahn-Meitner-Platz 1, 14109 Berlin, Germany

Abstract

We present a 52.6 kHz repetition-rate soft x-ray source with a broadband emission spectrum covering the water window. It is driven by an unprecedented average power (52 W), few-cycle, carrier-envelope phase stable, short-wave infrared (2.1 µm) optical parametric chirped pulse amplifier.

Time-resolved soft x-ray spectroscopy (TR-SXS) is an important technique to probe element-specific electronic structure dynamics in matter. High-harmonic generation (HHG) provides temporally and spatially coherent, attosecond to few-femtosecond pulses potentially spanning the vacuum ultraviolet to soft x-ray (SXR) spectral regions [1]. HHG driven by short-wave infrared (SWIR) lasers enables high-time-resolution SXS in the water window (284-543 eV) on a laboratory scale [1]; however, low photon statistics are the principal limiting factor for associated experiments. SWIR sources with high average power are a promising route to enable such experiments with high signal-to-noise levels [2].

We present a SXR source driven by an optical parametric chirped pulse amplifier (OPCPA) that delivers 20 fs (few-cycle) pulses at 2.1 μ m central wavelength at a 52.6 kHz repetition rate [3]. The carrier-envelope phase (CEP) is stabilized and measured to be $\approx 600\,\mathrm{mrad}$ with single-shot resolution. The output SWIR pulses possess high spatial beam quality (M² < 1.3) and high average power of 52 W. An average power of 45 W is currently available on target for SXR generation.

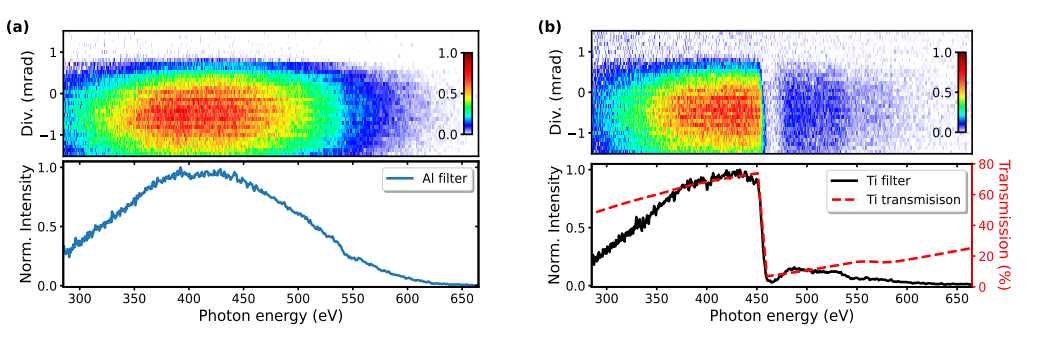


Figure 1: SXR spectra measured with an exposure time of 60 s after filtering with a) two aliminium filters, b) one aliminium and one titanium filter. The dotted line shows the titanium-filter transmission.

In an initial application of the SWIR source, a SXR beam is generated in helium gas in a 1.65 mm-long gas cell (backing pressure 9 bar) by focusing few-cycle SWIR pulses to a peak intensity of $\approx 7 \times 10^{14} \, \mathrm{W/cm^2}$. The emitted broadband beam is spectrally filtered using thin metal filters, and the spatially resolved SXR spectra are measured with an x-ray CCD detector after being diffracted by a flat-field grating (2400 grooves/mm). In Figure 1, the resulting SXR spectra are shown for two different filter combinations, demonstrating extended broadband emission above 600 eV and a low divergence of < 2 mrad (half-angle). The latter indicates good phase matching, which can contribute to higher photon-collection efficiency and energy resolution when respectively refocusing or monochromatizing the SXR beam for experiments. Current work focuses on extending the photon flux of SXR source beyond the state of the art and developing SXR beam lines for TR-SXS experiments.

- [1] D. Popmintchev *et al.*, "Near- and Extended-Edge X-Ray-Absorption Fine-Structure Spectroscopy Using Ultra-fast Coherent High-Order Harmonic Supercontinua", Physical Review Letters **120**, 093002 (2018).
- [2] J. Pupeikis et al., "Water window soft x-ray source enabled by a 25 W few-cycle 2.2 μm OPCPA at 100 kHz", Optica 7, 168-171 (2020).
- [3] D. Walke et al., "High-average-power, few-cycle, 2.1 μm OPCPA laser driver for soft-X-ray high-harmonic generation", Optics Express 33, 10006-10019 (2025).

²UltraFast Innovations GmbH, Dieselstr. 5, 85748 Garching (Munich), Germany

 $^{^*}$ azize.koc@helmholtz-berlin.de



Generation of multi-GW, sub-10 fs tuneable visible pulses

Martin Gebhardt, Joleik Nordmann, Michael Heynck, Nikoleta Kotsina, Teodora Grigorova, Christian Brahms, and John C. Travers*

School of Engineering and Physical Sciences, Heriot-Watt University, Edinburgh, EH14 4AS, United Kingdom *j.travers@hw.ac.uk

Abstract

We obtain multi-GW peak power few-cycle visible pulses through resonant dispersive wave emission in a gas-filled capillary. Generated in the fundamental fibre mode without the need for post compression, these pulses are well-suited for driving strong-field experiments such as high-harmonic generation.

Few-cycle strong-field drivers in the visible (VIS) hold great promise to overcome the conversion efficiency bottlenecks of extreme ultraviolet high-harmonic generation (HHG). Compared to the infrared, the fast field oscillations of VIS lasers reduce quantum diffusion during the HHG process and allow for high driving intensities, ultimately boosting efficiency—provided the pulses are sufficiently short [1]. However, true few-cycle nonlinear compression, starting from attractive Yb-based second harmonic sources, remains challenging due to limited bandwidth and damage thresholds of VIS pulse compression mirrors [1]. As an alternative to broadband parametric amplification [2] (typically >400 nm), and nonlinear high-order fibre mode mixing [3], we present energy scaling of a new route toward VIS strong-field drivers: resonant dispersive wave (RDW) emission in gas-filled capillaries [4]. This approach does not require subsequent pulse compression and features inherently high beam quality due to operation in the fundamental fibre mode.

Our experiments are driven by an optical parametric amplifier and a subsequent nonlinear pulse compression stage providing sub-15 fs pulses centered at $1800 \,\mathrm{nm}$ with up to $2 \,\mathrm{mJ}$ energy. A fraction of these pulses is coupled to a $\sim 4 \,\mathrm{m}$ long Ar-filled capillary (700 µm core diameter). Due to the interplay between nonlinearity and dispersion, the infrared pulses self-compress within the fibre and generate phase-matched RDWs. Figure 1a presents a RDW tuning curve, shifting the phase matching from the ultraviolet across the VIS as the Ar pressures is progressively increased. The total RDW energy in a $1/e^2$ bandwidth is, depending on the Ar pressure, in the range of $40-70\,\mu\mathrm{J}$ ($\sim\!15\,\%$ conversion efficiency). The spectral modulation at $550-650\,\mathrm{nm}$ arises from f-3f interference (between the RDW and a weak third harmonic of the infrared) which we use to determine a passive carrier-envelope phase (CEP) noise of <250 mrad RMS on a ~ 1 s timescale. A typical beam profile in the VIS confirming fundamental mode operation is shown in the inset. When tuned to 515 nm, we use dispersion-minimised optics to separate the VIS RDW from the driving pulse. We subsequently demonstrate the potential of our source as a strong-field driver using the tunneling ionisation with a perturbation for the time-domain observation of an electric field (TIPTOE) method. The relative ionisation yield δN from an Ar target, time-domain retrieved pulse, the spectrum of the separated RDW, as well as the match between TIPTOE/spectrometer data are presented in Figure 1b,c. With >4 GW peak power, sub-10 fs duration and prospects for robust slow-loop CEP stabilisation, we demonstrate isolation of a strong-field few-cycle VIS RDW for the first time, which opens the door to their use in driving efficient HHG. Additionally, our future work will include pushing the RDW emission to higher energies and shorter pulse durations as well as implementing active CEP control.

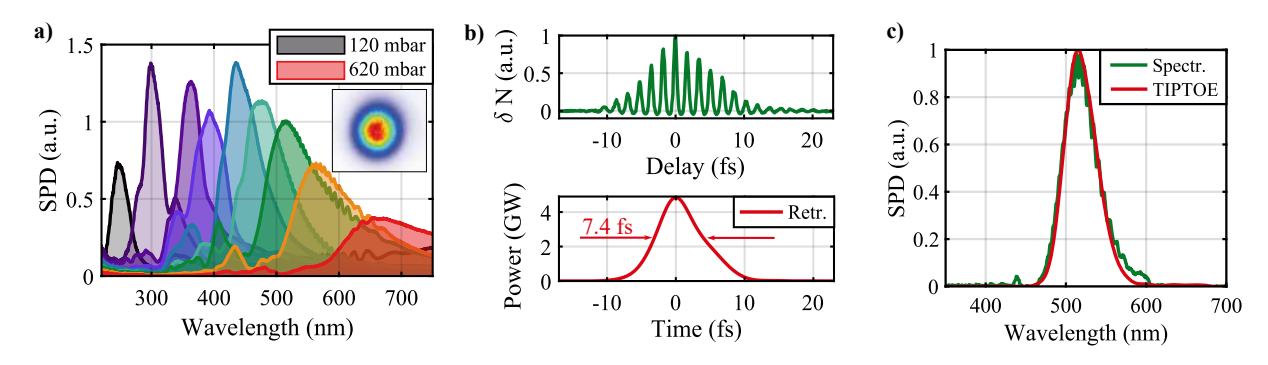


Figure 1: a) Spectral tuning of RDWs. b) Time domain and c) spectral TIPTOE measurement results.

- [1] R. Klas et al., PhotoniX 2:4 (2021). [2] J. Odhner et al., Opt. Lett. 40, 3814-3817 (2015).
- [3] R. Piccoli et al., Nat. Photon. 15, 884–889 (2021). [4] C. Brahms et al., Phys. Rev. Res. 2, 043037 (2020).

Optical Parametric Multi-Pass Cell Amplifier: A High-Efficiency Ultrashort Pulse Amplification scheme

Supriya Rajhans,^{1,*} Nikolas Rupp,¹ Esmerando Escoto,¹ Arthur Schönberg,¹ Ingmar Hartl,¹ Christoph M. Heyl, ^{1,2,3} and Tino Lang¹

Abstract

We present a novel method combining multi-pass cell (MPC) technology with optical parametric amplification. The resulting simulated optical parametric MPC (OPMPC) amplifier exhibits excellent beam quality and a pump-to-signal efficiency approaching the Manley-Rowe limit.

Multi-pass cell (MPC)-based post-compression enables high compression ratios, efficient transmission, and excellent beam quality, making it a key technology for high-power few-femtosecond laser pulse generation [1]. However, the method is limited in spectral tunability and temporal contrast. Optical parametric chirped pulse amplification (OPCPA) offers superior spectral flexibility and temporal contrast but is typically limited to <20% pump-to-signal conversion efficiency and suboptimal beam quality [2]. This work introduces the optical parametric MPC (OPMPC) amplifier, combining the advantages of MPC-based post-compression with OPCPA.

We present (3+1)D numerical simulations using the chi3D software [3] to model parametric amplification in an MPC. Collinear pump $(1.03\,\mu\text{m})$ and signal $(1.6\,\mu\text{m})$ pulses propagate through the MPC, with the idler filtered on each pass to suppress back-conversion [4]. As shown in Fig. 1(a), the setup features cell mirrors (ROC: 4 m) with four $0.15\,\text{mm}$ thick KNbO₃ crystals symmetrically positioned near the focus, spaced $25\,\text{mm}$ apart. The 1 ps, 1 mJ pump pulses are temporally overlapped with a seed pulse spanning $1.3-2.1\,\mu\text{m}$. Fig. 1(b) presents the seed and the amplified signal spectra after 20 passes in the MPC. Linear losses considered at crystal interfaces and mirrors reduce the multi-pass cell transmission to 80%. Simulations predict conversion efficiencies exceeding 50% within a key spectral range, relevant e.g. for high harmonic generation. The observed signal saturation at \sim 50% efficiency is attributed to cell transmission losses, limiting performance below the 64% quantum limit. Optimizing second and third order dispersion yields a 20 fs compressed pulse (FWHM) close to the 18 fs Fourier limit (Fig. 1(d)). The inset of Fig. 1(d) confirms an excellent signal beam profile attributed to quasi-waveguiding properties of the MPC.

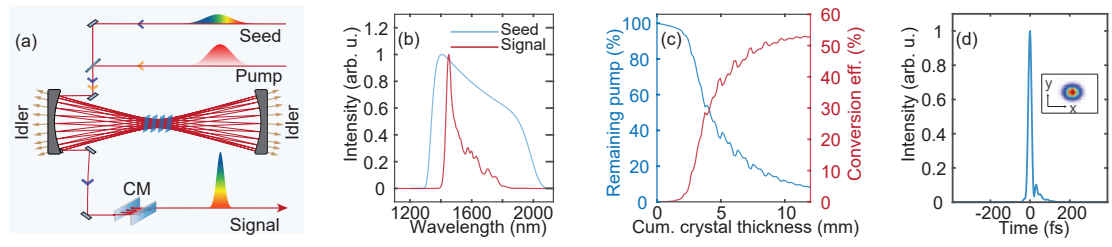


Fig. 1 (a) Schematic of the OPMPC with collinearly propagating seed and pump pulses (cell length: 2.76 m). CM: Chirped mirrors (b) Spectra of the simulated input seed and output signal pulses. (c) Calculated pump depletion and conversion efficiency of the OPMPC. (d) Compressed output pulse shape. Inset: Spatial profile of the signal beam at the output.

In conclusion, we introduce an optical parametric multi-pass scheme integrating nonlinear amplification within an MPC. Simulations confirm excellent spatio-temporal pulse quality at record efficiency, paving the way to a new ultrashort pulse laser platform.

- [1] A-L. Viotti, et al., "Multi-pass cells for post-compression of ultrashort laser pulses," Optica 9, 197 (2022).
- [2] H. Fattahi, et al., "Third-generation femtosecond technology," Optica 1, 45 (2014).
- [3] T. Lang, et al., "Impact of temporal, spatial and cascaded effects on the pulse formation in ultra-broadband parametric amplifiers," Opt. Express 21, 949 (2013).
- [4] T. H. Jeys, "Multipass optical parametric amplifier," Opt. Lett. 21, 1229 (1996).

¹Deutsches Elektronen-Synchrotron DESY, Notkestraße 85, 22607 Hamburg, Germany

²Helmholtz Institute Jena, Fröbelstieg 3, 07743 Jena, Germany

³GSI Helmholtzzentrum für Schwerionenforschung GmbH, Planckstraße 1, 64291 Darmstadt, Germany

^{*}supriya.rajhans@desy.de

Fast a-swing ptychographic pulse retrieval

Cristian Barbero,1,* Íñigo J. Sola,1,2 and Benjamín Alonso1,2

¹Grupo de Investigación en Aplicaciones del Láser y Fotónica (ALF), Universidad de Salamanca, Spain ²Unidad de Excelencia en Luz y Materia Estructuradas (LUMES), Universidad de Salamanca, Spain *cristianbp@usal.es

Abstract

Here, we propose a ptychographic algorithm to retrieve scalar and vector pulses from amplitude swing measurements, in all its configurations. This fast and robust algorithm enhances the capabilities of amplitude swing, benefiting the ultrafast science community.

In ultrafast optics, temporal characterization of laser pulses is crucial both for understanding and optimizing the experiments, with a continuously increasing demand for simple and versatile setups. Amplitude swing (a-swing) [1] meets this demand by means of a compact inline setup, easily adaptable to different pulse durations and bandwidths [2], and central frequencies [3]. Furthermore, a-swing integrates the temporal and polarization detections, retrieving vector pulses from a single trace [4]. In previous works, Levenberg-Marquardt [1-2,4,5] and differential evolution algorithms [3] have been employed. Here, we present a specially designed ptychographic iterative engine (PIE) algorithm, based on a unified a-swing theory [6]. It improves the performance of said algorithms in terms of speed, robustness against energy fluctuations during the scan, complexity of the phase to be retrieved, capability of simultaneously retrieving amplitude and phase, and applicability to generalized configuration [5] for vector pulses. To illustrate this, we show some retrievals in Fig. 1.

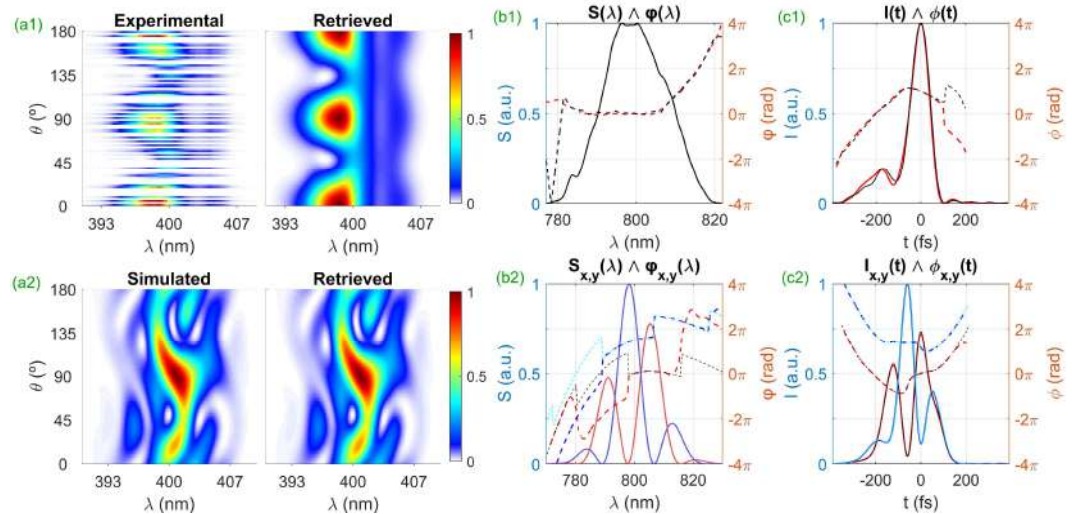


Figure 1: (a) Experimental/Simulated and retrieved traces. Retrieved pulses in spectral (b) and temporal (c) domains. Row 1: scalar pulse retrieved from full trace (black) and after removing some trace slices (red). Row 2: simulated (black and cyan) and retrieved (red and blue) projections of a vector pulse. The spectra are not retrieved in these cases.

In conclusion, we present a fast and robust ptychographic algorithm to retrieve scalar and vector pulses from all a-swing implementations, including single-shot architectures. We expect it will benefit the ultrafast physics field by enhancing the capabilities of such a simple and versatile pulse characterization method.

- [1] B. Alonso, W. Holgado, and Í. J. Sola, "Compact in-line temporal measurement of laser pulses with amplitude swing", Opt Express 28, 15625-16640 (2020).
- [2] M. López-Ripa, Ó. Pérez-Benito, B. Alonso, R. Weigand, and Í. Sola, "Few-cycle pulse retrieval using amplitude swing technique," Opt Express **32**, 21149–21159 (2024).
- [3] M. López-Ripa, Í. J. Sola, and B. Alonso, "Amplitude swing ultrashort pulse characterization across visible to near-infrared," Opt Laser Technol **164**, 109492 (2023).
- [4] C. Barbero, B. Alonso, and İ. J. Sola, "Characterization of ultrashort vector pulses from a single amplitude swing measurement," Opt Express **32**, 10862–10873 (2024).
- [5] M. López-Ripa, Í. J. Sola, and B. Alonso, "Generalizing amplitude swing modulation for versatile ultrashort pulse measurement", Opt Express **31**, 34428–34442 (2023).
- [6] C. Barbero, Í. J. Sola, and B. Alonso, "Ptychographic retrieval for complete ultrashort pulse amplitude swing reconstruction" Opt Laser Technol 188, 112939 (2025).

Ultrabroadband few-cycle and chirped pulses measured with amplitude swing

Íñigo Sola^{1,2,*}, Miguel López-Ripa¹, Óscar Pérez-Benito³, Benjamín Alonso^{1,2}, and Rosa Weigand³

¹Grupo de Investigación en Aplicaciones del Láser y Fotónica (ALF), Universidad de Salamanca, Salamanca, Spain ²Unidad de Excelencia en Luz y Materia Estructuradas (LUMES), Universidad de Salamanca, Salamanca, Spain ³Department of Optics, Faculty of Physics, University Complutense, Plaza de Ciencias 1, 28040 Madrid, Spain * ijsola@usal.es

Abstract

This work establishes a-swing technique as a precise and robust approach for characterizing few-cycle laser pulses, offering a compact and adaptable setup for ultrafast optics applications across broad spectral ranges.

We show the amplitude swing (a-swing) technique [1,2] for characterizing ultrashort few-cycle laser pulses [3]. This method relies on modulating the relative amplitude of two delayed pulse replicas with an in-line and compact setup. Recent works show that a-swing can also characterize vector pulses [4] and operate in single-shot mode [5].

Using a Ti:sapphire oscillator generating pulses with a Fourier limit of 5.50 fs, the study demonstrated pulse characterization both near-optimal compression (5.98 fs) and under highly chirped conditions, where group delay dispersions up to ± 160 fs² stretched the pulses to approximately 15–20 times their original duration [3]. The results for the compressed case are presented in Fig. 1. Comparisons with the d-scan technique [6] showed excellent agreement across all conditions, confirming the accuracy of a-swing in both compressed and chirped regimes.

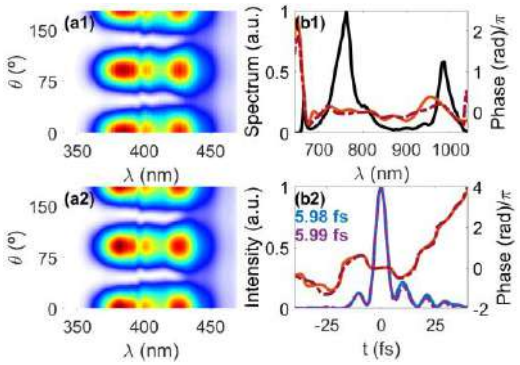


Figure 1: (a1) Experimental and (a2) retrieved a-swing traces. Comparison of the pulse retrieved near compression: (b1) measured spectral intensity (black) and retrieved spectral phase (a-swing: solid orange; d-scan: dashed red) and (b2) retrieved temporal intensity (a-swing: solid blue; d-scan: dashed purple) and phase (a-swing: solid orange; d-scan: dashed red).

The adaptability of a-swing to ultrabroadband pulses and its capability to operate over a wide spectral range [7] make it well-suited for advanced ultrafast optics applications, such as attoscience and time-resolved spectroscopy. The setup remains straightforward, utilizing standard laboratory components like birefringent plates and nonlinear crystals, and holds potential for characterizing even shorter pulses or extending it to different spectral regions.

- [1] B. Alonso, W. Holgado, and Í. J. Sola, "Compact in-line temporal measurement of laser pulses with amplitude swing," Opt. Express 28, 15625–15640 (2020).
- [2] Í. J. Sola and B. Alonso, "Robustness and capabilities of ultrashort laser pulses characterization with amplitude swing," Sci Rep 10, 18364 (2020).
- [3] M. López-Ripa, Ó. Pérez-Benito, B. Alonso, R. Weigand, and Í. Sola, "Few-cycle pulse retrieval using amplitude swing technique," Opt. Express **32**, 21149–21159 (2024).
- [4] C. Barbero, B. Alonso, and Í. J. Sola, "Characterization of ultrashort vector pulses from a single amplitude swing measurement," Opt. Express **32**, 10862–10873 (2024).
- [5] C. Barbero, Í. J. Sola, and B. Alonso, "Measuring ultrafast laser pulses using a single-shot amplitude swing implementation", arXiv:2503.08824 (2025).
- [6] M. Miranda, C. L. Arnold, T. Fordell, F. Silva, B. Alonso, R. Weigand, A. L'Huillier, and H. Crespo, "Characterization of broadband few-cycle laser pulses with the d-scan technique," Opt. Express **20**, 18732–18743 (2012) [7] M. López-Ripa, Í. J. Sola, and B. Alonso, "Amplitude swing ultrashort pulse characterization across visible to near-infrared," Opt. Laser Technol **164**, 109492 (2023).

Recent developments in L3 HAPLS

Jakub Novák,^{1,*} Petr Szotkowski,¹ Emily Sistrunk Link,² James McLaughlin,² Leily Kiani,² Thomas Galvin, ² Katherine Velas, ² Jan Černý, ¹ Jitka Sedmidubská, ¹ Alexandros Sarafis, ¹ Martin Cuhra, ¹ Lucia Jarboe, ¹ Bohdana Lopushanska, ¹ Jan Moučka, ¹ Thomas Spinka, ² and Bedřich Rus¹

¹ELI ERIC, Beamlines Facility, Za Radnicí 835, 252 41 Dolní Břežany, Czechia
²Lawrence Livermore National Laboratory, 7000 East Ave., Livermore, CA 94550, USA
*Jakub.Novak@eli-beams.eu

Abstract

The L3 HAPLS laser system at ELI Beamlines has reliably delivered pulses with energy up to 10 J compressed to a 30 fs duration for several years, supporting a broad range of experiments in both shot-on-demand and 3.3 Hz repetition modes. Recent upgrades have extended the system's potential to approach energy of 15.5 J and 0.5 PW peak power maintaining high output stability and a near diffraction-limited focal spot. This talk will outline the technical innovations and key modifications that enabled this milestone and will present the way to ramp-up to 1 PW.

L3 HAPLS

The L3 HAPLS (High-repetition-rate Advanced Petawatt Laser System) at ELI Beamlines has reliably delivered pulses with energy up to 10 J compressed to a 30 fs duration for several years, supporting a broad range of experiments for users in both shot-on-demand and 3.3 Hz repetition modes [1]. In both regimes it has shown high output stability and a near diffraction-limited focal spot. Recent upgrades have extended the system's potential to approach energy of 15.5 J and 0.5 PW peak power.

The primary upgrades were focused on the pump laser of the final Ti: Sapphire amplifier. First, the pump energy was increased to 140 J. Additionally, we rebuilt the SHG conversion and pump beam delivery, introducing a delay leg as a major enhancement. We reached converted pump energy of 119 J with 85% conversion efficiency at 0.2 Hz repetition rate, which is a remarkable achievement for this type of laser system (see fig. 1). Splitting the pump pulse and delaying a portion of it increased the efficiency of the Ti: Sapphire amplifier and more importantly decreased laser load on optics. We are currently extending this result to 3.3 Hz operation at this energy by implementing a Faraday rotator in the pump laser to mitigate depolarization effects [2]. We are now focusing on further improvements of energy extraction to reach 1 PW peak power.

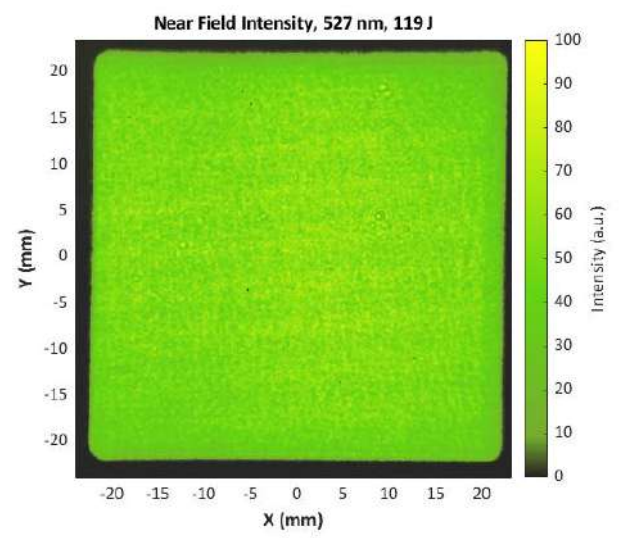


Figure 1: Beam profile of a SHG pump pulse with energy of 119 J

References

[1] C. L. Haefner et al, "High average power, diode pumped petawatt laser systems: a new generation of lasers enabling precision science and commercial applications," Proc. SPIE 10241, 1024102 (2017)

[2] F. Batysta et al, "Characterization of a multi-kW, large-aperture gas-cooled Faraday rotator," Opt. Express 33, 7372-7379 (2025)

Spatiotemporal measurement of astigmatically focused beams using BLASHI

Benjamín Alonso^{1,2,*}, Miguel López-Ripa, and Íñigo J. Sola, 1,2

¹Grupo de Investigación en Aplicaciones del Láser y Fotónica (ALF), Universidad de Salamanca, Spain

Abstract

We investigate the suitability of Bulk LAteral SHearing Interferometry (BLASHI) for measuring non-collimated beams. We theoretically analyze the effect of numerical aperture (NA), finding that it is effective for moderate NA < 0.1 out of the focal region. We apply BLASHI to measure astigmatically focused beams.

Precise spatiotemporal characterization of laser beams is crucial for optimizing laser applications [1]. However, some techniques face limitations, e.g. interferometric methods like STARFISH [2] can introduce wavefront noise due to instabilities [3]. The BLASHI technique [4] overcomes it by combining spectral and lateral interferometry in a compact, ultra-stable bulk setup using birefringent crystals, which introduce both walk-off and delay.

Until now, BLASHI has been demonstrated with collimated beams [4,5]. Non-collimated beams can experience distortions after passing through a uniaxial crystal due to angle-dependent birefringence effects. In this work, we develop a theoretical model for light propagation, incorporating refraction, birefringence, and lateral displacement effects. It is combined with numerical simulations to analyze how non-plane waves acquire distortions. Our analysis suggests that BLASHI remains effective for characterizing non-collimated beams when measurements are taken far from the focal point and the beam is focused with a moderate NA < 0.1.

Experimentally, we use BLASHI to measure the spatiospectral distribution of an ultrashort laser beam (60 fs, 800 nm) after focusing with an astigmatic lens (focal lengths of 100 cm and 197 cm), which introduces a spatial phase structure with two distinct focal planes along orthogonal axes. Measurements were taken at two propagation planes: 49 cm after the lens (before the first focus) and 137 cm (between the two foci). The retrieved spatial phase profiles (wavefronts) exhibited a bi-convergent shape at the first measurement plane and a convergent-divergent profile at the second (Fig. 1), as expected and validated with the theory.

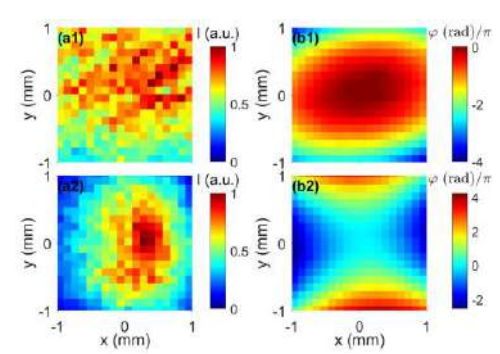


Figure 1: Spatial intensity (a) and phase (b) for the central wavelength of the spatiospectral characterization at two propagation distances after the astigmatic lens, before the first focus (a1,b1) and between the two foci (a2,b2).

This experimental validation confirms that BLASHI effectively characterizes both convergent and divergent beams, even with complex spatiospectral dependencies, supporting the described theoretical finding.

References

[1] B. Alonso, A. Döpp, and S. W. Jolly, "Space–time characterization of ultrashort laser pulses: A perspective," APL Photonics **9**, 070901 (2024).

[2] B. Alonso, I. J. Sola, O. Varela, J. Hernández-Toro, C. Méndez, J. Román, A. Zaïr, and L. Roso, "Spatiotemporal amplitude-and-phase reconstruction by Fourier-transform of interference spectra of high-complex-beams," J Opt Soc Am B **27**, 933 (2010). [3] B. Alonso, R. Borrego-Varillas, O. Mendoza-Yero, Í. J. Sola, J. San Román, G. Mínguez-Vega, and L. Roso, "Frequency resolved wavefront retrieval and dynamics of diffractive focused ultrashort pulses," J Opt Soc Am B **29**, 1993–2000 (2012). [4] M. López-Ripa, Í. J. Sola, and B. Alonso, "Bulk lateral shearing interferometry for spatiotemporal study of time-varying ultrashort optical vortices," Photonics Res **10**, 922–931 (2022).

[5] M. López-Ripa, Í. J. Sola, and B. Alonso, "Visible optical vortices measured with bulk lateral shearing interferometry," arXiv:2503.24218 (2025).

²Unidad de Excelencia en Luz y Materia Estructuradas (LUMES), Universidad de Salamanca, Spain

^{*} b.alonso@usal.es

Generation of multi-octave millijoule-level radial vector beams

Michael Heynck^{*}, Nikoleta Kotsina, Joleik Nordmann, Martin Gebhardt, Teodora Grigorova, Christian Brahms, and John C. Travers

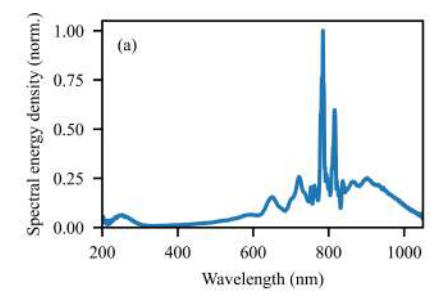
School of Engineering and Physical Sciences, Heriot-Watt University, Edinburgh, EH14 4AS, United Kingdom *mh2065@hw.ac.uk

Abstract

We demonstrate the generation of ultra-broadband radial vector beams. Through the use of soliton self-compression dynamics in gas-filled hollow-core fibres on the XSOL (Extreme Soliton) beamline, mJ-level pulses with multi-octave spectra reaching down to 140 nm are generated.

If radial vector beams are tightly focused, the resulting longitudinal field in the propagation direction can be used to accelerate electrons [1]. In order to maximise the peak intensity at focus, either the pulse energy has to be increased or the pulse duration has to be decreased. When using segmented waveplates for the conversion of linearly polarised light to radial vector beams, the limited bandwidth of these optics sets a limit to the minimum pulse duration. While previous work has overcome this by spectrally broadening radially polarised beams in gas-filled hollow-core fibres [2], the pulse duration in that case is still at the few-cycle level, due to the limited bandwidth of chirped mirrors. Our work aims to overcome these limits by self-compressing radially polarised light in gas-filled hollow-core fibres using soliton dynamics [3].

The beamline used is called XSOL (Extreme Solitons), a three-stage hollow-core fibre setup that is capable of generating mJ-level pulses that cover a multiple-octave spanning spectrum. In brief, it is built of three helium filled fibre stages. The first two stages compress 40 fs linear polarised pulses down to 5.5 fs with pulse energy up to 5 mJ. These pulses are sent into the third stage, where soliton dynamics cause spectral broadening and temporal self-compression at the same time [3], making the generation of sub-femtosecond pulses possible. In the current work, before sending the pulses into the soliton stage, they are converted to radially polarised beams with a segmented achromatic waveplate. This input state preferentially couples to the TM_{01} mode of a 4 m long, 530 µm core diameter, helium filled hollow-core fibre. These pulses experience soliton dynamics, causing their spectral broadening and temporal self-compression. The wavelength of the generated ultraviolet light is dependent on the gas pressure. For 1.4 bar it reaches the deep ultraviolet, as shown in Figure 1. By reducing the pressure even further, the spectrum extends into the vacuum ultraviolet, reaching down to 140 nm so far. This spectral bandwidth, together with an output pulse energy of 1.4 mJ, allows the generation of several hundred GW-scale, sub-femtosecond, radially polarised beams. While the full temporal characterisation for radial polarisation is still pending, this claim is supported by our recent characterisation of 0.77 fs, multi-mJ self-compressed linearly polarised pulses generated on the same beamline.



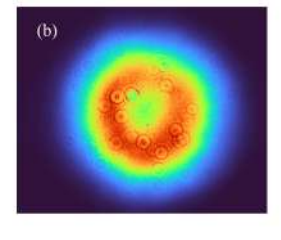


Figure 1: (a) Spectrum of our radially polarised beam for a gas pressure of 1.4 bar, keeping the spectral extension within the deep ultraviolet. (b) Corresponding beam profile.

- [1] S. Payeur et al., "Generation of a beam of fast electrons by tightly focusing a radially polarized ultrashort laser pulse," Appl. Phys. Lett. **101**, 041105 (2012).
- [2] F. Kong et al., "Generating few-cycle radially polarized pulses", Optica 6, 160-164 (2019).
- [3] J.C. Travers et al., "High-energy pulse self-compression and ultraviolet generation through soliton dynamics in hollow capillary fibres," Nat. Phot. 13, 547–554 (2019).

Polarization-resolved ultrashort pulse characterization using an air-based knife-edge

Marie Ouillé^{1,*}, Gaëtan Jargot¹, Mayank Kumar¹, Stephen Londo¹, Édouard Hertz², Pierre Béjot², Heide Ibrahim¹, François Légaré¹ and Adrien Leblanc³

Abstract

We present a simple pump-probe technique combining an air-based knife-edge with time-domain ptychographic retrieval for ultrashort pulse characterization. Thus far limited to orthogonally polarized pump and probe pulses, we introduce a novel setup enabling characterization of the temporally varying polarization, as well as the phase and amplitude of ultrashort pulses.

Ultrashort laser pulse temporal characterization methods typically rely on nonlinear processes, therefore having a limited spectral range of application, and require the use of transmissive optics which can potentially modify the pulse's spatio-temporal structure prior to its characterization. Recently, a simple, phase-matching free pump-probe technique using a transient plasma lens generated in ambient air and a time-domain ptychographic retrieval algorithm, was demonstrated [1,2]. However, this technique has thus far been limited to orthogonally polarized pump and probe pulses. Here, we present a novel setup that is independent of the probe polarization, thus enabling characterization of not only the phase and amplitude, but also the temporally varying polarization state of ultrashort pulses, as shown in Figure 1. We illustrate its capabilities by measuring polarization-shaped pulses, such as those used for polarization gating of high harmonic generation in order to generate isolated attosecond pulses. Additionally, we demonstrate the extreme versatility of the technique by performing measurements at up to 2 MHz repetition rate and over extended spectral bandwidths through the characterization of a supercontinuum generated in YAG.

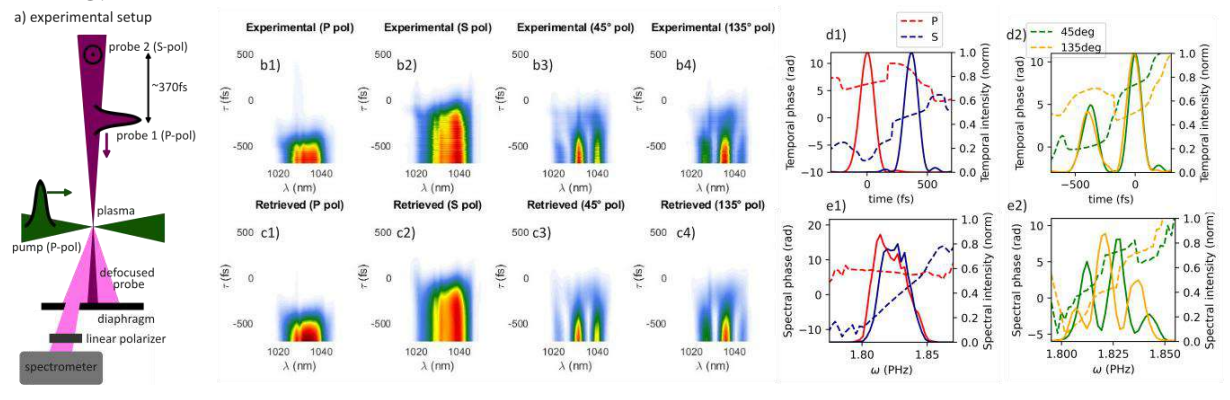


Figure 1: Characterization of two orthogonally polarized $\sim 130 \text{fs}$ FWHM duration "probe" pulses with a $\sim 370 \text{fs}$ relative delay from an ytterbium laser. Top view of the experimental setup (a). Experimental (b1-4) and reconstructed (c1-4) traces for different orientations of the linear polarizer, where τ is the pump-probe delay. Retrieved temporal (d) and spectral (e) amplitudes and phases of the probe pulses.

References

[1] R. K. Bhalavi *et al.*, "Phase-matching-free ultrashort laser pulse characterization from a transient plasma lens", in Optics Letters **49**, 1321–1324 (2024).

[2] P. Béjot *et al.*, "Temporal characterization of laser pulses using an air-based knife-edge technique", in Advanced Photonics Research **6**, 2400074 (2025).

¹Advanced Laser Light Source (ALLS), Centre Énergie Matériaux Télécommunications, Institut National de la Recherche Scientifique (INRS-EMT), 1650 Boulevard Lionel-Boulet, Varennes, Québec, J3X1P7, Canada ²Université Bourgogne Europe, CNRS, Laboratoire Interdisciplinaire Carnot de Bourgogne ICB, UMR 6303, Dijon F21000, France

³Laboratoire d'Optique Appliquée, Ecole Polytechnique, ENSTA, CNRS, Université Paris Saclay, 181 Chemin de la Hunière, 91762 Palaiseau, France

^{*}marie.ouille@inrs.ca

△ UFO XIV Azores 2025

Broad-band second harmonic generation in a multi-pass cell

Arthur Schönberg, 1,* Nikolas Rupp, 1 Ana Oliveira e Silva, 1,2 Lorenzo Pratolli, 1,2 Vincent Wanie, 1,2 Francesca Calegari, 1,2,3 and Christoph M. Heyl 1,4,5

Abstract

We experimentally demonstrate phase- and group-delay optimized broad-band second-harmonic generation using a thin BBO-crystal placed inside a multi-pass cell, resulting in 15 fs, 5μ J pulses at 515 nm.

Multi-Pass-cells (MPCs) have been widely adopted for post-compression [1]. Benefiting from the unique degrees of freedom for tailoring nonlinear processes, their range of applications is currently being adapted to other nonlinear processes including wavelength-tuning [2] and second-harmonic generation (SHG) using nanosecond pulses [3]. Here, we experimentally explore SHG inside an MPCs and demonstrate phase- and group velocity matching across a broad phase-matching bandwith, defined by a single-pass though the thin SHG crystal. We employ 17 fs, infrared (IR) 1030 nm, 15 μ J driving pulses, resulting in 15 fs, 5 μ J pulses at 515 nm, (Fig 1(d-e)), corresponding to a conversion efficiency of 33 %. We use an MPC with R=1 m radius-of-curvature, N=4 round-trips (8 passes), k=1 and a length of about L=29 cm (Fig.1(a)), placed inside a vacuum chamber. A thin BBO crystal (type I phase-matching, cut angle of $\theta=23.4^{\circ}$, thickness: 78 μ m) used for SHG is placed at the cell center. The custom MPC mirrors compensate for a relative group-delay between the IR and SHG pulses introducing Δ GD = -15 fs per reflection. Figure 1(b) shows the SHG spectra as a function of Krypton gas pressure inside the vacuum chamber, used for dispersion-tuning. At an optimum pressure (here: 560 mbar) relative phase and group-delay are both matched, resulting in a maximum conversion efficiency of 33 % (Fig. 1(b)). Simulations reproduce the experimental results very well (Fig. 1(c)).

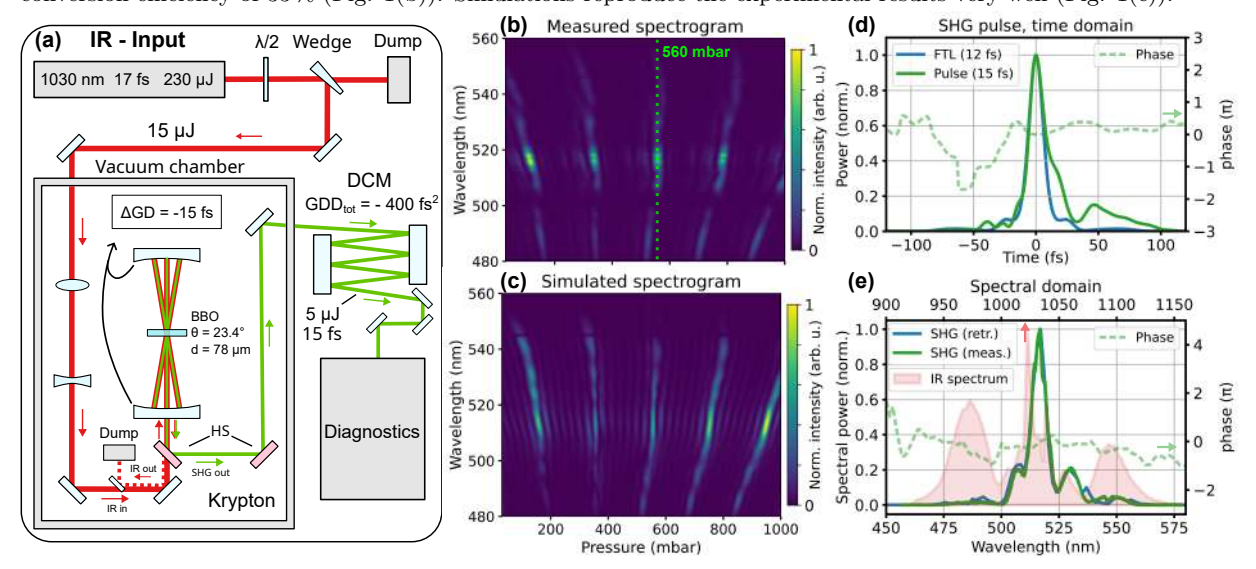


Figure 1: (a) Experimental setup. HS: Harmonic separator. DCM: Double-Chirped Mirror. (b,c) Measured/simulated SHG spectrogram. (d,e) Measured pulses and spectra (at green line in (b)).

In conclusion, we demonstrate SHG in an MPC using BBO as the nonlinear medium. Our experiments demonstrate the phase-tuning capabilities of MPCs in general, indicating the potential for tailoring other nonlinear optical processes in MPCs.

- [1] A.-L. Viotti et al., "Multi-pass cells for post-compression of ultrashort laser pulses," Optica 9, 197-216 (2022).
- [2] P. Balla et al., "Ultrafast serrodyne optical frequency translator", Nature Photonics 17, 187 (2023).
- [3] N. Kovalenko et al.,"Free-space quasi-phase matching", Opt. Lett. 48, 6220-6223 (2023) .

¹Deutsches Elektronen-Synchrotron DESY, Notkestraße 85, 22607 Hamburg, Germany

²Center for Free-Electron Laser Science CFEL, DESY, Hamburg, 22607, Hamburg

³Department of Physics, Universität Hamburg, 22761 Hamburg, Germany

⁴Helmholtz-Institut Jena, Fröbelstieg 3, 07743 Jena, Germany

⁵GSI Helmholtzzentrum für Schwerionenforschung GmbH, Planckstraße 1, 64291 Darmstadt, Germany

^{*}arthur.schoenberg@desy.de



Ultraviolet pulse shaping through four-wave-mixing-based upconversion

Linshan Sun,^{1,2,*} Hao Zhang,^{1,3} Cameron Leary,¹ Connor Lim,¹ Chad Pennington,¹ Gia Azcoitia,¹ and Sergio Carbajo^{1,2,3,4}

Abstract

Customized temporal shapes of femtosecond pulses are key challenges in ultrafast optics. Programmable pulse shapers are restricted to the visible and near-infrared because of the limited transmission range. We demonstrate an anti-symmetric dispersion transfer from near-infrared femtosecond pulses to ultraviolet through four-wave mixing.

Temporal shaping of ultrafast ultraviolet (UV) lasers is a pivotal technique for the coherent control of quantum systems¹, advanced dispersion control, and nonlinear optics, leading to enhanced performance across various applications. It allows precise control over energy distribution, stretching, and peak intensity². The duration control in the UV regime is also crucial for free electron lasers and DC-gun photoemission science because of emittance reduction³.

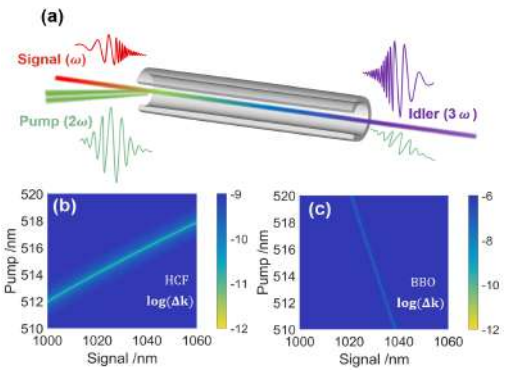


Fig. 1. Chirp transfer of the CFWM process in HCF. (b)(c) are the phase mismatching of the FWM for HCF and SFG in BBO crystal, respectively. The 2 axes are the signal and pump wavelength while the color bar represents the mismatching magnitude.

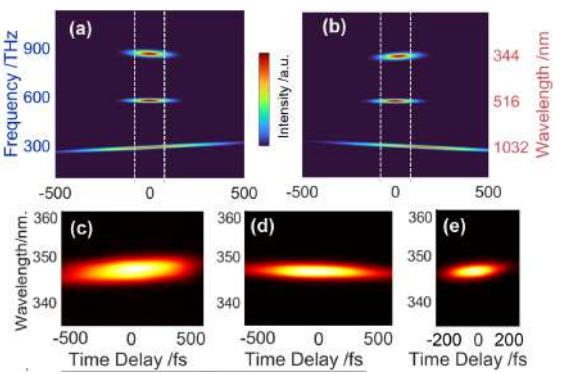


Fig. 2. Numerical calculation and experiment results.
(a)(b) are the numerical calculations of the FWM spectrogram under the delay positions of 0 fs (150 fs).
(c)~(e) are experimental spectra trace maps at UV idler pulse for a linear chirped signal pulse.

We demonstrate the second-order dispersion of the near-infrared pulse can transfer anti-symmetrically to the UV pulse with the opposite sign in the chirped four-wave mixing (CFWM) process^{2,4}. This technique broadens the foundation for ultrafast pulse indirectly temporal shaping. Fig. 2 shows the theoretical and experimental results under the low energy regime to avoid high self-phase modulation. Negatively chirped-high power UV pulses (over 10 μ J) are generated from the hollow capillary fiber (HCF) with 13.6% conversion efficiency by the broadband phase matching in argon gas where the wavevector mismatching is 4 orders lower than traditional crystals, as shown in Fig. 1(b)(c). It should have broad applicability because pulses usually suffer from positive dispersion and the pre-compensated UV pulse could solve the questions. A high-power handling spatial light modulator (SLM) is being applied in the Fourier plane to programmably shape the signal. We are currently doing more case studies based on the SLM.

- Rabitz, H., de Vivie-Riedle R, Motzkus, M. & Kompa, K. Whither the future of controlling quantum phenomena? Science 288, 824–828 (2000).
- Zhang, H. et al. Optimizing spectral phase transfer in four-wave mixing with gas-filled capillaries. Opt. Express 32, 44397–44412 (2024).
- 3. Zhang, H. *et al.* The Linac Coherent Light Source II photoinjector laser infrastructure. *High Power Laser Science and Engineering* **12**, e51 (2024).
- 4. Linshan, S. *et al.* Anti-symmetric chirp control by four-wave-mixing in gas-filled hollow capillary fibers. *arXiv* [physics.optics] (2025).

¹Department of Electrical Computer Engineering, University of California Los Angeles, Los Angeles, CA 90095, USA

²California NanoSystems Institute, 570 Westwood Plaza, Los Angeles, CA 90095, USA

³SLAC National Accelerator Laboratory, Stanford University, Menlo Park, California 94025, USA

⁴Physics and Astronomy Department, University of California Los Angeles, CA 90095, USA

^{*}lssun@ucla.edu

△ UFO XIV Azores 2025

Generation of extreme-ultraviolet spatiotemporal optical vortices

Rodrigo Martín-Hernández,^{1,2} Guan Gui,³ Henry C. Kapteyn,³ Margaret M. Murnane,³ Luis Plaja,^{1,2} Chen-Ting Liao,^{3,4} Miguel A. Porras,⁵ Carlos Hernández-García ^{1,2,*}

- ¹ Grupo de Investigación en Aplicaciones del Láser y Fotónica, Universidad de Salamanca, 37008, Salamanca, Spain
- ² Unidad de Excelencia en Luz y Materia Estructuradas (LUMES), Universidad de Salamanca, Salamanca, Spain
- ³ JILA and Department of Physics, University of Colorado and NIST, Boulder, CO 80309, United States of America
- ⁴ Department of Physics, Indiana University, Bloomington, IN 47405, United States of America
- ⁵ Grupo de Sistemas Complejos, ETSIME, Universidad Politécnica de Madrid, Ríos Rosas 21, 28003 Madrid, Spain *carloshergar@usal.es

Abstract

Spatiotemporal optical vortices (STOVs) are structured light wavepackets entangled in the spatial and temporal domains. Their generation has been limited to the infrared and visible regimes, restricting their potential applications. Here we theoretically and experimentally demonstrate for the first time generation of extreme-ultraviolet STOVs through nonlinear up-conversion of infrared STOVs.

Spatiotemporal optical vortices (STOVs) are unique structured light fields with a e intertwined phase distribution in the spatial and temporal domains. Contrary to standard spatial/longitudinal optical vortices (LOV), STOVs are not propagation eigenmodes [1]. The non-trivial propagation dynamics make STOVs well-suited candidates for diverse applications: from information carriers to probing ultrafast dynamics in novel materials. However the generation of STOVs has been limited to the infrared/visible regimes [2], due to low efficiency of optical elements beyond the ultraviolet. Here we demonstrate both theoretically and experimentally the generation of extreme-ultraviolet (EUV)-STOVs for the first time [3]. Thanks to the high nonlinear process of high-order harmonic generation (HHG), EUV STOVs with high topological charge can be produced. We study the up-conversion process, which, contrary to LOV-driven HHG [4], is strongly affected by the non-trivial propagation dynamics of STOVs, whose comprehension is fundamental to understand the duality between spatio-temporal and -spectral optical vortices (SSOV), (see Fig. 1).

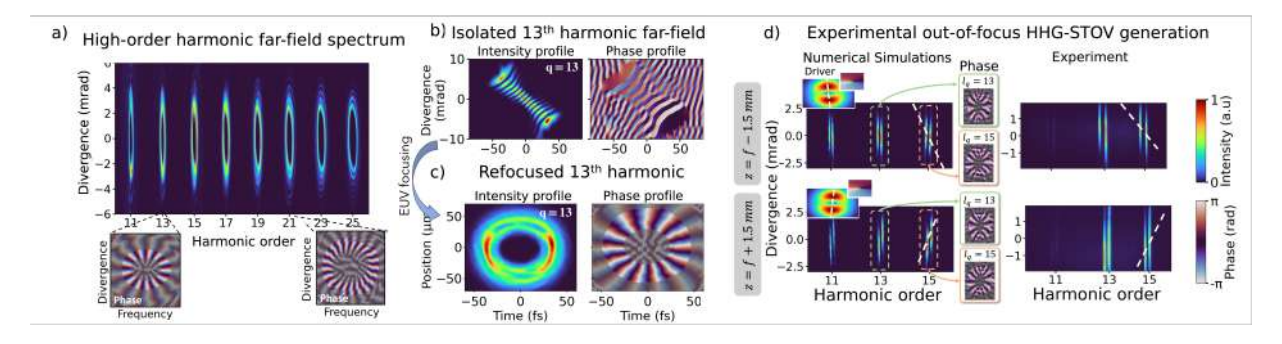


Figure 1: Generation of EUV STOVs through high-order harmonic generation. a) Simulated HHG far-field spectrum driven by IR STOVs. b) Far-field and c) refocused spatiotemporal intensity and phase distribution of the 13th harmonic order. d) Theory vs experiment comparison in the generation of inhomogeneous EUV STOVs at two gas jet positions along the propagation direction.

- [1] M. A. Porras, and J. W. Spencer "Procedure for imparting transverse orbital angular momentum by focusing spatiotemporally coupled ultrashort pulses." Physical Review A 109, 033514 (2024).
- [2] G. Gui, et al. "Second-harmonic generation and the conservation of spatiotemporal orbital angular momentum of light." Nature Photonics 15, 608-613 (2021).
- [3] R. Martin-Hernández, et al. "Extreme-ultraviolet spatiotemporal vortices via high harmonic generation." arXiv:2412.01716 [physics.optics]. Nature Photonics, in press (2025).
- [4] C. Hernández-García, et al. "Attosecond extreme ultraviolet vortices from high-order harmonic generation." Physical Review Letters 111, 083602 (2013).

Burst-mode multi-GHz pulse repetition rate ps laser with kW average power for high throughput laser processing

Hanyu Ye¹, Lilia Pontagnier¹, Abdelkrim Bendahmane¹, Annalisa Guandalini ², Matthias Kemnitzer², Martin Gorjan², Jürg Aus der Au², André Loescher³, Florian Bienert³, Marwan Abdou Ahmed³, Giorgio Santarelli¹ and Eric Cormier^{1,*}

Abstract: Fully configurable picosecond pulses at 1 to 7.5 GHz with tens to thousands pulses per burst are demonstrated at the kW average power level and several mJ energy per burst.

Recent advancements in high-power lasers that can produce GHz pulse bursts represent a major leap in industrial laser processing. This technology addresses the growing need for precision and efficiency in tasks like materials machining, surface texturing, and microfabrication. Achieving optimal results depends on the material and process, making it essential to have flexibility in parameters such as pulse repetition rate and energy per burst. Here, we report on a unique high-power laser system capable of generating bursts of pulses whose repetition rate is continuously adjustable from 1 to 7.5 GHz at a maximum average power of 1 kW and a maximum energy per burst of 10 mJ.

The system consists of 3 modules: a GHz all fibered pulse-burst generator, a solid-state pre-amplifier and a thin-disk booster amplifier all based on Yb-doped materials and operates at the wavelength of 1030 nm. The main feature of the system concerns the ability to generate arbitrary bursts of picosecond pulses (below 2 ps). In fact, the parameter space includes the pulse repetition rate which can be continuously varied from 1 to 7.5 GHz, the number of pulses per bursts ranging from 1 to several thousands and the burst repetition rate limited to a minimum of 100 kHz. An example is given in fig. 1 where 5 pulses where selected from a train at 7.5 GHz and a final burst repetition rate of 100 kHz. Note here that a special configuration allows to generate pulses with a repetition rate as low as 50 MHz for particular applications simply by reprogramming the system without any additional hardware. The electro-optical modulation technology at the core of the system allows to produce and amplify pulses with typical duration between 800 fs and 2 ps as depicted in Fig.2 (center). Finally, the temporally shaped bursts of GHz can be amplified up to 250 W in the commercial amplifier (Spectra-Physics) used as a pre-amplifier and up to 1 kW in a multipass thin-disk amplifier with excellent beam quality as shown in Fig. 2 (right).

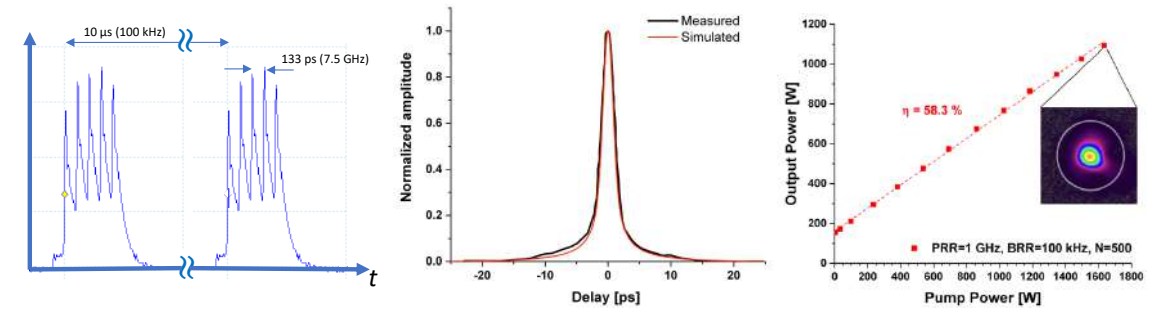


Fig. 2. Left: Typical generated burst with 5 pulses at 7.5 GHz for a burst repetition rate of 100 kHz). Center: Autocorrelation trace of the amplified pulses with 1.8 ps duration. Power curve of the main amplifier to the kW level (uncompressed) with bursts of 500 pulses at 1 GHz.

We have demonstrated a complete laser system producing fully configurable bursts of pulses (from 1 to several thousands) with GHz intra-bursts repetition rate continuously ranging from 1 to 7.5 GHz. Typical compressed durations are below 2 ps and average power of close to 1 kW and 10 mJ energy per burst. The system with state-of-the art performances will be used to demonstrate record performances in precision manufacturing and laser processing.

¹Laboratoire Photonique Numérique et Nanosciences (LP2N), UMR 5298, CNRS-IOGS-Université Bordeaux, 33400 Talence, France

² Spectra-Physics, MKS Instruments, Inc., Feldgut 9, 6830 Rankweil, Austria

³ Universität Stuttgart, Institut für Strahlwerkzeuge (IFSW), Pfaffenwaldring 43, 70569 Stuttgart, Germany

^{*}eric.cormier@u-bordeaux.fr



Spectral phase interferometry for direct electric-field reconstruction of synchrotron light from tapered undulators

Takao Fuji,^{1,*} Takashi Tanaka,² Tatsuo Kaneyasu,³ Yuichiro Kida,⁴ Kei Imamura,⁴ Satoshi Hashimoto,⁵ Aoi Gocho,⁶ Keisuke Kaneshima,⁶ Yoshihito Tanaka,⁶ and Masahiro Katoh^{3,7}

Abstract

We have characterized the synchrotron light from tapered undulators using spectral phase interferometry for direct electric-field reconstruction. The measured spectral phases of the chirped waveforms are consistent with the theoretical prediction.

An undulator is a device which is widely used in the modern synchrotron light sources to produce light with high optical power density. Standard undulators produce quasi-monochromatic light by modulating the electron with sinusoidal magnetic field. To generate light with broad spectrum from the undulator, tapered undulators are designed. The gap between the permanent magnets in the undulator linearly changes and the amplitude of the sinusoidal magnetic field changes along the longitudinal axis. It results that the wavelength of the radiation changes in time, namely, the radiated light wave is chirped. Such a chirp can be predicted through special theory of relativity but has not been measured so far. In this contribution, we present the waveform characterization of chirped waveforms from tapered undulators using spectral phase interferometry for direct electric-field reconstruction (SR-SPIDER) [1].

The experiment was carried out at BL01 of the NewSUBARU storage ring. Two identical undulators were installed together with a three-pole electromagnet as a chicane. The undulator was composed of 12 magnet modules, each of which corresponds to a single undulator period. The taper of the undulator was controlled by changing the magnetic gap of the modules independently [2].

We performed SR-SPIDER measurements for three cases, namely, down chirp, up chirp, and chirp-free. The taper for the chirp was created by setting the gap difference to 3.4 mm for the 2 m length of the undulator. The center wavelength of the radiation was set to 750 nm, which corresponds to the gap of 54.7 mm.

Figure 1 shows the power spectra and the retrieved spectral phases of the synchrotron light. We can clearly see the down and up chirp corresponding to the up and down parabolic curves of the spectral phase although the step function that comes from the square shaped envelope remains. The group delay dispersions of the up and down chirped waveforms were calculated by fitting the central part of the spectral phase and these were ± 15 fs², respectively, which is in agreement with theory.

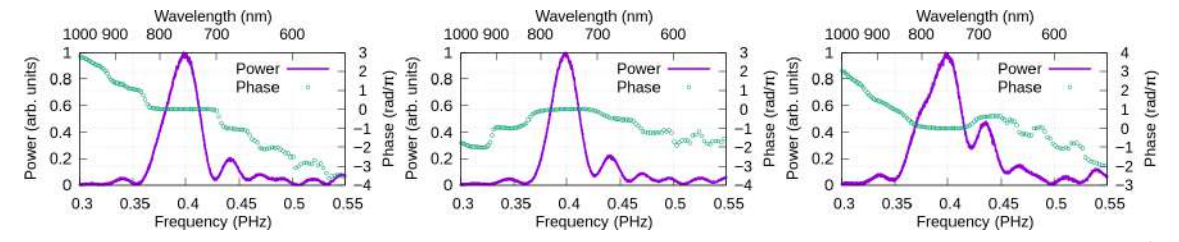


Figure 1: Power spectra and retrieved spectral phases of the electric fields generated by the untapered (left), down chirp tapered (middle), and up chirp tapered (right) undulator, respectively.

- T. Fuji, et al. "Spectral phase interferometry for direct electric-field reconstruction of synchrotron radiation," Optica 10, 302–307 (2023).
- [2] T. Tanaka, et al. "Development of a tapered undulator for the NewSUBARU synchrotron radiation facility," J. Synchrotron Rad. 28 404–409 (2021).

¹Laser Science Laboratory, Toyota Technological Institute, Nagoya, 468-8511, Japan

 $^{^2\}mathrm{RIKEN}$ S
Pring-8 Center, Koto 1-1-1, Sayo, Hyogo 679-5148, Japan

 $^{^3 {\}rm Institute}$ for Molecular Science, Okazaki 444-8585, Japan

⁴ Japan Synchrotron Radiation Research Institute, Sayo, Hyogo 679-5198, Japan

⁵Laboratory of Advanced Science and Technology for Industry, University of Hyogo, Kamigori, Hyogo 678-1205, Japan

⁶Graduate School of Science, University of Hyogo, Kamigori, Hyogo 678-1297, Japan

⁷Research Institute for Synchrotron Radiation Science, Hiroshima University, Higashi-Hiroshima 739-0046, Japan

^{*}fuji@toyota-ti.ac.jp

△ UFO XIV Azores 2025

Sub-80-fs 2 µm thulium-holmium-doped fluoride fiber oscillator

Hiroki Kawase,^{1,2} Nur Atika Azali,¹ and Takao Fuji¹

¹Laser Science Laboratory, Toyota Technological Institute, Nagoya, 468-8511, Japan

Abstract

We report a femtosecond mode-locked oscillator at $\sim 2.1 \, \mu m$, based on a thulium-holmium-doped fluoride fiber. The oscillator generates positively chirped 349 fs pulses with a pulse energy of 2.34 nJ. The pulse was compressed to 74 fs using six 10 mm BK7 glass plates.

Holmium (Ho)-doped lasers are attracting attention as high-energy, ultrafast short-wavelength infrared sources for high-field physics. Their emission around 2 μ m benefits from the absence of water vapor absorption and a high emission cross section. However, it is difficult to generate sub-100-fs pulses in such lasers due to the inherently narrow spectral bandwidth of Ho.

In this work, we developed a femtosecond oscillator at $\sim 2.1~\mu m$ based on a thulium (Tm)- and Ho-doped double-clad fluoride fiber (Tm:Ho:ZBLAN), pumped by a 0.79 μm laser diode. While femtosecond oscillators using Tm-Ho-doped silica fibers were demonstrated, their pulse durations were limited to 160 fs without external nonlinear spectral broadening [1]. We expect that shorter pulses can be generated using fluoride fibers that have less anomalous dispersion in the wavelength range. In particular, we previously demonstrated the generation of 45 fs pulses from a Tm-doped fluoride fiber laser, the shortest to date for Tm-doped fiber lasers [2, 3].

Our oscillator employs a ring cavity and nonlinear polarization rotation mode-locking. The gain medium was a double-clad Tm:Ho:ZBLAN fiber (8.6 μ m core, dispersion of -0.013 ps²) with Tm and Ho doping concentrations of 40,000 ppm and 2,000 ppm, respectively. At 1.81 W pump power, the oscillator produced 179 mW output power at 76.5 MHz. The pump power dependence of the output spectrum, shown in Fig. 1, reveals a redshift and spectral broadening with increasing the pump power. The oscillator's output pulses, characterized by a home-built SHG-FROG, exhibited a duration of 349 fs and a dispersion of 7,650 fs². By employing six 10 mm thick BK7 plates for dispersion compensation, we successfully compressed the pulses to 74 fs, achieving the shortest pulse duration reported for a Ho-doped fiber laser oscillator without external nonlinear spectral broadening.

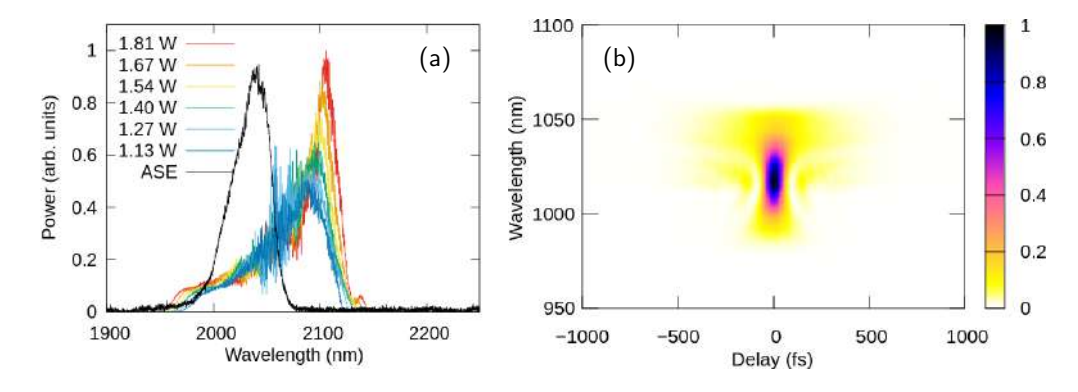


Figure 1: (a) Pump power dependence of the output spectrum of the oscillator. The black curve shows the spectrum of the amplified spontaneous emission from the active fiber. (b) SHG-FROG trace of the oscillator output compressed with six BK7 glass plates with a thickness of 10 mm.

- [1] P. Li, A. Ruehl, U. Grosse-Wortmann, and I. Hartl, "Sub-100 fs passively mode-locked holmium-doped fiber oscillator operating at 2.06 μ m," Opt. Lett. **39**, 6859 (2014).
- [2] Y. Nomura and T. Fuji, "Sub-50-fs pulse generation from thulium-doped ZBLAN fiber laser oscillator," Opt. Express 22 12461 (2014).
- [3] Y. Zhang, et al. "Advances and challenges of ultrafast fiber lasers in 2–4 μm mid-infrared spectral regions," Laser Photon. Rev. 18, 2300786 (2024).

²RIKEN Center for Advanced Photonics, RIKEN, Wako, 351-0198, Japan

^{*}fuji@toyota-ti.ac.jp

Multichannel Yb:YAG laser architecture for peak and average power scaling

Ivan Kuznetsov*, Sergey Chizhov, Nikolay Karpov, and Oleg Palashov

A.V. Gaponov-Grekhov Institute of Applied Physics of the Russian Academy of Sciences, 46 Ul'yanov Street, Nizhny Novgorod, 603950, Russia *kuznetsov@ipfran.ru

Abstract

A new architecture of a MOPA laser system with a 4-channel Yb:YAG single-rod amplifier was proposed and brought to life. Tiled aperture coherent beam combining with 20W average power, 17mJ pulse energy, 57% power in the central beam lobe, and ~1% RMS of residual intensity fluctuations was demonstrated.

Today Yb:YAG lasers is a leading laser technology, providing both, high peak and high average power radiation. With its development, power increasing becomes more and more problematic, approaching its limit [1]. A promising option for the further power scaling is switching to a multi-channel laser scheme with coherent beam combination. The key problem here is the creation of identical channels, which is aggravated by the strong influence of thermal effects. We propose a new architecture of a multichannel laser amplifier that allows us to significantly simplify the task of channel multiplication. The idea is to amplify several beams in one rod active element (AE), when the beams are located symmetrically relative to the rod axis and along its cooled side surface. It provides effective cooling of the AE through the side surface and symmetric gain and thermal conditions for all beams. Based on the presented geometry, a MOPA laser system with a 4-channel Yb:YAG amplifier and coherent beam combining is implemented, the scheme of which is shown in Fig. 1.

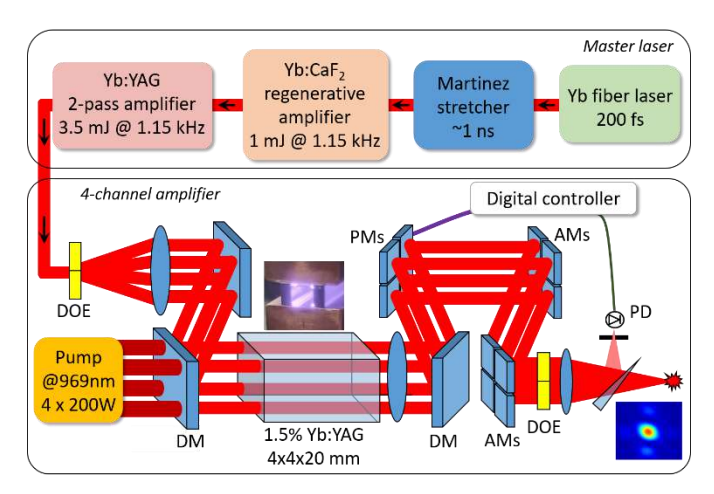


Figure 1: Optical scheme of laser system. DOE – diffraction optical element, DM – dichroic mirror, AMs – adjustment mirrors, PMs – mirrors on piezo actuator, PD - photodiode.

The signal beam is split into 4 replicas with a diffraction optical element and amplified in a single rectangular parallelepiped shaped AE, passing along its 4 edges. Coherent combination is realized with a "tiled aperture" scheme using the digital controller based on the "hill climbing" algorithm. To date, such a system has achieved full pulse energy >17 mJ at an average power of ~20 W, with 57% power in the central lobe of the beam and ~1% RMS of residual intensity fluctuations. The next step will be to increase the pulse energy in each channel up to ~50 mJ, which was successfully demonstrated in the single-channel rod "diverging beam amplifier" proposed in [2], as well as to increase the number of channels up to 16.

References

[1] C. Herkommer et. al., "Ultrafast thin-disk multipass amplifier with 720 mJ operating at kilohertz repetition rate for applications in atmospheric research", Opt. Express **28** (20), 30164-30173 (2020).

[2] I. Kuznetsov et. al., "Yb:YAG diverging beam amplifier with 20 mJ pulse energy and 1.5 kHz repetition rate," Opt. Lett. 48, 1292-1295 (2023).

MW-Peak-Power Ho:YAG Thin-Disk Laser

Yuya Koshiba, ¹ Jiří Mužík, ¹ Pavel Peterka, ² Pavel Honzátko, ² Miroslav Šlechta, ² Antonín Fajstavr, ³ Sabina Kudělková, ³ Martin Smrž^{1,*} a Tomáš Mocek ¹

Abstract

We report on 2.09- μ m-emitting Ho:YAG thin-disk lasers with mJ pulse energy. High-peak-power operation in single-mode beam was achieved using cavity-dumping technique, producing pulses with 6.2 mJ energy, 3.7 ns duration, 1.7 MW peak power at 500 Hz repetition rate. We compare diode pumping at 1.91- μ m with Tm-fiber-laser. Sub-picosecond MOPA system will be discussed as well.

Thanks to low water absorption, low scattering in atmosphere and operation in eye-safe spectral region, Ho-based lasers have found many applications in medicine, spectroscopy, remote sensing and detection of atmospheric gases, various military and defense applications, and free space communications. Thin-disk geometry is known for its power and energy scalability can bring improved performance in terms of pulse energy and brightness.

We demonstrate status of fully in-house developed Ho:YAG thin-disc technology, and compare direct diode pumping at wavelength of 1.91-µm with in-house developed Tm-doped fiber lasers emitting at 1908 or 1940 nm. Tm-fiber lasers up to 0.25 kW are under development at Institute of Photonics and Electronics in Prague now. At 50-W pump power level, our Ho:YAG SiC-bonded thin disc working in cavity-dumped regime was delivering 3.7 ns long pulses with 6.2 mJ pulse energy, 500 Hz pulse repetition rate and 1.7 MW peak power with wavelength of 2090 nm. In this regime, it was possible to increase repetition rate up to 2 kHz, and to reach pulse energy stability of 0.66% (RMS). At repetition rate of 2 kHz dropped output power level to 9.0 W. Performance of the laser system in the electro-optically cavity dumped operation (RTP Pockels cell) shows Figure 1.

The nanosecond laser is based on a simple V-shaped cavity. A Ho:YAG thin disk manufactured by Crytur, s.r.o. (crystal growth, coating, and heatsink bonding) with Ho³⁺ doping concentration of 1.5 at.%, diameter of 8 mm, and SiC heatsink was placed into a 72-pass thin-disk pump module. Pump fiber-coupled diode laser provided up to 50 W CW output at wavelength around 1910 nm (bandwidth ca. 10 nm FWHM). The pump spot diameter on the thin disk had a diameter of 2.4 mm. CW cavity dumped and Q-switched regimes as well as sub-picosecond MOPA system (under development) based on the in-house technology with optimized Ho:YAG diamond-bonded thin disc and upgraded Tm-fiber laser pumps will be reported at the conference as well.

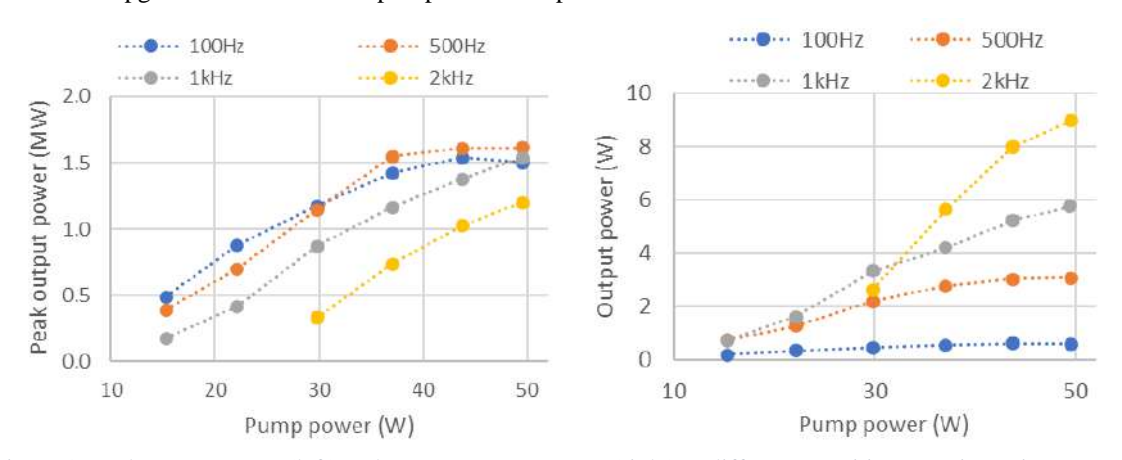


Figure 1: Peak output power (left) and average output power (right) at different repetition rates in cavity dumping operation.

This work was supported by European Union and the state budget of the Czech Republic under the project LasApp CZ.02.01.01/00/22 008/0004573.

¹Hilase centre, Institute of Physics AS CR, Za Radnicí 828, CZ-25241 Dolni Brezany, Czechia

²Institute of Photonics and Electronics AS CR, Chaberska 1014/57, CZ-18200 Prague 8, Czechia

³Crytur s.r.o., Na Lukách 2283, CZ-51101 Turnov, Czechia

^{*}martin.smrz@hilase.cz

Spatiotemporal Characterization of High-Power Light Springs Using Off-Axis Holography and IMPALA

Pablo San Miguel Claveria*¹, S. Smartsev², G. Vaz^{3,4}, R. Neumann¹, R. Almeida¹, R. Neumann¹, J. Pereira¹, C. Miranda¹, M. Fajardo¹, J. Faure², M. Piccardo^{3,4}

^{,1}GoLP / Instituto de Plasmas e Fusão Nuclear Instituto Superior Técnico, Lisbon, Portugal

Abstract

We synthesized and characterized Light Springs at a moderately high-power laser using off-axis holography, retrieving their orbital group velocity in good agreement with recently developed theory. To address challenges posed by low repetition rates, we explored IMPALA as a complementary diagnostic, enabling single-shot access to key spatiotemporal features of the beam.

Main Text

The ability to structure ultrashort laser pulses in both space and time has opened new frontiers in beam shaping, enabling novel light fields such as Light Springs—beams in which each spectral component carries a distinct orbital angular momentum [1]. These beams exhibit complex spatiotemporal couplings that require advanced diagnostics for complete characterization, especially as they are scaled to higher powers and lower repetition rates.

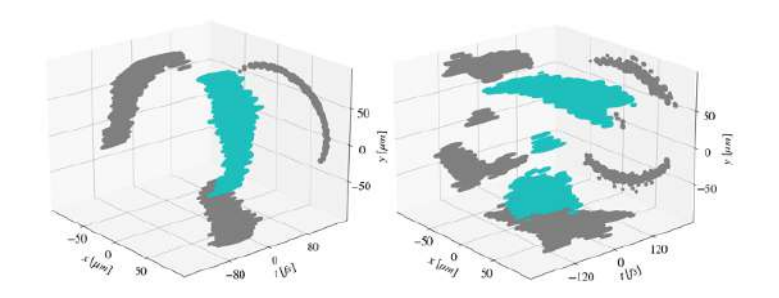


Figure 1: Isosurfaces of the measured lightsprings using off-axisholography. Left: single Light Spring. Right: Intertwined helices.

We report on the synthesis and characterization of a Light Spring generated at the TW-class VOXEL laser system using a diffractive axicon and a reflective spatial light modulator for spectral phase control. The beam exhibits a helical structure in space-time, and we first characterized it using off-axis holography to reconstruct its phase and amplitude in the far field. From this, we extracted the orbital group velocity, which showed excellent agreement with a recent theoretical model developed at IST.

Recognizing the limitations of interferometric techniques in high-power, low-repetition-rate systems, we then implemented and adapted the IMPALA diagnostic [2], to our Light Spring configuration. This required a novel optical relay setup and in-house fabrication of precision IMPALA masks. Preliminary measurements confirm IMPALA's ability to resolve the beam's modal structure, providing spatiotemporal information of the synthetised Light Springs.

This work represents a significant step forward in the metrology of complex spatiotemporal beams, demonstrating the combined use of interferometric and few-shot diagnostics for structured light in high-power laser systems.

References

[1] M. Piccardo, *et. al.*, "Broadband control of topological–spectral correlations in space–time beams", Nat. Photon. 17, 822–828 (2023)

[2] Slava Smartsev, *et. al.*, "Simple few-shot method for spectrally resolving the wavefront of an ultrashort laser pulse," Opt. Lett. 49, 1900-1903 (2024)

²LOA / CNRS, Ecole Polytechnique, ENSTA Paris, Institut Polytechnique de Paris, Palaiseau, France

³Department of Physics, Instituto Superior Técnico, Universidade de Lisboa, Lisbon, Portugal

⁴Instituto de Engenharia de Sistemas e Computadores - Microsistemas e Nanotecnologias (INESC MN), Lisbon, Portugal

^{*}pablo@san.miguel.claveria@tecnico.ulisboa.pt

Approaching kW-class λ^3 regime at ELI ALPS

Adam Borzsonyi,* Janos Csontos, Peter Jojart, Balint Kiss, Roland S. Nagymihaly, Imre Seres, Szabolcs Toth, Barnabas Gilicze, Prabhash P. Geetha, Viktor Pajer, Janos Bohus, Levente Lehotai, Eric Cormier, Rodrigo Lopez-Martens, Mikhail Kalashnikov, Katalin Varju, Gabor Szabo

ELI ALPS, ELI-HU Non-Profit Ltd., Wolfgang Sandner utca 3., Szeged, H-6728, Hungary *adam.borzsonyi@eli-alps.hu

Abstract

ELI ALPS offers beamtime for scientists around the world at state-of-the-art ultrafast pulse facilities with hundreds of watts of a verage power. This paper describes recent user-inspired laser developments towards even shorter pulses and improved spatial focusability while taking care of enormous thermal load on optics.

Ongoing developments of few-cycle, extreme average power lasers

As ELI ERIC recently opened its 7th call for proposals [1], researchers are invited to conduct multi-disciplinary scientific experiments in our facilities. ELI ALPS offers a broad range of ultrafast pulse sources, which include XUV, electron, proton and neutron beams and their driving laser sources. In this paper, we focus on this latter segment of our portfolio and review recent developments in the spatial and temporal improvements of the laser pulses. Following several dozens of user experiments successfully performed in previous calls, we received first-hand practical feedback on the most important aspects of beam quality and temporal shape of pulses and their stability at extreme thermal stress, and insight into the directions we should steer developments.

One common goal for all laser systems at ELI ALPS is to reach the few-cycle regime at the multi-100-W average power level [1], using fiber technology at 100 kHz repetition rate (HR lasers), OPCPA in the 1-100 kHz range (MIR and SYLOS lasers) and Ti:Sapphire at 10 Hz (HF PW). Since amplification is spectrally limited in all cases, we therefore explored numerous post-compression techniques to reduce the pulse duration. But how much is it worth pushing the spectral limits before post-compression? OPCPA configurations in SYLOS systems enabled us to reach 6.6 fs [2], but we learned that for everyday operational reasons, a less spectrally overloaded amplifier with a simple post-compression stage was found to operate more reliably. Among the available post-compression methods, particularly at high average powers, we found that multi-pass cells [3] or single pass thin plate compressors in a vacuum environment with loose focusing [4] constitute the most promising approach. For high repetition rates and long pulses, multi-pass cells offer reasonably high compression factors and long uninterrupted operation times. For shorter pulses in the 10-100 mJ energy range, limited compression factors can be best achieved in a single thin plate compressor with appropriate beam imaging, but beam homogeneity and n₂-induced beam graininess appear as the main bottleneck. Therefore, for applications towards the Joule regime, we created a testbed with beam apodization to study the optimal homogeneity required for thin plate compression.

As these examples showed us, spatial quality plays a critical role and poses serious technical challenges when aiming for pulse reduction. In our SYLOS systems, we successfully implemented vacuum spatial filters utilizing glass cones to overcome the beam profile issue. Wavefront correction with deformable mirrors is also a crucial part of the process. Thermalload related issues are connected to wavefront distortions in many areas. We showed that vacuum conditions significantly reduce rapid wavefront shimmering in an expanded beam already in the backend of the laser system. Optics and opto-mechanics also suffer mechanical distortions under heat stress, causing severe astigmatism in the beam, which – when coupled with nonlinear propagation in multi-pass cells – turned to be a critical challenge with the HR2 laser at kW-class average power. Consequently, distortion-free mounts, deformable mirrors and pointing stabilization loops are must-have components for these high average power systems. We discuss past experiences and countermeasures related to best practices in focusing these beams.

Characterizing spatiotemporal distribution of these focused pulses is another crucial area of development. We performed a comparative study of methods at different levels of compressed pulse durations [5]. We also report on our recent experiences with spatiotemporal characterization of our systems, especially on the 100kHz MIR [6] and HF PW systems [7].

References

[1] https://up.eli-laser.eu

[2] S Toth et al., J. Phys. Photonics **2**, 045003.

[3] B. Gilicze et al., Optica Open, preprint ID 121099

[4] S Toth et al., Optics Letters 48, 57.

[5] V.Pajer et al. Optics Express 32, 15710.

[6] R.S. Nagymihaly et al. Optics Express 33, 17551.

[7] R.S. Nagymihaly et al. Optics Express 31, 44160.

HYPerspectral Ultrafast Source - HYPUS

É. Doiron¹, M. Ivanov^{1,2}, M. Scaglia¹, P. Abdolghader¹, M. Stratmann-Meouchi¹, X. Zheng^{1,2}, G. Tempea¹, G. Vampa³, B. E. Schmidt¹

Abstract

Employing two cascaded hollow-core fibers (HCFs) 55W, 1.3mJ, sub 7fs are achieved with ~70% efficiency and long-term hands-off operation. We exploit these pulses to derive new wavelengths via various nonlinear conversion techniques ranging from the deep UV (200 nm) up to the far IR (12 um).

Main Text

Starting from an 80W, 2mJ Yb laser (Light-Conversion Carbide), we achieved 1.3mJ, sub-3 cycle pulse compression (grey curves in fig. 1) with 70% efficiency with excellent short- and long-term stability [1]. We use these pulses to derive widely tunable secondary outputs in an "OPA free" fashion. Few uJ-level deep UV pulses (purple curves) are generated in a third HCF via resonant dispersive wave (RDW) generation [2]. Up to several watts of 50fs VIS pulses can be achieved via SHG and durations as short as 9fs can be achieved in a sandwiched SHG configuration with 5% efficiency (green curves). The supposedly CEP stable mid (red curves) - and far IR ranges (black lined) are accessible via intra-pule DFG. NIR wavelength between 1.3 – 1.9um can be obtained as an idler wave emerging from a second, DFG booster crystal. Noteworthy, since all outputs are derived from the same 3 cycle driver at 1030nm, they are temporally synchronized.

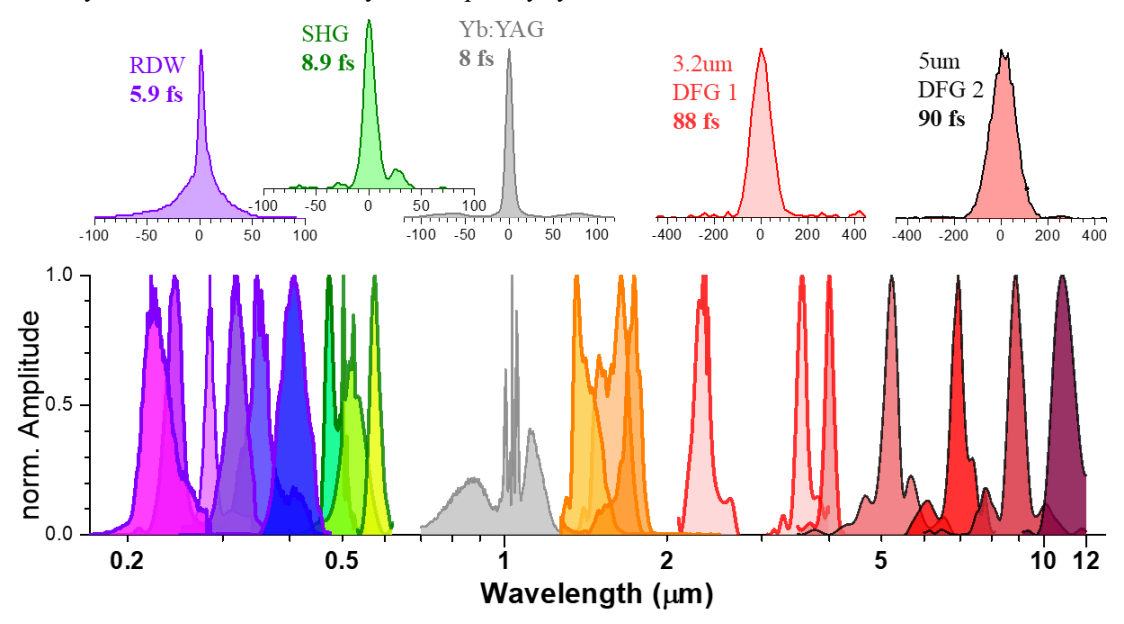


Figure 1: HYPUS spectral tuning range (bottom) and corresponding temporal pulse shapes. The tuning range can be covered by 6, independently tunable channels that can be available at the same time.

References

[1] M. Ivanov et al., "Advancing high power hollow-core fiber pulse compression," *IEEE JSTQE*, **30**, 6, 1-10 (2024).

[2] J. C. Travers et al., "High-energy pulse self-compression and ultraviolet generation through soliton dynamics in hollow capillary fibres," Nat. Phot. 13, 547 (2019).

¹few-cycle Inc., 1650 Blvd. Lionel Boulet, J3X 1P7, Varennes, QC, Canada

²INRS-EMT, 1650 Blvd. Lionel Boulet, J3X 1P7, Varennes, QC, Canada

³University of Ottawa and National Research Council of Canada, Ottawa, Canada USA

^{*}schmidt@few-cycle.com

Single-Shot Measurements of Carrier-Envelope Phase at 293 kHz Pulse Repetition Frequency

Paulo T. Guerreiro, 1,2,* Jose C. Alves, 3,4 Celso P. Figueiredo, 3 Vitor A. Amorim, 1,2 Miguel Miranda, 1,2 Chen Guo, 5 Anne-Lise Viotti, 5 Cord L. Arnold, 5 Anne L'Huillier, 5 Helder Crespo, 1 and Rosa Romero 1,2

Abstract

We present carrier-envelope phase (CEP) laser pulse measurements of single-shot and every-shot at 293 kHz pulse repetition frequency using a digital line sensor. We also demonstrate the possibility of doubling the acquisition frequency by synchronizing two line sensors.

As ultrashort few-cycle pulses from amplified laser systems become available at pulse repetition frequencies (PRF) of many hundreds of kHz, there is a requirement for faster single-shot every-shot carrier-envelope phase (CEP) diagnostics. CEP measurements at 200 kHz [1], and recently at 586 kHz, has been demonstrated using optical Fourier transform interferometry, overcoming constraints of digital line sensor speeds and data transfer. Here we present measurements at 293 kHz using a digital sensor, and show the possibility of measuring at twice this PRF.

The laser source is a CEP-stable Pharos (Light Conversion) that generates 170 fs pulses at PRF of 586 kHz and sub-multiples. We direct the beam through a white-light generation f:2f interferometer so each pulse produces a spectrally modulated pattern that encodes in the pattern phase the CEP of the pulse [2]. The beam is then split into a double spectrometer with two different fast linear sensors connected to FPGAs. The master spectrometer is synchronized to the laser pulse output, and provides the second spectrometer with a synchronization signal with adjustable delay. The master spectrometer can measure every shot up to 100 kHz, while the second spectrometer can measure every shot up to 300 kHz. We use the FPGA that acquires the data from the sensor to calculate the Fourier transform and CEP, and only transfer to the computer the time-tagged CEP data, therefore reducing constrains on data transfer. To correlate the CEP measurement of the two detectors, we set the laser PRF to 293 kHz, and synchronize the two detectors to measure every pulse (at 293 kHz) with the second spectrometer, and every third pulse (at 97.7 kHz) with the master spectrometer. Figure 1 shows the CEP measured with both spectrometers over a period of 1 ms (the phase offset between the two measurements is arbitrary). By adjusting

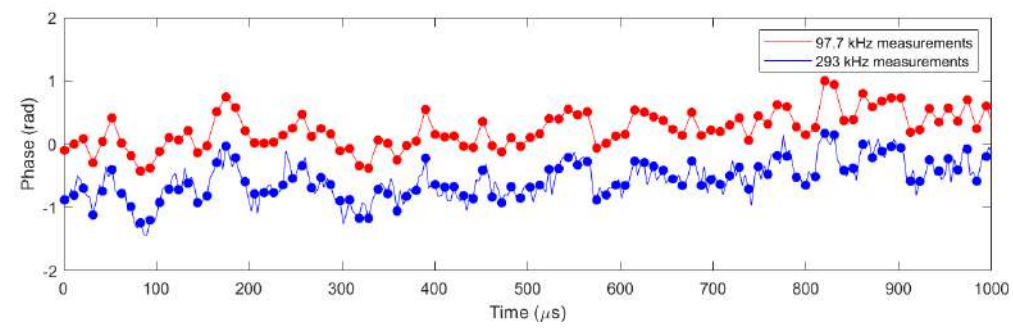


Figure 1: CEP measurements with two synchronized digital spectrometers; the 97.7 kHz spectrometer only measures one in every third pulse measured by the 293 kHz spectrometer; dots indicate same pulse measurements

the delay of the synchronization signal to the second spectrometer, we are able to capture spectra from different pulses on the two spectrometers, demonstrating the possibility to perform CEP measurements at 586 kHz PRF, when using two synchronized spectrometers measuring alternate pulses at 293 kHz.

- [1] C. Guo, et al., Opt. Lett. 48, 5431-5434 (2023).
- [2] M. Kakehata, et al., Opt. Lett. 26, 1436-1438 (2001).

¹ Sphere Ultrafast Photonics, Rua do Campo Alegre, 1021, Ed. FC6, 4169-007 Porto, Portugal

² IFIMUP-IN, Universidade do Porto, Rua do Campo Alegre 687, 4169-007 Porto, Portugal

³ Faculdade de Engenharia da Universidade do Porto, Rua Dr. Roberto Frias, 4200-465 Porto, Portugal

⁴INESCTEC Rua Dr. Roberto Frias, 4200-465 Porto, Portugal

⁵ Department of Physics, Lund University, P. O. Box 118, SE-22100 Lund, Sweden

^{*}pguerreiro@sphere-photonics.com

Advanced High Harmonic Generation Beamline for Tailored XUV at ELI Beamlines

Matyáš Staněk^{1,2*}, Lucie Jurkovičová^{1,2}, Jan Vábek^{1,2}, Fauzul Rizal^{1,2}, Martin Albrecht¹, Jaroslav Nejdl^{1,2}, and Ondřej Hort¹

¹ELI Beamlines Facility, Extreme Light Infrastructure ERIC, Za Radnicí 835, 252 41 Dolní Břežany, Czech Republic ²Czech Technical University in Prague, FNSPE, Břehová 7 115 19 Prague 1, Czech Republic *matyas.stanek@eli-beams.eu

Abstract

High Harmonic Generation (HHG) provides compact source of coherent XUV for ultrafast studies but faces flux and spectral matching challenges. Using ELI Beamlines' L1 laser, we enhance XUV yield and introduce tunable HHG designs, online diagnostics, and a 41.8 nm soft X-ray laser, enabling advanced applications including XUV-XUV pump-probe experiments.

Main Text

High Harmonic Generation (HHG) is a key technique for producing compact, coherent extreme ultraviolet (XUV) radiation, indispensable for probing ultrafast atomic and molecular processes. Despite its potential, HHG faces challenges due to limited photon flux and spectral mismatches with the electronic structure of target samples, particularly in nonlinear XUV applications.

Recent advancements in high-power Optical Parametric Chirped-Pulse Amplification (OPCPA) lasers, exemplified by the L1 laser at ELI Beamlines (45 mJ, 15 fs, 1 kHz), have significantly improved XUV photon yields [1]. A synchronized auxiliary beam with electronically adjustable delay is currently under development, enabling XUV-XUV pump-probe experiments. The independent timing of dual driving beams opens pathways to experiments with two distinct XUV sources, further expanding the landscape of nonlinear XUV physics.

To tailor XUV output for specific applications, we introduce two HHG process designs that provide spectral control without the use of XUV optics, thereby reducing energy losses and preserving pulse integrity. The first approach utilizes modulation of the fundamental and second harmonic components of the driving laser to achieve tunable single-frequency XUV generation, offering 2 eV tunability within the 20.4–22.4 eV range [2]. The second approach improves spectral selectivity by modulating the gas medium density in combination with a Bessel-Gauss driver beam [3].

Demonstrating the flexibility of our HHG Beamline, we present a high-repetition-rate soft X-ray laser (SXRL) at 41.8 nm, operating at 1 kHz, the highest repetition rate reported for plasma-based SXRL sources [4]. Additionally, we have implemented a routine online XUV energy measurement technique for real-time diagnostics [5].

- [1] O. Hort et al., "High-flux source of coherent XUV pulses for user applications", Opt. Expr. 27, 8871-8883 (2019).
- [2] L. Jurkovičová et al., "Bright continuously tunable vacuum ultraviolet source for ultrafast spectroscopy", Comm. Phys. 7, 26 (2024).
- [3] O. Finke et al., "Monochromatic high-order harmonic generation by a Bessel-Gauss beam in periodically modulated media", PRA 109, 033517 (2024).
- [4] F. Tissandier et al., "Demonstration of a kHz-repetition-rate extreme ultraviolet laser at 41.8 nm", Opt. Lett. 49, 21, 6321-6324 (2024).
- [5] M. Staněk et al., "Photoelectric charge from metallic filters: An online XUV pulse energy diagnostics", Appl. Phys. Lett. **125**, 091109 (2024).

Microjoule Level 10fs Visible Pulse Generation Via Frequency Doubling of Hollow Core Fibre Driven by an Yb Amplifier

Pedram Abdolghader^{1*}, Beniwal Madhu², Marco Scaglia¹, Étienne Doiron¹, Maksym Ivanov¹, Gabriel Tempea¹, Ximeng Zheng¹, Pooya Abdolghader¹, Giulio Vampa^{3,4}, Bruno E Schmidt^{1#}

Abstract

We demonstrate the generation of 10 fs visible pulses with 3 μ J energy per pulse at a 10 kHz repetition rate. The system employs a dual-stage hollow-core fiber driven by a commercial Yb-based femtosecond laser amplifier. After spectral broadening, second-harmonic generation is achieved using two β -barium borate crystals.

We report the generation of ~10 fs visible pulses via second-harmonic generation (SHG) from a broadband near-infrared source. The input was provided by a Yb:KGW regenerative amplifier delivering 2 mJ, 340 fs pulses at 80 W average power. After spectral broadening through two sequential hollow-core fibers (HCFs) and subsequent compression using chirp mirrors, sub-10 fs pulses were obtained [1]. To address the limited phase-matching bandwidth in SHG, we implemented a dual-crystal 'sandwich' configuration using two 100 µm-thick type-I BBO crystals cut at 26°. Each crystal was phase-matched to opposite ends of the broadened spectrum—one to the blue side, the other to the red—enabling efficient frequency doubling across almost the entire bandwidth. The resulting visible pulses were characterized using TG-FROG (few-cycle Inc.), showing a pulse duration of ~10 fs and pulse energy of 3 µJ centred at 530nm, which is shown in Fig.1 (a). Power stability was measured over 4.5 hours of continuous operation, yielding a relative standard deviation of just 0.96%, confirming the robustness of the system.

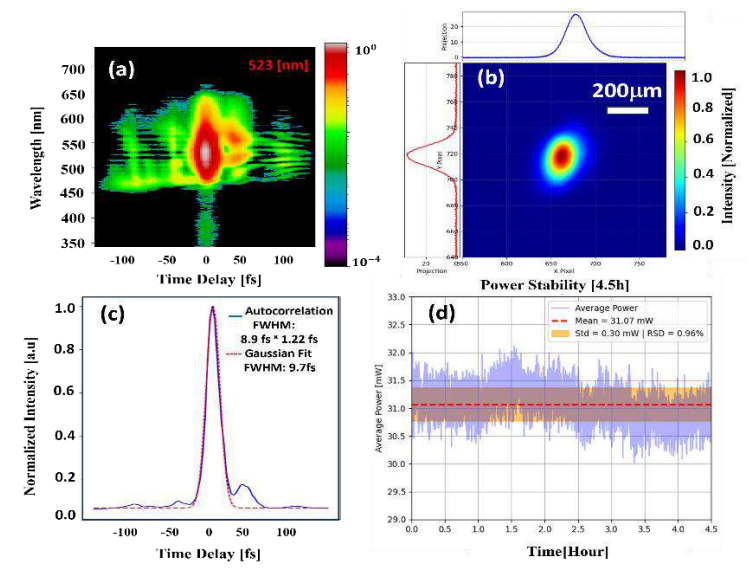


Figure 1: (a) TG-FROG trace, (b) Beam profile after at focus of a 1.5m focusing mirror, (c): Autocorrelation which represent the pulse duration of ~10fs, (d): Average power stability over 4.5 hours.

References

[1] M. Ivanov et al., "Advancing high power hollow-core fiber pulse compression," IEEE JSTQE, 30, 6, 1-10 (2024).

¹ few-cycle Inc, 1650 Boulevard Lionel-Boulet, J3X 1P7 Varennes, QC, Canada

²Institut national de la recherche scientifique, 1650 Boulevard Lionel-Boulet, J3X 1P7 Varennes, QC, Canada

³NRC-uOttawa Joint Centre for Extreme Photonics, Ottawa, ON, K1N 6N5, Canada

⁴National Research Council of Canada, 100 Sussex drive, Ottawa ON, K1N 0R6, Canada

^{*}pedram.ghaderi@few-cycle.com

[#]schmidt@few-cycle.com



Single-stage multipass spectral broadening and compression of 90 fs, 400-µJ laser down to 10 fs

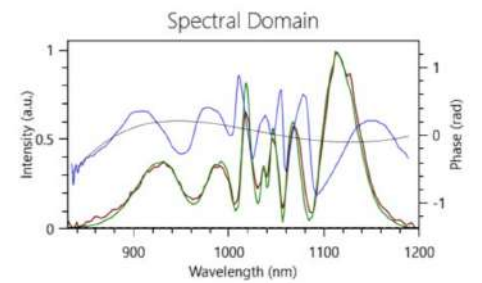
T Joy1*, K Fritsch1, T Stanislauskas2, V Maslinskas2, O Pronin1,3

Abstract

We report nonlinear broadening and pulse compression in a single multipass cell based on dielectric mirrors. The 90 fs and 400 μ J pulses from industrial-grade laser were compressed to 10 fs with 8 W average power and over 80 % efficiency.

Spectral broadening and compression of ultrashort pulses is a widely employed technique. The applications range from ultrafast pump-probe spectroscopy to the development of X-ray and XUV sources. A fundamentally new approach for spectral broadening and pulse compression using a quasi-waveguide system, namely the Herriott-type multi-pass cell (MPC), was introduced recently [1]. The technique was implemented with MPCs filled with bulk and gaseous media, thereby covering an impressive input peak power range from 9 MW up to 81 GW. So far, only a few demonstrations reached the sub-10 fs regime, mainly due to two challenges: The limited bandwidth of optics and the high demands on dispersion management inside the MPC. In this work, we report on our system breaking the 10 fs limit by employing custom-made dispersive mirrors covering the bandwidth from 850 to 1300 nm and Argon gas as a nonlinear medium.

The industrial-grade driving laser (PHAROS-UP by Light Conversion) delivered 90 fs and 400 μ J pulses at 25 kHz, resulting in 10 W average- and ~4 GW peak power. After coupling inside the multipass cell operating under absolute 3.6 bars of Argon, the output pulses were broadened to cover the 850 to 1300 nm range. The compression was performed with dispersive mirrors, providing an overall dispersion of approximately -500 fs2 of GDD and 120 fs³ TOD. The compression was verified with a commercial D-scan device from Sphere Photonics (Fig.1). The output pulse duration was measured to be 10 fs, with the main peak containing 89 % of energy as compared to the Fourier-transform limit. This corresponds to the peak power boost of 6.7 x and peak power of ~27 GW. The transmission of the cell and dispersive mirror compressor remained over 80 %. The long-term operation over 100 h is to be performed. The whole multipass compression unit (MIKS1_L) has a footprint of 1.5 x 0.24 m2. We plan to perform further energy scaling of this approach ultimately reaching the compression of 1 mJ, 90 fs pulses.



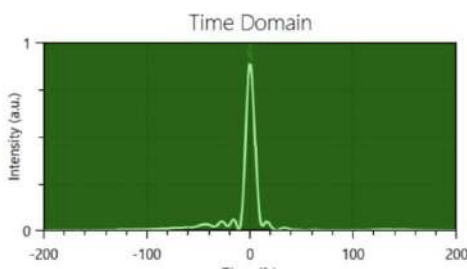


Figure 1. Compressed output spectrum and pulse duration measured with D-scan.

References:

[1] Jan Schulte et al., Optics Letters 41, no. 19, 4511–14 (2016)

¹n2-Photonics GmbH, Hamburg, 22§049, Germany

²Light Conversion, Vilnius, 10234, Lithuania

³Helmut Schmidt University, Hamburg, 22043, Germany

^{*}oleg.pronin@n2-photonics.de; tomin.joy@n2-photonics.de;

Ultrafast deep-UV pulse shaping for optimal electron beam production for the AWAKE experiment at CERN

Anahita Omoumi,* and Eduardo Granados

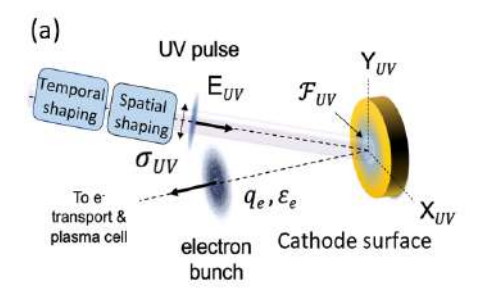
(AWAKE Collaboration)

CERN, Espl. des Particules 1, 1217 Geneva, Switzerland

Abstract

Producing and injecting ultrafast, tailored electron bunches is crucial for wakefield accelerators. This requires precise shaping of ultrafast deep-UV pulses at the photoinjector level. However, the transduction of ultrafast optical parameters into electronic ones is not straightforward. In this work, we propose a model to estimate the corresponding transfer function.

The Advanced Wakefield Acceleration Experiment (AWAKE) at CERN explores proton-driven plasma wakefield acceleration using ultra-relativistic proton drive bunches [1]. After its first experimental run, which demonstrated 2-GeV electron acceleration in a 10 m long Rb plasma, Run 2 focuses on sustaining 0.5–1 GV/m accelerating fields over longer distances, while preserving the electron beam emittance, controlling its energy spread, and demonstrating scalability in length [2]. Mapping the effects of electron bunch injection parameters on charge capture, underscores the importance of estimating the transfer function from UV-beamline settings to the resulting bunch characteristics [3]. To address this, here we present an extension of the Fowler–Dubridge photoemission model to account for the dynamic modulation of the cathode's Schottky barrier during the emission of high-brightness electron bunches.



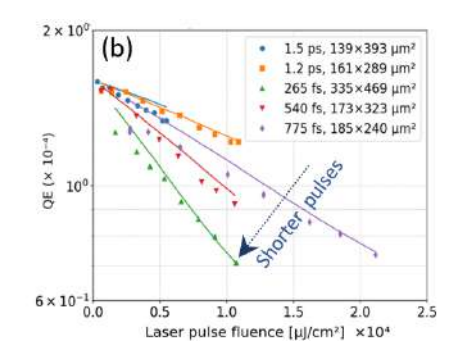


Figure 1: a) The deep-UV pulse energy (E_{UV}), temporal shape, and transverse energy distribution (σ_{UV}) impinging on the photocathode is tailored to produce high brightness electron bunches with optimal characteristics for injection into a plasma. b) Simulated (solid lines) and experimental (markers) quantum yield vs. fluence for deep-UV pulses with different illumination parameters at the cathode surface.

- [1] (AWAKE Collaboration). Acceleration of electrons in the plasma wakefield of a proton bunch. *Nature*, 561(7723): 363–367, 2018.
- [2] E. Gschwendtner and others (AWAKE Collaboration). The awake run 2 programme and beyond. Symmetry, 14 (8):1680, 2022.
- [3] E. Granados, L. Verra, A.-M. Bachmann, E. Chevallay, S. Doebert, V. Fedosseev, F. Friebel, S. Gessner, E. Gschwendtner, S. Y. Kim, et al. Mapping charge capture and acceleration in a plasma wakefield of a proton bunch using variable emittance electron beam injection. arXiv preprint arXiv:2206.14075, 2022.

^{*}anahita.omoumi@cern.ch

Poster Session 2

Broadband Astrocomb Spectral Shaper with Single-Comb-Mode Control

William Newman,^{1,*} Jake M. Charsley,¹ Yuk Shan Cheng,¹ Richard A. McCracken,¹ and Derryck T. Reid ¹

¹ School of Engineering and Physical Sciences, Heriot-Watt University, Edinburgh EH14 4AS, UK *cwn2000@hw.ac.uk

Abstract

We demonstrate independent intensity control of individual comb modes in a 20-GHz Ti:sapphire astrocomb spanning 550–950 nm. Arbitrary spectral shaping is performed directly on the output of a cross-dispersion astrophysical spectrograph, enabling dynamic spectral flattening, spectrograph free-spectral-range demarcation, single-comb-mode isolation and measurement, and comb-mode sparsification yielding the spectrograph instrument-response function.

Astrocombs—laser frequency combs (LFCs) engineered for use as calibration sources in high resolution astronomical spectrographs [1]—achieve broadband spectral coverage through supercontinuum generation processes that typically result in significant spectral structure. To obtain the highest calibration precision, the dynamic range of these intensity variations must be substantially reduced by employing a spectral flattening procedure [2]. Previously, spectral flattening has been performed by dispersing light in 1D across a spatial light modulator (SLM), whose programmable birefringence is used with suitable polarization optics to control the spectral intensity [2,3]. Here, using a 20 GHz astrocomb spanning 550–950 nm, we demonstrate a spectral shaper enabling flattening with individual comb-mode control, as well as other shaping / calibration procedures.

The 2D shaper (Figure 1(a)) places a liquid-crystal-on-silicon SLM at the focal plane of a spatially comb-mode-resolving cross-dispersion spectrograph and directly monitors the output of a separate cross-dispersion spectrograph (R = 95,000), serving as an astronomical spectrograph [4]. Dynamically addressing the SLM by using direct feedback from this diagnostic spectrograph enables spectral flattening (Figure 1(b)) as well as arbitrary shaping (Figure 1(c)), and can reveal the free spectral range/wavelength solution of the detector (Figure 1(c) inset).

In this context, we will present calibration procedures and results of spectral flattening, as well as capabilities and limitations for arbitrary shaping.

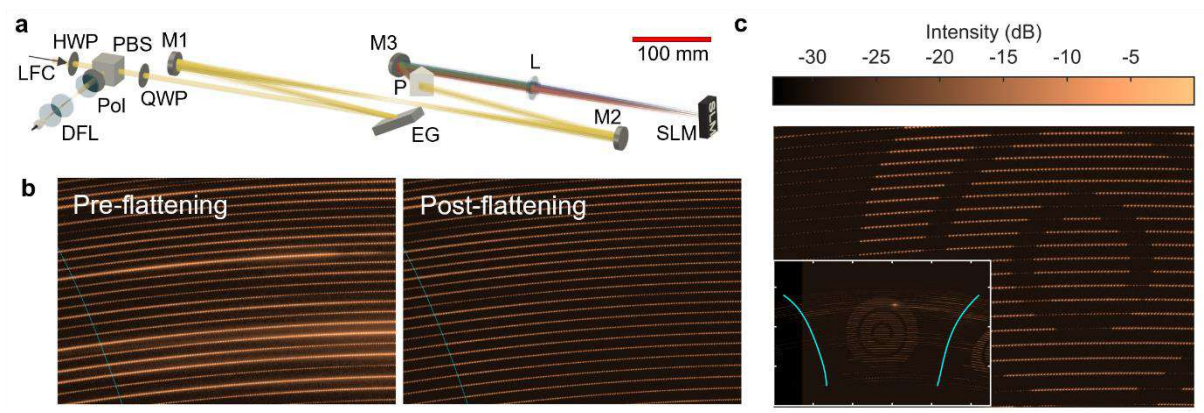


Figure 1: (a) High resolution cross-dispersion shaping spectrograph, with polarization optics (HWP, PBS, QWP, Pol), echelle grating (EG), silver concave mirrors (M1, M2), N-SF11 prism (P), silver plane mirror (M3), achromatic doublet lens (L), SLM, and diagnostic fibre launch (DFL). (b) Pre- and post-flattening images. (c) Example of arbitrary shaping.

- [1] R. A. McCracken, *et al.*, "A decade of astrocombs: recent advances in frequency combs for astronomy [Invited]," Opt. Express **25**, 15058 (2017).
- [2] R. A. Probst, *et al.*, "Spectral flattening of supercontinua with a spatial light modulator," SPIE Proceedings **8864**, 88641Z (2013).
- [3] P. Sekhar, et al., "Dynamic spectral tailoring of a 10 GHz laser frequency comb for enhanced calibration of astronomical spectrographs", arXiv:2502.05401v1 (2025).
- [4] W. Newman, et al., "Cross-dispersion spectrograph calibration using only a laser frequency comb," Opt. Express 32, 23617 (2024).

Towards a single-diode-pumped Ti:sapphire-based astrocomb

Ewan Allan,^{1,*} Abdullah Alabbadi,² Hanna Ostapenko,¹ Pablo Castro-Marin,¹ Yuk Shan Cheng,¹ Richard A. McCracken,¹ Pascal Del'Haye,² and Derryck T. Reid.¹

Abstract

We present a route to a compact optical astrocomb based on a single-diode-pumped 1-GHz Ti:sapphire laser and a Si_3N_4 waveguide to generate an octave spanning supercontinuum, which is mode filtered by a Fabry-Perot etalon to achieve a 20-GHz mode spacing and stabilised to a NIST-traceable reference.

Laser frequency combs are promising atomically-referenced wavelength calibrators for astronomy [1], with the extension to the near-UV possible by using Ti:sapphire-based systems [2]. The essential requirements can be satisfied by combining a 1-GHz modelocked laser source, a method to generate an octave spanning supercontinuum and a Fabry-Pérot filtering cavity [3]. Here, we present a route to a complete astrocomb based on a compact, diode-pumped 1 GHz Kerr-lens-modelocked Ti:sapphire laser [4] and a Si_3N_4 waveguide [5], to generate an octave-spanning supercontinuum, which can be stabilised to a NIST-traceable reference to create a turnkey and affordable calibration source for astronomy.

The Ti:sapphire laser comb-mode spacing, $f_{\rm rep}$, was controlled by a feedback loop shown in Fig. 1(a), and achieved a 760 mHz (frequency-counter limited) rms stability over 1 hour. The 80-fs output pulses had an average output power of 200 mW and pumped a Si₃N₄ waveguide to generate an octave-spanning 556–1121 nm supercontinuum (Fig. 1(b)). This is the first example of an octave-spanning spectrum from a GHz diode-pumped Ti:sapphire laser, and to our knowledge only the second demonstration of an octave-spanning Ti:sapphire-pumped supercontinuum achieved in Si₃N₄ [6]. The comb offset, $f_{\rm CEO}$, was stabilised by deriving a heterodyne beat between the Ti:sapphire laser and a single-frequency reference laser, achieving a locked linewidth of <100 kHz. We will present further details of the laser design and stabilization, together with progress towards implementing a Fabry-Pérot etalon to filter the supercontinuum spectrum to achieve a 20-GHz mode spacing.

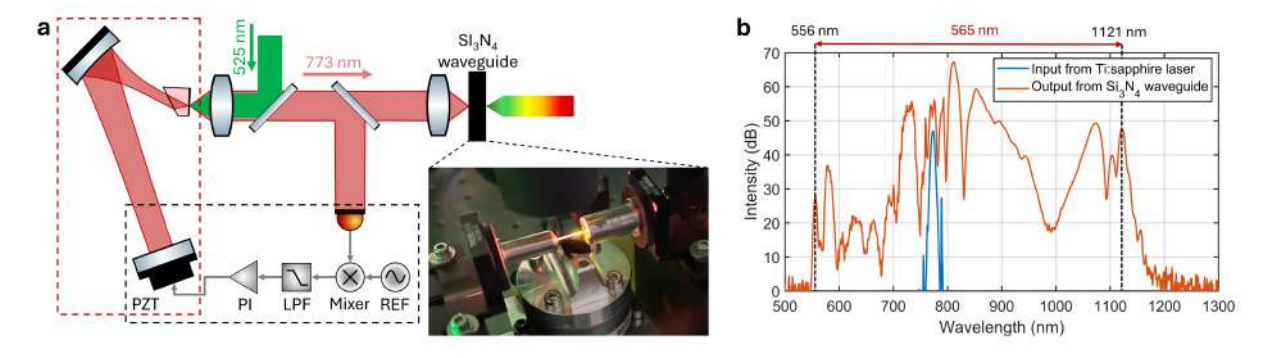


Figure 1: (a) Ti:sapphire laser and Si₃N₄ waveguide (inset). (b) Octave-spanning Si₃N₄ output.

- [1] R. A. McCracken et al., Opt. Express 25, 15058-15078 (2017).
- [2] Y.S. Cheng et al., Nat. Commun. 15, 1466 (2024).
- [3] C.-H. Li et al., Nature 452, 610 (2008).
- [4] H. Ostapenko et al., Opt. Express 30, 39624-39630 (2022).
- [5] K. Zhong et al., Laser Photonics Rev 2301366 (2024)
- [6] H. Zhao et al., Opt. Lett. 40, 2177-2180 (2015).

¹School of Engineering and Physical Sciences, Heriot-Watt University, Edinburgh EH14 4AS, UK.

²Max Planck Institute for the Science of Light, Staudtstrasse 2, 91058, Erlangen, Germany.

^{*}E.Allan@hw.ac.uk

Timing stabilization of femtosecond optical laser system for pump-probe experiments in SACLA

Tadashi Togashi, 1,2,* Shigeki Owada, 1,2 Toshinori Yabuuchi, 1,2 and Makina Yabashi, 1,2

Abstract

We developed a synchronization system using a balanced optical-microwave phase detector (BOMPD) along with a timing control system featuring an arrival-timing monitor (ATM) for pump-probe experiments at SACLA. The timing stabilization has been realized to less than 50 fs (RMS) over ~49 hours.

X-ray free-electron lasers (XFELs) are promising sources of femtosecond X-ray pulses that can explore ultrafast dynamics of chemical reactions and phase transitions on a femtosecond time scale through a pump-probe technique utilizing femtosecond optical lasers. When these optical lasers are synchronized with a reference signal from an XFEL machine via a standard phase-locking system, certain sources of error introduce sub-picosecond timing jitters, limiting time resolution in pump-probe experiments. To fully utilize the ultrashort-pulse nature of the XFEL, shot-to-shot diagnostics of the arrival timing between the XFEL and optical laser pulses are essential. By employing a post-processing sorting method with an arrival-timing monitor (ATM) that detects transient optical property changes in gallium arsenide during XFEL excitation, a sub-10 fs resolution has been achieved at SPring-8 Angstrom Compact free-electron LAser (SACLA). However, a more precise timing stabilization system is necessary to increase the number of events at specific delay timings. In this paper, we developed a synchronization system using a balanced optical-microwave phase detector (BOMPD) along with a timing control system featuring an ATM for timing stabilization.

The synchronized optical laser system, based on chirped pulse amplification (CPA) of a Ti:sapphire laser, provides output pulses of 12 mJ with an approximate pulse duration of 40 fs for user experiments [2]. The timing between the pulse train from the oscillator and the 5.7-GHz RF signal for the accelerator is detected by the BOMPD as a phase-error-dependent intensity imbalance from a Sagnac-loop interferometer [3]. The repetition rate of the oscillator is locked by applying this phase error signal to the linear actuator in the oscillator cavity. While this system reduced short-term timing jitter to about 50 fs (RMS), a long-term timing drift of 0.5 ps persists over a day.

To improve long-term timing drift, we developed a timing control system between the XFEL and optical laser pulses by applying the ATM data to an optical delay line, which was installed before the first regenerative amplifier in the CPA system. Consequently, we succeeded in reducing the timing fluctuation, including both short-term jitter and long-term drift between the XFEL and optical laser pulses, to less than 50 fs over 49 hours, as shown in Fig. 1. [2, 4]

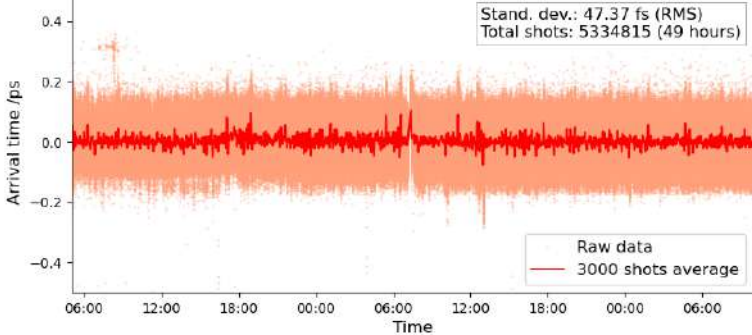


Fig. 1, Trends of the arrival timing measured by the ATM over 49 hours. The orange dots are raw data, while the red and brown traces are average and standard deviation in 3000 shots respectively

- [1] T. Katayama et al. "A beam branching method for timing and spectral characterization of hard X-ray free-electron lasers" Structural Dynamics 3, 034301 (2016).
- [2] T. Togashi et al. "Femtosecond optical laser system with spatiotemporal stabilization for pump-probe experiments at SACLA", Applied Science 10, 7934 (2020).
- [3] J. Kim et al. "Femtosecond synchronization of radio frequency signals with optical pulse trains", Opt. Lett. **29**, 2076 (2004).
- [4] T. Togashi et al. "Long-term timing stabilization for pump-probe experiments at SACLA", J. Synchrotron Rad. **32**, 269-274 (2025).

¹ Japan Synchrotron Radiation Research Institute (JASRI), Sayo-cho, Sayo-gun 6795198, Japan

² Riken SPring-8 Center, Sayo-cho, Sayo-gun 6795148, Japan

^{*}tadashit@spring8.or.jp

Exploring Spontaneous Multimode Solitary Wave Generation

Maghsoud Arshadipirlar^{1,*}, Francois Légaré¹, Reza Safaei²

¹ Advanced Laser Light Source (ALLS), Institut National de la Recherche Scientifique (INRS-EMT), 1650 Boulevard Lionel-Boulet, J3X 1P7, Varennes, Canada

² MPB Communications Inc. 147 Hymus Boulevard, H9R 1E9, Pointe-Claire, Canada *Maghsoud.Arsahdipirlar@inrs.ca

Abstract

We investigate the stability and energy transfer limits of multidimensional solitary states (MDSS) in Raman-active gas-filled hollow-core fibers. Combining theory, simulations, and experiments, we reveal that MDSS can coexist with instabilities while maintaining their structure. Our findings offer insights into multimode nonlinear dynamics, enabling advancements in ultrafast optics.

Main Text

MDSS in gas-filled hollow-core fibers (HCFs) exhibit unique energy transfer dynamics governed by Raman scattering and intermodal nonlinear interactions [1]. Here, we investigate the stability of MDSS and the fundamental limits of energy transfer in Raman-active gas-filled HCFs. Specifically, we show that beyond a critical input energy, a secondary red-shifted Raman component emerges due to Raman gain in higher-order modes. Similar to other multimode systems, this instability originates from spatiotemporal modulation instabilities (STMI), which influence the system's attractor [2].

To achieve this, we employ a Yb-based laser with a pulse duration of 700 fs and a central wavelength of 1030 nm. The laser is directed into a 2.5 m long HCF with a core diameter of 500 μ m, which is filled with N₂O gas. Figure 1 presents the variation of spatial beam profiles in the red-shifted and blue-shifted regions (Fig. 1a) and the corresponding spectral features (Fig. 1b) as a function of increasing gas pressure, with input pulse energy of 0.5 mJ. Initially, as the gas pressure increases, a red-shifted beam is created. Its size is smaller than that of the input beam, and it maintains a symmetric shape. This suggests the presence of higher-order symmetric modes in this

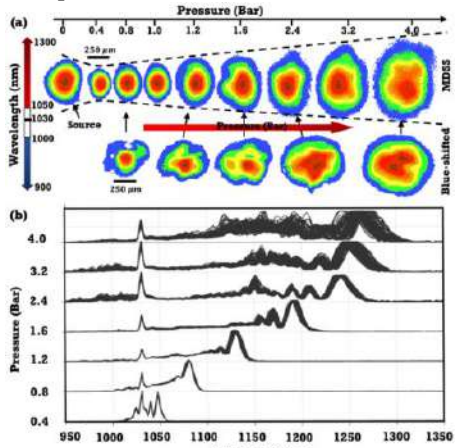


Figure 1. a) Beam profile of the MDSS and blue-shifted regions using a spectral short-pass and long-pass filters. b) Spectral broadening of the output beam by MDSS at different N_2O gas pressures with an input pulse energy of 500 μJ .

region, marking the formation of an attractor [2]. At the same time, the blue part of the spectrum is also observed. At first, the beam in blue part exhibits a symmetric shape but is significantly smaller than the fundamental beam, indicating strong self-focusing in this region. As the gas pressure increases further, the blue-shifted component begins to diverge, and the beam in this region becomes unstable. Simultaneously, MDSS in the red-shifted region starts to develop additional spatiotemporal structures around itself, leading to an increase in beam size and marking the onset of attractor instability. As seen from the spectral evolution, the entire spectrum exhibits increasing instability with higher gas pressure. Another intriguing observation is that as self-focusing strengthens in the blue part of the spectrum, a second red-shifted spectral component emerges, which becomes prominent at 2.4 bar. This effectively divides the red-shifted region into two parts, with the newly formed red-shifted component being significantly more unstable. This instability further disrupts the primary attractor. These observations provide clear evidence of the rich and complex physics underlying attractor formation. Using a combination of a theoretical model and multimode numerical simulations, we investigated these experimental results in greater detail to uncover the underlying physics behind our observations.

Our results offer new insights into the interplay between stability and multimode nonlinear dynamics in structured light systems. By demonstrating that MDSS can maintain coherence even in the presence of spectral instabilities, we open new possibilities for their use in ultrafast optics, high-energy pulse propagation, and nonlinear multimode fiber systems.

- [1] R. Safaei and et al., "High-energy multidimensional solitary states in hollow-core fibres," Nat. Photonics, 14 (2020).
- [2] L. G. Wright and et al., "Self-organized instability in graded-index multimode fibres," Nat. Photonics, 10 (2016).

Ultrafast time-resolved demagnetization imaging in a ferromagnet

Alessandro Baserga^{1,*}, Federico Visentin^{1,2}, Davide Benettin¹, Giovanni Gandini¹, Christian Rinaldi¹, Ettore Carpene², Giulio Cerullo^{1,2}, Stefano Dal Conte¹, Franco V.A. Camargo²

- ^{1.} Politecnico di Milano, Piazza L. da Vinci 32, 20133 Milano, Italy
- ². IFN-CNR, Piazza L. da Vinci 32, 20133 Milano, Italy.
- * alessandro.baserga@polimi.it

Abstract

We present ultrafast imaging of light-induced demagnetization in a Pt/CoFeB/MgO ferromagnet using holographic microscopy. With femtosecond and sub-micrometer resolution, we uncover spatially dependent magnetization dynamics, revealing variations in lateral demagnetization behavior and decay times, offering deeper insight into ultrafast magnetic phenomena at the nanoscale.

Main Text

Ultrashort laser pulses are powerful tools for studying out-of-equilibrium magnetism [1]. While pump-probe techniques track femtosecond magnetization dynamics [2], spatially resolved studies remain limited [3]. Using self-referencing ultrafast holographic microscopy [4], we image light-induced demagnetization in Pt/CoFeB/MgO with 100-fs and sub-µm resolution, revealing spatially dependent magnetization dynamics.

Our widefield transient absorption microscope employs holographic multiplexing to measure the polarization ellipse of the probe beam and a self-referencing technique to reduce noise to near shot-noise levels [4]. When an intense light pulse excites a magnetized metal, hot electrons transfer energy to phonons, rapidly reducing magnetization. Our technique captures perturbations with sub- μ m and fs space/time resolution, which we use to study the ultrafast spatial dynamics of this demagnetization.

Figure 1a shows a Faraday rotation image 0.2 ps following photoexcitation with diffraction limited pulses with a diameter of approximately 0.75 μm FWHM of a Pt/CoFeB/MgO sample. As seen in Figure 1b, a central positive signal, corresponding to magnetization reduction, is surrounded by a negative halo that is much larger than the excitation pulses. We hypothesize that this is due to the closing of magnetic field lines at the excitation periphery.

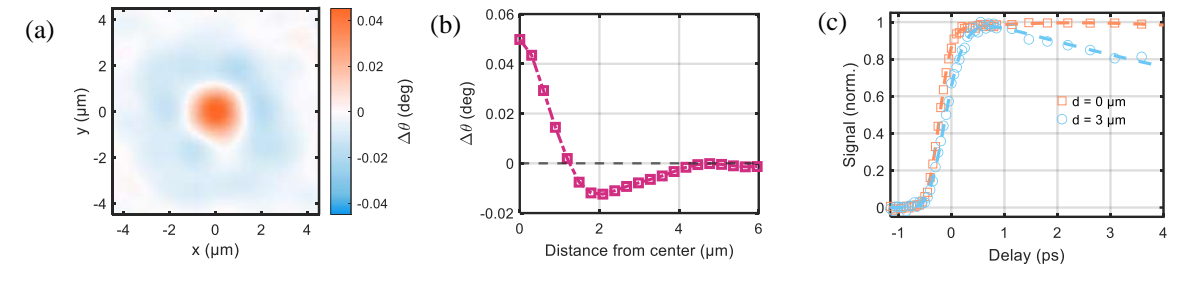


Figure 1: (a) Differential Faraday rotation signal and (b) its radial average Faraday at 0.2 ps. (c) Normalized Faraday rotation kinetics at the center and 3 µm away from it (points experimental, line biexponential fit).

The demagnetization dynamics depend on distance from the excitation center. Within 1 μ m, decay is minimal, while between 1.5 and 3 μ m, it accelerates, consistent with heat dissipation via electrons, phonons, and magnons. Differences in the signal rise at early times offering insights into spin diffusion and spin wave propagation.

- [1] A. Kirilyuk et al., "Ultrafast op tical manipulation of magnetic order", Rev. Mod. Phys. 82 (3): 2731–84 (2010).
- [2] E. Beaurepaire et al., "Ultrafast Spin Dynamics in Ferromagnetic Nickel", Phys. Rev. Lett.76 (22): 4250-53 (1996)
- [3] Y. Hashimoto et al.; "Ultrafast time-resolved magneto-optical imaging of all-optical switching in GdFeCo with femtosecond time-resolution and a μ m spatial-resolution", Rev. Sci. Instrum; 85 (6): 063702, (2014).
- [4] M. Hörmann et al., "Self-referencing for quasi shot-noise-limited widefield transient microscopy," Opt. Express 32, 21230-21242 (2024)

Optimization of thin plate post-compression based on 2+1D numerical simulations

Viktor Pajer,^{1,*} Levente Lehotai,¹ János Bohus,¹ Nóra Csernus-Lukács,¹ Balázs Tari, ¹ Mikhail Kalashnikov,¹ Ádám Börzsönyi,¹ and Roland S. Nagymihály¹

¹ELI-HU Nonprofit Ltd, Wolfgang Sandner utca 3, H-6728 Szeged, Hungary *viktor.pajer@eli-alps.hu

Abstract

We numerically investigate the effect of material properties on the spectral broadening and compressibility in thin plate post-compression setups where the evolution of the spatial-spectral profile is also considered. We show that the achievable compression factor after a quadratic compressor is limited despite the intensity or the material.

Motivation and results

To increase the peak power of the driver pulses in high field science [1], either one needs to boost the pulse energy or to reduce the pulse duration by post-compression [2]. The latter one is possible with the thin-plate method in high energy laser systems. On the other hand, testing different materials or arrangements using a large, high-energy beam is a difficult and time-consuming task. In addition, it is crucial to preserve the beam profile and the temporal quality of the recompressed pulse. Here, we present the results derived from 2+1D numerical simulations about the expected spectral broadening and optimal compression factor in a single thin plate arrangement.

We performed a series of simulations considering different materials (fused silica, sapphire, YAG) and intensity levels to see the evolution of the spectral broadening and recompressed pulse quality. The model takes into account self-phase modulation, self-steepening, and material dispersion (by using Sellmeier-equations). Figure 1. shows the spatio-spectral profile of an originally 25 fs short pulse after propagating through a 2 mm and a 4 mm thin fused silica plate. The intensity was set to obtain approximately the same B integral. The profile is more homogeneous than what we got from the thinner plate (Fig. 1. (a) and (b)), especially around the central wavelength. Though this could be beneficial, we also found that the maximum obtainable compression factor after a quadratic compressor is limited and saturates during the propagation despite that spectral broadening still in progress. From the above results, we can derive an optimal plate thickness to have high quality post-compressed pulses from a high-energy setup.

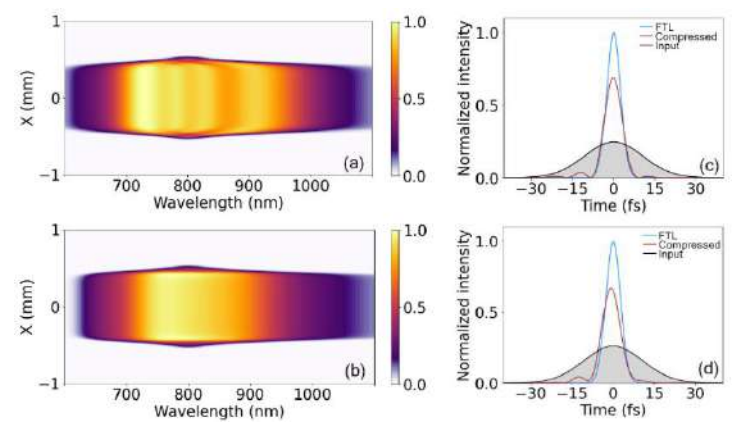


Figure 1. Left: Simulated spatio-spectral profile after a fused silica plate with (a) 2 mm and (b) 4 mm thickness. Right: (c) and (d), corresponding FTL and compressed intensity profiles.

References

[1] J. A. Wheeler et al., "Science of high energy, single-cycled lasers," Rev. Accel. Sci. Technol. **10**, 227-244 (2019). [2] T. Nagy et al., "High-energy few-cycle pulses: post-compression techniques," Advances in Physics: X **6**(1), 845795 (2021).

High power HHG source driven by a Black Dwarf laser system

B. Manschwetus¹, T. Braatz¹, S. Starosielec¹, H. Goudarzi¹, M. Wieland³, M. J. Prandolini^{1,3}, M. Schulz¹, T. Gorkhover³, M. Drescher³, C. M. Heyl^{2,4,5}, R. Riedel^{1,*}

Abstract

Power scaling of our high harmonic generation based XUV source using the Class 5 Black Dwarf laser system at 17 W and 50 W of average power, as well as, the next steps within our MEGA-EUV collaboration project are presented. The ultimate goal is to deliver up to 1 mW of XUV flux at the industrial relevant wavelength of 13.5 nm.

High harmonic generation (HHG) sources [1] provide fully coherent laser-like radiation in the extreme-ultraviolet (EUV/XUV) and soft X-ray spectral range with femto- or attosecond pulse duration. These sources are ideal metrology tools for scientific or industrial applications: The short wavelength allows very high spatial resolution in scattering or imaging of nanostructures created by state-of-the-art microchip EUV lithography.

In our contribution, we will present the current status of our Moonlander HHG source driven by the Class 5 Black Dwarf laser. The Black Dwarf utilizes a multipass cell (MPC) nonlinear compression with an integrated Yb driver laser in a compact package [2]. This particular system delivered 17 W average power at 100 kHz repetition rate and a pulse duration of 29 fs. We measured an XUV output power of $1.4~\mu W$ for an argon target gas and $2.8~\mu W$

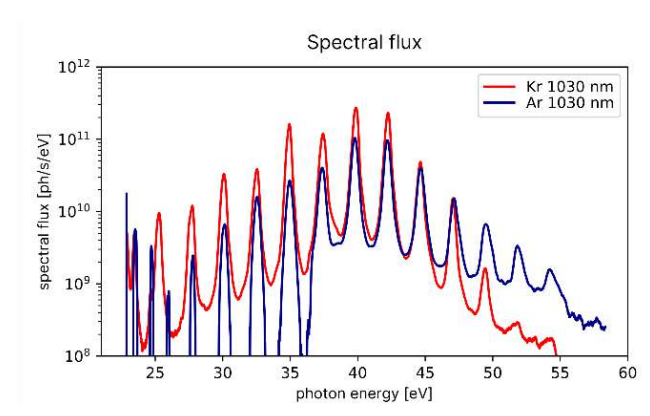


Figure 1: Measured XUV spectral photon flux using a Class 5 Black Dwarf with 17 W average power at 100 kHz.

for a krypton target gas within the aluminum filter window (22-75 eV). The measured key parameters are shown in Figure 1.

We will also show first results with a driver at an average power of 50 W at a much high repetition rate of 750 kHz. Class 5 Photonics is developing the Moonlander HHG source to fullfil the requirements of photoelectron emission, XUV absorption spectroscopy and coherent diffraction imaging, as well as, advanced semiconductor metrology applications. Our next steps are the demonstration of stable operation of our HHG source for driver lasers at 200 W and 500 W average power within the joint research project MEGA-EUV with DESY, University of Hamburg and AMPHOS. We will discuss the technical challenges and prospects in the power scaling of these XUV sources.

References

[1] X. F. Li et al., Phys. Rev. A 39, 5751-5761 (1989)

[2] A.Viotti et al., Optica 9, 197-216 (2022)

¹Class 5 Photonics GmbH, Notkestrasse 85, D-22607 Hamburg, Germany

²Deutsches Elektronen Synchrotron (DESY), Notkestraße 85, 22607 Hamburg, Germany

³Universität Hamburg, Institut für Experimentalphysik, Luruper Chaussee 149, 22761 Hamburg, Germany

⁴Helmholtz-Institut Jena, Fröbelstieg 3, 07743 Jena, Germany

⁵GSI Helmholtzzentrum für Schwerionenforschung GmbH, Planckstraße 1, 64291 Darmstadt, Germany

^{*}robert.riedel@class5photonics.com

Ultrafast SHG microscopy enhanced by deep learning for rapid, low-power tissue imaging

Arash Aghigh,1,* Bhawna Dhawnan,1 Reza Safaei,1 and François Légaré1

¹ Centre Énergie Matériaux Télécommunications, Institut National de la Recherche Scientifique, Varennes, Québec, Canada.

*arash.aghigh@inrs.ca

Abstract

This work presents two deep learning-based strategies that enhance ultrafast second harmonic generation (SHG) microscopy under challenging imaging conditions. Through denoising and super-resolution methods, laser power was reduced by up to 70% and acquisition time by over 95%, respectively, enabling low-damage and high-throughput nonlinear imaging of biological tissue.

Main Text

SHG microscopy enables high-resolution, label-free imaging of non-centrosymmetric structures such as collagen and myosin [1]. Polarization-resolved SHG (P-SHG) extends this by allowing fiber alignment analysis. However, low signal-to-noise ratios (SNR), long acquisition times, and photodamage risks pose significant limitations for large-scale or dynamic imaging [1].

Two deep learning pipelines were employed to address these challenges. The first pipeline used convolutional neural networks—specifically, content-aware image restoration (supervised) and Noise2Void (self-supervised)—for denoising SHG images acquired at reduced laser power [2]. This approach allowed up to 70% power reduction while preserving tissue microstructure, as validated in zebrafish muscle and tumor-edge tissue [2].

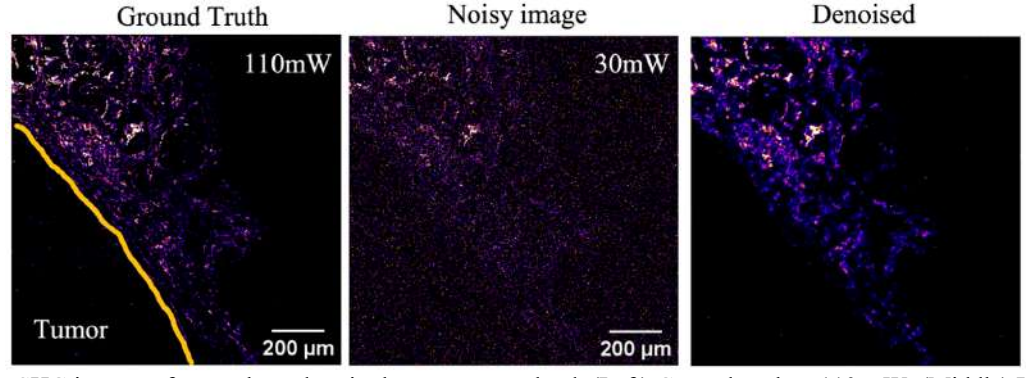


Figure 1: SHG images of tumor boundary in the mammary gland. (Left) Ground truth at 110 mW. (Middle) Low-SNR acquisition at 30 mW. (Right) The denoised results using deep learning. A 70% power reduction is achieved while preserving structural features essential for analysis.

The second pipeline applied an Enhanced Super-Resolution Generative Adversarial Network (ESRGAN) to reconstruct high-resolution P-SHG images from fast, low-resolution acquisitions. This method reduced acquisition time by over 95% while maintaining structural and polarimetric fidelity [3].

Together, these studies outline a deep learning-enabled roadmap for SHG microscopy that overcomes traditional speed and power constraints. While denoising and super-resolution were applied independently, they lay the foundation for a future hybrid pipeline combining low-power acquisition with fast imaging and real-time enhancement. This vision integrates ultrafast optics with machine learning to advance biomedical SHG imaging throughput and accessibility.

- [1] A. Aghigh, S. Bancelin, M. Rivard, M. Pinsard, H. Ibrahim, and F. Légaré, "Second harmonic generation microscopy: a powerful tool for bio-imaging," *Biophys. Rev.*, vol. 15, no. 1, pp. 43–70, Feb. 2023, doi: 10.1007/s12551-022-01041-6.
- [2] A. Aghigh *et al.*, "A comparative study of CARE 2D and N2V 2D for tissue-specific denoising in second harmonic generation imaging," *J. Biophotonics*, vol. 17, no. 6, p. e202300565, 2024, doi: 10.1002/jbio.202300565.
- [3] A. Aghigh *et al.*, "Accelerating whole-sample polarization-resolved second harmonic generation imaging in mammary gland tissue via generative adversarial networks," *Biomed. Opt. Express*, vol. 15, no. 9, pp. 5251–5271, Sep. 2024, doi: 10.1364/BOE.529779.

Compression of ultrafast laser pulses at the SXP instrument of the European XFEL

P. Grychtol^{1,*}, P. Bhardwaj¹, Yi-P. Chang¹, R. Carley¹, L. Mercardier¹, D. Rompotis¹, M. Emons¹, J. Meier¹, M. Lederer¹, A. Scherz¹, and M. Izquierdo¹

¹European XFEL, Holzkoppel 4, 22869 Schenefeld, Germany

Abstract

This contribution presents the pump-probe laser infrastructure in general and more specifically the laser pulse compression scheme of the SXP instrument at the European XFEL.

At the European X-ray Free Electron Laser (XFEL) facility, a new instrument, the Soft X-ray Port (SXP), has started its operation [1] complementing the other two soft X-ray baseline instruments: Spectroscopy and Coherent Scattering (SCS) and Small Quantum Systems (SQS). SXP is primarily designed for time- and spin-resolved X-ray photoelectron spectroscopy (TR-XPES), but investigations of complex chemical and bioinorganic molecular systems with fluorescence spectroscopy as well as research on highly charged ions are also envisioned [2]. All three instruments are located downstream of the SASE 3 soft X-ray undulator system providing ultrafast photon pulses with variable polarization in the energy range between 260 eV and 3000 eV, at MHz repetition rates in a 10 Hz burst mode. Up to 10¹² photons per pulse can be focused in the interaction region at a micrometer spot size, resulting in an intensity of more than $10^{18} \,\mathrm{W/cm^2}$. These outstanding specifications will enable the complete electronic, chemical and atomic characterization of solids, surfaces, and interfaces using TR-XPES. For this purpose, two powerful pump-probe lasers envisioned to operate in a broad spectral range from the mid-infrared to the extreme ultraviolet region will be available. Herriott-type multi pass cells (MPC) will be used to compress their pulses into the few femtosecond range paving the way for ultrafast time-resolved investigations at the SXP instrument combining intense and tunable soft X-rays with versatile optical laser capabilities.

In addition to a standalone Yb fiber laser system, the SXP instrument is equipped with a dedicated pump-probe laser centered at 1030 nm as well as 800 nm that is shared among all three instruments at SASE 3 [3]. This powerful laser delivers 850 fs (15 fs) short and 4 mJ (0.2 mJ) strong laser pulses at a repetition rate of about 1.1 MHz in the XFEL characteristic 10 Hz burst mode pattern [4]. First steps have been taken in collaboration with SCS and the laser group of the European XFEL to compress the 1030 nm pulses into a regime where high harmonic generation (HHG) and other nonlinear wavelength conversion schemes become more efficient to allow for covering a large spectral range of pump-probe photon energies with ultrafast pulse durations [5]. To this end, the initially 850 fs long pulses are first of all broadened in a MPC comprising two dielectric broadband mirrors with a radius of curvature of 700 mm and a diameter of 50 mm separated by approximately 1.4 m encapsulated in a custom-designed vacuum vessel filled with Argon gas to a pressure of about 3.5 bars above atmosphere. The original laser spectrum widens significantly after 26 round trips of the laser beam, and it is eventually compressed by 18 bounces on chirped mirrors, compensating for a total dispersion of 6300 fs². A compression ratio of about 20 has been achieved, shortening the laser pulse length to approximately $40\,\mathrm{fs}$ with an efficiency of more than $80\,\%$ delivering about $3\,\mathrm{mJ}$ pulses to the experiment, at a MHz repetition rate in a 10 Hz burst mode pattern synchronized to the European XFEL. This development will pave the way for groundbreaking ultrafast TR-XPES studies by enabling an expanded pump-probe wavelength range, thereby enhancing the capabilities of the SXP instrument and nonlinear optical investigations at the European XFEL.

- [1] Grychtol et al., "The SXP instrument at the European XFEL", J. Phys.: Conf. Ser. 2380, 012043 (2022).
- [2] Izquierdo, "Technical Design Report: Scientific Instrument Soft X-Ray Port Part A Science Cases", http://xfel.tind.io/record/2647 (2022).
- [3] Pergament et al. "Versatile optical laser system for experiments at the European X-ray free-electron laser facility" Opt. Exp. 24, 29349 (2016).
- [4] Grychtol et al., "The Laser Infrastructure at the SXP instrument of the European XFEL", J. Phys.: Conf. Ser. **2380**, 012114 (2022).
- [5] Grychtol et al., "Generation of Ultrafast Laser Pulses at the SXP Instrument of the European XFEL" CLEO/Europe-EQEC (2023).

grychtol@xfel.eu



Relevant effects for the pulse post-compression with VEGA-2

Irene Hernández-Palmero, *,1,2,3 Julio San Román,2,3 and Enrique Conejero Jarque^{2,3}

*ihernandez@clpu.es

Abstract

We present numerical simulations to find the best conditions for bulk material post-compression of high intensity laser pulses. The validity of the code has been tested by comparison simulated propagation and measurements obtained during an experimental campaign using the Thin Film Compression technique with VEGA-2 at CLPU facility.

Laser driven particle acceleration in compact laboratories demands laser pulses with increasing peak power. Due to the limitations of current technology (amplification crystals size or diffraction grating size due to damage threshold), it is difficult to continue increasing the peak power. A possible solution is the temporal shortening of the present laser pulse outputs at the already operational facilities. A shorter pulse could be achieved thanks to a spectral broadening induced by Self-Phase Modulation (SPM) and the subsequent spectral phase correction with a compressor [1]. The theoretical modeling of this process is essential to understand and identify the most relevant effects, and to guide the design of new compression strategies.

The spectral broadening due to SPM introduced in the material is simulated numerically using Generalized Nonlinear Schrödinger Equation (GNLSE) to model the nonlinear propagation of a laser pulse through a material. The measurements used were taken during an experimental campaign with VEGA-2 beamline at CLPU (200 terawatt laser) with the Thin Film Compression technique in a research line in ELI-NP [2].

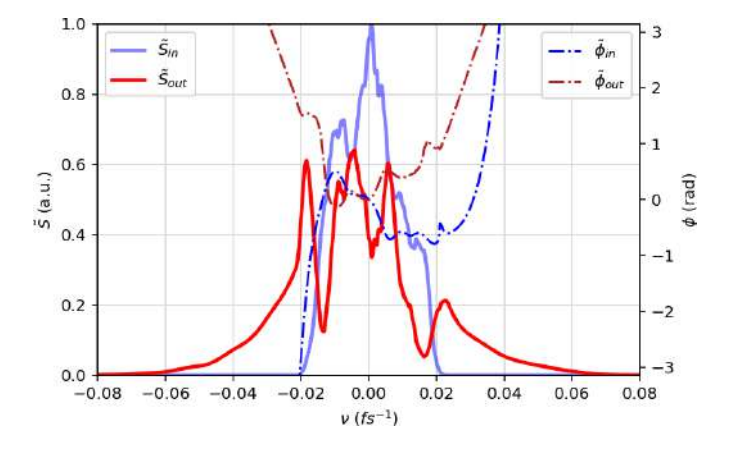


Figure 1: Measured spectrum at the output of the compressor (S_{in} in blue), simulated output after Fused Silica plate of 3 mm thickness (S_{out} in red). The frequency axis is shifted from the central frequency.

The code has allowed us to explore the influence of the spectral phase of the incident pulse and to have an idea of the amount of Group Delay Dispersion (GDD) accumulated during the nonlinear propagation that we should compensate to finally achieve a shorter pulse.

- [1] E. A. Khazanov, "Post-compression of femtosecond laser pulses using self-phase modulation: from kilowatts to petawatts in 40 years," Quantum Electron., **52**, no. 3, 208–226 (2022).
- [2] P.-G. Bleotu et al., "Post-compression of high-energy, sub-picosecond laser pulses," High Pow. Laser Sci. Eng., 11, e30 (2023).

¹Centro de Láseres Pulsados (CLPU), Villamayor, 37185 Salamanca, Spain

²Grupo de Investigación en Aplicaciones del Láser y Fotónica, Departamento de Física Aplicada, Universidad de Salamanca, 37008 Salamanca, Spain

³Unidad de Excelencia en Luz y Materia Estructuradas (LUMES), Universidad de Salamanca, 37008 Salamanca, Spain

Ultrafast intracavity measurement of resonant microcavity modes dynamics

Ouri Karni,1,* Etienne Lorchat,1 Chirag Vaswani,1 and Thibault Chervy1

¹ Physics and Informatics Laboratories, NTT-Research Inc., 940 Stewart Drive, Sunnyvale, California 94085, USA *ouri.karni@ntt-research.com

Abstract

We report ultrafast measurement of optical fields resonating in high-quality microcavities, utilizing secondorder nonlinearity-based optical gating scheme inside the cavity. Instead of waiting for light leakage from the cavity, we extract its instantaneous state on-demand, basing future characterization of ultrafast dynamics of intracavity fields in polariton or quantum-optical systems.

Optical micro-cavities have become established platforms for quantum simulations, quantum photonics, and information, relying on the manipulation of the optical fields resonating in the cavity [1]. Thus, it is imperative to be able to directly measure these fields. So far, the intra-cavity fields were mapped through their leakage out of the cavity, over the timescale of cavity decay. This brings about a conundrum: to show more pronounced quantum effects, cavities are designed to slow-down the light leakage process, reducing its detection efficiency outside the cavity. Moreover, since this detection scheme is based on an incoherent loss process, any quantum information carried out of the cavity is scrambled.

In this work, we solve this problem by introducing a wide-band second-order optical nonlinearity into a high-quality wavelength-selective microcavity, to extract the intra-cavity field information in an ultrafast manner, ondemand. In our demonstration (see schematics in Figure 1a), we incorporated a slab of LiNbO3 into a distributed Bragg reflector (DBR) microcavity resonating around 750 nm. Following a pulsed (~100 fs) excitation of the cavity resonant modes, a pulse (~100 fs) at 1040 nm (outside the stopband of the DBRs) at a controlled delay is launched at the cavity to gate the resonant light. The sum-frequency-generated (SFG) signal at ~436 nm is also not reflected by the DBRs, thus easily escapes the cavity. Since it is linearly dependent on the intra-cavity resonant field, the SFG signal extracts its instantaneous quantum-state in a well-defined mode. This allows to characterize its spectrum, phase and polarization together with its real- and momentum-space distributions and their evolutions along the ~200 ps long cavity decay process. We demonstrate the dynamics of the intracavity light following the excitation of different cavity modes and their superpositions, showing how it migrates across the cavity plane.

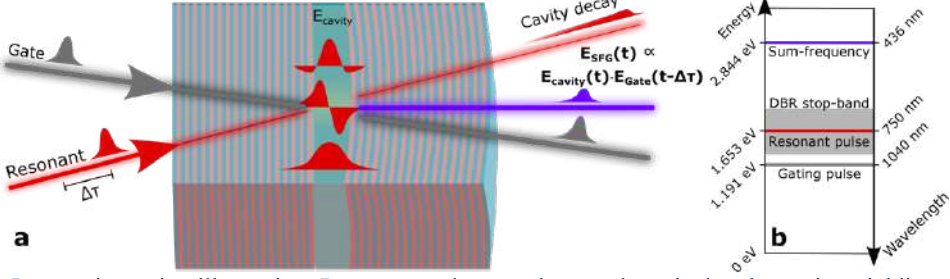


Figure 1: **a.** Intracavity gating illustration: Resonant and gate pulses are launched at the cavity, yielding a fast SFG pulse which is the product of the intracavity resonant field and the gating pulse. **b.** Spectral configuration of the experiment. Only the resonant signal is reflected well by the DBRs of the cavity, thus resonate in it. The other signals pass once and escape the cavity.

We expect this technique to impact the exciton-polariton and quantum-photonics communities, by offering ultrafast measurements of the coherent interplay of the cavity with excitonic systems, or for coherent measurements of quantum-states of light excited in the cavity [2], and their dynamics.

- [1] Daniele Sanvitto and Stéphane Kéna-Cohen, "The road towards polaritonic devices," Nature Materials 15, pages1061-1073 (2016)
- [2] A. Delteil et al., "Second-order photon correlation measurement with picosecond resolution using frequency upconversion," Optics Letters 44, 3877-3880 (2019)



Photon Transport Neural Networks: A Digital Twin Approach

Justin M. Baker^{1,*}, Jack Hirschman,^{2,3}, Abhimanyu Borthakur², Harris Hardiman-Mostow¹, Sergio Carbajo^{1,2}, and Andrea L. Bertozzi¹

Abstract

The Frantz-Nodvik equations, foundational in modeling ultrafast optics, arise from the photon transport conservation law. We incorporate this physical constraint into the latent memory of a neural network (NN) to enhance the explainability and fidelity of a NN digital twin for chirped pulse amplifiers (CPA).

Photon Transport Neural Networks

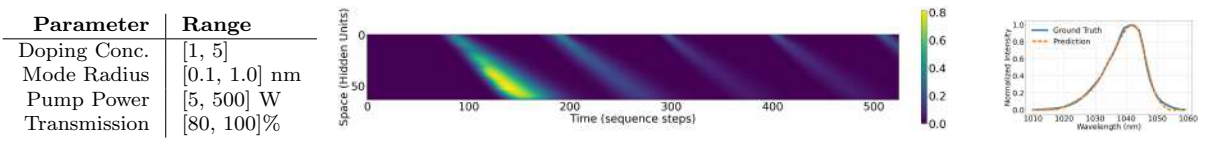
Numerical modeling based on the modified Frantz-Nodvik equations has provided insights into the dynamic behavior of pulse amplification [1]. Although these traditional methods have proven effective, NNs are emerging as powerful tools to model optical amplifiers, offering improved accuracy, computational efficiency, and capturing the nonlinear dynamics and memory effects in amplifiers [2]. However, black-box modeling of an NNs latent memory limits their full utility. Building on recent work [3] using convolution operators (*) to explain NN memory, we incorporate physical conservation laws by enforcing a latent continuity constraint. This approach may offer new insights into predicting power excursions or pulse-shape control, thereby enhancing amplifier design and optimization.

The photon density n(x,t) in a CPA is modeled by the continuity equation 1 and driven by the population inversion $\Delta = N_1 - N_2$, where N_1 and N_2 denote the density of steady and excited state atoms in the gain medium, c is the velocity of light and σ is the resonance absorption cross section. In a supervised learning framework, we are given gain medium features $x \in \mathbb{R}^n$, the intensity of an incoming pulse $I_{\text{in}} \in \mathbb{R}^T$ and outgoing pulse $I_{\text{out}} \in \mathbb{R}^T$. The NN is parameterized so that the latent state h^{t+1} is the forward solution of a continuity equation 2 from the state h^t , with learnable weight matrices W_x, W_{enc} and W_{dec} , and a projection matrix P_{bc} for the boundary conditions. This ensures the network weights model a discrete nonhomogeneous continuity equation, paralleling photon transport. The model is trained on labeled data to minimize the mean squarred error of the output, i.e., min $\mathcal{L}(W_{\text{dec}}h^T, I_{\text{out}})$.

$$\frac{\partial n}{\partial t} + c \frac{\partial n}{\partial x} = 2\sigma \Delta n, \text{ with bc. } n(0, t) = g, \qquad \frac{\partial \Delta}{\partial t} = -2\sigma \Delta n, \text{ with condition } N_1 + N_2 = C \qquad (1)$$

$$\mathbf{h}^{t+1} = \operatorname{softmax}(\mathbf{W}_x \mathbf{x}) \star \mathbf{h}^t + \Delta^t \mathbf{h}^t + \mathbf{P}_{bc.} \mathbf{W}_{enc} \mathbf{I}_{in}^t, \quad \mathbf{h}^0 = \vec{\mathbf{0}}, \quad \Delta^{t+1} = \Delta^t - 2\mathbf{h}^t \Delta^t, \quad \Delta^0 = \frac{\operatorname{sigmoid}(\mathbf{W}_{enc} \mathbf{x})}{\|\operatorname{sigmoid}(\mathbf{W}_{enc} \mathbf{x})\|_2^2} \qquad (2)$$

$$\boldsymbol{h}^{t+1} = \operatorname{softmax}(\boldsymbol{W}_{x}\boldsymbol{x}) \star \boldsymbol{h}^{t} + \Delta^{t}\boldsymbol{h}^{t} + \boldsymbol{P}_{\text{bc.}}\boldsymbol{W}_{\text{enc}}\boldsymbol{I}_{\text{in}}^{t}, \ \boldsymbol{h}^{0} = \vec{\boldsymbol{0}}, \quad \Delta^{t+1} = \Delta^{t} - 2\boldsymbol{h}^{t}\Delta^{t}, \quad \Delta^{0} = \frac{\operatorname{sigmoid}(\boldsymbol{W}_{\text{enc}}\boldsymbol{x})}{\|\operatorname{sigmoid}(\boldsymbol{W}_{\text{enc}}\boldsymbol{x})\|^{2}}$$
(2)



(a) Amplifier parameters

(b) Latent state evolution

(c) Pulse reconstruction

Figure 1: The dataset is constructed from the set of Yterbium amplifier parameters detailed in (a) and split into 80/20% train/test partitions. The latent state evolution illustrated in (b) shows 5 passes of the laser through the gain medium. The ground truth versus predicted evolution after the final pass through the gain medium is illustrated in (c). The network reveals pulse broadening/narrowing in each pass through the CPA. This work was supported by NSF grant DMS-2436343.

- [1] P. Kroetz, A. Ruehl, K. Murari, H. Cankaya, F.X. Kärtner, I. Hartl, and R.J.D. Miller, "Numerical study of spectral shaping in high energy Ho:YLF amplifiers", Opt. Express 24, 9905-9921 (2016)
- [2] S. Yan, W. Shi and J. Wen, "Review of neural network technique for modeling PA memory effect", 2016 IEEE MTT-S International Conference on Numerical Electromagnetic and Multiphysics Modeling and Optimization (NEMO), Beijing, China, 2016.
- [3] K.T. Anderson, L. Muller, T. Sejnowski, and M. Welling, "Traveling Waves Encode the Recent Past and Enhance Sequence Learning", The Twelfth International Conference on Learning Representations, 2024.

¹ University of California, Los Angeles, CA 90095, USA

² Stanford University, Stanford, CA 94305, USA

 $^{^3}$ SLAC National Accelerator Laboratory, Menlo Park, CA 94025, USA

^{*}justin@math.ucla.edu



Advancing X-ray Sources with Digital Twin Surrogates for Ultrafast Optics

Jack Hirschman,^{1,2,*} Hao Zhang,^{2,3} Abhimanyu Borthakur,³ Linshan Sun,³ Justin Baker,³ Andrea L. Bertozzi,³ Randy Lemons,² Frederick Cropp,² Razib Obaid,² Ryan Coffee,² Auralee Edelen,² and Sergio Carbajo^{2,3}

¹Stanford University, Stanford, CA 94305, USA

²SLAC National Accelerator Laboratory, Menlo Park, CA 94025, USA

³University of California, Los Angeles, CA 90095, USA

*jhirschm@stanford.edu

Abstract

We demonstrate digital twin surrogates for ultrafast optics applied to XFEL photoinjector systems. Integrating start-to-end simulations of the photocathode laser including $\chi^{(2)}$ and $\chi^{(3)}$ nonlinear processes, we couple resultant ultraviolet pulses to photocathode and FEL simulations, showing promising avenues to synergistically combine simulation and experiment through machine learning.

SLAC's LCLS-II is undergoing upgrades to push the frontiers of X-ray Free-Electron Lasers (XFELs), significantly advancing brightness, energy tunability, attosecond pulse generation, and repetition rate [1]. Fully harnessing these enhancements necessitates real-time optimization of accelerator beamlines to control X-ray characteristics precisely. Central to this optimization is the photoinjector laser, which initiates electron bunch formation via photocathode interaction (Fig. 1a) [2]. Leveraging the photoinjector laser's adaptability requires developing an accurate digital twin to produce customized laser profiles to interface with downstream accelerator simulations and to facilitate two-way information transfer-from model to experiment and experiment to model. Here, we introduce the core components of such a digital twin, starting with a comprehensive start-to-end (S2E) simulation framework of the laser system, including a spatial light modulator-based spectral pulse shaper, regenerative amplifier, and $\chi^{(2)}$ or $\chi^{(3)}$ nonlinear upconversion [3]. Upconversion, specifically via dispersion controlled nonlinear synthesis (DCNS)–a method contingent on noncollinear sum frequency generation (SFG)-or four-wave mixing (FWM), presents computational bottlenecks from solving the generalized nonlinear Schrödinger equation [4,5]. Thus, we implement a long short-term memory surrogate model for noncollinear SFG (Fig. 1b), achieving excellent fidelity with simulations and a 250× computational speedup [6]. Similarly, for FWM, we employ a hybrid neural network to reconstruct pump, signal, and idler pulses, demonstrating close agreement between simulation, machine learning (ML) predictions, and experimental data. These efficient and accurate ML surrogates accelerate digital twin development, enabling precise real-time optimization of ultrafast optical systems and enhancing downstream XFEL applications.

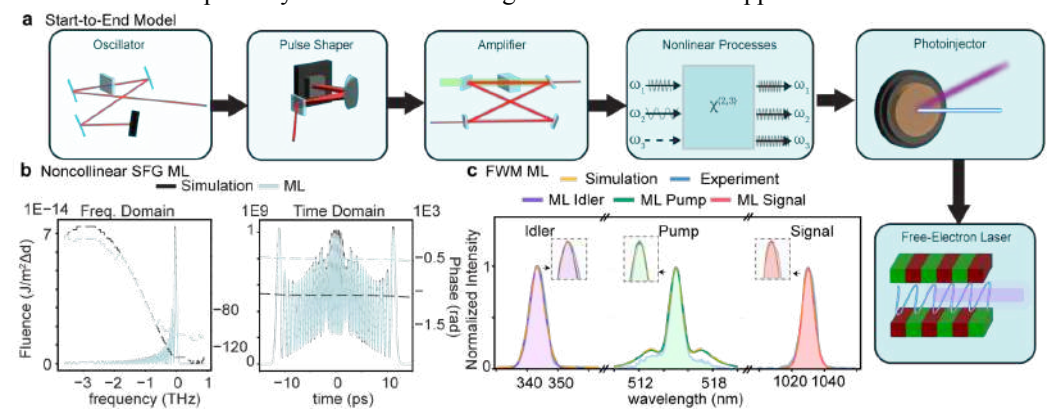


Figure 1. a) S2E software model linking oscillator, pulse shaper, amplifier, and nonlinear upconversion processes of photoinjector laser to injector and FEL processes; b) ML surrogate results for noncollinear SFG-based upconversion; c) ML reconstruction for FWM fiber dynamics compared to simulation and experiment.

- [1] H. Zhang, et al., HPLSE 12 (2024). https://doi.org/10.1017/hpl.2024.33
- [2] J. Duris, et al., Nat. Photonics 14 (2020). https://doi.org/10.1038/s41566-019-0549-5
- [3] J. Hirschman, et al., Opt. Express **32** (2024). https://doi.org/10.1364/OE.520542
- [4] R. Lemons, et al., PRAB 25 (2022). https://doi.org/10.1103/PhysRevAccelBeams.25.013401
- [5] H. Zhang, et al., Opt. Express **32** (2024). https://doi.org/10.1364/OE.542590
- [6] J. Hirschman, et al., Arxiv (2025). https://doi.org/10.48550/arXiv.2503.21198

CEP-stable High-power Ultra-short Ti:Sa laser system seeded by OPCPA

Jingfeng Chen¹, Raman Maksimenka^{2, *}, Solenne Favier¹, Philippe Demengeot¹, Yoann Pertot², Xiaowei Chen^{1, *}

Abstract

We present a high-power Ti:Sa laser system with stable Carrier-Envelope Phase (CEP) control, seeded by a Yb-pumped OPCPA injector. The CEP is passively stabilized through difference frequency generation in the OPCPA seeder, and slow drift in the Ti:Sa amplifier is corrected using a Dazzler device in the stretcher

The system, designed for attosecond science, uses a Ti:Sa CPA amplifier [1] (ARCO from Amplitude Laser), delivering 10 mJ at 1 kHz with pulse durations under 30 fs (see Figure 1 (a)). It is seeded by a custom OPCPA system with 800 nm pulses, a 150 nm bandwidth, and passive CEP stability achieved through difference frequency generation [2].

The seeder's pulse energy of several microjoules enables robust operation and broad bandwidth for the Ti:Sa amplifier, while the high pulse contrast improves temporal contrast. Over one-hour, passive CEP stability at the seeder output reaches a low 300 mrad without active correction, with only minor drift due to thermal or air fluctuations. Local CEP stability for 1000 consecutive shots at 10 kHz is around 200 mrad. To further stabilize CEP, an active correction loop using the Dazzler compensates for slow fluctuations and noise, resulting in 230 mrad CEP stability averaged over 10 shots for an hour (see Figure 1 (b)).

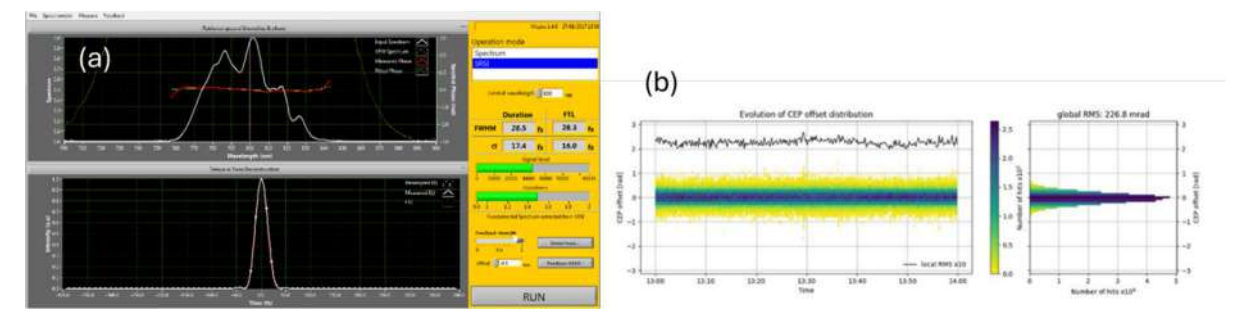


Figure 1: (a) Pulse duration measurement of the 10mJ, 1kHz Ti:Sa laser output. (b) Actively stabilized CEP over one hour averaged over 10 consecutive shots at 1 kHz.

This unique system architecture combines the best capabilities of both Ti:Sa laser amplification and OPCPA technologies in a single system leading to a cost-efficient high average and peak power with CEP stability for attosecond science such as high harmonic generation. While actual performances are already compatible with attosecond applications, we believe to significantly reduce the CEP noise level in the future.

- [1] D. Strickland and G. Mourou, "Compression of amplified chirped optical pulses," Optics Communications 6, 447-449 (1985).
- [2] R. Maksimenka & al, "A universal broadband and CEP stable seeder for high-power amplifiers", EPJ Web of Conferences, 309, 07003 (2024).

¹ Amplitude, 2-4 rue du Bois Chaland – CE 2926, 91029 Evry, France

² Fastlite by Amplitude, 165 rue des Cistes, 06600 Antibes, France

^{*}xiaowei.chen@amplitude-laser.com

250W, 2.5mJ, 7.3fs at 1030nm extracted from a dual-stage MPC-based post-compression

C. Grebing, S. Wunderlich, M. Tschernajew, E. Shestaev, F. Just, V. Hilbert, C. Kern, M. Kienel, H. Masood, T. Heuermann, C. Gaida, O. Herrfurth, <u>S. Breitkopf*</u>, T. Eidam, J. Limpert

Active Fiber Systems GmbH, Ernst-Ruska-Ring 17, 07745 Jena, Germany *publications@afs-jena.de

Abstract

World-record average power of 250W with 7.3-fs pulses. The driver laser system generates 290-fs pulses with up to 8mJ pulse energy, a fraction of it is post-compressed to 7.3fs (sub-3-cycle) at 2.5mJ and 100kHz, 250W respectively. Designed for long-term operation as part of a user-beamline at the Ohio-State-University [1]

Main Text

High-repetition-rate few-cycle laser systems with high average power and CEP-stable operation are essential for various scientific applications, including the generation of a continuum in the XUV for attosecond pulse generation and numerous ultrafast pump-probe measurements [2,3]. We present a sub-3-cycle laser system that combines high average power and pulse energy. This system is based on a fiber-based chirped-pulse amplification setup, incorporating the coherent combination of 14 main amplifier channels, similar to [4]. It emits 290-fs pulses with 8 mJ energy. A fraction of this energy is nonlinearly post-compressed to a few optical cycles in a two-stage multipass cell (MPC). The first MPC utilizes highly efficient dielectric mirrors, achieving an intermediate output of 5 mJ pulse energy, 500 W average power, and <40 fs pulse duration due to its 94% efficiency [similar to 5]. The second MPC further compresses the pulses to a duration of 7.3 fs (sub-3-cycle, see Fig. 1 left) at a pulse energy of 2.5 mJ, resulting in the highest compressed average power for few-cycle MPCs, with 250 W at a 100 kHz pulse repetition rate, nearly doubling previous, already impressive, results [6]. Furthermore, for such a complex device, the entire system demonstrates a remarkable power stability (see Fig. 1 right).

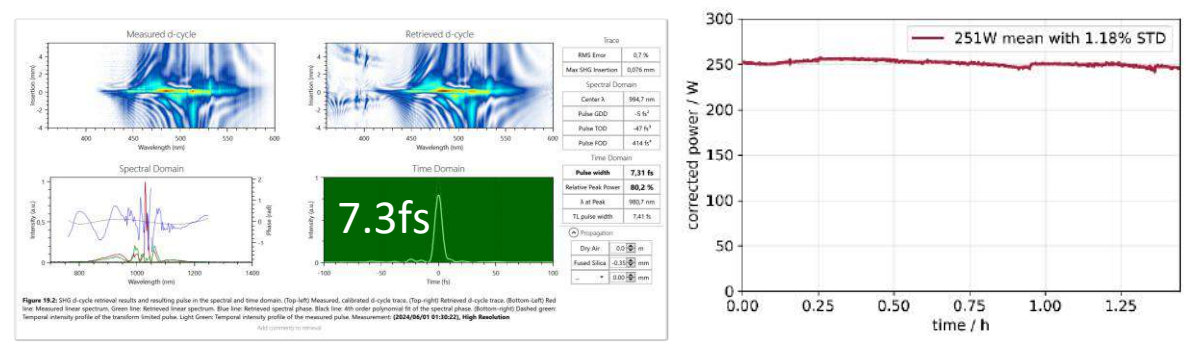


Figure 1 [Left] D-scan measurement [7] of the 2.5mJ output pulses at 100kHz. [Right] Long-term stability of the output at 250W of average power.

- [1] https://nsf-nexus.osu.edu/
- [2] J. J. Abel et al., "Non-destructive depth reconstruction of Al-Al2Cu layer structure with nanometer resolution using extreme ultraviolet coherence tomography," Mater. Charact. 211, 113894 (2024).
- [3] D. C. Haynes, et al., "Clocking Auger electrons," Nat. Phys. 17, 512-518 (2021).
- [4] M. Müller at al., "1 kW 1 mJ eight-channel ultrafast fiber laser," Opt. Lett. 41, 3439 (2016).
- [5] C. Grebing et al., "Kilowatt-average-power compression of millijoule pulses in a gas-filled multi-pass cell," Opt. Lett. 45, 6250–6253 (2020).
- [6] Semyon Goncharov et al., "Amplification-free GW-level, 150 W, 14 MHz, and 8 fs thin-disk laser based on compression in multipass cells," Opt. Lett. 49, 2717-2720 (2024)
- [7] F. J. Salgado-Remacha, et al., "Single-shot d-scan technique for ultrashort laser pulse characterization using transverse second-harmonic generation in random nonlinear crystals," Opt. Lett. 45, 3925-3928 (2020)

CEO Frequency Detection of Watt-Level Ho:CALGO Femtosecond Oscillator at 2.1 µm Wavelength

Sergei Tomilov^{1,*}, Yicheng Wang¹, Mykyta Redkin¹, Michael Müller^{1,2}, David R. Carlson³, Martin Hoffmann¹, Clara J. Saraceno¹

¹Photonics and Ultrafast Laser Science, Ruhr Universität Bochum, Universitätsstraβe 150, 44801 Bochum, Germany ²RayVen Laser, Universitätsstraβe 150, 44801 Bochum, Germany

³Octave Photonics, 325 W South Boulder Road, Louisville, CO 80027 USA

*Sergei.Tomilov@ruhr-uni-bochum.de

Abstract

We demonstrate $f_{\rm ceo}$ detection of a watt-level 100-fs Ho:CALGO oscillator at 2.1 μ m. The octave-spanning supercontinuum for self-referencing is generated in an integrated Ta₂O₅ waveguides. This result represents the first step toward fully stabilized watt-level frequency combs at 2.1 μ m.

Optical frequency combs operating beyond 1.5- μ m wavelength are attractive for a wide range of applications in fields such as attosecond science and spectroscopy. A central feature of a referenced frequency comb is a stabilized carrier-envelope offset frequency, f_{CEO} . Measuring and stabilizing f_{CEO} typically requires an f-to-2f interferometer, which necessitates an octave-spanning spectrum. For lasers based on broadband materials such as Cr:ZnS(e), octave-spanning spectra can be achieved by nonlinear spectral broadening in bulk media [1]. In contrast, f_{CEO} characterization of more power-scalable Tm- and Ho-based ultrafast lasers at this wavelength range is challenging, due to their relatively narrow emission bandwidths and typically long pulses. In this context, we recently demonstrated several novel solid-state Ho-lasers capable of watt-level and sub-100-fs pulses [2] with promising potential in this area.

In this work, we demonstrate f_{CEO} detection based on octave-spanning supercontinuum (SC) generation in chip-based Ta₂O₅ waveguides pumped by a 2.1-µm ultrafast laser, which is the first critical step toward full comb stabilization of this promising new Ho:CALGO laser technology [3]. The oscillator directly emits watt-level average power with 102-fs pulses at a center wavelength of 2.1 µm, a repetition rate of 71 MHz, a pulse energy of 14 nJ, and a peak power of 0.12 MW. Roughly 30% of the laser power is coupled into the waveguide. The generated SC spans from 0.9 µm to 2.6 µm at -30 dB, providing sufficient bandwidth for self-referencing of f_{CEO} . f_{CEO} detection is performed in a standard f-to-2f interferometer, as shown in Fig. 1(a). Without significant optimization, we were able to obtain an f_{CEO} beat note (~30 dB at 100-kHz resolution bandwidth (RBW)). To the best of our knowledge, this is the first f_{CEO} detection of a Ho-oscillator, which is important for the development of high-power infrared laser sources for metrological applications. Further passive improvements to the setup should enable a significantly higher signal-to-noise ratio and a full characterization of f_{CEO} . Furthermore, optimizing coupling efficiency for SC generation and realizing the control loop for f_{CEO} stabilization will allow us to obtain the comb with a much smaller fraction of the available laser power for future use of the system in applications.

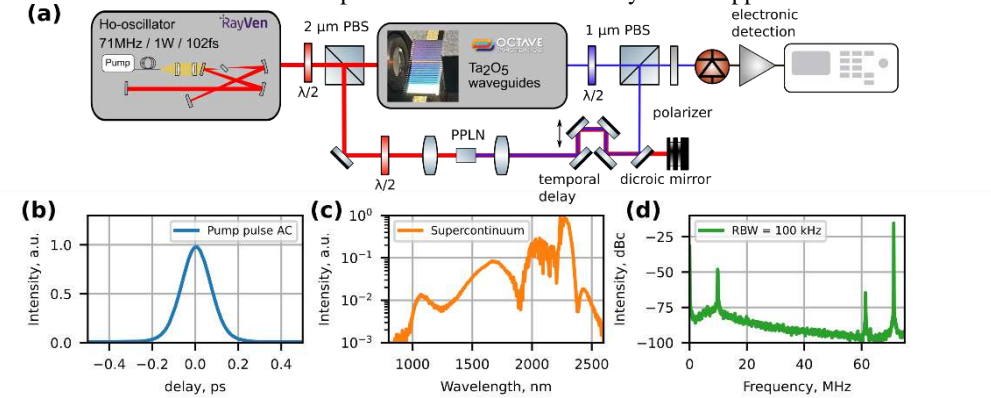


Figure 1: (a) Experimental setup for SC generation and f_{CEO} detection, PBS – polarized beam splitter; Autocorrelation (AC) trace of the pump pulse; (c) SC spectrum; (d) Radio-frequency spectrum featuring two f_{CEO} beat notes and fundamental repetition frequency of the pump laser.

- [1] M. Kowalczyk et al., "Ultra-CEP-stable single-cycle pulses at 2.2 µm," Optica 10, 801, (2023),
- [2] C. Gaida *et al.*, "High-power frequency comb at 2 μm wavelength emitted by a Tm-doped fiber laser system," Opt. Lett. **43**, 5178, (2008),
- [3] W. Yao *et al.*, "Low-noise, 2-W average power, 112-fs Kerr-lens mode-locked Ho:CALGO laser at 2.1 μm," Opt. Lett. **48**, (2023).

Passively Stable Free-space Coherent Combining in Nonlinear Pulse Compression

Nayla Jimenez,^{1,2,3,*} Victor Hariton,¹ Henrik Tünnermann,¹ Hüseyin Çankaya¹, Ingmar Hartl,¹ and Marcus Seidel^{1,2,3}

Abstract

We demonstrate passive coherent combining in multipass cells using free-space delay lines for spectral broadening and pulse compression. By dividing temporarily the initial pulse into two replicas, the pulses of 250-µJ energy and 1-ps pulse duration were compressed to 272-fs. The setup offers excellent passive stability, enabling efficient high-energy pulse compression.

Multi-pass cells (MPCs) provide an effective method for spectral broadening. However, one of the main challenges is their energy scalability, as the required cell length increases linearly with the input pulse energy [1]. To address this issue, several energy scaling methods have been proposed. Some of these involve temporally dividing the pulse using birefringent crystals [2,3]; however, this method is limited by the increasing thickness of the crystals, making it impractical for generating a large number of pulses. Therefore, we have implemented, to our knowledge, for the first time, in combination with MPCs, divided pulse spectral broadening with flexible free-space delay lines. The method is passively stable, largely energy scalable, and supports ultrabroadband pulses.

The experimental setup (Fig. 1a) features a burst-mode Yb:YAG amplifier emitting 950 fs pulses. The input pulse, with an energy of 250 μ J, is split into two replicas of 125 μ J each using a broadband 50/50 intensity beam splitter. One replica is sent through a 2-ns delay line. Its polarization is rotated by a half-wave plate (HWP), such that it is transmitted through a thin-film polarizer (TFP). Both replicas propagate along a common path through a 39 cm long MPC containing two 1-mm silica plates. After spectral broadening (Fig. 1b), the pulses were temporarily recombined using the same delay line with a height offset between the input and output beams to ensure proper separation. The pulses are then sent to a grating compressor and a diagnostics stage. A pulse duration of 272 fs was measured by FROG (Fig. 1c). Recombination efficiencies above 75 % were reached independent of the spectral broadening factor (Fig. 1d). As splitting and recombination paths are common, the approach exhibits very good passive stability (Fig. 1 e).

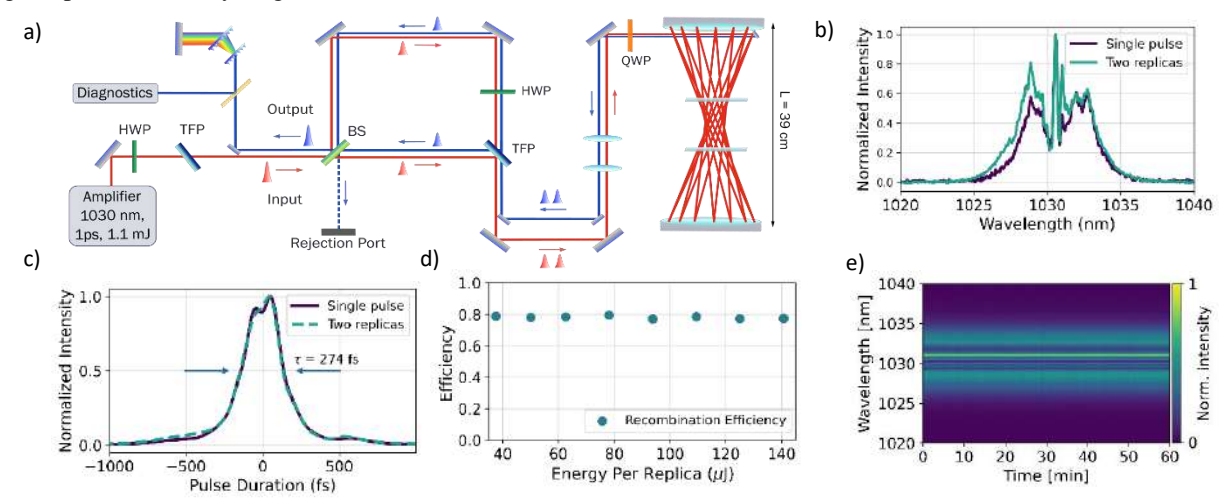


Fig. 1 a) Experimental setup. TFP: Thin Film Polarizer, BS: Beam Splitter. b) Spectrum of the Input and MPC output for a single pulse and two replicas. c) Pulse duration. d) System efficiency vs energy and e) Spectral stability.

- [1] A.-L. Viotti, M. Seidel, E. Escoto, S. Rajhans, W. P. Leemans, I. Hartl, C. M. Heyl, Optica 2022, 9, 197.
- [2] H. Stark, C. Grebing, J. Buldt, A. Klenke, J. Limpert, J. Phys. Photonics 2022, 4, 035001.
- [3] H. Schygulla, N. Jimenez, Y. Jiang, I. Hartl, M. Seidel, in EPJ Web Conf., EDP Sciences, 2024, p. 07011.

¹Deutsches Elektronen-Synchrotron DESY, Notkestraße 85, 22607 Hamburg, Germany

²GSI Helmhotzzentrum für Schwerionenforschung GmbH, Planckstraße 1, 64291 Darmstadt,

³Helmholtz-Institute Jena, Fröbelstieg 3, 07743 Jena, Germany

^{*}nayla.jimenez@desy.de

Broadband Dispersive mirrors for multipass cell with 100 GW peak power

V. Pervak^{1,2}, A. Kobiak², and A. Guggenmos²

¹ Ludwig Maximilians University, Am Coulombwall 1, 85748, Garching, Germany
² Ultrafast Innovations GmbH, Dieselstr. 5, 85748 Garching, Germany
e-mail correspondence: vladimir.pervak@lmu.de

Abstract: We present newly developed and produced high damage threshold and broadband multilayer mirrors for the multipass cell with the peak power toward 100GW. The mirrors cover the range of 800-1300 nm and exhibit exceptional reflectance exceeding 99.9%. The group delay dispersion of the mirrors is -100 fs2. The broadest mirrors set enable the generation of sub-7 fs pulses. In this work, we will discuss the critical points for such mirrors and provide solutions for sub-7 fs pulse or 100 GW peak power.

© 2025 The Author(s)

The pursuit of generating short laser pulses, limited by a single wave cycle of light, has been a long-standing goal since the invention of lasers. Laser pulses, comprising only a few wave cycles, enable more efficient exploitation of nonlinear optical effects, leading to remarkable advancements such as the generation of single subfemtosecond light pulses.

Recent years have witnessed significant development efforts focused on multipass cells as a simple and efficient way to convert Yb:YAG-based systems. These systems, capable of producing high-energy, relatively long pulses of about 500-1000 fs, can be converted to short pulses down to 7-fs with minimal losses.

A key component of multipass cells is dispersive mirrors, which play a crucial role in managing dispersion and extracting high intensities and energies. We present newly developed dispersive mirrors with exceptional smooth group delay dispersion (GDD), oscillating slightly around -100 fs2. Additionally, they exhibit high reflectance and a high damage threshold.

Magnetron sputtering (MS) deposition methods have gained increasing importance in producing ultrafast and high-resistive optical coatings. These methods allow for high packing density, enabling the deposition of dielectric multilayer coatings with optical losses of less than 100 ppm. This significantly reduces scattering losses and thermal load, which are major factors affecting the performance of high-power laser systems.

The mirrors were produced on a Helios, Bühler Alzenau GmbH magnetron sputtering coating machine. This machine enables the sputtering of coatings on substrates with a maximum diameter of 200 mm, making it suitable for the production of large-aperture optics.

Mid-frequency MS is known to produce sputtered layers with a high density of silicon (Si) defects. These defects have been shown to reduce the laser induced damage threshold (LIDT) of the coating. However, recently developed Radio Frequency (RF) magnetron sputtering allows for the direct sputtering of dielectric material from an oxide target. With RF MS, we can produce layers where all defects are transparent in the visible range because SiO2 has low absorption in this range. Transparent defects have a negligible impact on LIDT. The LIDT is very critical for reaching 100 GW peak power.

In this work, we demonstrate that the broadest mirrors produced using MS can support sub-7 fs pulses directly from a multipass cell. Further development of deposition technology and the closed development of multipass cell technology will enable us to achieve almost single-cycle regime from user-friendly and turn-key laser systems in the near future. This level of energy and pulse duration was not achievable with Ti:Sapphire-based systems.

△ UFO XIV Azores 2025

Multi-gigawatt peak power post-compression with higher-order vortex beams in a bulk multi-pass cell

Victor Koltalo, ¹ Saga Westerberg, ², * Melvin Redon, ² Gaspard Beaufort, ² Ann-Kathrin Raab, ² Chen Guo, ² Cord. L. Arnold, ² and Anne-Lise Viotti ²

Abstract

We present a compact bulk multi-pass cell employing higher-order Laguerre-Gaussian beams generated with a spatial light modulator. We achieve compression of $610\,\mu\mathrm{J}$, $180\,\mathrm{fs}$ pulses down to $44\,\mathrm{fs}$, boosting the peak power from $2.5\,\mathrm{GW}$ to $9.1\,\mathrm{GW}$.

High repetition rate ytterbium laser systems enable high flux high-order harmonic generation [1] and other strong-field applications. These systems typically produce pulses with durations of hundreds of femtoseconds, making it difficult to achieve high peak powers. Thus, they are often used in combination with pulse post-compression [2] based on self phase modulation in either a gaseous or bulk medium. One recently-demonstrated and efficient technique is nonlinear multi-pass cell (MPC) [3]. Bulk-based MPCs have the benefit of being more compact, as large vacuum chambers are not required. However, the input peak power in a bulk MPC is limited by the damage thresholds of the cell mirrors and the nonlinear material, and by eventual beam degradation due to operation far beyond the critical power for self-focusing. Several approaches have been investigated for increasing input pulse energy and thus peak power in post-compression setups, e.g., pulse division, concave-convex or folded geometries and beam shaping [4].

Here, we extend the latter to a compact bulk MPC utilizing higher-order Laguerre-Gaussian beams (LG_{0,l}, l=0-3), generated by a spatial light modulator (SLM). The pulse energy is redistributed into a larger spatial footprint, therefore decreasing the peak intensity. Figure 1 a) shows the laser parameters and a schematic of the compression setup. Figures 1 b) and c) display the input and output LG_{0,3} beams, carrying a pulse energy of 610 μ J. We demonstrate compression of 180 fs down to 44 fs (see figure 1 d)), corresponding to a peak power of 9.1 GW. Despite operating 600 times above the critical power for self-focusing in fused silica, the quality of the LG beam is maintained and the topological charge is conserved.

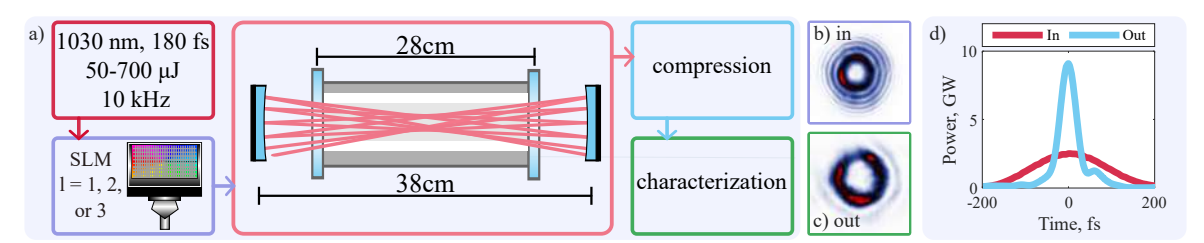


Figure 1: a) Schematic of the experimental setup. Beam profile of the LG_{03} mode b) before and c) after the MPC. d) Retrieved temporal profile of the pulse before (red) and after (blue) the post-compression setup.

- [1] R. Klas, W. Eschen, A. Kirsche, J. Rothhardt, and J. Limpert, "Generation of coherent broadband high photon flux continua in the XUV with a sub-two-cycle fiber laser," Opt. Express 28, 6188–6196 (2020)
- [2] T. Nagy, P. Simon, and L. Veisz, "High-energy few-cycle pulses: post-compression techniques," Advances in Physics: X 6, 1845795 (2021).
- [3] A.-L. Viotti, M. Seidel, E. Escoto, S. Rajhans, W. P. Leemans, I. Hartl, and C. M. Heyl, "Multi-pass cells for post-compression of ultrashort laser pulses," Optica 9, 197–216 (2022).
- [4] M. Kaumanns, D. Kormin, T. Nubbemeyer, V. Pervak, and S. Karsch, "Spectral broadening of 112 mJ, 1.3 ps pulses at 5 kHz in a LG10 multipass cell with compressibility to 37fs." Opt. Lett. 46, 929–932 (2021).

¹Laboratoire d'Optique Appliquée (LOA), Institut Polytechnique de Paris, ENSTA Paris - CNRS - Ecole Polytechnique, 91120 Palaiseau, France

²Department of Physics, Lund University, P. O. Box 118, SE-22100 Lund, Sweden

^{*}saga.westerberg@fysik.lth.se

High-Quality Soliton Compression in Hollow-Core Fiber

Callum R. Smith,* Erik N. Christensen, Rasmus D. Engelsholm, Patrick B. Montague

NKT Photonics A/S, Blokken 84, Birkerød, DK-3460, Denmark *casm@nktphotonics.com

Abstract

We present a simple soliton self-compression system consisting of a neon-filled anti-resonant hollow-core fiber. We achieved six-fold compression to 45.6fs whilst maintaining a pulse quality factor of 0.82. The pulse duration demonstrated excellent resilience against power fluctuations. Furthermore, the compression dynamics could be scaled to $\sim 10~\mu J$ level in the same fiber simply by varying the pressure.

High-power ultrafast laser systems delivering few-hundred femtosecond pulse durations facilitate a wide range of applications [1]. However, further decreasing the pulse duration of these systems whilst maintaining excellent pulse quality would be extremely beneficial in fields such as attosecond science [2], materials processing [3] and ophthalmology [4]. We present a simple pulse compression architecture consisting of input pulses coupled to a gas-filled anti-resonant hollow-core fiber (AR-HCF) to obtain compressed output pulses. In addition to the exceptional spatial and power handling properties of AR-HCF, their excellent flexibility in terms of length, gas species and pressure, can be utilized to achieve the desired compression ratio and compressed pulse quality [5]. To demonstrate this powerful technique we compress 275 fs pulses at 10 MHz from a 1033 nm mode-locked system with a maximum power of 10 W. To determine the optimal operating conditions for both high quality and compression factors we performed simulations based on a split-step Fourier method for solving the non-linear Schrödinger equation. Based on these simulations we opted for a soliton number of N \sim 2.5, experimentally achieved with 7.5 m of 27 µm core diameter AR-HCF filled with neon at 9.8 bar to achieve optimal compression at the fiber output (Fig. 1(c)). At the maximum available input power of 10 W we obtained an output power of 7.12 W (712 nJ pulse energy), a pulse duration of 45.6 fs (Fig. 1(a) inset), with a pulse quality factor of 0.82. The output pulse duration was very robust against changes in input energy, with only a slight decrease in pulse duration from 52.7 fs to 45.6 fs as the input pulse energy is increased from 800 nJ to 1000 nJ (Fig. 1(a)). Furthermore, we demonstrate scalability in pulse energy by compensating with a reduction in neon pressure, ensuring the nonlinear contribution remains unchanged. Since waveguide dispersion dominates around the pump wavelength of 1033 nm in smaller core AR-HCFs, such as the one used in these experiments, the dispersion landscape is also essentially unchanged. This allows us to achieve the same compression dynamics over a range of pulse energies in the same fiber simply by keeping the product of pulse energy and fiber pressure constant, as displayed in Fig. 1 (c). Additionally we will present further results on polarization properties and fiber delivery functionality.

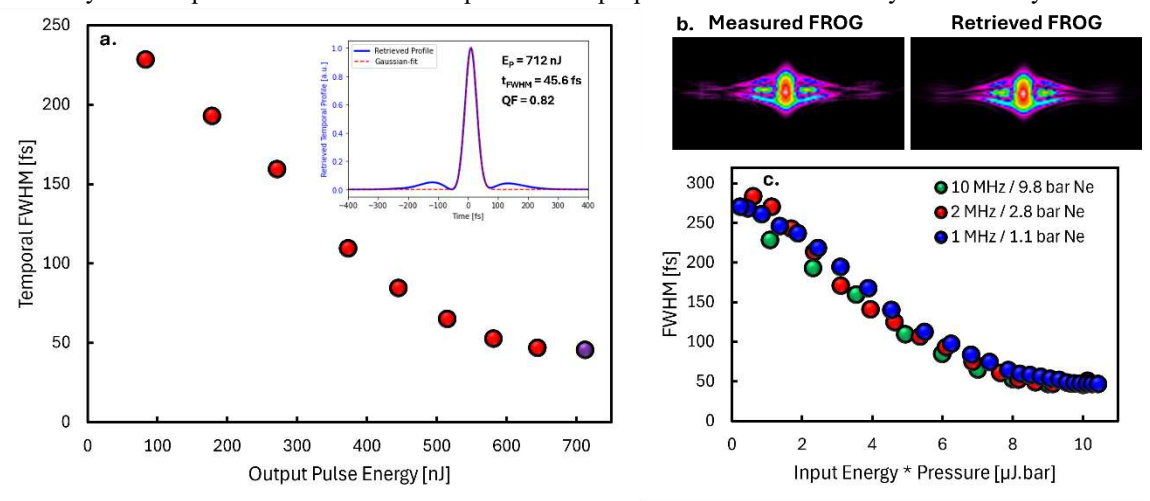


Figure 1: Compressed output pulse duration as a function of output pulse energy (a) with retrieved FROG pulse profile at maximum output power (inset), measured and retrieved FROG trace at maximum output power (b), and experimental set-up (c).

- 1. https://www.nktphotonics.com/products/ultrafast-fiber-lasers/aeropulse-fs-50/
- 2. F. Calegari, G. Sansone, S. Stagira, C. Vozzi, M. Nisoli, "Advances in attosecond science," J. Phys. B: At. Mol. Opt. Phys. 49 062001 (2016)
- 3. R. Gattass, E. Mazur, "Femtosecond laser micromachining in transparent materials," Nature Photon 2, 219–225 (2008)
- 4. B. Pajic, B. Pajic-Eggspuehler, C. Rathjen, M. Resan, Z. Cvejic, "Why Use Ultrashort Pulses in Ophthalmology and Which Factors Affect Cut Quality," *Medicina* 7 (2021)
- 5. D. Schade, et al, "Scaling rules for high quality soliton self-compression in hollow-core fibers," Opt. Express 29, 19147-19158 (2021)

Azores 2025

Towards (V)UV Dual Comb Spectroscopy with Femtosecond Temporal Resolution

Robert di Vora,^{1,*} Emily Hruska,¹ and Birgitta Bernhardt¹

¹Institute of Experimental Physics, Graz University of Technology, Petersgasse 16, 8010 Graz, Austria *divora@tugraz.at

Abstract

Dual Comb Spectroscopy (DCS) will be established in the (vacuum) ultraviolet (V)UV regime. The implementation of a pump-probe scheme enables the combination of the fast acquisition times and high spectral resolution of DCS with femtosecond temporal resolution.

Understanding light-matter interactions is of critical importance for molecular, chemical and optical physics, as well as material science. With ultrafast (femtosecond) pulses, photo-induced dynamics can be studied in real-time. Currently, research into improved spectroscopic methods suited for the UV regime is advancing rapidly. One powerful candidate which combines extreme relative spectral resolution (up to 10^{-11}) and fast acquisition times (down to µs) is DCS. While DCS has been established strongly in the NIR and THz domain, the ultraviolet regime has been explored only very recently with DCS [1, 2, 3]. As part of the ERC project "Electronic Fingerprint Spectroscopy"-ELFIS [4], Dual Comb Spectroscopy is expanded into the UV regime via High Harmonic Generation (HHG) enabling DCS to access the electronic energy structure in matter. Furthermore, a pump-probe scheme will be implemented. A sketch of the proposed experimental setup is shown in Figure 1. This unique combination of ultrahigh spectral and temporal resolution in the UV regime paves the way for the observation of subtle effects as for example wave packet dynamics in gases.

As a first example, high-repetition rate (10 MHz) pump-probe spectroscopy utilizing the fifth harmonic of the fundamental laser frequency ($\lambda_{\text{center}} = 206 \text{ nm}$) as a probe beam is currently realized. First results on time resolved UV dual comb spectroscopy in iodine will be presented.

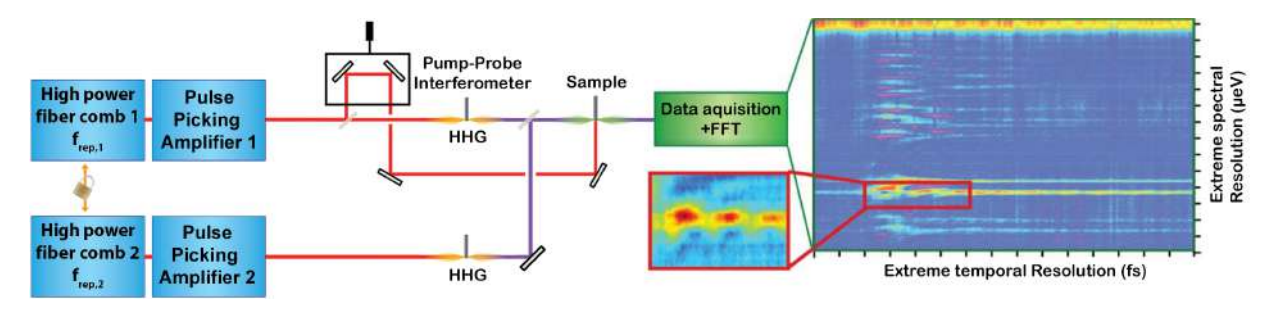


Figure 1: Overview of a UV Dual-Comb spectrometer setup including a pump-probe interferometer. This allows for a measurement combining both high spectral and temporal resolution simultaneously in a single experiment in the (V)UV regime. The data shown in the spectrogram are taken from [5].

- [1] L. Fürst, A. Kirchner, A. Eber, F. Siegrist, R. di Vora, and B. Bernhardt, "Broadband near-ultraviolet dual comb spectroscopy", Optica 11, 471-477 (2024). DOI: https://doi.org/10.1364/OPTICA.516783
- [2] B. Xu, Z. Chen, T.W. Hänsch, et al. "Near-ultraviolet photon-counting dual-comb spectroscopy", Nature 627, 289–294 (2024). https://doi.org/10.1038/s41586-024-07094-9
- [3] J. J. McCauley, M. C. Phillips, R. R. D. Weeks, Y. Zhang, S. S. Harilal, and R. J. Jones, "Dual-comb spectroscopy in the deep ultraviolet", Optica 11, 460-463 (2024). DOI: https://doi.org/10.1364/OPTICA.516851
- [4] ERC Grant 947288, DOI: 10.3030/947288, https://cordis.europa.eu/project/id/947288/de
- [5] A. R. Beck, et al. "Attosecond transient absorption probing of electronic superpositions of bound states in neon: detection of quantum beats", New J. Phys. 16 113016 (2014). DOI: https://doi.org/10.1088/1367-2630/16/11/113016

Nonlinear characterization of materials via low order surface harmonics driven by 100 fs pulses operating at 100 kHz

Hugo F. A. Pires, 1,* Hugo F. C. Gomes, 1 Gonçalo A. L. Vaz, 1 Gonçalo Figueira, 1 and A. G. Silva 2,*

Abstract

Low order surface harmonics provide insight into the atomic-scale structure and bonding at interfaces and surfaces of centrosymmetric materials. In this work, we show the experimental apparatus, automated detection systems, and the first results obtained in semiconductors, including novel reports of high order contributions and preliminary results in metallic samples.

Nonlinear optical phenomena, particularly second-harmonic generation (SHG), have long been used as a powerful tool to investigate the structural and electronic properties of materials. Surfaces and interfaces of centrosymmetric materials can be studied due to bulk contributions being forbidden due to inversion symmetry [1, 2, 3]. Despite these advancements, previous works have focused primarily on SHG, with limited exploration of higher-order nonlinear processes, particularly in reflective configurations.

In this work we study the surface second and third order harmonic emission of materials in the sub-ps regime. The harmonic signal dependence for different incident laser powers, incident laser polarization, outgoing laser polarization, and sample axis orientation are evaluated and discussed. The effect of pulse duration is also tested.

The laser used is a Yb:YAG delivering 1030 nm, 100 kHz, 1 ps, 1 mJ pulses coupled to a multipass cell that can compress the pulse duration down to 100 fs [4]. The availability of ultrashort mJ-level laser pulses operating at 100 kHz enables novel physics to be explored with fast acquisitions times.

The experimental setup, shown below, aims to characterize the crystalline symmetries and ultrafast laser light response of materials using the spectrum of the emitted radiation on a reflective configuration over a wide range of parameters. We will also present the system developed to automate the measurement of spectral data using a monochromator and an ADC (analog-to-digital converter), for precise measurement of very low intensity optical signals.

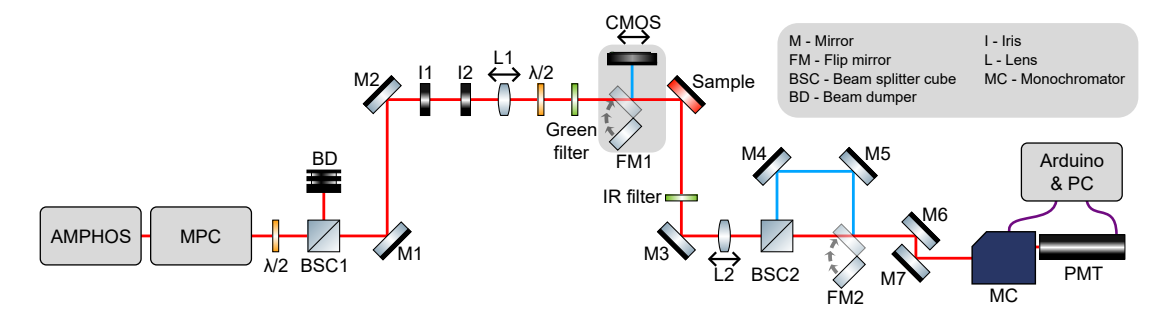


Figure 1: Experimental setup: AMPHOS- 1030 nm laser; MPC - MultiPass Cell; PMT - PhotoMultiplier Tube; CMOS - Camera

- J. F. McGilp, "Spectroscopic optical second-harmonic generation from semiconductor interfaces" Applied Physics A 4, 401–405 (1994).
- [2] R. M. Corn, "Optical second harmonic generation as a probe of surface chemistry" Chemical Reviews 1, 107–125 (1994).
- [3] A. Prylepa, "Material characterisation with methods of nonlinear optics" Journal of Physics D: Applied Physics 51, 043001 (2018).
- [4] G. Vaz et al., "Multidisciplinary laser facility driven by new-generation high-repetition laser" Photonics 12, 11 (2024).

¹GoLP/IPFN, Instituto Superior Técnico, Universidade de Lisboa, 1049-001 Lisboa, Portugal

²Universidade Nova de Lisboa, Campus da Caparica, 2829-516 Caparica, Portugal

 $^{^*}$ hugo.pires@tecnico.ulisboa.pt, acs@fct.unl.pt



Combining high temporal pulse quality and high compression factors via post-compression with chirped ellipse rotation

E. Escoto, A. Zablah, S. Rajhans, A. Schönberg, and C. M. Heyl^{1,2,3}

¹Deutsches Elektronen-Synchrotron DESY, Notkestraße 85, 22607 Hamburg, Germany

Abstract

Post-compression achieving large compression factors typically goes hand in hand with temporal pulse quality degradation. We numerically demonstrate a mitigation strategy using chirping and polarization rotation, achieving a very smooth spectrum with 99% of the compressed pulse energy in the main pulse.

Multi-pass cell (MPC) technology has enabled very high compression factors through self-phase modulation (SPM), while maintaining excellent spatial beam properties and high energy throughput. MPCs have therefore become a key technology for generating high-power, few- femtosecond laser pulses For many applications, a good temporal contrast is crucial. However, SPM causes modulations in the spectrum and also higher-order spectral phase components, which deteriorate the temporal contrast especially at high compression factors [1]. We propose an approach combining two pulse cleaning techniques: nonlinear polarization ellipse rotation (NER) [2] and enhanced frequency chirping (EFC) [3]. We refer to the combination as chirped ellipse rotation (CER).

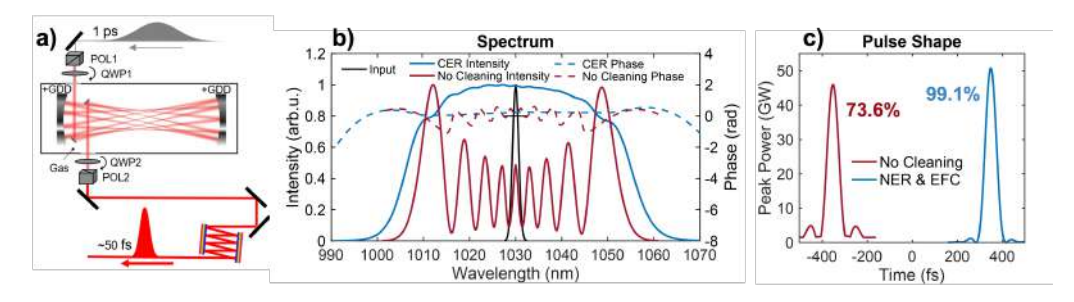


Figure 1: Fig. 1 (a) Schematic of the proposed CER scheme. POL: polarizer, QWP: Quarter-wave plate. (b) Comparison of the broadened spectra and corresponding phases, (c) temporal pulse shapes and percentage of output energy contained in the main peak.

CER can be implemented by simple addition of polarization optics to the post-compression setup and positive chirp within the MPC. Results of our numerical simulations are shown in Fig. 1(b-c). We here consider 5-mJ input pulses with a duration of 1 ps, centered at 1030 nm, post-compressed using a gas-filled MPC to reach a pulse duration 56 fs, i.e. a compression factor of 17. The two techniques can be synergistically combined: EFC helps NER to reach higher efficiencies, while the smoothening of the spectrum through EFC is enhanced even further by NER. The very smooth spectral intensity and phase shown in Fig. 1(b) enables compression of nearly the full output pulse energy within the main peak of the pulse, even though only second-order dispersion was removed in this simulation. Despite the losses intrinsic to NER (here almost 30%), the peak power reached exceeds the standard SPM case. At large compression factors, spectral broadening inside an MPC is then typically limited by parasitic four-wave mixing (FWM) [4]. In this contribution, we will also discuss strategies to mitigate this limit, thus paving the way towards even higher compression factors within a single MPC stage.

- [1] E. Escoto, A. L. Viotti, et al., "Temporal quality of post-compressed pulses at large compression factor," Optics Letters 39, 1694-1702 (2022).
- [2] E. Escoto, F. Pressacco, et al., "Improved temporal characteristics for post-compressed pulses via application-tailored nonlinear polarization ellipse rotation," Opt. Lett. 49, 6841-6844 (2024).
- [3] M. Benner, M. Karst, et al., "Concept of enhanced frequency chirping for multi-pass cells to improve the pulse contrast," J. Opt. Soc. Am. B 40, 301-305 (2023).
- [4] M. Hanna, N. Daher, et al., "Hybrid pulse propagation model and quasi-phase-matched four-wave mixing in multipass cells," J. Opt. Soc. Am. B 37, 2982-2988 (2020).

²Helmholtz Institute Jena, Fröbelstieg 3, 07743 Jena, Germany

 $^{^3}$ GSI Helmholtzzentrum für Schwerionenforschung GmbH, Planckstraße 1, 64291 Darmstadt, Germany

^{*}esmerando.escoto@desy.de

Bright, soft X-ray high harmonic source at 100 kHz repetition rate

Philipp Gierschke, ^{1,2*} Themistoklis Sidiropoulos, ² Lucas Eisenbach, ² Warunya Röder, ¹ Maximilian Karst, ^{3,4} Mathias Lenski, ² Ziyao Wang, ² Maximilian Benner, ²Arno Klenke, ^{1,2,3,4} Robert Klas, ¹ Jan Rothhardt, ^{1,2,3,4} Jens Limpert, ^{1,2,3,4}

Abstract

We report on bright soft X-ray emission via high harmonic generation in neon, driven by a $100 \, \text{kHz}$ ultrafast Thulium-fiber CPA system. We achieve a record photon flux exceeding $1.4 \times 10^8 \, \text{ph/s/1}$ BW at $300 \, \text{eV}$. This table-top, nW-class source renders an ideal platform for photon-hungry applications in the soft X-ray water window.

We present a table-top high harmonic soft X-ray (SXR) source that utilizes a power-scalable design based on Thulium-doped fiber chirped-pulse amplification (Tm:fCPA) [1] and subsequent pulse post-compression within a gas-filled hollow-core fiber [2]. Operating at a repetition rate of 100 kHz, this system delivers 67 W of average power with pulse durations of less than 11 fs at the generating target, which is a 2 mm neon gas jet at 4.25 bar backing pressure. The achieved photon flux at 300 eV reaches 1.4×10^8 photons/s/1% bandwidth and is approximately a factor 6 above the current state of the art [3,4], making this setup highly attractive for applications.

This work marks the first demonstration of a 100 kHz-repetition-rate SXR source that achieves these coherent flux levels around the carbon K-edge. The driving source high repetition rate, average output power, and few-cycle pulses are crucial, as they directly contribute to the increased photon flux of the SXR and highlight its capabilities as an ideal driving platform.

The demonstration of bright coherent SXR emission with a high repetition rate Tm:fCPA laser represents a significant step forward in lab-scale, laser-driven SXR sources and paves the way for future applications in advanced spectroscopy and table-top nanoscale imaging in the water window, which has so far been exclusive to synchrotrons [5]

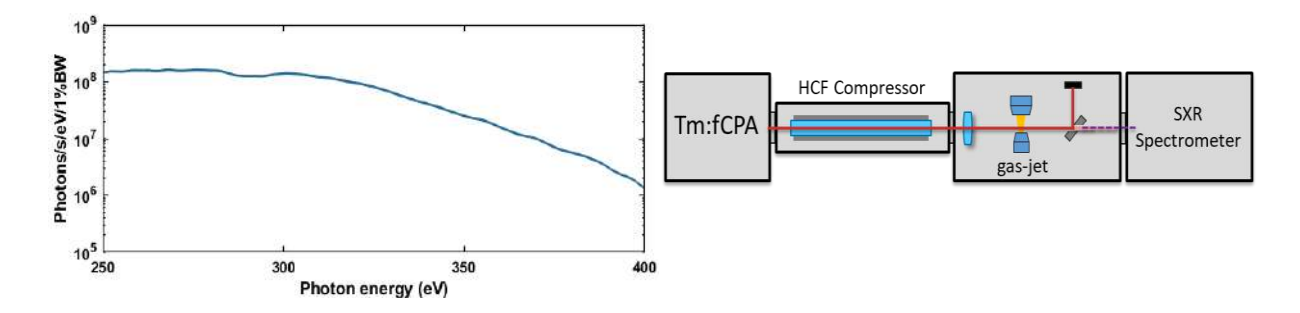


Fig 1: Optimized HHG spectrum (left), experimental setup including thulium-doped fiber chirped-pulse amplification (Tm:fCPA), hollow-core-fiber (HCF) compressor, high harmonic generation and soft X-ray (SXR) spectrometer (right).

- [1] T. Heuermann et al., "Ultrafast Tm-doped fiber laser system delivering 1.65 mJ, sub-100 fs pulses at 100 kHz repetition rate", Opt. Letters, 47, 3095 (2022)
- [2] Z. Wang, et al., "Nonlinear pulse compression to sub-two-cycle, 1.3 mJ pulses at 1.9 μm wavelength with 132 W average power," Opt. Lett. 48, 2647-2650 (2023).
- [3] S. Cousin et al., "High-flux table-top soft x-ray source driven by sub-2-cycle, CEP stable, 1.85 micron, 1-kHz pulses for carbon K-edge spectroscopy". *Opt. Lett.* **39**, 5383–5386
- [4] M. van Mörbeck-Bock et al, "High average power OPCPA MIR-systems for coherent soft x-ray generation accessing absorption edges of metals," Proc. SPIE **11777**, 117770C (2021).
- [5] N. Mille, et al., "Ptychography at the carbon K-edge," Commun. Mater. 3, 1–8 (2022)

¹Fraunhofer Institute for Applied Optics and Precision Engineering, Jena, Germany

²Institute of Applied Physics, Friedrich-Schiller-Universität Jena, Albert-Einstein-Str. 15, 07745 Jena, Germany

³Helmholtz-Institute Jena, Fröbelstieg 3, 07743 Jena, Germany

⁴GSI Helmholtzzentrum für Schwerionenforschung, Planckstraße 1, 64291 Darmstadt, Germany *philipp.gierschke@iof.fraunhofer.de

State of ELI ALPS high repetition rate lasers

Imre Seres,^{1*} Barnabás Gilicze,¹ Tamás Bartyik,¹ Zsolt Bengery,¹ Zsolt Kovács,¹ Bernát Vinkó,¹ Zoltán Várallyay,¹ Péter Jójárt,¹ Ádám Börzsönyi,¹ Evgeny Shestaev,² Maxim Tschernajew,² Nico Walther,² Christian Gaida,² Sven Breitkopf,² Tino Eidam,² Jens Limpert²

¹ELI ALPS, ELI-HU Non-Profit Ltd., Wolfgang Sandner utca 3., Szeged, H-6728, Hungary ²AFS - Active Fiber Systems GmbH | Member of the TRUMPF Group, Ernst-Ruska-Ring 17, 07745 Jena, Germany *imre.seres@eli-alps.hu

Abstract

The ELI ALPS High Repetition Rate laser lab provides mJ, CEP-stable, few-cycle pulses at up to 100 kHz repetition rate. HR2 laser reached 4 mJ, 6.2 fs pulses with excellent beam profile, and a new, extremely stable laser, HR-Alignment, was commissioned. These lasers are available through ELI ERIC user calls.

Introduction

Our laser systems, namely HR1, HR2, and HR-Alignment lasers, deliver few-millijoule pulses in the near-infrared (1030 nm) at repetition rates up to 100 kHz. High repetition rate enables experiments that require a large number of observations, or studying events with rare occurrence. These laser systems utilize ytterbium-based amplifiers generating sub-300 fs pulses, followed by multiple post-compression stages in multi-pass cells (MPCs) [1]. This flexible architecture allows tailoring pulse durations to various experimental needs. For instance, attosecond spectroscopy experiments [2] can utilize 30-50 fs pulses to generate attosecond pulse trains (APT) [3] via bypassing the further MPC stages. Alternatively, for experiments demanding high temporal resolution, such as single attosecond pulse generation, one can access CEP-stabilized 2-cycle pulses by using all of the MPC stages.

Results

Our flagship 100 kHz system, HR1, offers pulses up to 1.2 mJ at 30 fs or 1 mJ at 6 fs. This versatility has enabled numerous user experiments on the field of atto-science since 2018. [2,3].

The 100 kHz HR-2 laser system provides even higher energy than HR-1, delivering up to 6 mJ pulses tunable from 50 fs to 35 fs after the first 8 m long MPC stage. A second 8 m long stage further compresses the pulses down to sub-11 fs with 4.3 mJ energy. To achieve the sub-7 fs pulse regime necessary for CEP detection via the stereo-ATI method, a third 8 m long helium-filled MPC stage was recently added. This final stage delivers 4 mJ, 6.2 fs pulses, corresponding to 400 W average power, pushing the boundaries of ultrafast laser technology. Despite challenges in managing ionization threshold and nonlinear self-focusing within the long MPCs, we achieved excellent beam quality (Strehl ratio: 0.96, M2 =1.092, 0.04% astigmatism). The final 6.2 fs pulse duration was measured by D-scan method, where the relative peak power exceeding >90% according to the device.

To address demand for repetition rate flexibility in the HHG beamline during certain experiments, we commissioned the HR-Alignment laser system that shares the same beamline as HR-1 and offers similar pulse energy and sub-6 fs pulse duration, but with a wider range of repetition rates (single shot to 10 kHz). Based on a Light Conversion Pharos frontend and two post-compression stages, similar to HR-1, this system is a low-power and variable repetition rate alternative of the HR-1 [4]. It also provides several advantages, such as a warm-up time of less than 10 minutes, excellent beam pointing stability (with fluctuations below 25 µrad) and CEP stability (less than 300 mrad). Its robust nature supports long measurements including continuous 24-hour operation. During recent applications in photoelectron spectroscopy of gas-phase targets (C-ReMi measurements), we demonstrated over 100 hours long continuous measurement with extreme stability.

These advanced laser systems are available to researchers worldwide through ELI ERIC user calls.

- [1] S. Hädrich et al., "Carrier-envelope phase stable few-cycle laser system delivering more than 100 W, 1 mJ, sub-2-cycle pulses," Opt. Lett. 47, 1537 (2022).
- [2] D. Hammerland et al., "Reconstruction of attosecond pulses in the presence of interfering dressing fields using a 100 kHz laser system at ELI-ALPS," J. Phys. B At. Mol. Opt. Phys. **52**, 23LT01 (2019).
- [3] P. Ye et al., "High-Flux 100 kHz Attosecond Pulse Source Driven by a High-Average Power Annular Laser Beam," Ultrafast Sci. 2022, 2022/9823783 (2022).
- [4] B. Gilicze et al., "Tunable repetition rate, Compact, carrier-envelope phase stable sub-2-cycle, 1 mJ, laser system for high harmonic generation," Optica Open, preprint ID 121099

△ UFO XIV Azores 2025

High energy few-cycle flat-top beam single-plate post-compression

Gaudenis Jansonas,^{1,*} Dominykas Karvelis,¹ Pija Gadonaitė,¹ and Arūnas Varanavičius¹

¹Laser Research Center, Vilnius University, Saulėtekio Ave. 10, LT-10222 Vilnius, Lithuania *gaudenisjansonas@yahoo.com

Abstract

We report on efforts to shorten the $800\,\mathrm{nm}$ sub-8 fs pulse with a flat-top spatial profile by nonlinear spectral broadening in a single 1 mm thick fused silica plate. The results show a $3.8\,\mathrm{fs}$ pulse with a $64\,\%$ relative peak power. The achieved spatial-spectral homogeneity was $97\,\%$.

Main Text

In recent history, the post-compression became a very popular and useful tool for breaking the bandwidth limits of optical amplifiers [1]. Here we report on our recent efforts to overcome such a limit in the case of optical parametric chirped pulse amplification (OPCPA). Initially, our 200 Hz OPCPA system provided a passively carrier-envelope phase stabilized 800 nm output of around 5 mJ and 7.7 fs with a hyper-Gaussian beam profile. Spatiospectrally homogeneous nonlinear spectral broadening was achieved by relay imaging the flat-top beam from the final amplifier to a 1 mm thick fused silica plate, which was placed inside a vacuum chamber. Fused silica wedge and chirped mirror pairs were used in the same vacuum chamber for pulse compression and characterization via dispersion scan [2]. Spectrally-resolved wave-front analysis was performed to evaluate the spatial-temporal couplings. Deformable mirror wave-front correction and simple propagation model spectral properties prediction capabilities were tested with great success. The main results are presented in Figure 1. Here one can observe the temporal and spectral shape changes before and after the nonlinear spectral broadening and pulse re-compression. These properties were measured by averaging the information collected from the whole beam. The shown spatial-spectral homogeneity profile was measured at the image plane of the thin plate. It was found that the nonlinear spectral broadening did not change the spatial Strehl ratio, however, the beam quality parameter degraded by up to 1.5 times. The efficiency was measured to be around 40 %. This was mainly caused by metal (silver or aluminium) mirrors and uncoated glass components.

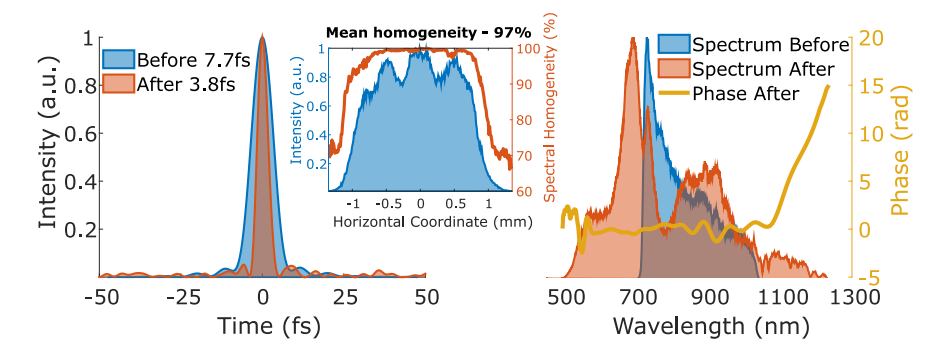


Figure 1: The visualization of main results. The illustration shows pulse shape and spectrum differences before and after post-compression. Measured spectral phase after the post-compression is presented as well. The horizontal cut of the beam profile with the calculated spatial-spectral homogeneity is shown in the inset.

In conclusion, a twofold pulse shortening (from 7.7 fs to $3.8^{+0.36}_{-0.25}$ fs) was shown with 40 % efficiency. The achievable relative peak power dropped from around 100 % to 64^{+4}_{-8} %. The flat-top beam provided the weighted average near-field spatial-spectral homogeneity of 97 % with only a single pass through a single thin plate of glass.

- T. Nagy, P. Simon, L. Veisz, "High-energy few-cycle pulses: post-compression techniques," Advances in Physics: X 6, 1845795 (2021).
- [2] F. Silva, M. Miranda, B. Alonso, J. Rauschenberger, V. Pervak, H. Crespo, "Simultaneous compression, characterization and phase stabilization of GW-level 1.4 cycle VIS-NIR femtosecond pulses using a single dispersion-scan setup," Optics Express 22, 10181-10191 (2014).

Composition-controlled recovery dynamics of GaSb-based **SESAMs in the SWIR**

M.C. Schuchter^{1,2,*}, M. Gaulke¹, N. Huwyler¹, M. Golling¹, M. Guina², U. Keller^{1,3}

¹ETH Zurich, Department of Physics, Institute for Quantum Electronics, 8093 Zurich, Switzerland

²Optoelectronics Research Centre, Physics Unit (TAU), FI-33720 Tampere, Finland

³ETH Zurich, Department of Electrical Engineering and Information Technology, 8093 Zurich, Switzerland *maximilian.schuchter@tuni.fi

Abstract

We present composition-controlled recovery times in SWIR GaSb-based SESAMs. Quantum well strain in quaternary InGaAsSb and the composition of AlGaAsSb barrier materials allows engineering of absorption recovery times from 1 picosecond to the nanosecond timescale.

The short-wave infrared (SWIR) regime is of growing interest for medical, sensing and spectroscopic applications. So far GaSb-based SESAMs operating at a center wavelength around 2 µm have used InGaSb quantum well layers embedded in GaSb barriers with sufficiently fast recovery times (<30 ps) [1], and have successfully modelocked both diode-pumped semiconductor [2], [3] and ion-doped solid-state lasers [4], [5], [6]. However, two-photon absorption (TPA) resulted in an early rollover of the nonlinear reflectivity at lower saturation fluences, limiting shorter pulse generation and high-fluence operation. The surprising result was that replacing the GaSb barrier material with AlAs_{0.08}Sb_{0.92} to reduce TPA, resulted in significantly slower recovery time of 605 ps.

We addressed this problem with a systematic investigation of the material-composition-dependent recovery times in the 2-µm to 2.4 µm wavelength range [7]. Each SESAM is a standard antiresonant low-finesse design with a Distributed Bragg Reflector (DBR) of 20 pair AlAs_{0.08}Sb_{0.92}/GaSb layers, 2 QW saturable absorber layers (11.5 nm thickness) around the antinode, and the semiconductor air interface located at a node of the standing wave of the design wavelength. The QWs are different ternary (InGaSb, GaAsSb) and quaternary (InGaAsSb) materials. The barrier materials are Al_xGa_{1-x}Al_ySb_{1-y} with varying aluminum (Al) content. Figure 1a) shows the strain dependence (e.g. lattice mismatch (LMM)) on the recovery time using ternary InGaSb (pink region), GaAsSb (green region) and quaternary InGaAsSb (orange region) QWs embedded in GaSb. The 2-µm SESAMs exhibit a QW LMM, with respect to the GaSb barrier, ranging from compressive strain (-1.71 %) to tensile strain (+0.92 %).

This investigation shows that the interband recovery time can be controlled via strain, with a maximum interband recovery time of 340 ps using -0.1 % lattice-matched QWs, whereas a -0.05 % LMM QW at 2.3 µm even reached 2.7 ns. Both compressively and tensile strained QWs result in a shorter interband recovery time, independent of arsenic concentrations but only dependent on the amount of strain in the QW. Furthermore, Figure 1b) shows the recovery time for a set of InGaSb QWs with constant strain (i.e. -1.71% LMM) using barriers with different Al content in the AlGaAsSb barrier. Increasing the Al content in the barrier increases the interband recovery time to a maximum of 605 ps using AlAs_{0.08}Sb_{0.92}. Combining the effects of lattice-matched QWs and AlAsSb barriers we can extend the recovery time into the nanosecond regime. Such a long recovery time is clearly a disadvantage for SESAM-based modelocking.

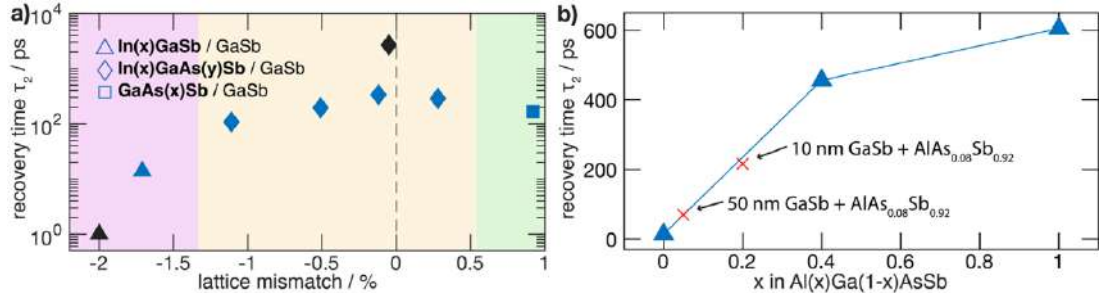


Figure 1: Recovery times of GaSb-based SESAMs at 2 -2.4 μm. a) Quantum well (QW) lattice mismatch (LMM) vs. recovery time τ₂ of 2-μm (blue) and 2.3 μm (black) SESAMs, using different InGaSb/GaSb (pink region), GaAsSb/GaSb (green region) and InGaAsSb/GaSb (orange region) QW designs. b) 2-µm SESAMs with fixed In₂₇GaSb QWs embedded in Al(x)Ga(1-x)AsSb (blue triangles connected). The red data points show two SESAMs embedded in a stacked barrier material of 50 nm resp. 10 nm GaSb followed by AlAs_{0.08}Sb_{0.92}.

- J. Paajaste et al., "Absorption recovery dynamics in 2 μm GaSb-based SESAMs," J. Phys. Appl. Phys., vol. 47, no. 6 (2014)

 A. Harkonen et al., "Modelocked GaSb disk laser producing 384 fs pulses at 2 μm wavelength," (2011)

 J. Heidrich et al., "324-fs Pulses From a SESAM Modelocked Backside-Cooled 2- μ m VECSEL," IEEE PTL, vol. 34, no. 6, pp. 337–340 (2022)

 A. Barh et al., "Watt-level and sub-100-fs self-starting mode-locked 2-4-μm CrZnS oscillator enabled by GaSb-SESAMs," Opt. Express, vol. 29, no. 4, p. 5934 (2021)

 A. Tyazhev et al., "Upconversion-pumped femtosecond thulium laser at 2309 mm mode-locked by a GaSb-based SESAM," Opt. Express, vol. 32, no. 9, p. 15093 (2024)
- S. Tomilov et al., "50-W average power Ho:YAG SESAM-modelocked thin-disk oscillator at 2.1 µm," Opt. Express, vol. 30, no. 15, p. 27662 (2022)
 M. C. Schuchter et al., "Composition-controlled recovery time of SWIR (2–2.4 µm) GaSb-based SESAMs," Opt. Express, vol. 33, no. 7, p. 14750 (2025)

Optical chip for carrier-envelope phase scanning of laser oscillator beams

Václav Hanus, 1 Beatrix Fehér, 1 and Péter Dombi 1,2,*

¹HUN-REN Wigner Research Centre for Physics, 1121 Budapest, Hungary ²ELI ALPS Research Institute, ELI ERIC, 6728 Szeged, Hungary *dombi.peter@wigner.hu, dombi.peter@eli-alps.hu

Abstract

We demonstrate an optical chip with which one can record a 3D map of the carrier-envelope phase (CEP) of nJ-level laser pulses in the focal volume with ~500 nm spatial resolution. We also show that CEP dependent signal levels can be significantly enhanced by metal-dielectric heterostructures.

The carrier-envelope phase (CEP) is a powerful knob to steer interactions of laser light with matter in the strong-field regime, as evidenced by numerous studies of ultrafast electron dynamics in atomic, molecular and solid-state media. Precise characterization of CEP or CEP changes in time or space is a key ingredient in applying electric-field sensitive techniques to study and control ultrafast electron processes in matter. Thus, characterizing and controlling CEP in space can support strong-field nanooptics experiments [1] or PHz optoelectronics [2].

Here, we present a novel, on-chip scanning CEP probe that is capable of measuring 3D CEP maps in the vicinity of a few-cycle laser beam focus for laser pulses having only ~nJ pulse energy without having to use vacuum equipment for this purpose [3]. The measurement principle and some results are depicted in Fig. 1. [4].

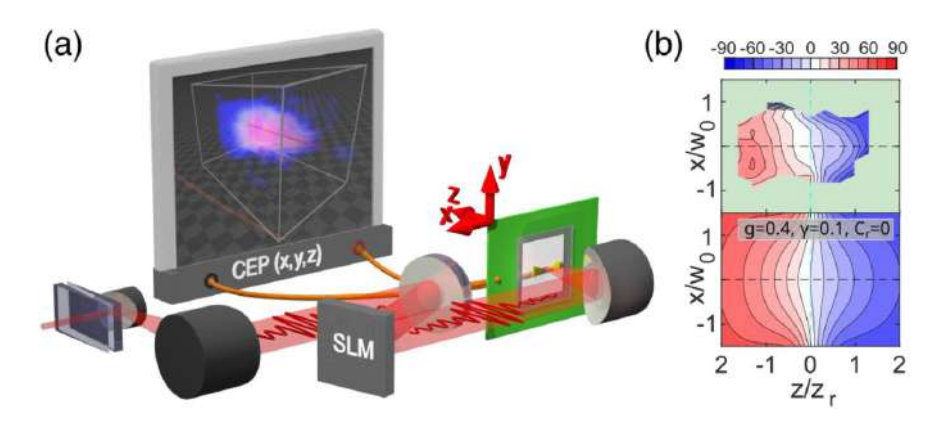


Figure 1. (a) Measurement setup with a false-color cloud showing measured values of the 3D CEP(x,y,z) distribution in the beam focus. Pink, white and blue color show positive, zero and negative CEP values respectively. (b) Measured CEP spatial distribution of a focused few-cycle laser beam (top panel). (bottom panel) Respective CEP distribution calculated with an analytical formula.

We will also feature recent results on how to use dielectric-metal heterostructures to enhance CEP dependent signal levels significantly. In addition, experiments on revealing the mechanisms of the ultrafast current generation process will also be presented. We also demonstrate a method to sculpt the CEP of few-cycle pulses in the vicinity of the focal volume.

In summary, our demonstration of a robust optical-to-electrical readout of CEP change using an engineered heterostructured material represents an important cornerstone for the development of few-cycle beam diagnostics and PHz devices.

- [1] P. Dombi et al., "Strong-field nano-optics," Rev. Mod. Phys. 92, 025003 (2020).
- [2] T. Boolakee et al., "Light-field control of real and virtual charge carriers," Nature 605, 251-255 (2022).
- [3] V. Hanus et al., "Light-field-driven current control in solids with pJ-level laser pulses at 80 MHz repetition rate" Optica **8,** 570-576 (2021).
- [4] V. Hanus et al., "Carrier-envelope phase on-chip scanner and control of laser beams," Nature Commun. **14**, 5068 (2023).

Mid-infrared supercontinuum generation up to 12 µm via intra-pulse difference frequency generation in Zinc Germanium Phosphide

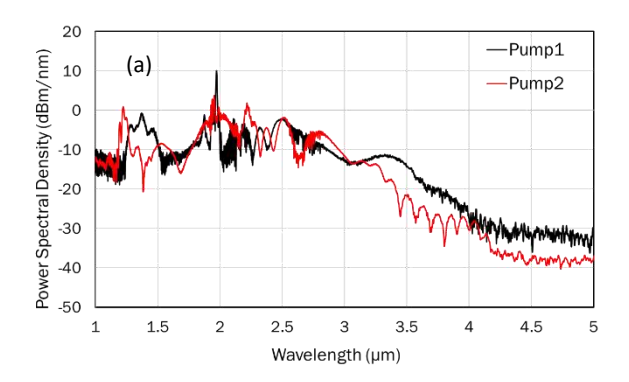
Ankita Khanolkar,^{1*} Chenchen Wan,¹ DongFeng Liu,¹ Sterling Backus, ^{1,2} Peter Fendel, and Reza Salem ^{1,3}

Abstract

We present a table-top, multi-octave, coherent mid-infrared light source by few-cycle pulse generation in an indium fluoride fiber and intra-pulse difference frequency generation in ZGP. Conversion efficiencies as high as 8.2% and wavelength coverage extending from $3.5~\mu m$ to $12~\mu m$ are demonstrated.

Summary

We demonstrate efficient IPDFG signals with up to 39 mW output and 8.2% conversion efficiency without using powerful pumps (μ J or mJ pulses) with complex architectures or employing elaborate pump pulse compression techniques [1,2]. We use a 50-MHz, all-fiber Tm-doped femtosecond laser at ~ 2 μ m generating 100 fs pulses with 600 mW average power (12 nJ). The fiber laser is spliced to a ~ 10 cm section of dispersion engineered indium fluoride (InF₃) fiber producing few-cycle pulses with 544 mW of power spanning from 1.3 μ m to ~ 3.5 μ m. The details regarding the non-linear fluoride fiber can be found in [3]. The output of InF₃ fiber is focused onto a 4 mm thick ZGP crystal using polarization projection method to facilitate Type-I phase matching. The output spectrum is recorded after a longpass filter with a 3.6 μ m cut-off using a Fourier-transform optical spectrum analyzer. Figure 1 (a) shows two pump spectra from two different fluoride fibers that enter ZGP. As these two pumps differ in spectral content, they result in two different IPDFG signals with distinct output power and spectral coverage as shown in Figure 1(b). The broadband spectrum extending up to 12 μ m in Figure 2 can be attributed to the use of a slightly larger core (hence more anomalously dispersive) fluoride fiber.



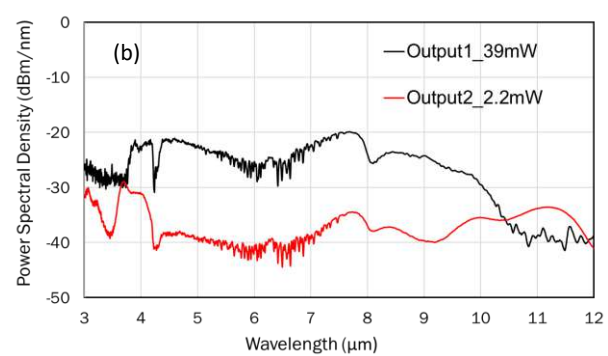


Figure 1: (a) Pump spectra from two different fluoride fibers (b) Output IPDFG signals corresponding to pump spectra in Figure 1(a)

References

[1] S. Vasilyev, I. Moskalev, V. Smolski, J. Peppers, M. Mirov, A. Muraviev, K. Zawilski, P. Schunemann, S. Mirov, K. Vodopyanov, and V. Gapontsev, "Super-octave longwave mid-infrared coherent transients produced by optical rectification of few-cycle 2.5-µm pulses," Optica 6, 111-114 (2019).

[2] T. Heuermann, Z. Wang, M. Lenski, J. Limpert, J., "Highly efficient, ultra-broadband mid infrared generation driven by a Tm-doped fiber laser system", Fiber Lasers XXI: Technology and Systems **12865**, 160-162 S (2024).

[3] R. Salem, Z. Jiang, D. Liu, R. Pafchek, D. Gardner, P. Foy, M. Saad, D. Jenkins, A. Cable, and P. Fendel, "Midinfrared supercontinuum generation spanning 1.8 octaves using step-index indium fluoride fiber pumped by a femtosecond fiber laser near $2 \mu m$," Opt. Express 23, 30592-30602 (2015).

¹Thorlabs Inc., 43 Sparta Avenue, Newton, New Jersey 07860 USA

²Colorado State University, Electrical and Computer Engineering, 1373 Campus Delivery, Ft. Collins, Colorado USA *AKhanolkar@thorlabs.com

Anomalous spin dynamics after dual optical excitation

Sergii Parchenko, 1* Peter M. Oppeneer, 2, and Andreas Scherz¹

¹European XFEL, Holzkoppel 4, 22869 Schenefeld, Germany

²Department of Physics and Astronomy, Uppsala University, Box 516, SE-75120 Uppsala, Sweden *sergii.parchenko@xfel.eu

Abstract

Dual noncollinear femtosecond pulses induce anomalous spin dynamics in copper, revealing a $2.5 \times$ slower spin relaxation and a unique negative reflectivity signal. Absent under single-pulse excitation, these effects indicate transient nonthermal modifications of electron-lattice coupling, offering a novel pathway for ultrafast control of quantum states via optical pulse engineering.

Main Text

Traditional perspectives regard optical excitation as a means of transferring thermal energy to electrons, leading primarily to electron-lattice thermalization. However, emerging evidence indicates that optical excitation may also perturb the fundamental electron interactions. In magnetic systems, dual-pump configurations have been shown to affect spin dynamics by delaying demagnetization and prolonging precession ^{1,2,3}. Motivated by these observations, our work investigates whether similar nonthermal modifications occur in nonmagnetic copper using circularly polarized near-infrared NIR pulses. We employ a dual-pump setup in which two noncollinear ultrashort NIR pulses are used to excite copper samples. Circularly polarized pulses are used to generate spin polarization via the inverse Faraday effect. The ensuing dynamics is monitored using time-resolved magneto-optical Kerr effect and transient reflectivity measurements.

Under single-pump excitation, the spin relaxation decay time is approximately 0.6 ps, consistent with conventional electron-lattice thermalization dynamics. Remarkably, dual-pump excitation extends the spin relaxation decay time to ~1.5 ps—a 2.5× increase—suggesting that the efficiency of angular momentum transfer is reduced under these conditions. Concomitantly, transient reflectivity measurements reveal a distinct negative signal at ~1.5 ps delay, a feature completely absent in single-pump experiments. This negative signal persists well beyond the typical thermal response timescale and correlates with both a ~3% reduction in amplitude and a 30 fs temporal shift in the ultrafast magnetic response. These observations rule out simple excitation efficiency artifacts.

Our findings challenge the traditional thermal paradigm of optical excitation by indicating that dual optical pulses can modify the electron-lattice coupling through nonthermal pathways. We propose that the interference between the pulses leads to a transient, long-lasting modification of the electron wavefunction. This modification, in turn, alters the dynamic coupling between the excited electrons and the lattice. This mechanism resonates with prior observations in magnetic materials, where dual-pump configurations have been shown to delay demagnetization processes. The fact that a similar effect is observed in nonmagnetic copper highlights the broader universality of this phenomenon and underscores the potential of dual-pulse engineering as a versatile technique for tailoring quantum states.

Our study demonstrates that by leveraging the interference of ultrashort NIR pulses, it is possible to "reprogram" electron dynamics without inducing structural modifications to the material. This approach not only broadens our understanding of nonthermal electron dynamics but also offers a new avenue for the development of next-generation spintronics and light-driven quantum materials. The ability to precisely manipulate spin and charge states on ultrafast timescales opens up exciting possibilities for future research and technological applications.

- [1] S. Parchenko et al., "Demagnetization dynamics after noncollinear dual optical excitation", Phys. Rev. B **110**, 054425 (2024).
- [2] S. Parchenko et al., "Magnetization precession after non-collinear dual optical excitation", J. Appl. Phys. **135**, 173902 (2024).
- [3] S. Parchenko et al., "Magnetization switching in GdFeCo induced by dual optical excitation", Phys. Rev. B 110, 174401 (2024).

From Green to EUV: Efficient Coherent Light Generation at 13.5 nm Driven by a 515 nm Source

Maximilian Karst^{1,2,3,*}, Lucas Eisenbach^{1,2,3,4}, Philipp Gierschke^{1,4}, Robert Klas^{1,2,3,4}, Jan Rothhardt^{1,2,3,4} and Jens Limpert^{1,2,3,4}

¹Institute of Applied Physics, Abbe Center of Photonics, Friedrich Schiller University Jena, Albert-Einstein-Str. 6, 07745 Jena, Germany

Abstract

We demonstrate a highly efficient source of coherent extreme ultraviolet (EUV) light based on high harmonic generation. The ultrashort green driver laser enables record flux and conversion efficiency with unprecedented scaling potential allowing for $>10 \,\mu\text{W}$ -class EUV sources.

The presented source of coherent extreme ultraviolet light is based on high-harmonic generation (HHG) in a helium gas-jet. The process is driven by ≤ 20 fs pulses with a center frequency of 515 nm. These are generated by frequency-doubling an Yb:fiber laser and consecutive nonlinear pulse compression in a multipass cell [1]. Figure 1 a) displays the building blocks of the generation scheme and b) a recorded HHG-spectrum. The advantage of utilizing the second harmonic rather than the fundamental near infrared (NIR) driving laser becomes apparent when looking at the very favorable efficiency scaling of the single-atom response with λ^{-6} [2], enabling a boost of more than an order of magnitude.

The presented preliminary results, achieved with only 1.2 W of average power at 5 kHz, already outperform a state-of-the art few-cycle NIR driver with 30 W [3]. To the best of our knowledge this is the highest flux HHG-source at 13.5 nm. For harmonic line 37 (\sim 91 eV) a conversion efficiency exceeding 10^{-7} is achieved.

Furthermore, upscaling of the driver to 100 kHz is currently underway which will allow for unprecedented photon flux enabling new possibilities for actinic inspection of lithography masks e.g. via ptychographic nanoscale imaging and scaling of existing photon hungry applications [4, 5].

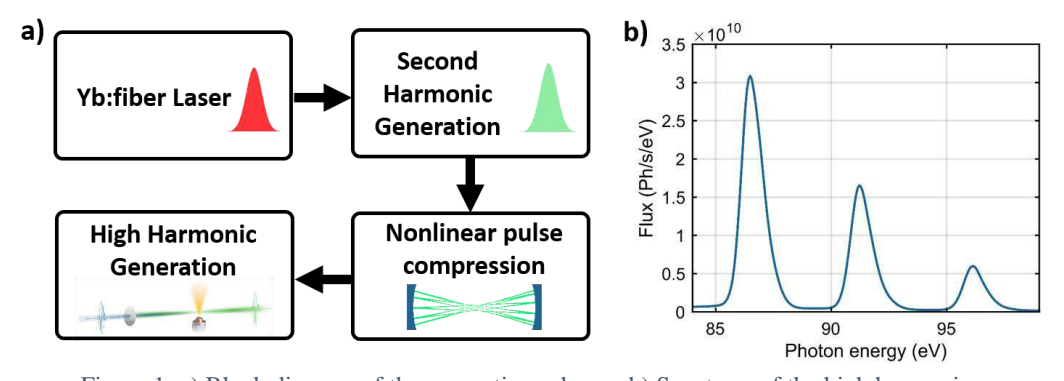


Figure 1: a) Block diagram of the generation scheme. b) Spectrum of the high harmonics.

- [1] M. Karst et al., "22-W average power high pulse energy multipass-cell-based post-compression in the green spectral range," Optics Letters 48, 1300 (2023).
- [2] A. D. Shiner et al., "Wavelength scaling of high harmonic generation efficiency," Physical Review Letters 103, 073902 (2009).
- [3] R. Klas et al., "Generation of coherent broadband high photon flux continua in the xuv with a sub-two-cycle fiber laser," Optics Express 28, 6188 (2020).
- [4] D. Kazazis et al., "Extreme ultraviolet lithography," Nature Reviews Methods Primers 4, 84 (2024).
- [5] W. Eschen, et al., "Material-specific high-resolution table-top extreme ultraviolet microscopy," Light: Science & Applications 11, 117 (2022).

² Helmholtz-Institute Jena, Fröbelstieg 3, 07743 Jena, Germany

³GSI Helmholtzzentrum für Schwerionenforschung, Planckstraße 1, 64291 Darmstadt, Germany

⁴Fraunhofer Institute for Applied Optics and Precision Engineering, Albert-Einstein-Str. 7, 07745 Jena, Germany *maximilian.karst@uni-jena.de

△ UFO XIV Azores 2025

Fast dispersion scan trace retrieval: neural networks vs. iterative algorithms

Miguel Canhota,^{1,*} Daniel Díaz Rivas,¹ Caroline Juliano,¹ Marzo C. López Cerón,¹ Ivan Sytcevich,¹ Chen Guo,¹ Anne-Lise Viotti,¹ and Cord L. Arnold¹

Abstract

In this work, we extend the current state-of-the-art dispersion scan retrieval algorithm based on neural networks, for the simultaneous retrieval of spectrum and phase, and compare it with an optimized iterative algorithm, in terms of quality and speed of retrieval.

Novel laser technologies provide high peak and average power and high repetition rate, with applications ranging from high-harmonic generation to terahertz generation [1], many of which call for single-shot pulse characterization capabilities. The dispersion scan (d-scan) is a simple, inline pulse characterization technique [2] with single-shot acquisition variants [3]. To complement the single-shot acquisition it is highly desirable to have a (near) single-shot retrieval ability. Towards that end, we implement neural networks based on a DenseNet architecture [4]. DenseNet is a neural network comprised of blocks of contiguous layers where each layer receives inputs from all preceding layers, which allows for feature reuse and better training efficiency.

To enable the retrieval of the spectrum, an inverse Fourier transform was introduced before the linear layers of DenseNet. This makes the training process more predictable to the neural network as its outputs are compared against a sparser representation of the training data, i.e., the electric fields in time-domain, instead of frequency-domain. This capability to simultaneously retrieve both the spectrum and spectral phase, generalizes the implementation that relied on a separately measured spectrum, and puts it on par, in this regard, with iterative methods. The neural networks performances are then compared against an optimized single-core implementation of the ptychographic retrieval algorithm [5] written in C++ language and leveraging Single Instruction Multiple Data (SIMD) operations.

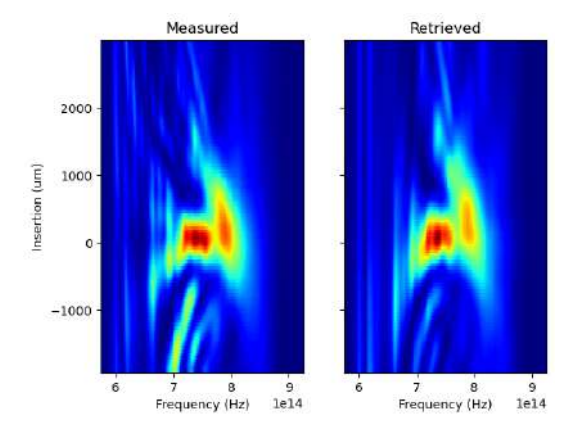


Figure 1: Left) Measured trace. Right) Retrieved trace using neural networks.

- [1] M Kling et al., J. Opt. 27, 013002 (2025)
- [2] M Miranda et al., Opt. Exp. 20, 688-697 (2012)
- [3] D Fabris et al., Opt. Exp. 23, 32803-32808 (2015)
- [4] S Kleinert et al., Opt. Lett. 44, 979-982 (2019)
- [5] A Wilhelm et al., Opt. Exp. 29, 22080-2209 (2021)

¹Department of Physics, Lund University, P. O. Box 118, SE-22100 Lund, Sweden

^{*}miguel.canhota@fysik.lth.se

Highly Efficient and Compact High-Harmonic Source at 45 to 65 eV for Magnetic Imaging

 $\label{eq:manual_manual_state} \begin{subarray}{ll} Mahmoud Abdelaal^{1,*}, Daniel S. Penagos Molina^{1,2,3}, Maximilian Karst^{1,2,3}, Robert Klas^{1,2,3,4}, Jens Limpert^{1,2,3,4} and Jan Rothhardt 1,2,3,4 and Jan Rothhardt 1,2,3,4 and Jan Rothhardt <math>^{1,2,3,4}$ and 1,2,3,4 a

Abstract

We demonstrate a high-flux XUV table-top source (45–65 eV, $>1\times10^{11}$ ph/s/harmonic) driven by a frequency-doubled Yb-fiber laser system, achieving record efficiency. This compact system targets $3p\rightarrow3d$ transitions in Fe/Co/Ni for studying ultrafast spin dynamics and nanoscale magnetic imaging.

Our compact HHG system is driven by a frequency-doubled Yb-fiber laser at 515 nm, post-compressed using a hollow-core fiber, delivering 58 μ J, 100 kHz pulses with 18 fs duration and M²=1.1×1.2 similar to the reported source [1]. The shorter wavelength of the driver improves HHG conversion efficiency by minimizing electron wave-packet spreading in the continuum, thereby increasing the probability of recombination. While the cut-off frequency decreases with shorter wavelengths, a shorter pulse duration compensates by increasing the cut-off energy limit [2,3]. The phase-matching conditions are fulfilled in front of the focus with a backing pressure of 1.4 bar neon and a 210 μ m diameter gas nozzle, as verified by 1D simulations [4]. This configuration delivers a state-of-the-art flux of 3.8×10^{11} ph/s/harmonic at 55.5 eV, as illustrated in Figure 1. Additionally, the system achieves an overall conversion efficiency of 1.5×10^{-7} , which is five times higher than that achieved through direct high-harmonic generation (HHG) using infrared post-compressed Yb-fiber CPA [5].

Many XUV applications can benefit from high-flux, high-efficiency table-top XUV sources with an extended spectral range of 20 to 70 eV using various gases. For instance, reflection ptychography has already demonstrated reliable performance for ptychographic imaging at 26 eV with argon [6]. Recent advancements have further broadened its capabilities to include 3p resonances of the 3d transition metals Fe (55.0 eV), Co (60.3 eV), and Ni (66.6 eV), enabling high-throughput nanoscale magnetic imaging and supporting pump-probe studies of femtosecond magnetization dynamics [7,8].

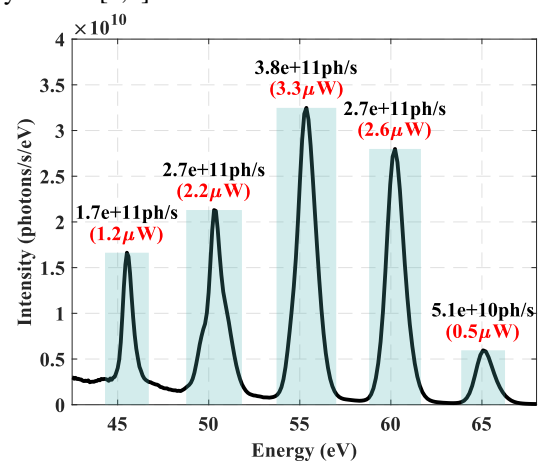


Figure 1: The HHG spectrum at the source. Each harmonic peak shows the photon flux (black) and average power (red), calculated by integrating over the shaded area.

- 1. R. Klas et al., PhotoniX 2, 1–8 (2021).
- 2. D. Shiner et al., Phys. Rev. Lett. 103, 073902 (2009).
- 3. G. Fan, et al. Optica, OPTICA 9 (2022).
- 4. E. Constant et al., Phys. Rev. Lett. 82, 1668 (1999).
- 5. Kirsche et al., Opt. Express 31, 2744–2753 (2023).
- 6. Seaberg, M.D et al., Optica 1.1, 39-44, (2014).
- 7. D. V. Christensen et al., J. Phys. Mater. 7, 032501 (2024)
- 8. K. Yao et al., Rev. Sci. Instrum. 91, 093110 (2020).

¹Institute of Applied Physics Friedrich-Schiller-University Jena, Albert-Einstein-Str 15 07745 Jena, Germany

²Helmholtz-Institute Jena, Fröbelstieg 3, 07743 Jena, Germany

³GSI Helmholtzzentrum für Schwerionenforschung, Planckstraße 1, 64291 Darmstadt, Germany

⁴Fraunhofer Institute for Applied Optics and Precision Engineering, Albert-Einstein-Str 7, 07745 Jena, Germany *mahmoud.abdelaal@uni-jena.de

UFO XIV Azores 2025

High-speed fly-scan ptychography with single-pulse diffraction

Augustas Karpavičius, 1,2,3,* Matthias Gouder, 1,2 and Stefan Witte 1,2,3

Abstract

We present a high-speed, synchronized fly-scan ptychography system combining continuous sample movement and a Timepix3 detector to capture single-pulse diffraction patterns at kilohertz rates. Achieving 2.3 Gpix/h throughput, we enable 30 ms-scale dynamic imaging of both object and illumination field with diffraction-limited resolution.

Main Text

Ptychography is a computational imaging technique that enables simultaneous reconstruction of both the complex object function (amplitude and phase) and the illumination probe from a series of intensity diffraction patterns acquired at highly overlapping scan positions [1]. Compared to conventional imaging methods, it provides considerably more comprehensive information about the object, including quantitative phase, and does so without requiring an aberration-free optical system, enabling the achievement of the world-record resolution [2]. This is made possible by the intrinsic redundancy in the recorded data, which makes the method robust, as it allows for correction of experimental instabilities such as sample-detector distance errors, angular misalignments and other measurement imperfections. However, this robustness comes at the cost of acquisition speed. The overall measurement time in conventional ptychography is limited by three main factors: the sequential scanning of the sample [3], the finite exposure times required due to the limited photon flux of the source, and the detector read-out time, which accumulates across the large number of diffraction patterns that must be recorded. These limitations significantly constrain the applicability of ptychography to the study of the dynamics of transient systems, as conventional measurement times typically span from several minutes to hours. With sufficient pulse energy, single-ultrafast-pulse diffraction patterns can be recorded at each position, making the sample scanning and camera readout the limiting factors in acquisition speed.

In this study, we address the fundamental bottlenecks limiting the speed of ptychographic imaging by developing a fully synchronized, high-throughput fly-scan ptychography system. Our setup integrates a high-flux picosecond modelocked Nd:YVO₄ laser source, a continuously scanning sample stage, and a high-speed event-based detector, all synchronized via pulse picking to ensure that each pulse is temporally aligned with the detector exposure and sample motion. The employed detector is a Timepix3 sensor capable of detecting individual events on each pixel of a two-dimensional array, with nanosecond time resolution for all pixels in parallel. This allows us to capture single-pulse diffraction patterns from $\sim 15\,\mathrm{ps}$ pulses at kilohertz repetition rates. By synchronizing this acquisition capability with continuous sample motion, we achieve acquisition times of 166 ms for a 0.95 mm² field of view and 30 ms for a 0.13 mm² region. These acquisition speeds, together with diffraction-limited reconstructions, result in the highest space-bandwidth product throughput reported for scanning ptychography to date: 2.3 Gpix/h. At this temporal resolution of 33 frames per second, we not only resolve object dynamics but also gain time-resolved access to the complex illumination field. This enables wavefront sensing with sensitivity to beam-pointing instabilities and spatiotemporal variations in the illuminating pulses.

While this demonstration uses the second harmonic of a Nd:vanadate laser pulses, future work aims to employ our in-house built high-harmonic source driven by spectrally broadened and temporally compressed pulses, with the goal of achieving dynamic high-resolution imaging at extreme ultraviolet wavelengths.

- [1] P. W. Hawkes and J. C. H. Spence, "Ptychography," in *Springer Handbook of Microscopy*, edited by P. W. Hawkes and J. C. H. Spence (Springer Nature, 2019), Chapter 17.
- [2] G. K. Tadesse *et al.*, "Wavelength-scale ptychographic coherent diffractive imaging using a high-order harmonic source," *Sci. Rep.* **9**, 1735 (2019).
- [3] J. Deng et al., "Continuous motion scan ptychography: characterization for increased speed in coherent x-ray imaging," Opt. Express 23, 5438–5451 (2015).

Advanced Research Center for Nanolithography (ARCNL), Science Park 106, 1098 XG Amsterdam, The Netherlands
 LaserLaB, Vrije Universiteit Amsterdam, De Boelelaan 1081, 1081 HV Amsterdam, The Netherlands

³Imaging Physics, Faculty of Applied Sciences, Technische Universiteit Delft, Building 22, Lorentzweg 1, 2628 CJ Delft, The Netherlands

^{*}akarpavicius@tudelft.nl

Bulk Multipass Cell Compression of Bursts of 11.424 GHz Repetition Rate, 50 μ J, Multi-Picosecond Photoinjector Laser Pulses

Michael W.L. Seggebruch,^{1,*} Ferenc Raksi,² Alex Amador,² Shawn M. Betts,² Adan Garcia,² Gennady Imeshev,² Patrick Lancuba,² Ricardo De Luna Lopez,² Mauricio Quinonez,² Trevor Reutershan,¹ Kelly Zapata,² Luis E. Zapata,² Allen J. Zhang,² and Christopher P.J. Barty^{1,2}

Abstract

We report on bulk multipass cell compression of bursts of one hundred 995.2 nm, 11.424 GHz repetition rate, 50 μ J pulses from 13.6 ps to 1.44 ps in an electro-optic pulse synthesis-based photoinjector laser architecture, enabling high-brightness and low emittance / energy spread electron beams from an X-band linac

The photogun laser (PGL) for the 11.424 GHz X-band linac at Lumitron Technologies is seeded by 8.75 ns, 100 Hz, pre-shaped bursts of 995.2 nm, 11.424 GHz repetition rate pulses. The pulses are generated via electro-optic pulse synthesis [1] clocked by the linac's RF oscillator. This approach to photogun laser design, to our knowledge never before implemented in an X-band linac, distributes electron beam charge over many RF buckets, thereby enabling high current electron beams while minimizing emittance and energy spread due to space charge effects. A cyrogenic Yb:YLF multipass amplifier is employed to amplify the PGL signal to 500 mW. [2] Due to gain narrowing in the cryogenic amplifier, the Fourier transform limit of the amplified spectrum is 11.9 ps FWHM. Because electron beam emittance and energy spread increase significantly with PGL pulse duration, a 23-pass bulk multipass cell (MPC) [3] and a 1250 l/mm grating Treacy compressor are employed to compress the PGL pulses from approximately 13.6 ps to 1.44 ps. The cell is 80 cm long with two 2 inch diameter, 500 mm radius of curvature end mirrors and two 17.33 mm thick, H-ZF7LA glass, AR coated windows each 8 cm from the center of the cell at their nearest faces. To exceed the work function of the photogun's copper photocathode, the compressed pulses are converted to UV via fourth harmonic generation. The flattest UV burst envelope is generated with a non-flat IR burst envelope, indicating that pulse durations may be variable across each IR burst. For optimal electron beam quality, the UV beam is apertured, and the aperture is imaged onto the photocathode.

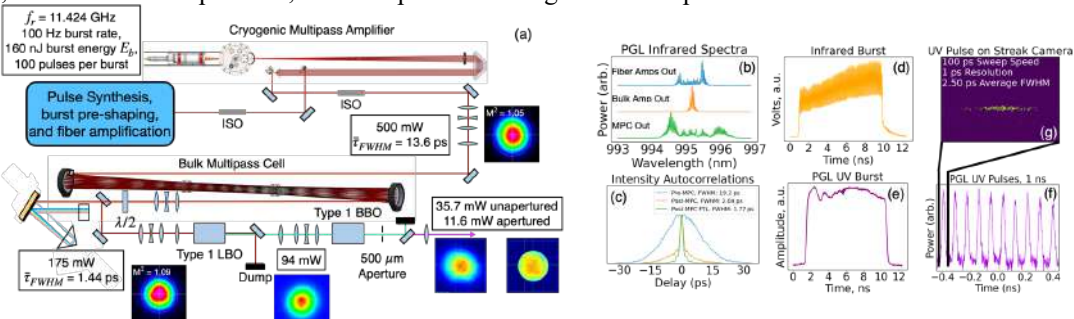


Figure 1: (a) Schematic of the X-band photoinjector laser. (b) PGL infrared spectra at key points. (c) Intensity autocorrelations before and after the MPC, as well as the post-MPC transform limited autocorrelation. FWHM 19.2 ps, 2.04 ps, and 1.72 ps, respectively. (d) Infrared burst after the multipass amplifier, measured with a 30 GHz fast photodiode. (e) and (f) are the streak camera measured UV burst and a sample 1 ns portion of the burst, respectively. (g) Sample UV micropulse measured with the streak camera's 100 ps sweep speed. The average measured pulse duration is 2.5 ps, although the measurement is limited by the streak camera's 1 ps resolution.

References

[1] Prantil, M. A., et al. (2013). "Widely tunable 11 GHz femtosecond fiber laser based on a nonmode-locked source." Optics Letters 38(17): 3216-3218.

[2] Barty, C. P., et al. (2024). "Design, construction, and test of compact, distributed-charge, X-band accelerator systems that enable image-guided, VHEE Flash radiotherapy." Frontiers in Physics 12: 1-18

[3] Viotti, A.-L., et al. (2022). "Multi-pass cells for post-compression of ultrashort laser pulses." Optica 9(2): 197-216.

¹University of California Irvine, Irvine, CA 92617, USA

²Lumitron Technologies, Inc., 5201 California Ave., Suite 100, Irvine, CA 92617, USA

^{*}mseggebr@uci.edu

Toward ultrafast parametric X-ray radiation using a compact electron beamline

Chad Pennington,^{1,2*} Gia Azcoitia,¹ Mariia Stepanova,³ Connor Lim,¹ Linshan Sun,¹ Mashnoon Alam Sakib,³ Cameron Leary,¹ Jackson Rozells,¹ Brittany Lu,¹ Liang Jie Wong,⁴ Tenio Popmintchev,⁵ Maxim Shcherbakov,³ Sergio Carbajo^{1,2,6}

Abstract

Abstract

The BELLS laboratory at UCLA is developing an ultrafast parametric X-ray radiation (PXR) source driven by a direct-current (DC) accelerator beamline. This work focuses on achieving spectral control, pulse shaping, and collimation of the emitted X-rays. By combining high-quality electron beams with tailored crystal targets, we aim to optimize PXR emission for applications in ultrafast optics.

Ultrafast, coherent X-ray pulses are essential tools for probing matter at molecular and atomic scales. Large-scale facilities like free-electron lasers (FELs) have made such capabilities possible¹, but replicating them in compact, accessible platforms such as university and industrial laboratories remains a scientific and technical challenge. The BELLS lab aims to bridge this gap by exploring parametric X-ray radiation (PXR), a process in which shaped electron beams interact with crystal lattices via bremsstrahlung² to generate tunable, coherent X-rays. Utilizing a compact beamline delivering 10–30 keV electron beams and advanced beam-shaping elements, we are developing PXR techniques with the potential for fine spectral control, ultrashort pulse durations, and directional emission. Preliminary estimates from our PXR setup suggest an expected flux of 10⁸-10¹⁰ photons per second in the 0.8–30 keV range with sub-100 fs X-ray pulses. We aim to compress these pulses to the single-digit femtosecond regime—or below—in future iterations of the system. These advancements would enable state-of-the-art performance in ultrafast optics applications, such as time-resolved spectroscopy and high-resolution imaging³ in compact research environments.

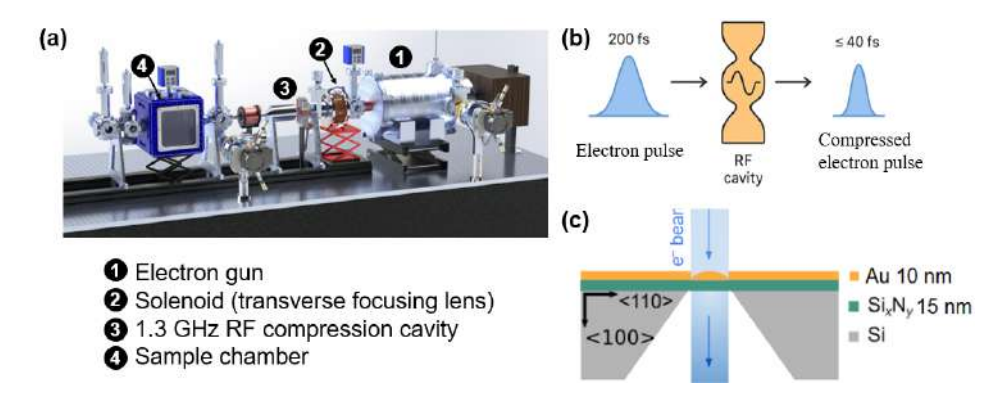


Fig 1. (a) Schematic of the BELLS beamline. (b) longitudinal compression scheme using an RF bunching cavity to generate ultrafast pulses. (c) Schematic of a sample phase plate for beam shaping and phase modulation for PXR.

- Galayda, J. The LCLS-II: A high-repetition rate superconducting linac free-electron laser. Nucl. Instrum. Methods Phys. Res. A 807, 69–74 (2016). https://doi.org/10.1016/j.nima.2015.03.089
- 2. Shi, X., Wong, L.W.W., Huang, S. et al. Transverse recoil imprinted on free-electron radiation. Nat Commun 15, 7803 (2024). https://doi.org/10.1038/s41467-024-52050-w
- 3. I.D. Feranchuk et al. Superradiant parametric x-ray emission. Phys. Rev. Accel. Beams 25, 120702 Published 23 December, 2022. DOI: https://doi.org/10.1103/PhysRevAccelBeams.25.120702

¹Department of Electrical and Computer Engineering, UCLA, Los Angeles, CA 90095, USA

²Physics and Astronomy Department, University of California Los Angeles, CA 90095, USA

³Department of Electrical Engineering and Computer Science, University of California, Irvine, CA 92697, USA

⁴Nanyang Technological University, 50 Nanyang Avenue, Singapore

⁵Physics Department, University of California San Diego, CA 92093, USA

⁶SLAC National Accelerator Laboratory, Stanford University, Menlo Park, California 94025, USA

^{*}chadpennington@g.ucla.edu

Ultrafast Energy Redistribution in Bimetallic Antenna–Reactor Nanoparticles

R. Dagar^{1,2*}, T. Yoon^{1,2}, S. Sahel-Schackis^{1,2}, T. Linker^{1,2}, M. Grassl¹, S. Kesarwani³, A. Colombo⁴, L. Hecht⁴, C. Pan⁴, E. Ott⁴, L. Schuepke⁴, A. Sanchez⁵, A. Sarracini⁶, K. Schnorr⁶, A. Al Haddad⁶, C. Bostedt⁶, Y. Ovcharenko⁷, S. Dold⁷, M. Meyer⁷, C. Aikens⁸, D. Rupp⁴, A. Summers¹, H. Lange³, M. Kling^{1,2}

¹SLAC National Accelerator Laboratory, Menlo Park, CA, USA; ²Stanford University, Stanford, CA, USA; ³University of Potsdam, Potsdam, Germany; ⁴Eth Zurich, Zurich, Switzerland; ⁵Deutsches Elektronen-Synchrotron, Hamburg, Germany; ⁶Paul Scherrer Institut, Villigen, Switzerland; ⁷European XFEL, Hamburg, Germany; ⁸Kansas State University, Manhattan, KS, USA; *dagar@slac.stanford.edu

Abstract

We report the direct observation of ultrafast photoinduced charge redistribution and its role in driving phonon-mediated energy transfer in Au–Pd nanoparticles, using laser-pump/X-ray-probe velocity map imaging at SwissFEL. The measurements reveal initial localization of charge and energy in the Pd satellites, followed by delayed Au ion emission from the antenna in bimetallic Au–Pd antenna–reactor nanoparticles.

Understanding the interplay between charge localization and thermal transport in heterogeneous plasmonic nanostructures is critical for advancing pulsed catalytic systems [1]. In this work, we investigate charge-driven phonon-mediated energy redistribution in Au-Pd antenna-reactor nanoparticles, where catalytically active Pd satellites are coupled to a central Au core. The system was probed using laser-pump/X-ray-probe velocity map imaging (VMI) at the Maloja endstation of SwissFEL, enabling time-resolved tracking of ionic fragment emission as a proxy for charge and thermal dynamics. Upon femtosecond laser excitation at 400 nm, the Pd satellites exhibited dominant ion emission at early delays (0–2 ps), while Au ion signals remained initially suppressed, despite the greater absorption cross-section of gold. This indicates that charge and energy were preferentially deposited in the Pd domains. Over a timescale of hundreds of picoseconds (measured upto 500 ps), a pronounced increase in Au+ ion yield was observed alongside a decline in Pd+ emission, marking a delayed transfer of energy from Pd to Au. We attribute this delayed Au response to phonon-mediated heat flow initiated by a photoinduced charge imbalance. Following initial charge localization in Pd, vibrational coupling between Pd and Au drives energy redistribution across the interface. This dynamic is consistent with sequential charge transfer followed by phonon-assisted thermal equilibration, a mechanism corroborated by our supporting molecular dynamics simulations [2].

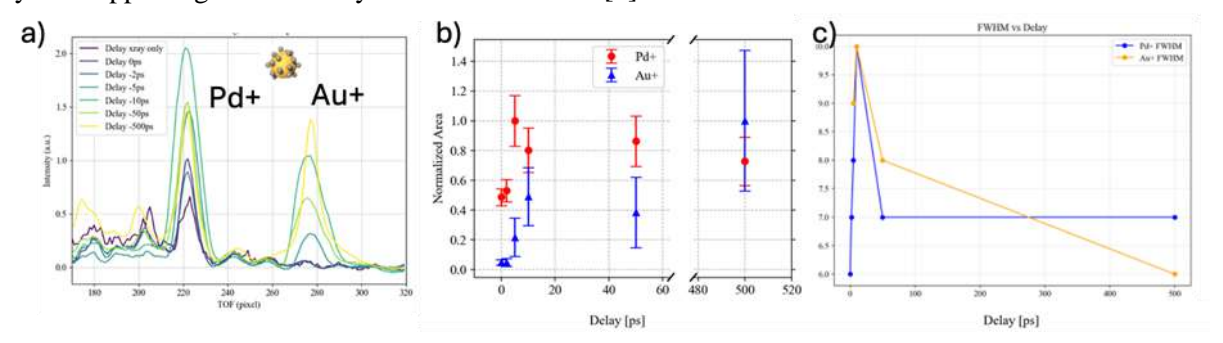


Figure 1: Variations in the ionic yields of Pd⁺ and Au⁺ at different time delays.

These results offer new insights into the spatiotemporal coupling of charge and vibrational energy in bimetallic nanostructures. Understanding and controlling such interactions is essential for tailoring nonequilibrium energy flow in pulsed catalytic applications.

- [1] Gargiulo, J., et al., Nat Commun 14, 3813 (2023)
- [2] Stete, F., et al., arXiv:2501.02566 [cond-mat.soft]

Real-Time Observation of Interfacial Charge Transfer in Hybrid Systems via fs-MIR spectroscopy

I Nadinov,* S Thomas, G Healing, H. N. Alshareef, and O. F. Mohammed

Division of Physical Sciences and Engineering, King Abdullah University of Science and Technology (KAUST), Thuwal 23955–6900, Kingdom of Saudi Arabia *issatay.nadinov@kaust.edu.sa

Abstract

Femtosecond mid-infrared spectroscopy, combined with density functional theory (DFT), reveals ultrafast carrier dynamics and vibrational interactions at hybrid interfaces. DFT calculations of both ground and excited states for periodic systems provide insights into lattice behavior. Interfacial charge separation mechanisms are elucidated in FAPbBr₃/IEICO-4F and PM6/CuSCN donor–acceptor systems.

At the heart of next-generation optoelectronic devices lies a complex and ultrafast world of charge transfer and molecular interactions, invisible to conventional techniques. By harnessing femtosecond mid-infrared (fs-MIR) spectroscopy, we directly capture the intricate interplay between lattice vibrations, organic cations, and interfacial carrier dynamics with femtosecond resolution.

We first examine the vibrational dynamics of methylammonium lead bromide (MAPbBr₃) and formamidinium lead bromide (FAPbBr₃), revealing that the larger FA⁺ cation induces weaker lattice coupling, resulting in reduced structural distortion and enhanced charge transport. In a breakthrough approach, we employ density functional theory (DFT) calculations of both the ground and excited states for FAPbBr₃ and MAPbBr₃ in a periodic system, performed for the first time, to extract infrared frequencies corresponding to vibrational changes in the organic cations. These calculations not only elucidate cation-lattice interactions but also reveal the structural stability and electronic behavior of perovskites under excitation.

Building on this understanding, we investigate electron transfer at the FAPbBr₃/IEICO-4F interface [1]. The fs-MIR spectroscopy reveals ultrafast electron injection within 150 fs, confirmed by distinct vibrational shifts in the C=N bond of the acceptor. This highlights the crucial role of interfacial interactions in optimizing charge separation, as molecular vibrations directly inform electronic coupling at donor-acceptor junctions.

Finally, we extend our study to hole transfer at the PM6/CuSCN interface. Fs-MIR spectra show hole injection within 168 fs, evidenced by a spectral shift in the C=N stretching mode of CuSCN [2]. The coherent nature of this transfer, supported by interfacial DFT models, emphasizes the importance of vibrational coherence in charge separation. Our findings further reinforce the predictive power of vibrational signatures in understanding and improving carrier transport across interfaces.

By integrating fs-MIR spectroscopy with advanced DFT calculations, we present a unified approach for probing ultrafast interfacial dynamics in hybrid materials. This work offers crucial insights into the stability, charge mobility, and vibrational coherence of perovskites, paving the way for the rational design of next-generation optoelectronic devices with optimized performance and longevity.

References

[1] I. Nadinov, ...O.F. Mohammed. "Real-time tracking of hot carrier injection at the interface of FAPbBr3 perovskite using femtosecond mid-IR spectroscopy," ACS Central Science, **10** (1), 43-53(2023).

[2] G. Healing, I. Nadinov, ...O.F. Mohammed, "Ultrafast Coherent Hole Injection at the Interface between CuSCN and Polymer PM6 Using Femtosecond Mid-Infrared Spectroscopy", ACS applied materials & interfaces, 17757–17766 (2025).

Azores 2025

Towards Realizing Schawlow-Townes Limited Dual-comb Spectroscopy with an Analog Feed-Forward Approach

Gregory Sercel,^{1,3*} Mirali Seyed Shariatdoust,^{1,3} Tao Qu,^{1,3} Jack Diab,^{1,3} Jack Hirschman,² Randy Lemons,² Sophia Beninati,¹ Prineha Narang,^{1,3} Suzanne Paulson,^{1,3} and Sergio Carbajo^{1,2,3}

Abstract

Near Schawlow-Townes noise-limited dual-comb spectroscopy can be realized through analog feed-forward stabilization of carrier envelope phase. We present such a system, for applications in precision atmospheric sensing.

Main Text

We present a dual-comb spectroscopy system nearing Schawlow-Townes noise limits for precision atmospheric sensing applications. Dual-comb spectroscopy presents a means of rapidly acquiring high-resolution transmission spectra by beating two optical frequency combs of slightly offset repetition rates. Each pair of optical comb teeth generates a unique low-frequency beat note, detectable with avalanche photodiodes. Optical absorptions of samples imprinted on one or both combs result in a corresponding change in RF beat intensity, meaning optical absorption information is encoded in an easily processed RF signal.[1] Our dual-comb spectroscopy system, depicted in Fig. 1, consists of two SESAM mode-locked Er:Yb:glass lasers with 324.998 and 325 Mhz repetition rates, emitting at 1550 nm, and utilizes a feed-forward carrier-envelope phase stabilization technique applied to each comb. Using this technique, we have historically demonstrated the ability to follow a frequency reference with integrated phase noise of 3.5 mrad (1 Hz–3 MHz)[2, 3]. With phase noise levels on this order, nearing Schawlow-Townes noise limits, an advantage of lower noise floors is theoretically gained in spectroscopic applications. As a result, more sensitive spectroscopy with shorter averaging times is possible. As a benchmark, greenhouse gases such as carbon dioxide and methane will be characterized using this ultra-stable comb system, followed by complex bioaerosols.

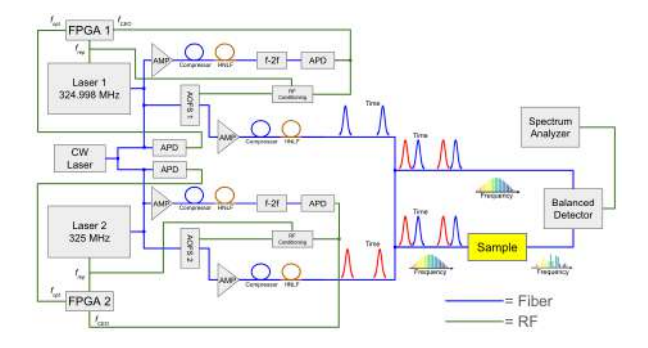


Figure 1: Schematic of dual-comb system. RF signals are shown in green, optical signals are shown in blue.

- [1] I. Coddington, N. Newbury, and W. Swann, "Dual-comb spectroscopy," Optica 3, 414–426 (2016).
- [2] R. Lemons, W. Liu, I. F. de Fuentes, S. Droste, G. Steinmeyer, C. G. Durfee, and S. Carbajo, "Carrier-envelope phase stabilization of an er:yb:glass laser via a feed-forward technique," Opt. Lett. 44, 5610–5613 (2019).
- [3] J. Hirschman, R. Lemons, E. Chansky, G. Steinmeyer, and S. Carbajo, "Long-term hybrid stabilization of the carrier-envelope phase," Opt. Express 28, 34093–34103 (2020).

 $^{^1}$ Department of Electrical and Computer Engineering, University of California, Los Angeles, Los Angeles, CA 90095,

 $^{^2}$ SLAC National Accelerator Laboratory, Stanford University, Menlo Park, CA 94025 USA

 $^{^3}$ California Nano Systems Institute, 570 Westwood Plaza, Los Angeles, CA 90095, USA

^{*}gsercel2@ucla.edu.edu

100 kHz Repetition Rate Extreme Ultraviolet Beamlines at the Artemis Facility

Bruce Weaver*, Yu Zhang, Charlotte Sanders, James Thompson, Tiffany Walmsley, Oliver Smith, Adam Wyatt, Richard Chapman, Greg Greetham, Emma Springate

STFC Central Laser Facility, Rutherford Appleton Laboratory, Harwell Campus, Didcot, OX11 0QX, UK. *bruce.weaver@stfc.ac.uk

Abstract

Artemis is the UK's user facility for ultrafast extreme ultraviolet spectroscopy. We present the recently completed and ongoing work to upgrade the facility to 100 kHz repetition rate and expand the end-station capabilities in femtosecond time-resolved materials science, gas-phase atomic and molecular science, ptychographic imaging, and liquid phase chemical dynamics.

The Artemis laboratory at the UK's Central Laser Facility (CLF) is a user facility offering access to high average power femtosecond laser systems and HHG sources for a variety of ultrafast extreme ultraviolet (XUV) experiments. The XUV beamlines provide the capability for time-and angle- resolved photoemission spectroscopy (TR-ARPES) on solid samples, and photoelectron spectroscopy (PES) on gas-phase small molecules, with tunable optical pump pulses and XUV probe pulses. In the gas-phase, recent experiments include the first alignment frame PES measurement with a monochromated HHG-based light source [1] and measuring the full excited state dynamics of 1,2-Dicholoroethene [2].

TR-ARPES with high harmonic probe pulses have enabled studies of electron dynamics in charge-ordered 2D materials [3]. We use a 100 kHz optical parametric chirped pulse amplification system [5] to drive the HHG source. We have also upgraded our TR-ARPES endstation with a new Fermi surface mapping analyser, enabling efficient acquisition of high-quality ARPES spectra of optically pumped excitations close to the Fermi surface level [5].

We have recently secured funding for a £17M major upgrade [6] of all the CLF's ultrafast facilities. The upgraded Artemis will offer a 100 kHz Yb-based laser system, with 1.5 mJ, <50 fs pulses at 1 micron for HHG, and tunable <50 fs pulses from 235 nm to 10 microns. A new gas-phase endstation will offer dual electron and ion coincidence spectrometers, with gas-jet and laser desorption sources. A new materials science end-station will offer a momentum microscope and a hemispherical analyser for time- and angle-resolved photoemission.

Finally, we aim to expand the facility's capabilities with the addition of a new beamline that will generate broadband XUV pulses for time-resolved XUV and soft-X-ray absorption spectroscopy in liquid- and gas-phase samples and perform XUV ptychographic imaging of microscopic samples.

The new capabilities will be available to access starting in 2026.

- [1] J. L. Woodhouse et al., Phys. Rev. A 111, 012815, (2024).
- [2] H. G. McGhee et al., Phys. Chem. Chem. Phys., 26, 28406-28416 (2024).
- [3] C. J. Sayers et al., Phys. Rev. Lett. **130**, 156401 (2023).
- [4] N. Thiré et al., Sci. Rep., 13, 18874 (2023).
- [5] P. Majchrzak et al., Rev. Sci. Instr., 95, 063001 (2024).
- [6] https://www.clf.stfc.ac.uk/Pages/HiLUX.aspx

Introduction to Advanced Attosecond Laser Infrastructure

Kun Zhao,1* Sheng Meng,1 Xinkui He,1 and Hongxiang Wei1

¹Institute of Physics, Chinese Academy of Sciences, No. 8, 3rd South Street, Beijing 100190, China *<u>zhaokun@iphy.ac.cn</u>

Abstract

The Advanced Attosecond Laser Infrastructure (AALI), a comprehensive ultrafast electron dynamics research facility in China, is characterized primarily by attosecond temporal resolution. With the curiosity of electron motion and electron correlations in mind, it seeks to explore the fastest ever evolution of electronic states, providing a unique tool for breakthroughs in multiple fundamental research fields.

In 2021, Institute of Physics, Chinese Academy of Sciences initiated the Center for Ultrafast Physics (CUP), aiming to bridge ultrafast optics and condensed matter physics/material sciences. With the constructiong of the Advanced Attosecond Laser Infrastructure (AALI) as the primary target, CUP strives to establish a new high ground of scientific research and technological development in a broad range of frontier fields especially ultrafast science with global influence. Next to the China Spallation Neutron Source, CUP is located in the city of Dongguan, a key hub in the Guangdong-Hong Kong-Macao Greater Bay Area. CUP currently has 80+ principal investigators and 50+ post-doctoral fellows and postgraduate students. Research Areas include but not limited to:

- Femtosecond and attosecond laser technologies;
- ◆ Ultrafast measurements;
- Nonlinear optical detection of quantum materials;
- Novel laser-induced quantum state;
- Ultrafast control of quantum state;
- High harmonics generation in condensed matters;
- ◆ Terahertz spectroscopy, ultrafast spectroscopy and coherent phonons;
- ◆ Time-dependent density functional theory, GW method and ultrafast dynamics simulation.

AALI is being constructed at this moment as a comprehensive ultrafast electron dynamics research facility, characterized primarily by attosecond temporal resolution and high spatiotemporal coherence of its light sources. The facility aims to achieve tracking, measurement, and manipulation of electron motion and electron correlations. From the perspective of electromagnetic interaction theory, starting from and based on electron motion, it seeks to explore evolutions of material and/or quantum states, providing a unique tool for breakthroughs in fundamental research in areas including atomic/molecular physics, condensed matter physics, quantum mechanics, materials science, chemistry, and life sciences.

Figure 1: Rendering of the AALI main building



CUP and AALI are experiencing a rapid expansion of their research abilities together. There are multiple openings at all levels from junior tenure-track assistant professors, senior full professors to high-level senior engineers in multiple research and development areas. Talented applicants from worldwide who have the capacity or have exhibited the potential of running a world-recognized independent R&D program are welcome.

Nonlinear photophysics of rare-earth ions under femtosecond excitation

Helena Cristina Vasconcelos, 1,2* Maria Gabriela Meirelles, 1,3

¹Faculty of Science and Technology, University of the Azores, Ponta Delgada, S. Miguel, 9500-321 Azores, Portugal ²Laboratory of Instrumentation, Biomedical Engineering and Radiation Physics (LIBPhys, UNL), Department of Physics, NOVA School of Science and Technology, 2829-516 Caparica, Portugal

³Research Institute of Marine Sciences of the University of the Azores (OKEANOS), Horta, Faial, 9901-862 Azores, Portugal

*helena.cs.vasconcelos@uac.pt

Abstract

Rare-earth ions under femtosecond excitation exhibit nonlinear responses including multiphoton and excited-state absorption, along with ultrafast relaxation. We present a theoretical analysis based on rate-equation models, showing how host matrices and dopant concentration affect emission dynamics. The study supports applications in upconversion, optical amplifiers, ultrafast photonics, and light sources.

Theoretical Framework and Results

Rare-earth ions are widely used in photonics due to their sharp intra-4f transitions, long-lived excited states, and efficient emission properties [1]. Their excitation with femtosecond pulses introduces strongly nonlinear processes, such as multiphoton absorption, excited-state absorption (ESA), and ultrafast nonradiative relaxation [2]. Understanding these mechanisms is crucial for designing next-generation broadband ultrafast amplifiers. We model the ground (N_g) and excited (N_e) populations using rate equations:

$$\frac{dN_g}{dt} = -W_{mp}(t)N_g + \frac{N_e}{\tau_{rad}} + \frac{N_e}{\tau_{nr}}$$

$$\frac{dN_g}{dt} = W_{mp}(t)N_g - \frac{N_e}{\tau_{rad}} - \frac{N_e}{\tau_{nr}} - W_{ET}N_e^2$$

where $W_{mp}(t) \propto I(t)^m$ describes multiphoton excitation and $I(t) = I_0 exp\left(-\frac{t^2}{2\sigma^2}\right)$ models a Gaussian femtosecond pulse. Shorter pulses $(\sigma\downarrow)$ enhance multiphoton processes, modifying the early-time population distribution. Simulations predict: (i) faster, multi-exponential decays for fs pumping compared to ps excitation, (ii) broadening of the emission spectrum, and (iii) nonlinear power dependence with multiphoton scaling at low fluences. Figure 1 illustrates the predicted spectra; as an example, the simulation considers the Yb³+ emission band around 1 μ m, widely used in broadband ultrafast amplifiers. These results indicate that femtosecond pumping may alter emission bandwidth in rare-earth-doped gain media, providing guidelines for the design of ultrafast broadband laser systems.

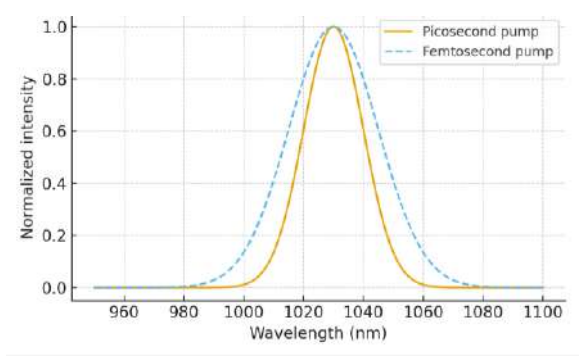


Figure 1: Simulated Yb³⁺ emission spectra around 1 μm under ps (narrower) and fs (broader) pumping conditions.

References

[1] Applications of Ultrafast Spectroscopy to Solid State Laser Materials. In: Di Bartolo, B., Gambarota, G. (eds) Ultrafast Dynamics of Quantum Systems. NATO Science Series: B:, vol 372. Springer, Boston, MA. https://doi.org/10.1007/0-306-47080-2_19

[2] Yao, Y., Xu, C., Zheng, Y., Yang, C., Ma, Y., Song, Z., & Xu, S. (2016). Femtosecond laser-induced upconversion luminescence in rare-earth ions by non-resonant multiphoton absorption. The Journal of Physical Chemistry A, 120(28), 5553–5558. https://doi.org/10.1021/acs.jpca.6b04444